A novel human stem cell platform for probing adrenoceptor signaling in iPSC derived cardiomyocytes including those with an adult atrial phenotype

Faizzan Syed Ahmad

St. Cross College

University of Oxford

A thesis submitted for the degree of

Doctor of Philosophy

Michaelmas 2017

Dedication

In memory of my dearest mother Sabiha Ahmad

For the joy and warmth you brought

For the irreplaceable void you left

You shall never be forgotten

A novel human stem cell platform for probing adrenoceptor signaling in iPSC derived cardiomyocytes including those with an adult atrial phenotype

Faizzan Syed Ahmad, St. Cross College, University of Oxford. A thesis submitted for the degree of Doctor of Philosophy, Michaelmas 2017

Scientific research is propelled by two objectives: Understanding and recognizing the essential biology of life, and deciphering this to uncover possible therapeutics in order to improve quality of life as well as relieve pain from disease. The aim of the work described in this thesis was to dissect the fundamental requirements of induced pluripotent stem cells both in pluripotency and differentiation with a particular focus on atrial specificity.

Drug targeting of atrial-specific ion channels has been difficult because of lack of availability of appropriate cardiac cells, and preclinical testing studies have been carried out in non-cardiac cell lines, heterogeneous cardiac populations or animal models that have been unable to accurately represent human cardiomyocyte physiology. Therefore, we sought out to develop a preparation of cardiomyocytes showing an atrial phenotype with adult characteristics from human induced-pluripotent stem cells.

A culture programme involving the use of Gremlin 2 allowed differentiation of cardiomyocytes with an atrial phenotype from human induced-pluripotent stem cells. When these differentiated cultures were dissociated into single myocytes a substantial fraction of cells showed a rod-shaped morphology with a single central nucleus that was broadly similar to that observed in cells isolated from atrial chambers of the heart. Immunolabelling of these myocytes for cardiac proteins (including RyR2 receptors, actinin-2, F-actin) showed striations with a sarcomere spacing of slightly less than 2um. The isolated rod-shaped cells were electrically quiescent unless stimulated to fire action potentials with an amplitude of 100 mV from a resting potential of approximately -70 mV. Proteins expressed included those for IK_1, IK_{ur} channels. Ca^{2+} Transients recorded from spontaneously beating cultures showed increases in amplitude in response to stimulation of adrenoceptors (both alpha and beta).

With the aim of identifying key signaling mechanisms in directing cell fate, our new protocol allowed differentiation of human myocytes with an atrial phenotype and adult characteristics that show functional adrenoceptor signaling pathways and are suitable for investigation of drug effects.

Acknowledgements

Enclosed within the ensuing pages is a summary of the work that has often encompassed the last 4 years of my life. The mission of completing a DPhil often seems overwhelming, nonetheless fortunately I was not unaided in this larger than life task. It may appear that my name being on this thesis is a gross unrepresentative reflection of the number of people who really contributed to it, through the advice, encouragement, and support they generously offered.

I would like to express my sincere gratitude to my supervisors Professor Derek A. Terrar, Professor Ming Lei and Professor Sir Magdi Yacoub for their patience, trust, guidance and continuous support throughout my D.Phil. Professor Derek Terrar's optimistic enthusiasm, support and belief enabled me to follow my interest in the cardiovascular stem cell field. I must thank him for inviting me to work in his laboratory and also for his wisdom and encouragement.

Besides my advisors, I would like to thank the Pharmacology administrative team, in particular Paula Savin without whose constant support my journey would have not been a successful one. Also, Meng Yuan, Dr. Sam Lin, Razik Mu-min, Alaa Hachem, Danni Zhu, and Dr. Bobo Nazarov, without whom working in Oxford would have been less enjoyable and I am extremely pleased that our paths crossed.

I must also thank my daughter Sana Sabiha Ahmad, who was born during my final year in Oxford. She has provided a continuous supply of joy and inspiration as well as much needed state of insomnia.

Finally, my heartfelt gratitude goes out to my family: my father Syed M.T. Ahmad, without whom this goal would be unattainable, my brother Feraz Ahmad and my sister Adiba Ahmad, the biggest pillars of my life for their never-ending belief in me. Most importantly, I owe more thanks that I can express to my wife Dr. Wajiha Hyder who has been a source of

unending love and patience, and who – in many ways – put her own life on hold to allow me to complete this DPhil.

Sincerely, thank you all.

Full publications

Bethany L. Johnson-Kerner, Faizzan S. Ahmad, Alejandro Garcia Diaz, J. Palmer Greene, Steven J. Gray, R. Jude Samulski, Wendy K. Chung, Rudy Van Coster, Paul Maertens, Scott A. Noggle, Christopher E. Henderson, Hynek Wichterle, Gigaxonin binds intermediate filaments and corrects peripherin aggregation in giant axonal neuropathy patient-derived motor neurons Hum Mol Genet. 2015 Mar 1;24(5):1420-31. doi: 10.1093/hmg/ddu556. Epub 2014 Nov 4.PMID: 25398950

Raynaud, CM, Ahmad, FS, Allouba, M, Abou-Saleh, H, Lui, KO & Yacoub, M (2014). Reprogramming for cardiac regeneration. Glob Cardiol Sci Pract. 2014 Oct 16;2014(3):309-29. doi: 10.5339/gcsp.2014.44. eCollection 2014. Review. PMID: 25763379

Raynaud CM, Butler JM, Halabi NM, Ahmad FS, Ahmed B, Rafii S, Rafii A. Endothelial cells provide a niche for placental hematopoietic stem/progenitor cell expansion through broad transcriptomic modification. Stem Cell Res. 2014 Aug 9;11(3):1074-1090. doi: 10.1016/j.scr.2013.07.010. PMID: 23978474

Liberski AR, Al-Noubi MN, Rahman ZH, Halabi NM, Dib SS, Al-Mismar R, Billing AM, Krishnankutty R, Ahmad FS, Raynaud CM, Rafii A, Engholm-Keller K, Graumann J. Adaptation of a commonly used, chemically defined medium for human embryonic stem cells to stable isotope labeling with amino acids in cell culture. J Proteome Res. 2013 Jul 5;12(7):3233-45. doi: 10.1021/pr400099j. Epub 2014 Jun 25. PMID: 23734825

Kahler DJ, Ahmad FS, Ritz A, Hua H, Moroziewicz DN, Sproul AA, Dusenberry CR, Shang L, Paull D, Zimmer M, Weiss KA, Egli D, Noggle SA. Improved methods for reprogramming human dermal fibroblasts using fluorescence activated cell sorting. PLoS One. 2014;8(3):e59867. doi: 10.1371/journal.pone.0059867. Epub 2013 Mar 29. PMID: 23555815

Lotz S, Goderie S, Tokas N, Hirsch SE, Ahmad F, Corneo B, Le S, Banerjee A, Kane RS, Stern JH, Temple S, Fasano CA. Sustained levels of FGF2 maintain undifferentiated stem cell cultures with biweekly feeding. PLoS One. 2013;8(2):e56289. doi: 10.1371/journal.pone.0056289. Epub 2014 Feb 20. PMID: 23437109

Invited Lectures

Ahmad, Faizzan S., iPS at QCRC. Qatar Heart Science Series 2015 https://www.youtube.com/watch?v=i09XTJ0xny8

Ahmad, Faizzan S., Hallmarks of Regenerative Medicine: An update on preclinical testing of iPSCs technology in Qatar. BD Biosciences ""Middle East Stem Cell Symposium: Opportunities and Challenges in Stem Cell Research and Therapy Development" 2015

Ahmad, Faizzan S., Increased Reprogramming Efficiency Through Fluorescence Activated Cell Sorting. BD Biosciences "1st Middle East Research Flow User's Meeting" 2012

SELECTED ABSTRACTS

Faizzan S. Ahmad[1*], Ming Lei[1], Matthew Daniels[2], Magdi Yacoub[3], Derek A. Terrar[1]. A NOVEL APPROACH TO DERIVE ATRIAL CARDIOMYOCYTES FOR THE STUDY OF ATRIAL FIBRILLATION (BRTISH HEART FOUNDATION CENTRE OF RESEARCH EXCELLENCE), AUGUST 2017

Ahmad, Faizzan S., Daalis, Arwa,Mu-u-min, Razik, Kahler, David J., Noggle, Scott A., Bollensdorff, Christian. MENDING REPROGRAMMING AND HIGH THROUGHPUT METHODOLOGIES: IMPROVED METHODS FOR IPSC DERIVATION AND FUNCTIONAL CHARACTERIZATION ISSCR (International Society for Stem Cell Research), Vancouver 2014

Ahmad, Faizzan S., Daalis, Arwa,Mu-u-min, Razik, Kahler, David J., Noggle, Scott A., Bollensdorff, Christian. MENDING REPROGRAMMING AND HIGH THROUGHPUT METHODOLOGIES: IMPROVED METHODS FOR IPSC DERIVATION AND FUNCTIONAL CHARACTERIZATION (11th International Symposium on Stem Cell Therapy & Cardiovascular Innovations), Madrid 2014

Ahmad, Faizzan S., Kahler, David J., Noggle, Scott A. IMPROVED METHODS FOR REPROGRAMMING HUMAN DERMAL FIBROBLASTS USING FLUORESCENCE ACTIVATED CELL SORTING. H3 Symposium: Cellular approaches for cardiac repair: a physiological perspective (The Physiological Society), London 2014

Ahmad, Faizzan S., Kahler, David J., Noggle, Scott A. Hallmarks of regenerative medicine: Improved methods For reprogramming human fibroblasts using fluorescence activated cell sorting. Read More: http://www.qscience.com/doi/abs/10.5339/qfarf.2013.BIOP-076. QF ARF, Doha 2013

Kahler, David J., Ahmad, Faizzan S., Ritz, Anita, Hua, Haiqing, Moroziewicz, Dorota N., Sproul, Andrew A., Dusenberry, Carmen R., Shang, Linshan, Paull, Daniel, Zimmer, Matthew, Weiss, Keren A., Egli, Dieter, Noggle, Scott A. IMPROVED METHODS FOR REPROGRAMMING HUMAN DERMAL FIBROBLASTS USING FLUORESCENCE ACTIVATED CELL SORTING. ISSCR (International Society for Stem Cell Research), Boston 2013

Abbreviations

AC	Adenylyl Cyclase
ACh	Acetylcholine
AF	Atrial Fibrillation
AP	Action Potential
B27	Serum Replacement for Growth
B3	HuESM supplemented with Microspheres Every Third Day
BMP	Bone Morphogenetic Protein
bpm	Beats per minute
CaM	Calmodulin
CaMKII	Ca^{2+}/calmodulin-dependent protein kinase II
cAMP	Cyclic adenosine monophosphate
CBA	Cytometric Bead Array
CGP	CGP20712A
CHIR	CHIR99021 – WNT Agonist
CICR	Calcium-induced Ca^{2+} release
CM	Conditioned Media
CPA	Cyclopiazonic acid
DEX	Dexamethasone
DMSO	Dimethyl sulfoxide
E/EE Axis	Embryonic/Extra-Embryonic Axis
ED	HuESM Daily Control
ESCs	Embryonic Stem Cells
FGF2	Fibroblast Growth Factor 2
FGFRs	FGF Receptors
GIRK	G protein-coupled inwardly-rectifying potassium channel
hESCs	Human ES cells
HuESM	hESC Media
Hz	Hertz
ICM	Inner Cell Mass
I_f	Funny current
IGF	Insulin-Like Growth Factor
I_{NCX}	Sodium- Ca^{2+} exchange current
IPSC-CM	iPSC Cardiomyocytes
iPSCs	Induced Pluripotent Stem Cells
Iso	Isoprenaline
I_{st}	Sustained inward current
K_r	Rapid-activated voltage-gated delayed rectifier K^+ channel
K_s	Slow-activated voltage-gated delayed rectifier K^+ channel
KSR	Knockout Serurm Replacement Media
K_v	Voltage-gated K^+ channel

LCR	Localized Ca^{2+} release
MEFs	Mouse Embryonic Fibroblasts
min	Minute
MOI	Multiplicity of Infection
NCX	Sodium- Ca^{2+} exchanger
NPCs	Neural Precursor Cells
PBS	Phosphate Buffered Saline
PCR	Polymerase chain reaction
PDE	Phosphodiesterases
PE	Phycoerythrin
Phen	Phenylephrine
PIP_2	Phosphatidylinositol 4,5-bisphosphate
PKA	Protein Kinase A
PLB	Phospholamban
PLGA	Poly(lactic-co-glycolic acid)
Praz	Prazosin
PSS	Physiological Salt Solution
PVA	Poly(vinyl alcohol)
qRT-PCR	Quantitative Real Time-Polymerase Chain Reaction
RA	Retinoic Acid
Reb	Reboxetine
ROCK	Rho Associated Protein Kinase
RT-PCR	Reverse transcription polymerase chain reaction
RY	Ryanodine
RYR	Ryanodine receptor
SAN	Sino atrial node
SERCA	Sarcoendoplasmic reticulum Ca^{2+} ATPase
SR	Sarcoplasmic reticulum
SSEA	Stage-Specific Embryonic Antigen
TGF	Transforming Growth Factor
TTX	Tetrodotoxin
UV	Ultraviolet
WNT	Wingless

Table of Contents

CHAPTER 1: INTRODUCTION

Chapter 1: Introduction

General Introduction

Previously, it was not feasible to study diseases of the human cardiovascular system through the use of living tissue. Cardiac muscle cells in the heart are inaccessible to routine biopsy without causing damage to the subject. In lieu of human tissue, mouse models have been the principal way to study diseases of the cardiovascular system. While we have gained valuable insight from these animal models, they are also ripe with many limitations. Namely, the disease has to be caused by known genetic mutations, the mouse genome has to have a homolog to the human gene, and the phenotype has to recapitulate key aspects of pathology. While this approach has worked for some diseases, many diseases do not have useful mouse models. The way in which we can study human diseases of the cardiovascular system changed with the introduction of human embryonic stem cell and human induced pluripotent stem cell (iPS) technology. For the first time, we can generate stable pluripotent cell lines directly from patients with mutations and modifiers causing disease in patients. These induced pluripotent stem cells (iPSCs) can be differentiated into the very cardiac muscle cells inaccessible to biopsy. Moreover, large quantities of cardiomyocytes can be generated for biochemistry and drug discovery on human cells. Here, I demonstrate the use of human cardiomyocytes derived from pluripotent stem cells for studying key aspects of both development of atrial versus ventricular subtypes and Ca^{2+} handling properties.

Little is understood about the development of human atrial myocytes. Efforts to better understand cardiovascular diseases have been focused primarily on using human ventricular myocytes derived from iPS cells. Cardiovascular diseases that affect the atrium are less understood i.e. atrial fibrillation, because the disease has been hindered by mouse models that do not recapitulate the human disease.

Overall, I will discuss our current understanding of cardiovascular diseases. First, I review the clinical aspects of cardiovascular disease, I then review basic principles of cardiovascular development. I then go on to describe current knowledge of calcium (Ca^{2+}) dynamics within adult cardiac myocytes. I conclude, by reviewing the uses of ES and iPS-derived cardiomyocytes for disease modeling and normal atrial development. From this survey, it is clear that further work needs to be done to a) develop a human cellular model utilizing atrial myocytes from iPSCs and b) identify key aspects of Ca^{2+} signaling within disease mechanisms as a first step towards understanding the mechanisms of various cardiac diseases.

Cardiovascular Disease in Humans

Heart disease is the leading cause of death worldwide. For the past decade, the incidence of cardiac related death has continued to rise globally, with the World Health Organization naming cardiovascular disease the number one cause of death, worldwide, in 2012 (World Health Organization, 2012). Similarly, in 2013 the Centers for Disease Control and Prevention indicated that heart disease was the leading cause of death within the United States(Moorman *et al*., 2007). Cardiovascular disease usually stems from vascular dysfunction which leads to heart failure. For centuries heart failure was termed dropsy, and was considered incurable. However, by the twentieth century, fascinating discoveries in the role of hemodynamics and neuroregulation of the heart, collectively with the development of effectual treatments altered disease progression of heart failure into a chronic disease. As the prevalence of heart failure increases globally with high rates of morbidity and mortality, it has proven to be cumbersome both socially and economically (Rosamond *et al*., 2008)

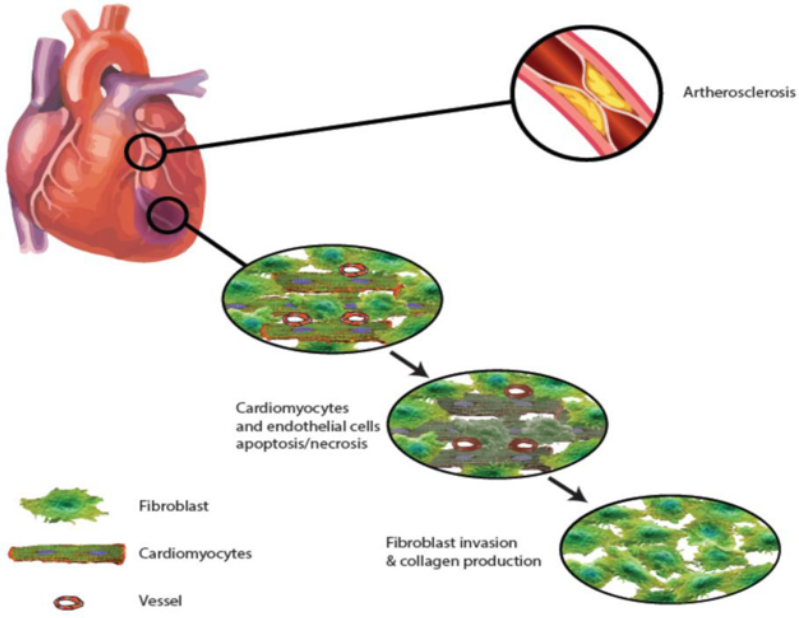

Figure 1.1 Schematic representation of myocardial infarction leading to cardiomyocytes and vasculature replacement by fibroblasts. Following coronary artery disease by arteriosclerosis, blood flow to the heart muscle is jeopardized, and tissue death occurs. The cardiomyocytes in that region soon enter apoptosis and necrosis. The surrounding fibroblasts invade the necrotic tissues and produce large areas of avascular scar tissue resulting in contractile dysfunction.

Cardiovascular disease and in particular heart failure (HF) causes great burden to patients, families and our healthcare and social service budgets. The damaged myocardium has very limited regenerative and repair capacity so that loss of cardiac function is often chronic, progressive and the leading cause of death worldwide (Moorman *et al.*, 2007). Heart transplantation is to date the treatment of choice for advanced HF, but remains limited due to the number of organ donors available (Zimmermann *et al.,* 2004). HF is most commonly caused by myocardial infarction (MI) which leads to the loss of billions of cardiomyocytes and endothelial cells within hours (Lohse et al., 2003, Eschenhagen et al., 2015, Cardin et al., 2003). Since the heart's regenerative capacity is almost entirely lost soon after birth, the apoptotic/necrotic cardiomyocytes and endothelial cells are slowly replaced by fibrotic tissues leading to severe myocardial dysfunction (Yamamizu et al., 2017, Moretti et al., 2006, Kattman et al., 2006). Therefore, strategies to repopulate the defective myocardium with

healthy mature myocytes have generated considerable excitement. However, to date, the concomitant replacement of subtype specific cardiomyocytes has been relatively neglected and other counterpart cells such as endothelial cells might help improve transplantation studies (Yamamizu et al., 2017, Moretti et al., 2006, Kattman et al., 2006).

Without prior re-vascularization, replacement of cardiomyocytes in a low oxygenated, poor in nutrients tissue environment may lead to inadequate engraftment or successive loss of engrafted cardiomyocytes (Yang et al., 2015). This might partially explain the failure of multiple pre-clinical and clinical trials. Moreover, endothelial cells provide key signals that direct vasculoprotective and acute differentiation signals. This is why, I propose here to develop a strategy for cellular therapeutics addressing cell type specificity (atrial, ventricular and nodal cardiomyocytes as well as endothelial cells), combining current strategies in maturing subtype specificity that will help augment some of the limitations we see in therapeutic strategies.

Signaling Mechanisms in the adult heart

A comprehensive series of molecular signaling cascades are thought to be involved in health and disease of an adult heart cell. An important class of signal transduction pathway receptors are the seven-transmembrane helix receptors (7TM). These receptors have 7 α-helices that span the membrane in snake-like fashion and therefore, may also be referred to as serpentine receptors (Lewis et al., 2012). Primary messengers such as hormones, neurotransmitters, or synthetic drugs can bind to the pocket from the extracellular side of the receptor in some cases and the 7TM receptor can have additional protein domains attached on the intracellular side. In the case of the epinephrine signal transduction pathway, the agonist binds on to a 7TM receptor called the β-Adrenergic Receptor (β-AR). The β-AR receptor contains a heterotrimeric domain on the intracellular side consisting of an α,β and ɣ domains

(Lewis et al., 2012). The α-domain is a G protein because it binds guanyl nucleotides. When epinephrine is not bound, the G protein binds guanosine disphosphate (GDP). This keeps the trimeric domain intact and attached to the 7TM domain (Lewis et al., 2012).

Upon binding, the epinephrine induces conformational changes in the 7TM that stimulates the G protein to release GDP and bind GTP. This also causes the β and ɣ –dimer to dissociate from the Gα protein. A single epinephrine molecule can cause many G proteins to exchange GTP for GDP which creates an amplified effect. The Gα domain in the GTP state moves and binds to another transmembrane protein called adenylate cyclase. It stimulates the adenylate cyclase to begin transforming ATP to cAMP. The cAMP molecules are secondary messengers. Since many are formed, this leads to a second level of amplification. cAMP then goes on and stimulates the activation of protein kinase A (PKA). PKA goes on to phosphorylate target molecules, which activates many different processes (Graham et al., 2001).

Within the adult heart, stimulation of adrenergic signaling pathways target a number of Ca^{2+} homeostatic proteins which in turn regulate gene transcription. There is a body of evidence suggesting that β-adrenergic stimulation activates Ca^{2+}/calmodulin-dependent protein kinase II (CaMKII). β-adrenergic signaling is important to consider as it is the major physiological means for the regulation of cardiac inotropy and chronotropy. Sympathetic nerve endings and β-adrenoceptors are widely distributed in the heart. β-adrenoceptors are G-Protein Coupled Receptors (GPCRs) that contain 7 transmembrane spanning domains and couple to heterotrimeric GTP-binding proteins (with α and βγ subunits); in the case of the β_1-adrenoceptor it is G_s (stimulatory) while β_2-adrenoceptors couple to G_s and G_i (inhibitory) and β_3-adrenoceptors are coupled to G_i to produce a negative inotropic effect that is dependent on nitric oxide (NO) (Gauthier et al., 1998). When β_1-adrenoceptors are activated

by agonists, bound GDP is exchanged for GTP and the $G\alpha_s$ subunit is activated and remains so until it hydrolyses the GTP. $G\alpha_s$ dissociates from $\beta\gamma$ and activates ACs to produce cAMP. The cAMP then binds to and activates PKA, which then phosphorylates LTCCs, PLB, TnI and possibly RyRs to produce an increase in the force of contraction and in the rate of relaxation. In addition to these effects on atrial and ventricular myocytes, β-adrenergic signaling will increase heart rate by direct actions on SAN pacemaker cells. The increase in cAMP in SAN myocytes will increase the amplitude of the hyperpolarisation activated inward current I_f that contributes to the diastolic depolarization (DiFrancesco, 1986). In addition, it will increase Ca^{2+} transient amplitude by increasing the amount of Ca^{2+} stored in the SR and the amount of Ca^{2+} entry. This may have additional stimulatory effects on pacemaker rate (Yang et al., 2002; Lakatta et al., 2003; Maltsev et al., 2004; Bogdanov et al., 2006).

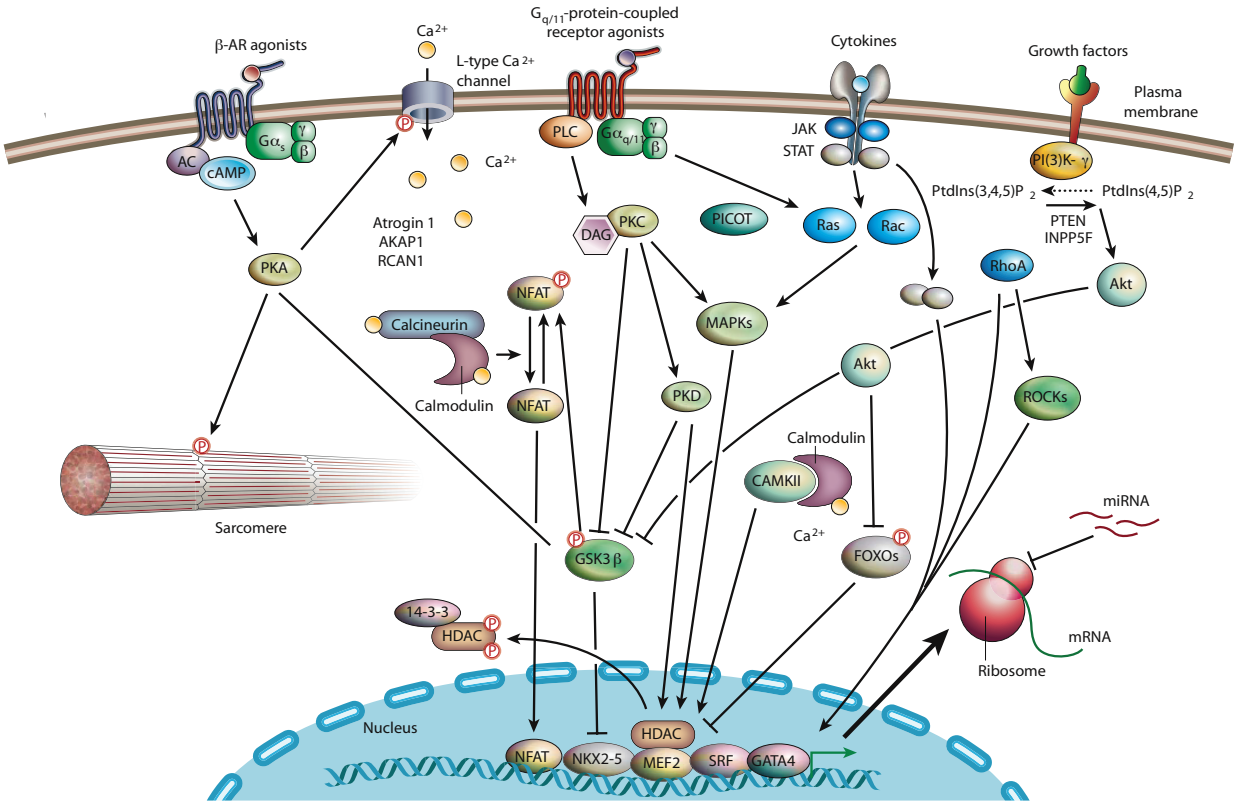

Figure 1.2: Cardiomyocyte signaling mechanisms. Adapted from (Mudd and Kass, 2008) Engaging intracellular signaling cascades ultimately result in changes in cardiomyocyte function and viability. Stimuli include neurohormones (such as natriuretic peptides and angiotensin II), β-adrenergic receptors (β-ARs), cytokines and growth factors.

Ca^{2+} as an intracellular messenger

The ability of a cell to react to extracellular stimuli is an essential characteristic for the coordination of a multi-cellular organism. The cell membrane is a relatively impermeable barrier to ions and solutes. As a result, proteins have evolved which respond to extracellular stimuli to produce a change inside a cell. The transduction of the extracellular stimuli into an intracellular change often occurs via the production of 'second messengers'. Ca^{2+} (Ca^{2+}) is a ubiquitous cellular messenger that is involved in a diverse array of cellular processes including fertilisation, transcription, muscle contraction and apoptosis (Ringer, 1883; Miyazaki et al., 1993; Dolmetsch et al., 1998; Szalai et al., 1999). Ca^{2+} is a divalent cation that interacts with a wide range of proteins in a cell, often through the activation of calmodulin (CaM). As a result

of its many signaling roles, the level of free Ca^{2+} in the cytosol of a cell is tightly controlled by various ATPases, exchangers and channels. The majority of the Ca^{2+} inside a cell is stored in the endoplasmic reticulum (ER), an organelle that is responsible for protein folding, though the mitochondria and lysosomes are also potential Ca^{2+} stores. Ca^{2+} can be released from the ER and other intracellular Ca^{2+} stores by the actions of second messenger molecules.

The heart as a pump

The heart is a synchronised muscular pump that serves to circulate blood around the body so that every cell in the body is supplied with nutrients and oxygen and so that waste products can be removed for excretion. The hearts of amphibians and mammals operate in a double circulatory system where the heart is separated into two pumps. As a result, the right side collects deoxygenated blood from the body and pumps it to the lungs (pulmonary circulation) while the left side pumps oxygenated blood to the body (systemic circulation). The main advantage of a double circulatory system is that it allows blood to be pumped to the body at a higher pressure than if it always had to pass through the lungs. The heart has two phases during each pumping cycle and these are termed diastole and systole. During diastole, the heart is relaxed and is refilled with blood. During systole, the heart contracts in a coordinated fashion that results in the ejection of blood into the arteries. The coordination of the contraction-relaxation cycle is achieved using electrical signals. The major pacemaker region of the heart is the sino-atrial node (SAN) and this is where the electrical signal that initiates contraction originates. The signal initially spreads throughout the atria so that they contract and complete the re-filling of the ventricles. The electrical signal is unable to pass directly from the atria to the ventricles, as there is a region of electrically insulating tissue between them. Instead, there is a specific conduction pathway that conveys the electrical impulse from the atria to the ventricles. The first key component of the conduction pathway is the atrio-ventricular node (AVN). The primary function of the AVN is to delay the impulse from the atria by

approximately 100 ms to allow the atria to contract before the ventricles. After the AVN, impulses pass through the bundle of His to the Purkinje fibres, which transmit the stimulus to the apex of the heart. This ensures that contraction of the ventricles begins at the apex so that blood is pushed towards the exit vessels. The wave of excitation spreads between myocytes through gap junctions that electrically connect cells of the heart so that the whole organ functions as an electrical syncytium.

Cardiac muscle

Cardiac muscle appears striated when observed under a light microscope due to the alternating presence of thick and thin contractile filaments. The thin filaments consist predominantly of actin, with associated troponin and tropomyosin, and are located at the I-bands as well as extending to the H-bands while the thick filaments consist of myosin located in the A-bands. Ventricular myocytes contain a large number of T-tubules, which are invaginations of the cell surface membrane that run along the Z-discs. The presence of T-tubules has been shown using membrane stains such as Di-8-ANEPPS or using scanning ion conductance microscopy (Glukhov *et al.*, 2015). The presence of T-tubules allows a homogenous rise in the intracellular level of Ca^{2+} when the cells are electrically stimulated. Atrial and SA nodal myocytes generally do not have T-tubules and so the rise in intracellular Ca^{2+} in them occurs initially at the cell surface before it propagates through to the center of the myocytes (Glukhov *et al.*, 2015) . The nuclei of cardiac cells are most frequently found towards the center of the cell while other organelles are concentrated at each pole of the nucleus. This mitochondria-rich region is also characterized by its relative lack of contractile filaments and in atrial myocytes also contains a very extensive Golgi system that is important for the storage and release of atrial natriuretic peptide. The presence of a large number of mitochondria is important for ensuring that the majority of energy production that occurs in the heart is based on aerobic respiration.

Cardiovascular Development

The heart is one of the first organs that develop in early fetal life (Christoffels and Pu, 2013) Starting soon after gastrulation, an early differentiating pool of precursor cells called the first heart field (FHF) forms the initial heart tube (Brade *et al.*, 2013) . In later stages, cells from FHF contribute to the left ventricle. Other precursor cells from bilateral pools called the second heart field (SHF) are late differentiating cells. They migrate symmetrically to the embryo midline adding cells to the tubular heart, which then elongates, loops and expands to distinct regions (Brade *et al*., 2013). The second heart field contributes to the inflow tract, outflow tract, atrial chambers and the right ventricle. While both SHF and FHF cell lineages are marked by expression of the Nkx2.5 transcription factor gene, it was found that the Isl1 gene is expressed only in SHF and Hcn4 expression marks the FHF population (Liang *et al.*, 2013) . A third heart field precursor population that is Tbx18+ has been found to form the sinus node. After distinct regions become distinguishable, "ballooning" of the ventricle and atrial chambers occur, followed by septation. This marks the point at which the heart is fully functional to propel separated systemic and pulmonary blood flows (Franco *et al.*, 2014) .

Embryonic and induced pluripotent stem cells

Until recently, the study of human cardiovascular disease has been limited by the lack of accessibility to sub-type specific human cardiomyocytes (CMs) for *in-vitro* testing (Takahashi and Yamanaka, 2006). Embryonic stem cells (ES) are cells that are derived from totipotent cells of the early mammalian embryo which primarily consist of two cardinal properties. The first of which is the unlimited proliferation potential of undifferentiated cells. The second property is that they consist of cells which can be coaxed to give rise to any of

the cell types found in the embryo proper. Historically, stem cells can be allocated to three subtypes: embryonic stem cells which are derived from the inner cell mass of blastocyst-stage embryos, induced pluripotent stem cells which are derived from adult somatic cells via reprogramming techniques, and lastly adult stem cells, which primarily come from adult tissues that contain stem cell niches.

ES cells, quintessentially are the classical stem cell archetype which can differentiate into all cell types in the body, including diverse sets of neurons, cardiomyocytes and pancreatic β-cells (Bradley *et al.*, 1984, Stubbs *et al.*, 2011). This allows scientists the fundamental framework to uncover possible therapeutics in order to improve quality of life as well as reduce pain from disease. Monumental work came out of Sir Martin Evans laboratory where he first reported isolation of mouse embryonic stem cells in 1981(Evans and Kaufman, 1981). The advent of mouse ES cells allowed researchers for the first time to investigate developmental questions by establishing genetically modified mice which is quite elegantly displayed in Rudolf Jaenisch's work (Jaenisch, 1988) and subsequently through Capecchi in 1989 (Capecchi, 1989).

Induced pluripotent stem cells

The creation of induced pluripotent stem cells (iPSCs) which were first derived almost 10 years ago (Takahashi and Yamanaka, 2006) has transformed our approach in accessing early fate decisions in a methodical manner for applications in target, disease and translational biology. Derivation of stable iPSC lines by viral transduction of fibroblasts is a slow (4-6 weeks) and inefficient (<.01%) process. Current methods of identifying colonies of bona fide iPSCs early in the reprogramming process (2–3 weeks post-infection) utilize light microscopy and manual isolation of candidate colonies, which requires training and expertise in advanced cell culture techniques. To enable future clinical applications requiring *de novo* iPSC

derivation, there remains a need for standardized and validated methods for isolating and purifying reprogrammed cells. Previous imaging studies based on tracking of cell-of-origin suggest that early events occur during defined factor reprogramming, including a change in cell proliferation rates and morphology (Terrenoire et al., 2013), downregulation of CD13, a marker of mesenchymal cells including fibroblasts (Kahler et al., 2013), as well as upregulation of the cell surface markers of pluripotency SSEA4 and TRA-1-60 (Kahler et al., 2013). These studies demonstrate that both partially and fully reprogrammed iPSCs can be identified by combined use of surface expression of multiple markers. Recently, a method of enriching reprogrammed fibroblasts by fluorescence activated cell sorting (FACS) for cells with dual expression of the pluripotency surface markers SSEA4 and TRA-1-81 arising late during reprogramming was described (Kahler et al., 2013). While a step forward, this method relies heavily on the use of a defined small molecule cocktail, and multiple rounds of sorting and extensive screening to identify fully reprogrammed clones. This suggests that pluripotency markers alone are not sufficient to purify fully reprogrammed iPSCs. Additionally, it is likely that the high variability among clones seen within this population is compounded by the use of integrating vectors to deliver the reprogramming factors. We are also beginning to address this limitation, through the ability of these cells to be differentiated in to functional cardiomyocytes *in vitro*. Furthering this, the ability to create CMs from iPSCs has enabled the study of human heart disease from patient specific samples to aid in disease modeling, drug development, and assessment of drug toxicity (Carlsson, 2006). The ability to produce large quantities of CMs from pluripotent stem cells has opened up the possibility of creating functional cardiac tissues to replace damaged myocardium (Carlsson, 2006). Given this great potential for disease modelling and regenerative medicine, subtype specific derivation of CMs is an important first step to harnessing the full potential of human pluripotent stem cells (hPSCs).

Cardiac disease modeling using iPSCs

Several cardiac diseases have been successfully modeled using patient specific human iPSCs (Moretti et al., 2006, Moretti et al., 2010, Hinson et al., 2015) and have been used for small-scale drug screening purposes (Liang et al., 2012). As of 2017, the likelihood of approval for cardiovascular drugs transitioning from phase 1 to phase 2 clinical trials stands at 8.7% (Hay *et al*., 2014). A major concern for drug safety is the possibility of life threatening toxicity presented by off target drug effects (Zeevi-Levin *et al*., 2012, Doherty *et al*., 2015). In order to prevent the risk of cardiotoxicity the Federal Drug Administration now requires newly developed drugs to undergo early in-vitro screening for any known cardiac risks (Fermini *et al*., 2016). A major concern for new compounds in development is the inhibition of the potassium channel I_{KR} (hERG) which, when blocked, may induce prolonged QT intervals subsequently inducing arrhythmias; in response, new assays, taking advantage of human iPSCs are currently being developed to specifically monitor hERG activity with new compounds of interest (Fermini *et al.,* 2016). Although only in limited studies, iPSC-CMs have been shown to successfully recapitulate *in vitro* drug effects consistent with clinical responses observed (Peters *et al.,* 2015). Nevertheless, these studies are limited to small numbers of cell lines from the same manufacturers who often use strategies such as engineering selectable markers to enhance CM purity and yield. However, such selection strategies do not currently scale well when manufacturing genetically distinct patient specific CMs in a high throughput manner (Burridge *et al*., 2014, Guan *et al*., 2015, Yang *et al*., 2015). As we now have the ability to produce large numbers of human iPSCs from genetically diverse populations (Kahler *et al*., 2013, Paull *et al*., 2015), the platforming and optimizing of differentiation protocols will broaden our modeling capability. This can be achieved by differentiating multiple cell lines in parallel, thus allowing genetically diverse studies to be performed *in vitro.*

Whilst primary cultures are a powerful tool for screening, there is a limitation of supply and consistency of CMs (Kahler *et al*., 2013, Paull *et al*., 2015). For example, replenishing the number of cells lost after a myocardial infarction would require a substantial number of cells, measured in the billions (Murry *et al*., 2006, Chong *et al*., 2014, Peters *et al*., 2015). For this purpose, cells would have to be expanded and differentiated in an efficient manner in order for this approach to be obtainable and economically feasible. Scaling automated production would address the demand for the increased throughput of subtype specific CMs required for research in regenerative medicine (Lundy *et al*., 2014, Shiba *et al*., 2012).

Atrial Fibrillation

Atrial fibrillation (AF), is the most common sustained arrhythmia, affecting nearly 1% of the population (Savio-Galimberti and Darbar, 2014). The manifestation of AF is the association of an irregular pulse, associated with heterogeneous atrial activity and first described in 1827 by Robert Adams. The first known recording of atrial fibrillation was recorded when William Einthoven invented the electrocardiography (ECG) (Sheng *et al*., 2014). The advent of the Framingham Heart Study (FHS) further exemplified the need to perform extensive community based studies that linked AF to pathogenesis, risk factors (RF) and clinical outcomes of the disorder.

In general, AF is characterized by a high-frequency excitation of the atrium that results in both dyssynchronous atrial contraction and irregularity of ventricular excitation. Other abnormalities affecting atrial cardiomyocytes include arrhythmogenic right ventricular cardiomyopathy(ARVC) which is one of the most common cardiac arrhythmia in clinical practice and can occur as a result of abnormalities of generation or conduction of electrical impulse. More specifically, ARVC is an inherited muscle disease associated with a higher risk of arrhythmias and sudden cardiac death (Yap and Liew, 2014). The disease manifests as

an autosomal dominant inherited disease, although recessive subtypes have been observed (Marcus *et al.*, 2010, Lodder and Rizzo, 2012) . Mutations in genes coding for desmosomal proteins, including desmoplakin, plakoglobin, plakophilin 2 (PKP 2), desmoglein 2, and desmocollin 2, have been identified in a significant number of patients. The clinical presentation of ARVC varies widely; diagnosis is often complex and involves structural, histological, electrocardiographic, arrhythmic, and genetic tests for the disease (Marcus *et al.*, 2010) . Studies from Huie-Sheng Vincent Chen's group indicated dysregulation of calcium-handling properties in the ventricular myocytes population. They found that compared to baseline Ca^{2+} expression in normal human embryonic stem cell lines, mutant iPSC-CMs demonstrated slower intracellular calcium. Comparing expression levels via qRT-PCR showed that relevant Ca^{2+} modulators e.g. SERCA were down regulated. They postulated that further mechanistic studies were required in order to determine the role of Ca^{2+} handling deficits in mediating pathogenesis of arrhythmias (Kim *et al.*, 2013) .

Atrial cardiomyocytes in the pathogenesis of rhythm disorders

Essentially the impetus to derive atrial cardiomyocytes began with interests in disorders that constitute an abnormal arrhythmic state. As such, ectopic activity, which is the generation of electrical impulses outside the SA node can trigger the AF state and maintain it. Abnormalities of electrical impulse conduction can be related to several factors. For example, heart failure (HF) is another common condition associated with AF, in which atrial myocytes were shown to remodel such that atrial tissue at the macroscopic level have increased fibrosis and reduced contractility, therefore greater chance of non-coordinated contraction of the atria (Anter *et al.*, 2009) . AF is not immediately a life-threatening disease. However, stagnation of the blood in the atria during fibrillation might lead to formation of thrombus. Hence, thromboembolism is a significant complication, and more than 15% of all strokes occur in patients with AF (Lubitz *et al.*, 2010, Reiffel, 2014) . Also, during the period of high blood

demand, absence of coordinated atrial mechanical function will affect the volume of blood propelled into the ventricles. Consequently, the blood pumping capacity of the heart might be reduced by a third (Bootman *et al.*, 2011) . In several studies, atrial myocytes were found to have abnormal expression of proteins involved in Ca^{2+} signaling. Therefore, it's believed that calcium-signaling dysregulation is a main factor in the progression and maintenance of AF. In normal cardiac physiology, electrical stimulation of an action potential opens fast-activating voltage-gated sodium channels (Na-v 1.5) followed by L-type voltage-operated Ca^{2+} channels (VOCCs). Ca^{2+} flows into the cell activating ryanodine receptors type-2 (RyR2) of the sarcoplasmic reticulum (SR) leading to Ca^{2+} –induced Ca^{2+} release (CICR) and initation of cardiac myocytes contraction (Fearnley, Roderick *et al*. 2011). Eventually, to restore resting (diastolic) levels, Ca^{2+} is re-sequestered into SR by the action of SERCA (sarcoplasmic and endoplasmic reticulum Ca^{2+} ATPase), and extruded from the myocyte across the sarcolemma by the sodium– Ca^{2+} exchanger (NCX) and sarcolemma Ca^{2+} ATPase (PMCA) (Fearnley *et al.*, 2011) .Several studies also have shed the light on the genetic factors contributing to development of AF. Mutations in genes encoding ion channels were identified and may be contributing to development and course of the disease (Lubitz *et al.*, 2010) .

Current treatment plans for AF include several interventions. Thromboembolism is a major risk for AF patients; therefore, the anticoagulant drug warfarin is usually prescribed to reduce risk of developing strokes. Ventricular rhythm and rate control represents another major goal in AF treatment strategies. It can be achieved by pharmaceuticals that work to slow the heart rate. However, atrioventricular nodal ablation and pacemaker placement were found to be more effective than medications in controlling ventricular rate (Lubitz, Benjamin *et al*. 2010). A third consideration for AF treatment is controlling the SA node rhythm. Pharmaceuticals that alter the electrical properties of cardiac cells are used to maintain sinus rate but they have major side effects such as ventricular proarrhythmia and extra-cardiac

toxicity. Furthermore, in some cases these drugs might be ineffective (Ames and Stevenson, 2006). Other interventions include catheter ablation to burn the abnormal area where the spontaneous firings of action potentials occur. Pharmacological agents are commonly used to control symptoms and reoccurrence of AF including β-Adrenergic blockers, angiotensin converting enzyme inhibitors and angiotensin receptor blockers (Prystowsky, Benson *et al*. 1996).

Current treatments for cardiovascular diseases are lacking

Most of our current knowledge of Cardiovascular Disorders and cardiac function in patients with cardiovascular disease has been obtained from post-mortem tissues that often represent the end stage of the disease (Cardin et al., 2003). The inability to sample live cardiac tissue inhibits our ability to understand the cardiovascular pathology over the course of the disease. Animal models can mimic genetic forms of human cardiovascular diseases, and our understanding of the mechanisms of neurological disease has been significantly advanced by transgenic and knockout animal models. However, this approach is limited to monogenetic disorders and thus only represents a minority of diseases. Additionally, in many cases of cardiovascular disorders with a defined causal gene, modeling with animal transgenic technology is inadequate due to species differences, genetic backgrounds or other challenges. Importantly, numerous candidate drugs with promise in models have failed when translated to human clinical trials. Combined, this indicates that complementary human models are needed to accurately study cardiovascular disorders (Hayashi et al., 2017).

Adult stem cells and reprogramming to cardiomyocytes

Stem cells are unspecialized cells with potentially unlimited proliferation attributes (self-renewal) and the capacity to differentiate into specialized cell types (Takahashi and Yamanaka, 2006). These cells, though, can be further classified into subtypes of stem cells

according to how many specialized cell types they can differentiate into, often called their "potency" or "differentiation potential" from "totipotent" in the fertilized egg, cells specialize along embryo development and only "multipotent", "oligopotent" and "unipotent" cells can be found in adults. These adult stem cells, however, all maintain the property of self-renewal and a certain differentiation capacity. The feasibility of cell therapy has been investigated in several of these adult stem cell populations. First reported in 1999, adult stem cells such as bone marrow mesenchymal stem cells (BM-MSCs), for which the possibility of autologous stem cell isolation has long been known, were shown to be reprogrammable into cardiomyocytes (CMs) (Pittenger *et al.*, 1999). Since that time, colossal efforts have been made to employ MSCs (in particular BM-MSCs) in heart failure clinical application, and there was a focus on improving in vitro or in vivo differentiation of MSCs into CMs. Thus, the use of bone marrow cells (BMCs) for treating myocardial infarction and heart failure have been reported in a large number of clinical trials. However, conflicting results, limited in vitro and in vivo reprogramming of human MSCs into CMs and the limited clinical benefits obtained, have led to research on other adult stem cell types such as cardiac stem cells (Hayashi *et al*., 2017).

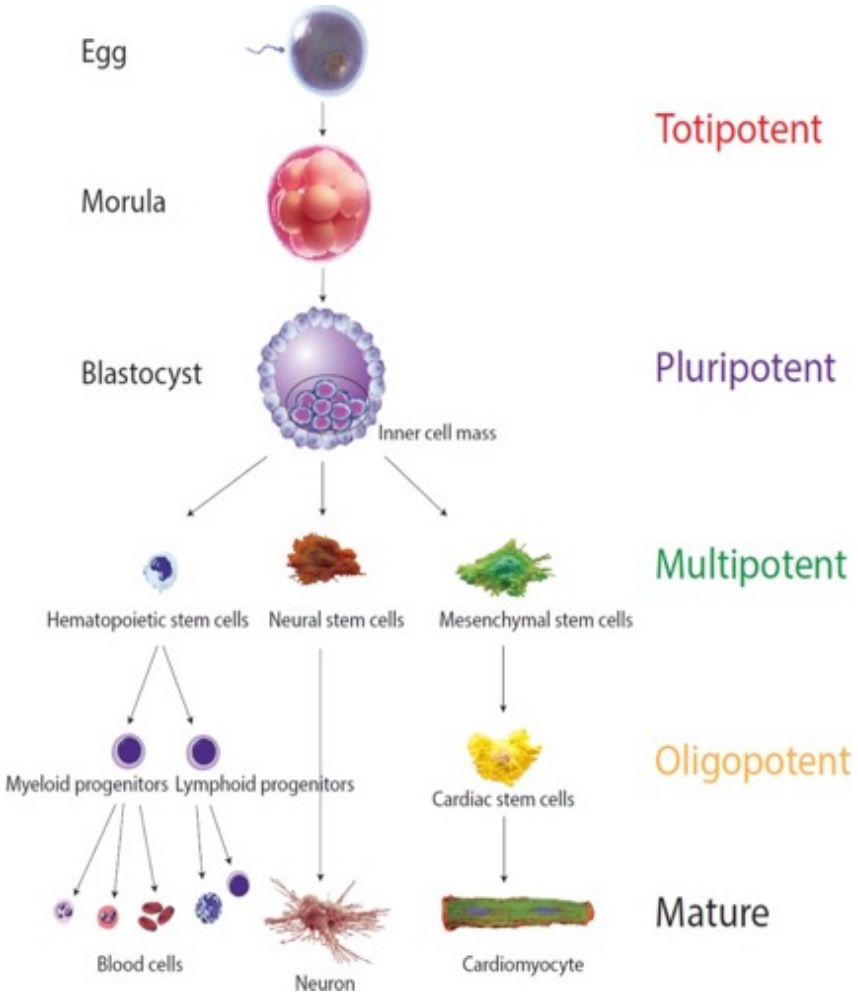

Figure 1.3 Different cells' "potency". The "potency" of a cell is defined by the number of cell types it has the capacity to differentiate into. The fertilized egg is "totipotent", cells having the potential to develop into an entire organism and therefore possesses the totality of potentials. This totipotent cell will divide in human for 4 days retaining this full capacity until a blastocyst develops, where these cells acquire some specialization. The cells from the inner cell mass cannot develop anymore into an entire organism, as they are unable to form the placenta but can still differentiate into all cell types within the organism. They are therefore qualified as "pluripotent". Pluripotent cells will further multiply and acquire more specialization. The resulting "multipotent" cells retain the capacity to differentiate into various cell types. They are already specialized into ectoderm, endoderm or mesoderm. Finally, cells are considered "oligopotent" when they can only differentiate into very limited cell types. (adapted from (Raynaud *et al.*, 2015))

Within the heart, different populations of cardiac stem cells (CSCs) have been extensively described and isolated based on extracellular marker expression or isolation processes. We can quote five main types of CSCs: cardiac c-kit$^+$ cells (defined by Lin$^-$ c-kit$^+$ markers), cardiac Sca-1$^+$ progenitor cells (defined by Sca-1 expression), side-population

cells (defined by their capacity to efflux Hoechst dye when analyzed in flow cytometry), cardio sphere-derived cells (CDCs) (defined by their capacity to form a sphere by tissue explanting technology) and genetically engineered cells such as Isl1-expressing cells. Among these five CSCs type described, only two populations of CSCs (c-kit$^+$ and CDCs) have been escalated to phase I clinical trials, yet the clinical benefit following implantation of the c-kit$^+$ CSCs has been challenged recently (Raynaud *et al.*, 2015). The outcomes of these trials at phase I only delineate the safety and tolerability of transplantation of those cells but present limitations on understanding the benefits for patients means that further clinical trials will be approached cautiously.

ES/iPS-CMs offer an opportunity for in vitro screens on human tissue

Successful derivation of induced pluripotent stem cells (iPSCs) from patient skin fibroblasts provides an opportunity to model the pathogenesis and treatment of human heritable diseases in cell culture. Cardinal work by Shinya Yamanaka for the first time demonstrated that somatic cells could be reprogrammed into an embryonic-like, pluripotent state by the forced expression of a defined set of transcription factors (Takahashi and Yamanaka, 2006). Yamanaka's elegant experiments utilized somatic cells which were subjected to ectopic expression of 24 genes active in embryonic stem cells. They showed that four genes/factors – Oct4, Sox2, Klf4, and c-Myc collectively stochastically reprogrammed a small percentage of cells into a pluripotent stem cell state.

Potential of cardiomyocytes derived from human pluripotent stem cells

As discussed, AF and related arrhythmias are complex disorders in which multiple factors play different roles among affected individuals. These conditions present a big challenge to develop new therapeutic strategies that are safe and effective. Animal models tremendously helped in understanding disease mechanisms and development of new treatment approaches. However, these approaches remain limited in recapitulating physiology and

disease pathophysiology in humans. Furthermore, toxicity of pharmaceuticals is a major concern in clinical research and trials. However, studies have shown that only up to 63% of toxic effects on humans can be predicted using animal models (Olson *et al.*, 2000) .

Since the generation of human induced pluripotent stem cells (hiPSCs), evidently it has become a major tool in the advancement of personalized medicine. Along with human embryonic stem cells (hESCs), hiPSCs can be directed to differentiate into specific lineages including cardiomyocytes. Thus, disease-specific, as well as patient-specific, cell models can be derived from hiPSCs. This enables scientists to study disease molecular mechanisms and perform drug screening. Several protocols for differentiation of human pluripotent stem cells (hESCs and hiPSCs) towards cardiac fate are published (Jiang, Han et al. 2012, Lian, Zhang et al. 2013)). These protocols report successful derivation of beating cardiac-like cells with variable efficiencies, reaching up to 98% functional cardiomyocytes (Lian, Zhang et al. 2013). Differentiation protocols usually yield a mixture of cardiac myocyte subtypes including ventricular, atrial and nodal cell lineages. However, as a tool for transplantation therapy and drug screening analysis, purified populations of subtype specific cardiac cells are critically needed. For example, to be used for cell transplantation in the left ventricle after myocardial infarction, it's essential to use ventricular-like cardiomyocytes. Likewise, to study mechanisms of nodal and atrial dysregulation disorders and perform cardio-toxicity and drug screening, nodal and atrial cells are fundamentally needed, respectively. Therefore, development of methodologies to generate pure populations of specialized cardiac cells would be a major advance in clinical research and personalized medicine. A study from Laflamme's group has investigated the effect of the NRG-1β/ErbB signaling pathway on the abundance of cardiac subtypes in differentiating hESC cardiomyocytes (hESC-CMs). They found that ~ 80% of differentiating hESC-CMs are ventricular and atrial subtype, while nodal cells constituted ~20%. Treatment of exogenous NRG-1β increased expression of atrial/ventricular genes, along

with an increasing percentage of atrial and ventricular myocytes in the differentiating hESC-CMs. On the other hand, with inhibition of the NRG-1β/ErbB signaling pathway there was an increase in the percentage of nodal-like cardiomyocytes (Zhu, Xie *et al*. 2010).

Another study from Jalife's group has employed the use of a selection marker (GFP) sub-cloning under the control of chamber-specific gene promoters to enrich and purify lineage-specific hiPSCs-CMs. They chose promoters of human ventricular and atrial myosin light chain genes, MLC2v and MLC2a, respectively. After generation of adenoviruses carrying the shuttle vector, hiPSC-CMs were infected, purified using fluorescence-activated cell sorting (FACS), and their biochemical and electrophysiological properties were analyzed. Their results demonstrated that MLC2v and MLC2a promoters can be used to purify and enrich ventricular and atrial cell populations, which were stable in culture and expressed chamber-specific transcription factors and contractile proteins. However, ventricular-like population that was purified using the MLC-2v promoter was more homogenous than the atrial-like population. This might be attributed to expression of MLC-2a in both atrial and ventricular cells early in the differentiation stages. As ventricular myocytes become more specialized, MLC2-a expression is down regulated while MLC2-v is up-regulated and restricted to this subtype of cardiac myocytes (Bizy, Guerrero-Serna et al. 2013).

Differentiation of cardiomyocytes with atrial fate

Atria and ventricles myocytes display differential expression of genes that serves as the basis for their structural, electrophysiological and contractile distinct properties. Important structural genes were found to be expressed in a chamber-specific manner. For example, the previously mentioned MLC-2a isoform is a protein responsible for cardiac sarcomere formation and is important in contractile function of the atrial myocytes.

Based on evidence from both developmental studies in animals as well as tissue culture, indications of a role for retinoic acid (RA) signaling in atrial specification has been recently explored (Devalla *et al.*, 2015) . Building on this, Tanwar and colleagues published studies utilizing mouse development (Tanwar *et al.*, 2014) , and deciphered transcription factor based studies which were more effective in targeting of atrial specific gene transcription. By modulating gene transcriptional activation or repression we hypothesize that in human cells, we can initiate atrial specification via incorporation of Grem2 and RA signaling to drive generation of atrial cardiomyocytes.

Until last year, there existed no known protocols for the successful derivation of purified populations of atrial cardiomyocytes. Most protocols that attempt to derive cardiac cells from hESCs/hiPSCs, yield cells biased towards ventricular myocytes. Differentiation paradigms continue to use cell-based systems where the conditions are undefined. We hope to improve differentiation of human pluripotent stem cells towards atrial cardiomyocytes via temporal regulation of WNT and BMP signaling to drive specification of cardiomyocytes towards an atrial phenotype.

Previous directed differentiation studies from Prof. Gordon Keller and colleagues identified ways to direct differentiation towards cardiomyocytes with high frequency albeit these were 3D embryoid body formations (Yang *et al*., 2008). More recent studies describe a novel, rapid, feeder cell-free cardiac induction paradigm in which ventricular cells are induced in less than 2 weeks (Lian *et al*., 2012) . This defined protocol enables, for the first time, systematic assessment of the molecular steps in early human cardiac induction and identification of the critical regulators of atrial/ventricular/nodal specification. Evidence for the “default” cardiomyocytes specification has been gathered by many labs, however the role of this in specification of atrial fates has not yet been fully assessed.

Combining advances in differentiation techniques in the context of a disease model looking at atrial cardiomyocytes and their role in arrhythmogenic perturbations have been largely unsuccessful. We hope to bring together our expertise in pluripotent stem cell biology, disease modeling, and pharmacological testing in order to create a more accurate representation of normal and disease mechanisms to decipher how we will eradicate cardiovascular diseases.

Alternative approaches: nuclear transfer embryonic stem cells

Somatic cell nuclear transfer embryonic stem cells (SCNT-ESCs) are cells that are obtained by substituting the oocyte genome with a somatic cell donor genome. Once artificially activated, embryonic development begins. As the embryo reaches the blastocyst stage, and as is typical in embryonic stem cell derivation, the inner cell mass gives rise to patient-specific pluripotent stem cells. This method involves various chemicals such as caffeine, fetal bovine serum, puromycin, kinase inhibitor 6-DMAP, HDAC inhibitor scriptaid, and Ca^{2+} depletion, which all intersect at different stages during development of SCNT-ESCs.

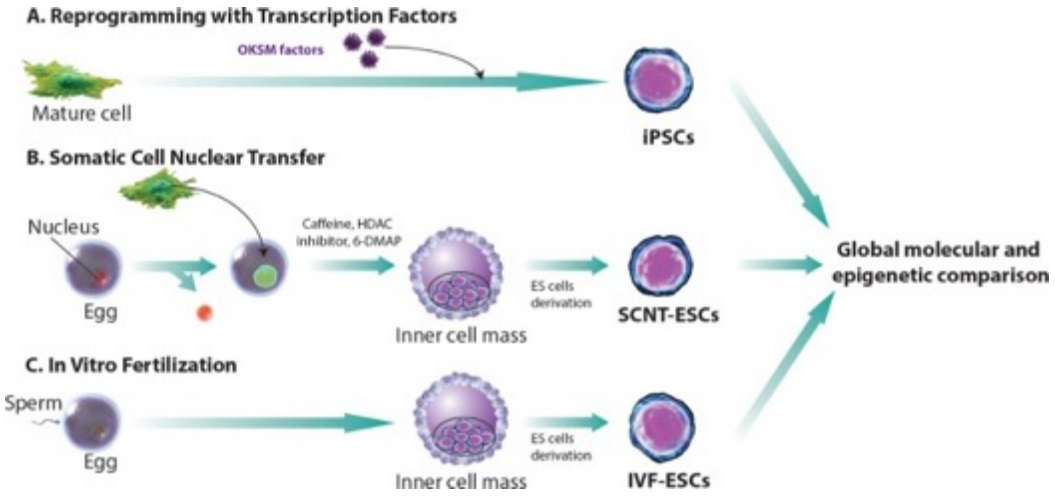

Figure 1.4 Comparing techniques for generating stem cells. There are three distinct ways to derive pluripotent stem cells*in vitro*. (A) iPS cell derivation is achieved via conversion of somatic cells with the addition of a cocktail of transcription factors, originally described as "Yamanaka factors". (B) tradtional embryonic stem cell derivation can be augmented by replacing the nucleus of an egg with a nucleus from a somatic cell at an early stage, as the cells mature and form the blastocyst. The inner cell mass (ICM) is isolated to form Nuclear Transfer embryonic stem (NT ES) cells. (C) *in vitro* fertilization is performed and ES cells are derived when reaching the blastocyst level to obtain IVF-ESCs (adapted from(Raynaud *et al.*, 2015) .

Given the recent successes in the derivation of patient-specific pluripotent stem cells via somatic cell nuclear transfer, groups have begun to decipher the epigenetic differences at the mechanistic level between SCNT-ES and iPSCs. Understanding the molecular determinants for these two cell types should further elucidate methodologies that will improve current limitations of pluripotent cell derivation for both *in vitro* disease modeling and cellular replacement strategies. Ma *et al.* performed this much-needed comprehensive experiment that profiles the molecular characteristics of iPSCs and SCNT-ESCs. These experiments compared and contrasted iPSCs, SCNT-ESCs and *in vitro* fertilization (IVF) produced ESCs. They demonstrated that iPSCs derived with transcription factor-based methodologies displayed inadequate epigenetic reprogramming. While the same somatic cells derived via SCNT were epigenetically and transcriptionally similar to control IVF-ESCs, there is residual DNA methylation in cells derived by transcription factor-based reprogramming. It is interesting to note that genome-wide microarray-based DNA

methylation techniques demonstrated that iPSCs, at a frequency eightfold higher than SCNT-ESCs, contain somatic patterns of CpG methylation, which is consistent with previous studies demonstrating that iPSCs retain an "epigenetic memory" of the somatic cells they are derived from. Hence, SCNT-ESCs are better at retuning genomics of reprogramming more faithfully than iPSCs. Taken together, these subsequent data highlight the importance of investing more in studies that will lend insight into improving current reprogramming paradigms. Methodologies of reprogramming will have to take into account reprogramming factors upstream of pluripotency. One place to look in order to identify possible strategies will be the ooplasm which may possibly contain processes that demethylate the somatic genome more faithfully compared with the more subdued or passive demethylation process during transcription factor-based reprogramming. In any case, the development of hiPSCs has emerged as a promising source of PSCs for tissue engineering, cell-based therapies, novel drug screening, and disease modeling. The drastic improvement of hiPSCs reprogramming has reduced the time and cost of iPSCs generation and has fostered even more the enthusiasm toward PSCs use in cellular therapy. Beside the improvement of hiPSCs generation, major improvements have been made in the differentiation, purification, and maturation of iPSCs derived CMs, precluding iPSCs cardiac clinical use.

Future challenges

After the first retinal cells derived from iPSCs were transplanted into a woman with eye disease in early 2014(Kamao *et al.*, 2014), reprogramming into iPSCs before differentiation into CMs seems to be the most advanced area of research for cardiac cellular therapy. However, many problems remain to be addressed before that stage can be reached with cardiomyocytes. Firstly, even if differentiation efficiency has been achieved recently, the purification of genetically unmodified cardiomyocytes needs to be worked out. Even if

teratoma formation encountered with PSCs is avoided and a time gain is anticipated, the path remains long before application of PSCs becomes a clinical reality for cardiac injuries. The cell maturity prior to implantation definitely needs to be improved. The potential immune-rejection of cells, even autologous, needs to be further studied and anticipated. Beyond these main points, an optimization of cell delivery with potential tissue engineering and scaffolds has to be addressed, as this could affect the maturity, the engraftment capacity, the electro-mechanical coupling and the survival of the cells. Nevertheless, the subsequent milestones achieved over the past decades make PSC clinical use for cardiac regeneration more promising than ever, and efforts should be pursued in that direction.

As exciting as direct reprogramming is, this approach could be even more challenging. When considered for primary *in vitro* differentiation before cell-based therapy, one might consider that differentiation of PSCs into CMs is a more advanced field. The same hurdles encountered with PSC derived CMs will have to be ruled out before clinical translation of directly reprogrammed cells can be envisioned. Besides, even at the *in vitro* level, it remains difficult to compare the various TF cocktails reported and future work should attempt to compare those cocktails side by side. Also, despite successful expression of cardiac markers, not all studies could demonstrate functionality of the iCMs and the focus should now be on functionality (analyzing spontaneous contractility or induced action potential measurements) rather than on single gene expression. Similarly, characterization of iCM subtype (atrial, ventricular or nodal) and their maturity needs to be addressed and fine-tuned. The efficiency of differentiation also remains to be improved in order to reach clinical levels and close the gap with PSCs differentiation efficiency. The possibility of an *in situ* direct reprogramming represents an exciting blueprint for this technique. Even if some of the drawbacks previously discussed were avoided, a large number remain. Besides, in contrast to problems encountered in gene therapies, other efforts need to be made to optimize

direct reprogramming before any treatment can be envisioned. Indeed, the first lesson from mice models could be that the cocktail of TFs used in the human context might need to be validated and consolidated for humans. In lieu of mouse studies, human reprogramming towards CMs has been less straightforward. Successful direct reprogramming of human cells had initially been discovered to make functionally immature neurons with lower efficiencies than in mouse. Therefore, it seems that human cells are typically more resistant and require activation of innate immunity for efficient reprogramming. It is prudent to speculate that human reprogramming requires more acute control of regulatory elements to convert cells towards a different cell fate lineage. Early larger mammalian animal models would deliver more certainty regarding the validity of this approach in humans. Finally, specific delivery of TFs needs to be optimized and validated for clinical use by drug dosing and toxicology testing. Optimization of the promoter used (allowing for the gene expression to be turned off after differentiation) also needs to be performed, and similar to PSCs derived CMs cell-based therapy, the maturity of the cells achieved *in situ* needs to be validated.

CHAPTER 2: METHODS

Isolation of fibroblasts from patients with cardiovascular disorder

Dermal fibroblasts were obtained from five patients with different types of cardiovascular mutations through skin biopsy. Each of the samples were taken before the study, and written informed consent of the parents/guardian of patients was obtained for the identifiable samples per the protocol approved by the Internal Research Board (IRB) of Oxford University. The types of demographic data collected were age, date of birth, and the mutation, if known.

Cell Culture

Human cardiovascular and control fibroblasts were maintained in DMEM medium supplemented with 10% fetal bovine serum (FBS) and penicillin/streptomycin at 37°C with 5% CO_2. All fibroblast samples were tested for mycoplasma while positive GAN fibroblasts (GAN1 and 3) were treated with Plasmocin (1:5000, InvivoGen) for two weeks, and they were then re-tested after a week in antibiotic-free media to determine whether they were cleared of the infection. GAN and control iPSCs were maintained on irradiated mouse embryonic fibroblasts (MEFs) in HuESM (DMEM/F12 supplemented with 20% knockout serum replacement (KSR), non-essential amino acid (NEAA), L-glutamine, β-mercaptoethanol (BME) and 20 ng/mL of basic fibroblast growth factor (bFGF)). Under sterile standards, the media was changed every 24 hours and lines were passaged using dispase (Gibco, 1 mg/mL in HuESM for 30 minutes at 37°C).

Characterization of derived iPSC lines

iPSC lines were fully characterized by a. immunostaining, b. qPCR, c. tri-lineage differentiation d. teratoma essay e. karyotyping as follows:

a. Immunostaining was used to determine if iPSC express pluripotency markers. iPSC were grown onto irradiated mouse embryonic feeder cells and maintained undifferentiated in

serum-free media supplemented with 20% serum replacement (Invitrogen) and 4ng/ml human FGF2 (R&D). Cells were fixed in 4% PFA, cell membranes permeabilized and non-specific staining inhibited by treatment with a blocking solution (Dako). Cells were incubated with primary antibodies against Klf4, Nanog, Oct4, Sox2, SSEA-4 and c-myc, then washed and incubated with the appropriate secondary antibody and DAPI to counterstain the nuclei. For confocal microscopy, slides were analyzed with a Zeiss confocal microscope Laser Scanning Microscope 710 (Carl Zeiss). Pictures were analyzed with Zen 2008 V5,0,0228 software (Carl Zeiss).

b. qPCR analysis was used to confirm expression of the endogenous genes Oct4, Sox2, Klf4 and c-myc and simultaneous silencing of the 4 exogenous (retroviral or sendai virus) factors in each of the iPSC clones using published primers (Takahashi, Tanabe et al. 2007). Cells were collected and total RNA will be isolated (Qiagen). cDNA was generated using reverse transcription and qPCR was performed using cybergreen mix (Applied Biosystem), with results normalized to the level of a housekeeping gene, HPRT. Expression of the endogenous genes were compared to gene expression in hESCs, the gold standard of pluripotency. Moreover, I validated that the retrovirus expression for the 4 factors were largely silenced, demonstrating successful reprogramming. Initial analysis confirmed endogenous expression of the pluripotency genes and silencing of the transgenes in two iPSC clones.

c. Tri-lineage differentiation in vitro was used to demonstrate functionality. Bona fide pluripotent stem cells are able to give rise to all three germ layers: endoderm, ectoderm and mesoderm. Prior to differentiation, iPSCs were feeder-depleted by passaging onto matrigel. We used established protocols for tri-lineage differentiation based on two commonly used methods: the formation of three-dimensional aggregates called embryoid bodies (EBs) or culture of cell monolayers on extracellular matrix. To generate EBs, iPSC were dissociated into small clusters of 10-20 cells, and then plated in low attachment plates with the appropriate

differentiation media: Endoderm - serum-free media supplemented with 100ng/ml activin A for 5 days. Around D5, we saw that greater than 90% of the cells were c-kit^{+} CXCR4^{+} (detected by FACS analysis), demonstrating efficient induction of definitive endoderm. Mesoderm - StemPro-34 media (Invitrogen) supplemented with activin A, BMP4, bFGF, VEGF and the Wnt inhibitor DKK1. Around D6, I visualized detection by FACS analysis the emergence of 3 distinct cell populations, with the c-kit^{neg} KDR^{low} population signaling the beginning of cardiovascular differentiation. Ectoderm - induction will be done in monolayers in serum-free medium supplemented with Noggin and SB431542 for 11 days. We saw that at D11 greater than 80% of the cells will express Pax6, a marker of neural differentiation.

d. The teratoma assay is considered the definitive proof of bona fide iPSCs. Tri-lineage differentiation in vivo was obtained by injecting around 1 million iPSC into an immunocompromised mouse, typically sub-cutaneous. Around 6-8 weeks later, teratomas are removed and histological analysis is performed to show the presence of tissues from the 3 germ layers. A human nuclear marker was used to confirm the human nature of the tumor.

e. Karyotype analysis will be performed for bona fide iPSC clones. I sent cells to Cell Line Genetics to perform karyotyping using standard protocols.

Generation of iCMs from pluripotent stem cells

I obtained highly pure cultures of CM cells from iPSCs by combining the use of Noggin (a BMP4 inhibitor) and SB431542 (a TGF inhibitor) to drive mesoderm induction(Chambers, Fasano et al. 2009), However, the addition of activin A to improve CM yield (Corneo and Temple 2009). But the recent publication of sequential treatment of hPSCs with chemical inhibitors of Wnt signaling produced a high yield of virtually (up to 98%) pure functional human cardiomyocytesis is the most attractive procedure, and was used in this thesis (Lian, Hsiao et al. 2012). A summary of the protocol is given below (from Lian et al. 2012)

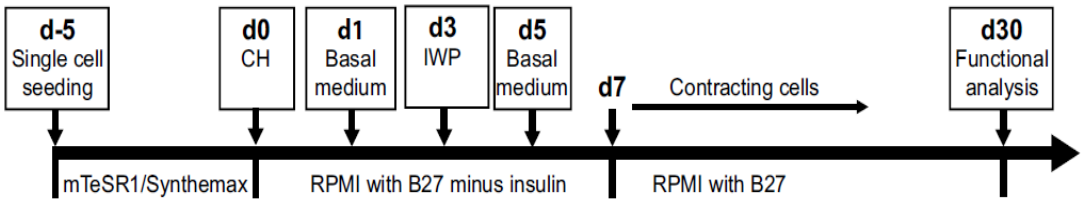

Schematic: Protocol of cardiomyocyte differentiation of iPSCs using Wnt signaling targeting molecules.

Colonies with characteristic CM morphology and polarization appear at day 25 and grow to form a highly enriched CM monolayer. Further maturation of the iCMs were performed prior to characterisation as previously published by our collaborators using scaffolds that will be provided by Dr. Adrian Chester's group (Rao, Prodromakis et al. 2013).

Analysis of expression of transcription factors and cardiac proteins

Validation and proteins expression level were determined by flow cytometry, confocal microscopy, western blot and q-PCR.

a. For flow analysis of intracellular markers staining of cardiomyocyte, BD cytofix/cytoperm kit (BD biosciences, #554722) was used according to manufacturer recommendations. The following primary antibodies were used: Anti-heavy chain cardiac Myosin antibody (abcam, # ab15), Anti-Nkx2.5 (abcam, # ab91196), Anti-alpha smooth muscle Actin (abcam, # ab7817), Anti-NCX1 (Abcam, # ab2869), anti-MRCL3 (Novus, # NBP1-44423), Anti-CTNI (R&D system, #MAB6887), anti-CTNT (abcam, # ab8295), anti-mesp1 (Abcam #77013). Secondary antibody from Invitrogen (goat anti-mouse IgG1-AF546, # A-21123; IgG2a-AF546, # A-21133; IgG2b-AF488, # A-21141) was used. Controls were performed omitting the primary antibody and applying only the secondary antibody. Anti-

GATA4-AF647 (BD Biosciences #550257) was used without secondary antibody. Briefly, 1.106 cells were harvested and non-specific sites will be blocked in PBS- 5%FBS-1%BSA-10%FcR Blocking Reagent (Myltenyi Biotec) for 30 minutes on ice. Cell suspensions were permeabilised with cytofix cytoperm for 30 min cells were incubated with specific antibodies for 1h on ice. Cells were washed in wash buffer and incubated with secondary antibody for 45 minutes. After washes in PBS and filtration on 45um strainer, cells will be analyzed by Fluorescence Activated Cell Sorting (FACS) on a SORP FACSAria3 (BD Biosciences). Data was processed with FACSDiva 7.1 software (BD Biosciences). Doublets were excluded by FSC-W x FSC-H and SSC-W x SSC-H analysis, single stained channels were used for compensation, and fluorophore minus one (FMO) controls were used for gating, 100,000 events were acquired per sample.

b. Western blot was performed as previously published.

c. Cells will be grown in 8 chamber slides under appropriate conditions. Cells will be fixed and stained using BD cytofix/cytoperm kit according to manufacturer recommendations. Slides were incubated with primary antibodies (previously described) 1h to overnight, followed by 1h of secondary antibody staining (as previously described). The same equipment presented in 3.a. was used.

d. PCR/q-PCR was used to assess the expression of the GOI and of cardiac proteins to determine the differentiation efficiency of fibroblast. RNA extraction: reverse transcription was performed using Qiagen RNA easy extraction kit following the manufacturer instructions with some modifications. Reverse transcription to create a cDNA bank: Applied biosystems High capacity RNA to cDNA kit (4387406)

Functional analysis

Following the first step of treatment optimization and characterization of resulting cardiomyocytes, a characterization of the level of maturity of the cardiomyocytes was performed, using transcriptomic analysis, flow cytometry, western blot and electrophysiological measurements.

a. Flow cytometry and western blot was performed as previously described using MLC2a (abcam #ab68086) and MLC2v (Novus #NBP1-0754) isoform directed antibody.

b. All transcriptomic analysis was performed in the department of pharmacology at the University of Oxford. RNA was isolated as previously described with RNA yields that produce satisfactory microarray data. Two quality control measures were carried out: (1) A spectrophotometric analysis (2) A size fractionation procedure using a microfluidics instrument (Agilent Technologies). 200ng of total RNA were analyzed on Affymetrix GeneChip Human Genome U133 Plus 2.0 Array. Data were analyzed using Partek Software (V6.09.1110-6; Affimetrix), Venny online software (BioinfoGP; CNB-CSIC) and Ingenuity Pathway analysis (Ingenuity Systems, Redwood City, CA.

c. Class comparison between primary cell, iPSCs, and iCMs (three biological replicates of each) was performed to identify gene expression changes with a significant expression differences ($P < 0.05$) and 2 fold increases or decrease expression. Commercially available human cardiomyocytes were also analyzed as reference (Celprogen #36044-15).

I used Ingenuity Pathway Analysis software to identify and analyze relevant pathways from the gene lists obtained after comparison of 2 different cell lines. Networks were constructed by overlaying the genes in the gene list onto a global molecular network developed from information contained in the Ingenuity Pathways. Knowledge database using keywords such as cardiomyocyte or cardiogenesis. Networks of the genes up- or down-regulated will then be algorithmically generated based on their connectivity. A network is a graphical representation

of the molecular relationships between genes. Genes were represented as nodes, and the biological relationship between two nodes is represented as a line. All edges are supported by at least one reference from the literature, from a textbook, or from canonical information stored in the Ingenuity Pathways knowledge database. P values for the enrichment of canonical pathways will then be generated based on the hypergeometric distribution and calculated with the right-tailed Fisher's exact t-test for 2 × 2 contingency tables.

d. As previously described (Terracciano, Harding et al. 2003), action potential (AP) measurements will be performed using an Axoclamp 2B system (Axon Instruments). High resistance microelectrodes were used (15e25 MU) (Harvard Apparatus). Cells superfused with 37 C Normal Tyrode's (NT) solution containing; 140mM NaCl, 6mM KCl,1mM MgCl2, 1 mM CaCl2, 10 mM glucose, 10 mM HEPES adjusted to pH 7.4 with 2 M NaOH (All Sigma Aldrich); and the microelectrode filling solution contained; 2 M KCl, 0.1 mM EGTA, 5 mM HEPES adjusted to pH 7.2 with 2 M NaOH (All SigmaeAldrich). Action potentials were recorded in current clamp mode and measured AP were analysed using pCLAMP 10.3 software (Molecular Devices).

e. Measurement of Ca2+ transients were performed as previously published (Rao, Prodromakis et al. 2013). Briefly, iPSC-CM were loaded with 20 mM Fluo-4 acetoxymethyl ester (Invitrogen) using 8 ml (250 nM) probenecid (Invitrogen) and 0.2% pluronic acid (Invitrogen), in 2 ml pre-warmed DMEM (Invitrogen) at 37C for 30 min. The myocytes were then be washed and incubated with pre-warmed DMEM containing 2% FBS (Invitrogen) and 250 nM probenecid for 30 min to de-esterify. The experimental dish was mounted on the stage of an upright Zeiss LSM710 confocal microscope (Carl Zeiss) and myocytes observed through a x40 water immersion objective. Line scanning was performed at suitable regions with the myocytes spontaneously beating or under field stimulation at 0.5 Hz, 1 Hz using an external pacing generator. During recording the cells super fused with 37C NT or Na^{+} and Ca^{2+} free

solution containing: 140 mM LiCl, 6 mM KOH, 1 mM MgCl2, 10 mM glucose, 10 mM HEPES, 0.1 mM EGTA adjusted to pH 7.4 with 2 M NaOH (All SigmaeAldrich). 50 mM caffeine (Sigmae Aldrich) will be used for sarcoplasmic reticulum (SR) studies. Linear time length images were converted into Ca^{2+} transients using ImageJ (National Institutes of Health) and analyzed using pCLAMP 10.3. Fluorescent values were normalised to baseline fluorescence (f/f0). tP will be taken as the time taken for the ratio signal to reach peak fluorescence from baseline fluorescence. Similarly, t50 and t90 will be taken as the time taken for the fluorescent transient to decline by 50% and 90% of the transient amplitude respectively (Terracciano, Harding et al. 2003).

Episomal human iPS cell line

The human iPSCs used for the differentiation experiments were provided by Gibco® by Life Technologies, Carslbad, USA. The iPSC line was generated from cord blood-derived CD34+ progenitor cells using a three-plasmid and seven-factor (Oct4, Sox2, Klf4, Myc, Nanog, Lin28 and SV40L T antigen) episomal system.

Matrigel plate coating

Matrigel Matrix (Corning) was stored at -20℃. 5ml of Matrigel was allowed thawing at 4℃ overnight and 0.5ml Matrigel aliquots were prepared on ice. The ready-to-use Matrigel aliquots were stored at -20℃. To coat plates, each aliquot was thawed on ice or at 4℃ for 1 hour. While thawing Matrigel, the 4-, 6-, or 24-well culture plates as well as the pipettes were placed in -20℃ for pre-cooling. The mTeSR™1 (STEMCELL™ Technologies) culture medium was kept cold at 4℃. When Matrigel was fully thawed, it was 1:60 diluted in the cold mTeSR™1 medium to coat the pre-cooled plates. Matrigel diluted in mTeSR™1 medium was added to the wells using the pre-cooled pipettes. For 6-well culture plates, the

coating medium was added 2ml per well and for the 4- and 24-well culture plates, the medium was added 0.5ml per well. Subsequently, the coated plates were stored at 4℃ overnight. Before use, they were incubated at 37℃ for 1h for the Matrigel layer to solidify.

Human iPSCs maintenance and passaging

Episomal Human iPSC Line was cultured on Matrigel-coated six-well culture plates with mTeSR™1 medium. Undifferentiated human iPSCs were maintained with daily medium change. The mTeSR™1 medium was pre-warmed under room temperature every time before medium change. The iPSCs were passaged every 4 to 5 days. An approximately 70% confluence was observed before passaging the cells. For passaging, human iPSCs were treated with 1U/ml Dispase (STEMCELL™ Technologies) at 37℃ for 5-7 min to detach the cells from the Matrigel layer. After three washes with fresh medium, the cells were collected and centrifuged at 800rpm for 4min using HERAEUS MEGAFUGE 8 centrifuge (Thermo Scientific). Then the cells were resuspended in fresh medium and plated in new Matrigel-coated culture plates. The cells were passaged at a 1:3 ratio.

Human iPSC stock preservation

Cell stocks of each passage were prepared in the freezing medium consisting of 40% Knockout Serum Replacement (Gibco® Life Technologies), 50% mTeSR™1 medium and 10% DMSO, and were stored at -80℃. The ready-to-use freezing medium was stored at 4℃ before use. Cells were first treated with 1U/ml Dispase at 37℃ for 5-7 min. After three washes with fresh medium, they were collected and centrifuged at 800rpm for 4min. Then the cells were resuspended in the freezing medium described above and transferred into cryovials. One well (of a 6-well culture plate) of iPSCs were transferred into one cryovial. The cell stocks were preserved at -80℃.

Resuscitation of frozen human iPSC lines

When thawing the frozen human iPSC lines, a frozen cell stock was placed at 37℃ until it was fully thawed. Then the cells were carefully collected and transferred into a tube containing fresh mTeSR™1 medium drop by drop. Next, the cells were centrifuged at 800rpm for 4min and resuspended using fresh mTeSR™1 with 10μM Y-27632 (Cambridge Bioscience). One vial of frozen human iPSCs were plated in one well of a Matrigel-coated 6-well culture plate. After resuscitation, the iPSCs were maintained with daily medium change (fresh mTeSR™1 wi.th 10μM Y-27632) for three days. Afterwards, the cells were cultured with mTeSR™1 medium only.

Purification of human iPSCs

Human iPSCs were purified when spontaneous differentiation was observed. The iPSCs were treated with 1U/ml Dispase at 37℃ for 5-7 min. After three washes with fresh medium, each well of a 6-well culture plate was added with 1ml mTeSR™1 medium. Under the microscope, undifferentiated iPSC colonies were picked with a 200μl pipette tip and transferred into a tube for centrifugation. Then the cells were centrifuged at 800rpm for 4min, resuspended in fresh mTeSR™1 medium and plated in new Matrigel-coated culture plates. The purified iPSC colonies were passaged at a 1:1 ratio.

Differentiation from human iPSCs to cardiomyocytes

The human iPSCs were dissociated into single cells for differentiation experiments. Cells were given a 3-4 min treatment of 1U/ml Dispase at 37℃. After three washes with fresh medium, the cells were then treated with ACCUTASE™ (STEMCELL™ Technologies) at 37˚C for 5-8 min. After the addition of 2-3 volume of fresh mTeSR™1 medium to terminate

the effect of ACCUTASE™, the cells were collected and centrifuged at 800rpm for 4min. Then the iPSCs were plated in Matrigel-coated 4- or 24-well culture plates and maintained daily using mTeSR™1 medium with 10μM Y-27632. Differentiation experiments were performed using PSC Cardiac Differentiation Kit (Gibco® Life Technologies) which contained Cardiac Differentiation Medium A, Cardiac Differentiation Medium B, and Cardiac Maintenance Medium (CMM). When the iPSCs reached an approximately 90% confluence, Medium A with 10μM Y-27632 was added to the plates, and the date of the addition of Medium A was labelled as Differentiation day 0 (Day 0). Medium B with 10μM Y-27632 was applied on Day 2. From Day 4, the cells were cultured with CMM and the medium was changed every other day. All the differentiation and culture media were pre-warmed under room temperature before applying to the cells. The undifferentiated cells were divided into experimental groups and control groups. For experimental groups, Gremlin 2 (R&D Systems; BioVision) was added to the culture medium at the concentration of 1μg/ml on Day 4, and RA (Sigma) was added at 1μM on Day 6 and Day 8. Control groups were differentiated using the same protocol excluding the addition of Gremlin 2 and RA.

RNA isolation

RNA samples were harvested on Day 0, Day 1, Day 3, Day 5, up to Day 15 from both experimental groups and control groups using RLT buffer from RNeasy® Mini Kit (QIAGEN) with 10μl/ml β-mercaptoethanol. The samples were stored at -80℃ and before purification, they were allowed thawing on ice. To purify the samples, 350μl of RLT buffer was used for one well of a 4- or 24-well culture plate. Samples were purified with RNeasy® Mini Kit following the manuals from the manufacturer. In brief, the unpurified samples were mixed with 70% 200 proof ethanol at 1:1 volume ratio and transferred directly into the RNeasy spin columns placed in 2ml collection tubes. After the centrifugation at 10,000rpm for 15s using

Centrifuge 5424R (Eppendorf), the flow-through was discarded. 700µl of Buffer RW1 was added into one column, and after the centrifugation at 10,000rpm for 15s, the flow-through was discarded. Buffer RPE were pre-mixed with 4 volumes of 96-100% ethanol to make working solution. 500µl of Buffer RPE working solution was applied to the samples for twice and the samples were centrifuged at 10,000rpm for 15s and 2min respectively after each RPE application. After disposing the flow-through, the RNeasy spin columns were placed into new 1.5ml collection tubes. Subsequently, 40µl of nuclease free water was added directly to the membrane of each column for RNA elution. The columns were centrifuged again at 10,000rpm for 1min to collect RNA. The RNA concentration of each sample was measured using Nanodrop 2000c (Thermo Scientific).

Reverse transcription

Reverse transcription was carried out with High Capacity RNA-to-cDNA kit (Applied Biosystems by Thermo Fisher Scientific) according to the manufacturer's instructions. The kit was kept in -20℃ and before use, it was allowed thawing on ice. 1µg of RNA was used for a total reaction volume of 20µl. In brief, for each 20µl reaction volume, 10µl of Buffer Mix (containing MuLV and RNase inhibitor protein) and 1µl of Enzyme Mix (containing dNTPs, random octamers and oligo dT-16) were used. 1µg RNA was applied in each qPCR tube, with a maximal volume of 9µl. Nuclease free water was added to the reactions when needed. Then the reverse transcription was performed using the Mastercycler Gradient 5331 (Eppendorf). The reaction program was set to the following: 1h at 37℃, followed by 5min at 95℃ before returning to 4℃. After the reverse transcription, cDNA samples were stored at -20℃.

Quantitative PCR (qPCR)

Gene expressions were analyzed using qPCR. The analyses were carried out for Gremlin 2 protein coding gene (GREM2), cardiac progenitor cell marker (NKX2-5), cardiac troponin coding gene (TNNT2), atrial-specific genes (NPPA, MYL7 and KCNJ5), other inward rectifier potassium channel coding genes (KCNJ4, KCNJ5 and KCNJ12), and adrenergic receptor coding genes (ADRA1A and ADRB1). The qPCR was performed with LightCycler®480 (Roche) using TaqMan® Gene Expression Master Mix (Applied Biosystems by Thermo Fisher Scientific) following the instructions from the manufacturer. The TaqMan® Gene Expression Assays and cDNA samples were stored at -20℃ and before qPCR experiments, they were allowed thawing on ice. A control for cDNA input was generated by amplifying human HPRT1 gene (Applied Biosystems by Life Technologies). In brief, the total volume for each reaction was 20µl, consisting of 10µl of Gene Expression Master Mix, 1µl of Gene Expression Assays, 1µl of human HPRT1 gene, 1µl of cDNA sample and 7µl of RNase-free water. Cycling parameters were set to 2 min at 50℃, followed by 10 minutes at 95℃ , then followed by 40 cycles of 15 seconds at 95℃ and 60 seconds at 60℃. The relative expressions of target genes were determined by comparing the Ct values of target genes with those of the house-keeping gene using -ΔCt method (equation as below). The results from two or three technical replicates were averaged. Four experimental groups were differentiated independently for qPCR experiments (n=4), and parallel analyses were done in two sets of experimental and control groups differentiated simultaneously using the human iPSCs from the same passage. The information of the TaqMan® Gene Expression Assays used in this study is provided in Fig 2.2.

$$\text{Relative expression}(\%) = \frac{\text{Expression of target gene}}{\text{Expression of house} - \text{keeping gene}} = 2^{-\Delta Ct}$$

$$\Delta Ct = Ct_{target} - Ct_{house\text{-}keeping}$$

Table of TaqMan® Gene Expression Assays
Supplied by Applied Biosystems by Thermo Fisher Scientific

Gene	Assay no.	Target species
TNNT2	Hs00943911_m1	Human
NKX2-5	Hs00231763_m1	Human
GREM2	Hs03986140_s1	Human
NPPA	Hs00383231_m1	Human
MYL7	Hs01085598_g1	Human
KCNJ5	Hs00168476_m1	Human
KCNJ4	Hs00705379_s1	Human
KCNJ12	Hs00266926_s1	Human
ADRA1A	Hs00169124_m1	Human
ADRB1	Hs02330048_s1	Human

Cardiomyocyte dissociation

Cardiomyocyte aggregates were dissociated using 100units/ml Collagenase I (Gibco® by Life Technologies). Collagenase I treatment was given to the cardiomyocyte aggregates for 45min at 37℃. After fully pipetted with a 1000µl pipette tip, the cells from one culture well (of a 4- or 24-well culture plate) were transferred directly into a 1.5ml tube and centrifuged at 1200rpm for 2min at 20℃ using Centrifuge 5424R (Eppendorf). The supernatant was discarded and the cells were washed with PBS. 0.05% Trypsin-EDTA (Gibco® by Life Technologies) treatment was applied to the cells for 2min at 37℃. CMM with 10% KnockOut™ Serum Replacement (Gibco® by Life Technologies) was subsequently added to the tube and the cells

were centrifuged at 1200rpm for 2min at 20℃. In order to fully dissociate the aggregates, the cells were pipetted for 5-10 times with a 1000µl pipette tip before each centrifugation. Then the supernatant was discarded and the cells were resuspended in CMM with 10µM Y-27632 and plated in new Matrigel-coated 4-well culture plates with coverslips. The cardiomyocytes were split at a ratio of 1:4 (used for the immunofluorescence analysis Protocol 1) or 1:12 (used for the immunofluorescence analysis Protocol 2 and patch clamp experiments).

Immunofluorescence analysis

The dissociated cardiomyocytes were cultured in CMM with 10µM Y-27632 for 2 days at 37℃. Immunofluorescence analysis of the single cardiomyocytes grown on coverslips were performed using the following protocols.

Protocol 1: The dissociated cardiomyocytes cultured on the coverslips were fixed first with 2% paraformaldehyde (PFA) with 0.1% glutaraldehyde at room temperature for 20min, followed by 0.1% PFA at room temperature for 10min. The cells were then washed for 3 times using 0.3% Triton X-100 in PBS, and permeabilized and blocked from non-specific bindings with the incubation of 0.3% Triton X-100 and 0.1% Bovine Serum Albumin (BSA) (Sigma) in PBS for 20min at room temperature. Next, the cells were incubated overnight at 4℃ with α-actinin primary antibody produced in mouse (Sigma) 1:200 diluted in the solution consisting of 0.3% Triton X-100 and 0.1% BSA in PBS. After the primary antibody incubation, the cells were washed with 0.1% Triton and 0.25% BSA in PBS for three times at room temperature, and incubated for 1h at room temperature with Alexa Fluor® 488 donkey anti mouse secondary antibody (Molecular Probes by Life Technologies) 1:1000 diluted in the solution consisting of 0.1% Triton and 0.25% BSA in PBS. After the secondary antibody incubation, the cells were washed for three times with 0.01% Tween-20 at room temperature. Finally, the coverslips were

transferred onto the slides and the cardiomyocytes were mounted with Prolong™ Gold Antifade Reagent with DAPI (Molecular Probes by Life Technologies). The mounted slides were allowed drying at room temperature for 24h and examined using Leica SP8 Inverted scanning confocal microscope with oil immersion. The immunofluorescence images were analyzed using ImageJ.

Protocol 2: This protocol was applied by the collaborator group from Southwest Medical University in China using the experimental group cardiomyocytes differentiated by me.

The dissociated cardiomyocytes cultured on the coverslips were fixed with 4% PFA for 15 min at room temperature, and were then blocked with 5% BSA for 1h. 0.1% Triton-X100 was used for membrane permeabilization. Then the cardiomyocytes were incubated with 1:100 diluted primary mouse anti-actinin 2 antibody (Boster, Wuhan, China) at 4˚C overnight. After washed with cold PBS, the cardiomyocytes were incubated for 1h at room temperature with DyLight® 488-conjugated donkey anti-mouse secondary antibody at 1:200 dilution (Abcam, Cambridge, UK). Cardiomyocytes were then incubated with Rhodamine phalloidin (Cytoskeleton, USA), an F-actin probe conjugated with red-orange fluorescent dye for 30 min. 5 min incubation of DAPI was used for the staining of cell nuclei. Immunofluorescence-labelled samples were examined using Nikon confocal laser scanning microscope (Tokyo, Japan).

Optical Mapping

Optical mappings were carried out after the cells started to contract. The responsiveness of the derived cardiomyocytes in experimental groups to β- and α- adrenergic receptor agonists and antagonists was measured. Fluo4 was selected as a fluorescence-labelled Ca^{2+} indicator. LED lights were used to illuminate the indicator and the excitation wavelength was set to

488nm. Intracellular Ca^{2+} transients were analyzed using a 128 x 128 EMCCD camera (Photometrics, Tucson, USA). In isoprenaline (ISO) experiment, the derived cardiomyocytes were pre-loaded with Fluo4 (Molecular Probes by Life Technologies) at a concentration of 1μM for 15min at 37˚C. Fluo4 was dissolved in DMSO and diluted with CMM. Ca^{2+} transients of the derived cardiomyocytes were first recorded without the addition of ISO as control. Recordings were then taken at 0min, 5min, 10min and 15min after 100nM ISO treatment. Using the same method, the responsiveness of the derived cardiomyocytes in the experimental group to 10μM phenylephrine (PE) treatment was tested. In adrenergic receptor antagonist tests, the cells were pre-treated with 600nM CGP20712A (CGP) (Sigma) dissolved in Fluo4 loading solution prior to 100nM ISO treatment. Recordings were taken in the same way as described above. Similarly, the cells were pre-treated with 1μM Prazosin dissolved in Fluo4 loading solution before the treatment of 10μM PE. Metamorph was used to take the recordings, and 4000 or 8000 frames were taken for each recording with a frame rate of 100Hz (for 4000 frames) or 333.33Hz (for 8000 frames). Regions of interest were selected using ImageJ. Raw traces were analyzed and baseline corrections were conducted using Clampfit. Raw traces are displayed as F-F0/F0 where F refers to the peak fluorescence intensity and F0 is the baseline fluorescence intensity. Ca^{2+} transient amplitude change was calculated based on averaged trace using the equation below. Four independent experiments were conducted for each treatment condition (n=4).

$$\text{Amplitude change}(\%) = \frac{Amplitude(treatment) - Amplitude(control)}{Amplitude(control)}$$

Electrophysiological analysis

The electrophysiological studies were conducted by the collaborator group from Southwest Medical University in China using experimental group cells differentiated by me.

Action potential recordings of the experimental group cells which were differentiated with Gremlin 2 and RA treatment were obtained by patch clamp under whole-cell configuration using Axon 200B amplifier system (Molecular Devices, USA) in the pipette solution consisting of 136 mmol/L K-aspartate (K-Asp), 5.4mmol/L KCl, 5mmol/L NaCl, 1mmol/L MgCl2, 1mmol/L HEPES, 5mmol/L EGTA, MgATP 5mmol/L and 5mmol/L Phosphocreatine. The pH value of the pipette solution was adjusted to 7.2 with KOH. The bath solution was composed of 136mmol/L NaCl, 5.4mmol/L KCl, 1.0mmol/L MgCl2, 1.8mmol/L CaCl2, 0.33mmol/L NaH2PO4, 5mmol/L HEPES and 10mmol/L Glucose. The pH value of the bath solution was adjusted to 7.4 with NaOH.

Karyotyping

Karyotype analysis was performed by Cell Line Genetics, LLC.

qRT-PCR

The total RNA was isolated using Trizol LS (Invitrogen) with 1 μg being treated with DNase (Invitrogen) and subsequently used o synthesize cDNA with iScript (Bio-Rad). I then performed quantitative RT-PCR using SYBR green (Bio-Rad) and the iCycler system (Bio-rad). Quantitative levels for all genes were normalized to endogenous B2M (for iPSC characterization) or GAPDH (for all other experiments). For pluripotency genes, levels were expressed relative to the levels in human ES line HUES42 whereas for viral genes, they were expressed relative to the levels in HEK293 cells infected with the reprogramming viruses for 2-3 days. I ran standard curves to ensure equal efficiency of all primers. RNA from 293 cells transfected with the plasmids encoding the transgenes were used as a positive control for viral transgene detection. My data was analyzed using the comparative quantitation by the 2-ΔΔCT equation. ΔΔCT = ΔCT (sample) – ΔCT (control), where ΔCT is the threshold cycle (CT) value of the housekeeping gene (B2M or GAPDH) subtracted from the Ct value of the target gene. Expression ratios were generated using the relative expression software tool

(REST) program, a mathematical model based on the PCR efficiencies and the mean crossing point deviation between sample and control groups (Pfaffl et al., 2002). Its also noted that the expression ratios of the 8 investigated transcripts were tested for significance by a randomization test.

Immunocytochemistry

I performed pluripotency marker stains of iPSCs after fixation overnight in 4% paraformaldehyde at 4°C as previously described (Dimos et al., 2008). cardiac cultures were then fixed in 4% PFA for 30 minutes at 4°C, permeabilized and quenched with 0.1-0.2% Triton-X in Wash buffer, PBS and 100mM Glycine (Sigma) for 20 minutes. I blocked these cells in Wash with 10% donkey serum for 30 minutes and then incubated them in primary antibody overnight and secondary antibodies for 1 hour. The primary antibodies used in this study are TRA1-60 (1:500, Chemicon, MAB4360), NANOG (1:500, R&D, AF 1997), OCT3/4 (1:500, Santa Cruz, sc-9081), ISL1 (1:200, DSHB, 40.2D6), HB9 (1:100, DSHB, MNR2 81.5C10-c), MAP2 (1:2,000, Neuromics, CH22103), NF-H (1:2000, Neuromics, CH22104), PRPH (1:500, provided by Dr. Ron Liem), anti-MYC (1:50, DSHB, 9E10-s), anti-GFP (1:5,000, Invitrogen, A11122). Secondary antibodies used were DyLight 488, 549, 647 conjugated (1:500, Jackson ImmunoResearch).

Microscope image acquisition

Images were acquired on an automated Ziess Observer Z1 epi-fluorescence microscope at standard stage positions (12-25 positions per well of a 96-well plate). Objectives used included:

Plan Apo 20X 0.8 DICII and Plan Apo 10X 0.45 DICII. Confocal images were acquired using a Zeiss LSM 510 META with a Plan Apo 100X 1.4 Oil objective. A consistent temperature for image acquisition was 22-24° Celsius. All images were acquired in Wash

buffer or Fluoromount-G (confocal). CoolSNAP HQ2 was the camera used to take these images and were acquired using AxioVision 4.8. Where indicated, the Trophos Platerunner was used to acquire whole-well images from 96-well plates.

Quantitative image analysis

Multi-Wavelength Cell Scoring module in MetaMorph (Molecular Devices) software was used to perform quantitative image analysis of differentiated neuronal cultures. Intensity thresholds were set (blinded to sample identity) to selectively identify positive cells which displayed an unambiguous signal intensity above local background. Each sample was handled with regard to these parameters, and only minimally adjusted for different staining batches as necessary. Script and Parameter files available upon request. I visually identified the cells and measures the average cell body intensity by drawing a region of interest that encompassed the cell body. In order to improve clarity, brightness and contrast of each grayscale channel were adjusted.

Protein isolation and western blot analysis

I isolated and suspended the cells in RIPA lysis buffer supplemented with protease and phosphatase inhibitor cocktail (Roche), triturated and centrifuged at 10,000 g for 15 minutes at 4°C. 1-10 μg of total protein was separated on 10% SDS-polyacrylamide gels. They were then transferred to a nitrocellulose membrane and probed with various primary antibodies, followed by horseradish-peroxidase-conjugated secondary antibody (1,:5000-10,000, for mouse or rabbit primaries respectively, Invitrogen). ECL chemiluminescence (Pierce) was used to visualize them. The primary antibodies used in this study consist of GIG (1:150, a generous gift from Dr. Pascale Bomont), HISH3, (1:500, Millipore, MAB052), PRPH (1:5000, kindly provided by Dr. Ron Liem), NF-L (1:200, Neuromics, MO22104), NF-M (1:200, Sigma, G9670), VIM (1:500, Sigma, V2258), TAU (1:150, DSHB, 5a6), MAP1B-LC (1:4,000, Santa Cruz, H-130), αTUB (1:10,000, Abcam, AB4074). For

quantification, band size and intensities were measured using Image J software. I normalized the values to their respective loading control followed by the control line to generate a fold change. Peripherin signal was undetectable in one WB; for a fold comparison, the HISH3 loading control was used to estimate expression since nIF levels did not vary significantly for the control line between experiments. For viral experiments, the membranes were stripped and re-probed for NF-L. PBS Tween was used to wash the membranes and incubated for 15 min at RT with stripping buffer, followed by 7 minutes at 37 deg. They were then washed again for 1 hour in PBS Tween, blocked, and probed with appropriate secondaries to confirm that the original signal was removed before reprobing.

Differentiation of control iPSCs

First, I had treated all my pluripotent stem cell colonies with dispase with a concentration of 1 mg/mL to separate colonies from feeder cells. They were then washed, triturated to 5-10 cell clumps and seeded in low-adherence dishes in HuESM medium with 20 ng/mL of bFGF, SB431542 (10 μM , SIGMA), LDN193189 (0.2 μM, Stemgent) and Y-27632 (20 μM Ascent) for the first 2 days. On day 3, EBs were switched to a neural induction medium (DMEM/F12 with L-glutamine, NEAA, penicillin/streptomycin, Heparin (2 ug/ml), N2 supplement (Invitrogen), BDNF (10 ng/mL) and Ascorbic acid (0.4 μg/mL) up until day 6. On day 7, RA (1 μM, Sigma), SAG (1 μM, Calibiochem smoothened agonist 1.3) and Purmorphamine (1 μM, Stemgent) were added. At day 17, Neurobasal (Invitrogen) was the new base medium used, along with all previous factors and with an addition of 10 ng/mL each of BDNF, GDNF, and CNTF (R&D) plus B-27 supplement (1:50, Invitrogen). On day 28, EBs were then dissociated with 0.05% trypsin (Invitrogen), and plated onto poly-lysine laminin-coated 96-well plates or 6-well plates at 10,000 or 1 million cells/well, respectively. Plated neuron cultures were cultured in the same medium with the addition of 25 μM

Betamercaptoethanol (Millipore) and 25 μM glutamic acid (Sigma). Where indicated, cell division was inhibited with 5-fluoro-2-deoxyuridine (UFdU, 1 μM, Sigma).

Statistical analysis

All quantitative data was analyzed using Microsoft Excel or GraphPad. I used the Kolmogorov-Smirnov test to compare the probable distribution of the peripherin intensities of GAN. To be able to control motor neurons, an XLSTAT macro in Excel was used. Non-Gaussian sample groups were compared with a Kruskal-Wallis test using GraphPad Software. Student's t test was used where indicated.

Immunocytochemistry of Cardiac Cells

Isolated cardiac cells were plated onto flamed coverslips and left to adhere for 15 min. Cells were first fixed in 4 % paraformaldehyde/PBS for 15 min. In order to dissolve the paraformaldehyde in PBS it was necessary to heat the mixture to 55 °C and to add 10 M NaOH. The paraformaldehyde (PFA)/PBS was then cooled to room temperature before the pH was adjusted to 7.4 with HCl. Once the cells were fixed they were washed in PBS (3 changes, 10 min each) and then permeabilised using the detergent Triton X-100 (0.1 % in PBS, Sigma-Aldrich) for 15 min. After the permeabilisation, the cells were washed in PBS (3 changes, 10 min each), blocked with PBS/10 % normal donkey serum for 60 min at room temperature to reduce non-specific binding. After blocking, the cells were incubated with primary antibodies at 4 °C overnight. The next day, cells were initially washed with PBS (3 changes, 10 min each) before being incubated with secondary antibodies at RT for 60 min (either AlexaFluor 488 or AlexaFluor 555 conjugates) then washed with PBS (3 changes, 10 min each). Finally, the cells were mounted using Vectashield® and permanently sealed. Cells were stored in the dark at 4 °C and visualised within 2 days. For control experiments either the primary or secondary antibody stage was omitted. Observations were carried out using a Leica DMIRB inverted

microscope modified for confocal laser-scanning microscopy (x63 water objective) and Leica TCSNT software or using a Zeiss LSM 510 (x40 oil objective). For detection of AlexaFluor 488, fluorescence excitation was at 488 nm with emission collected >515 nm. An excitation filter of 543 nm and an emission filter at 600 ± 15 nm were used to detect AlexaFluor 555.

Antibody	Supplier	Product Code	Dilution
AC1	Santa Cruz Biotechnology	sc25743	1:200
AC5/6	Santa Cruz Biotechnology	sc25500	1:100
AC8	Santa Cruz Biotechnology	sc32128	1:200
RyR2	Abcam	ab2827	1:400
PLB	Abcam	ab2865	1:200
CaMKII	Abcam	ab52476	1:100
IP_3R1	K. Mikoshiba	KM1112	1:1000
IP_3R2	K. Mikoshiba	KM1083	1:1000
IP_3R3	K. Mikoshiba	KM1082	1:1000

Western Blotting

Tissue for immuno-blotting was homogenized in 0.1 M phosphate buffered saline (PBS) containing protease inhibitors (Roche). Aliquots were stored at -80 °C. Protein concentration was measured using the BCA protein assay. Protein samples were resolved by SDS-PAGE with 50 μg protein per lane, and then transferred to nitrocellulose membrane for immunolabelling in sodium phosphate buffer (20 mM), pH 6.8 for 60 min at 50 V. To ensure that the separated bands of proteins were properly transferred to the nitrocellulose membrane, the membrane was incubated in 0.5 % Ponceau Red 1 % acetic acid for 1 min on the plate rocker to visualise the separated protein bands, and then the dye removed by washing in PBS/Tween-20 (0.5 %). I pre blocked the blots by incubation in blocking buffer (PBS, 5 % non-fat dry milk and 0.5 % Tween-20) overnight at 4 °C. Primary antibodies raised against AC1, AC5 and AC8 were diluted in blocking buffer and applied to the blots overnight at 4 °C or at RT for 60 minutes. I then washed the blots three times at 10 minute intervals in PBS/Tween-20 (0.5 %). The secondary peroxidase-conjugated antibodies (anti-rabbit for AC1 and AC5/6, anti-goat for AC8) were diluted 1:10000 in blocking buffer, and applied to the blot for 60 minutes at RT. Blots were washed in PBS/Tween-20 (0.5 %). Signal detection was carried out with ECL (GE Healthcare) and exposed to Kodak X-Omat L

CHAPTER 3: STUDIES OF IPSC DERIVATION AND CULTURE

3.1 Introduction

Scientific research is propelled by two objectives: understanding and recognizing the essential biology of life, and deciphering this to uncover possible therapeutics in order to improve quality of life as well as relieve pain from disease. Scientists can begin to tackle the above order by exploring fundamental mechanisms in health and disease. Induced pluripotent stem cells (iPSC) and human embryonic stem cells (hESC) provide a unique *in vitro* platform to probe molecular, cellular, and biophysical properties throughout the context of human development. iPSC/hESCs are pluripotent and have the potential to differentiate towards any of the cells within the three germ layers (ectoderm, mesoderm, and endoderm). This then allows us to probe for mechanistic insights hitherto, the process of human development (Thomson, 1998, Yamanka 2007).

Human embryonic development is characterized by distinctive phases. Embryo formation occurs when a sperm reaches the oocyte, and fusion of the gametes occurs which initiates successive cellular division until the fertilized oocyte reaches the morula. The morula undergoes invagination which forms the blastocoel and gives rise to the blastocyst, which is composed of two fundamental components that are fated to give rise to the trophectoderm and the inner cell mass form the body proper. Following the progression into gestation, the inner cell mass (ICM) cells are directed to specific germ fates, and eventually lose their multipotent potential as they mature towards an individual cell fate. ES cells are derived at the early-late blastocyst stage.

Breakthrough technologies emanating from early embryonic development findings from mouse (Evans, 2011) by Sir Martin Evans and Matthew Kaufman isolated a pluripotent stem cell line from haploid mouse embryos (Martin, 1981) by deriving the ICM and using cell culture techniques *in vitro* (Kaufman, 1983). Seminal work from the two groups paved the way for dissecting early developmental cues during human development. Lineage tracing studies

could not be performed during human embryogenesis. The discovery of human embryonic stem cells (Thomson, 1998) came almost two decades later which demonstrated that the ICM, once harvested could give rise to cell lines reminiscent of ES cell properties. **Figure 3.1** is a depiction of an ICM derived ES cell line that can if directed or randomly subjected to differentiation cues give rise to three germ layers that make up the entirety of the embryo proper. This led to a revolutionary approach for directly understanding human development, disease modelling, therapeutic drug discovery, and ultimately the hope and potential of its implications for cellular transplantation.

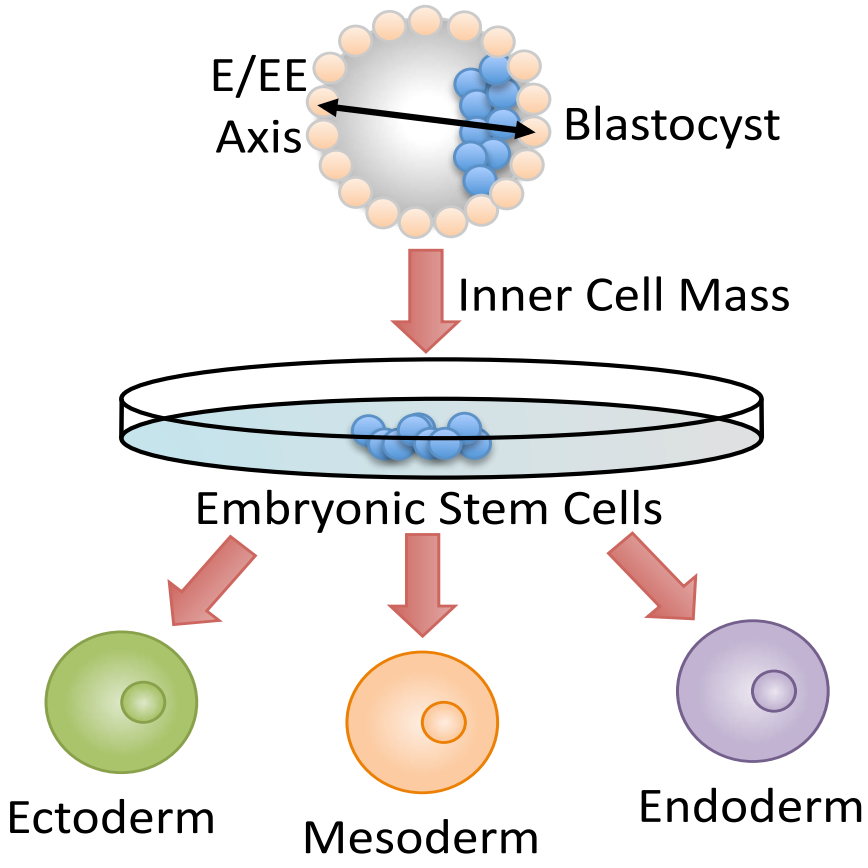

Figure 3.1: Human Embryonic Stem Cells. Blastocyst-stage embryos containing the inner cell mass (ICM) which can be propagated *in vitro*. Once ICM cells are successfully attached on to culture plates they can be expanded and stored. ES cells can then either indirectly or directly give rise to any cell in the human body.

Feeding paradigm for maintaining pluripotency: FGF converges.

How do iPSC/hESCs stay in the permissive stages of pluripotency? As with any entropic condition the state of stem cells is no different. iPSC/hESCs have an entropic disposition to constantly become more defined/differentiated most commonly known as the cells propensity for signaling pathway promiscuity (Banerji *et al*., 2013). A British developmental biologist by the name of Professor Conrad Waddington described this as what is now known as the Waddington landscape, which begins from an inclined plane that leads to various troughs down the valley. Stem cells have been described as the pluripotent cell at the top of the inclined plan that as it progresses down the various troughs is indeed an irreversible process as the cell moves further down and acquires a differentiated state. In order to prevent this differentiation potential, culture conditions have been optimized to circumnavigate differentiation cues via addition of mouse embryonic fibroblasts (MEFs) and supplemented with exogenous FGF2 or basic fibroblast growth factor within the culture medium.

Signaling pathways constituting transforming growth gactor (TGF)/nodal, FGF, and insulin like growth factor (IGF) have been shown to keep pluripotent stem cells in a proliferative and undifferentiated state(Chen *et al.*, 2011) . The amount of FGF proteins discovered to date in mammals exceeds 22 proteins that bind and trigger four tyrosine kinase receptors (Zhang *et al.*, 2006), all of which have distinct functions in tissue and cellular development(Beenken and Mohammadi, 2009). The recombinant protein for human-FGF is produced in *E.Coli* (Miltenyi), can be effectively used to maintain pluripotency and self-renewal of pluripotent stem cells (Akopian *et al.*, 2010). Mechanistically, basic FGF is able to block cellular death pathways through activating PI3 Kinase AKT/PKB (Dailey *et al.*, 2005) whilst activating activin/nodal and nanog (Lanner and Rossant, 2010). Signal transduction leads to stimulation of PLCγ which induces cytoskeletal re-organization, along with kinase activity through FRS2-RAS-MAP kinases to maintain self-renewal and

pluripotency **Figure 3.2**. Pathways downstream of FGF also help dampen transcription of differentiation associated genes. FGF signaling is kept in check by DUSP6/MKP-3, and mediated by ERK1/2 phosphorylation which acts as a negative feedback mechanism (Ekerot *et al.*, 2008). Therefore, ideally iPSC/hESCs cell culture seeks to maintain levels of FGF signaling in order to sustain both anti-apoptotic and pluripotency factors. Withholding FGF in pluripotent stem cell cultures leads to downregulation of FRS2-RAS-MAP kinase and initiates differentiation of these cells towards desired cell fates.

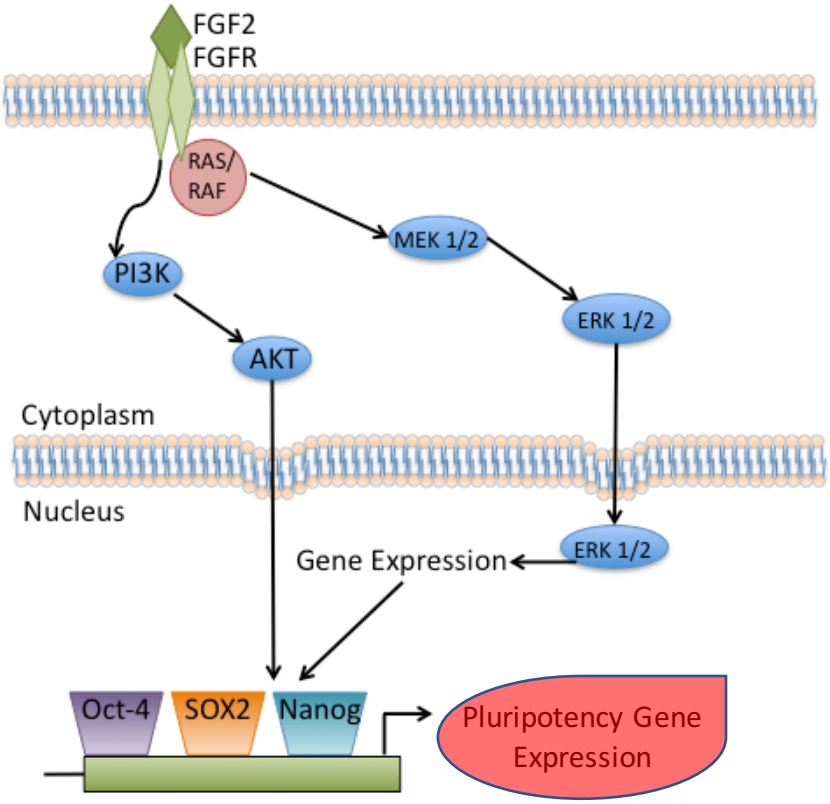

Figure 3.2: Basic FGF signaling mechanism. FGF signaling is critical in cellular proliferation and pluripotency within iPSC/hESCs. FGF binds receptors which in turn activate intracellular PI_3K and RAS/RAF. Pluripotency gene expression is activated by Nanog, Oct4 and Sox2 gene expression. (Adapted from Cell Signaling Technology)

Derivation of iPSC lines

Derivation of stable iPSC lines by viral transduction of dermal fibroblasts is a slow (4–6 weeks) and inefficient (≤0.01%) process. Current methods of identifying colonies of *bona fide* iPSCs early in the reprogramming process (2–3 weeks post-infection) utilize light

microscopy and manual isolation of candidate colonies, which requires training and expertise in advanced cell culture techniques. To enable future clinical applications requiring *de novo* iPSC derivation, there remains a need for standardized and validated methods for isolating and purifying reprogrammed cells. Previous imaging studies based on tracking of cell-of-origin suggest that early events occur during defined factor reprogramming, including a change in cell proliferation rates and morphology, downregulation of CD13, a marker of mesenchymal cells including fibroblasts, as well as upregulation of the cell surface markers of pluripotency SSEA4 and TRA-1-60(Raynaud *et al.*, 2015). These studies demonstrate that both partially and fully reprogrammed iPSCs can be identified by combined use of surface expression of multiple markers. Recently, a method of enriching reprogrammed fibroblasts by fluorescence activated cell sorting (FACS) for cells with dual expression of the pluripotency surface markers SSEA4 and TRA-1-81 arising late during reprogramming was described. While a step forward, this method relies heavily on the use of a defined small molecule cocktail, and multiple rounds of sorting and extensive screening to identify fully reprogrammed clones. This suggests that pluripotency markers alone are not sufficient to purify fully reprogrammed iPSCs. Additionally, it is likely that the high variability among clones seen within this population is compounded by the use of integrating vectors to deliver the reprogramming factors. Here, we confirm that throughout the reprogramming process a significant proportion of SSEA4+TRA-1-60+ cells retain the fibroblast surface marker, CD13. Through the use of negative selection against CD13, we were able to purify fully reprogrammed iPSCs from partially reprogrammed cells by FACS. This method removes contaminating cells at an early stage and can be used with a variety of cell populations including: cells reprogrammed with DNA-integrating or non-integrating viruses; fibroblasts harvested from healthy or specific disease patients.

3.2 Results

Optimizing Culture Conditions using PLGA beads for iPSCs

A major drawback within the cell culture paradigm for human stem cell research is the use of soluble FGF. iPSCs are cultured at 37°C in order to maintain survival. During a 24 hour incubation period if you were to culture cells at 25°C and 4°C mean survival decreases to about 70% (Heng *et al.*, 2006). The caveat to this is that FGF maintains its conformation between those temperatures, however it is significantly degraded at 37°C in part due to the compound's thermal instability (Levenstein *et al.*, 2006). Stem cell biologists have optimized culture conditions to counteract the degradation of FGF by supplementing culture conditions with excess amounts of FGF, upwards to a 100ng/ml dose, which constitutes non-physiological conditions, to maintain stem cell cultures. A drastically 10 fold higher than needed concentration of FGF may provide the necessary requirement to maintain pluripotency, but varying levels of FGF yields concern pertaining to the regulation of differentiation and pluripotency. We hypothesized that fluctuating levels of FGF may affect the on and off pendulum of various genes thought critical for maintaining an optimal culture condition. Hence, I've dedicated part of my work to optimizing culture conditions which I believe will be critical to enhance both derivation of pluripotency and subsequently differentiation of these cells to desired cell fates.

Historically, sustained release of FGF when loaded in microspheres on to rat mesenchymal cells in culture have supported growth (Liang *et al.*, 2012). Liang and colleagues have demonstrated that controlling FGF release along with dexamethasone under physiological (37°C) conditions improved differentiation of rat mesenchymal stem cells. Microspheres that were loaded with FGF showed a 40% retention of 10ng/ml FGF post 5 days at 37°C. Ultimately this showed us that once you load FGF on to microspheres you could provide sustained release of FGF over protracted phases of time. I then postulated that you could potentially treat

pluripotent stem cells with FGF loaded microbeads which would release FGF at physiological levels, thereby providing iPSC culture with adequate and sufficient amounts of FGF for their growth and survival.

Encapsulating FGF2

Controlling release of drug delivery to a particular site has been of paramount importance for the last decade. Researchers have utilized advances in nanotechnology and polymer biology to deliver drugs in controlled regimens. Traditionally, at 37°C under normal cell culture conditions following 24 hours of incubation, FGF degradation falls to levels well below the limit that is required for pluripotency in pluripotent stem(Furue *et al.*, 2008). I used poly-lactic-co-glycolic acid (PLGA) microspheres to load FGF2 and a stabilizing cofactor heparin. Our thought was if we added heparin, this would increase the binding affinity of FGF2 to FGFR(Furue *et al.*, 2008). Drug delivery techniques have required use of biodegradables like PLGA which degrades to lactic acid and glycolic acid and therefore, have extensively been used as a fairly harmless polymer for human-based drug delivery systems(Mohamed and van der Walle, Christopher F, 2008). This method allows me to polymerize PLGA as desired as well as load them with FGF2 and heparin to be used for slow release of pluripotent factor FGF2 in pluripotent stem cell cultures.

Synthesizing FGF on to PLGA Microspheres

Clinical trials have utilized a biocompatible form of PLGA copolymer as the basis for the microspheres (Liang *et al.*, 2012). Figure 3.3A shows PLGA microspheres loaded with FGF2 at a magnification of 400x. These FGF2 loaded microspheres are synthesized by dissolving PLGA in dichloromethane and mixing this dropwise into solution containing poly-vinyl alcohol (PVA). I used heparin in order to increase binding affinity to FGF receptors to aid in pluripotency regulation. Taken together, this was emulsified and stirred gently which

yielded FGF2 loaded microspheres which can be used to treat human stem cell medium (huESM) in order to achieve slow release of FGF2 in to pluripotent cell cultures.

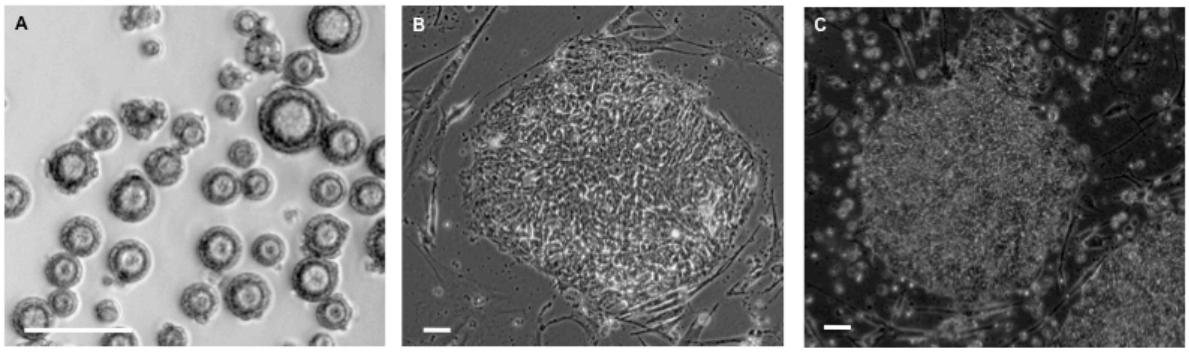

Figure 3.3 Images of FGF2 loaded microspheres and iPSC Colony. FGF2 and heparin loaded microspheres (2M) observed at 400x magnification prior to use as trophic supplement to mTeSR1 (A). Once optimized microspheres generally obtained spherical shape. A pluripotent iPSC colony observed at 100x magnification within mTESR1 (B). iPSC colonies that are highly pluripotent with low spontaneous differentiation have the morphology pictured here. Pluripotent iPSC colonies were also imaged at 100x magnification with mTeSR1 (C). Scale bars represent 10 μm

Stabilizing pluripotency with PLGA microspheres loaded with FGF2 at 37 °C

Cell culture paradigms particularly for pluripotent cells are often quite sensitive to subtle changes. I tested whether FGF2 loaded microspheres could potentially improve culture conditions comparable to FGF2. Therefore, cell cultures of iPSCs were supplemented with either soluble FGF2 or FGF2 loaded microspheres. Figure 3.3B shows iPSCs with the soluble FGF2 and Figure 3.3C shows iPSCs with FGF2 loaded PLGA microspheres. Table 1 describes the two conditions and media samples were taken at differing time periods and were analyzed with BD cytometric bead array (CBA) human basic FGF Flex Set (Invitrogen). The flex set protocol works by binding any available FGF2 in the culture dish to the capture beads and then activates phycoerythrin (PE) reagent.

Table 1: Preliminary Microsphere Feeding Paradigm					
Feeding Schedule:	**Harvest Times (Hours):**				
Every Day (Ctl)	0	4	24	48	72
Microspheres	X	X	24	48	72

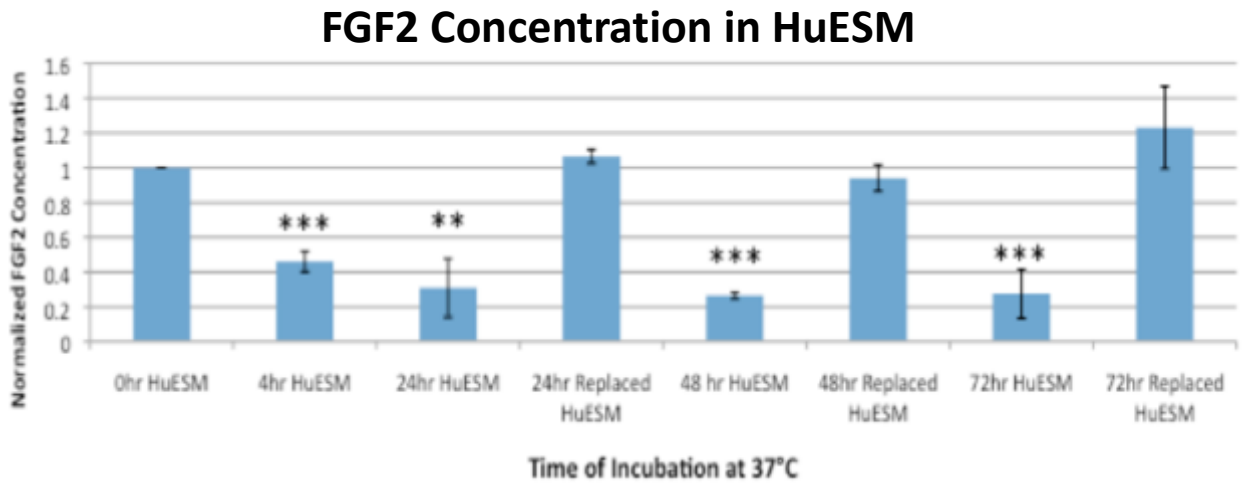

Figure 3.4 Soluble FGF degradation at 37°C. FGF2 concentrations were normalized to 0hr HuESM sample which is 10ng/ml. Student t-test provided statistical significance as *($p<0.05$) ** ($p<0.005$) ***($p<0.0001$). Error bars represent standard error. FGF2 loaded within microspheres is steadily released into HuESM and maintains stable levels in solution.

With this product, any FGF2 that was within the media binds to the Capture Beads and activates the phycoerythrin (PE) detection reagent. Analyzing these Capture Beads with flow cytometry then allows for a quantitative analysis of FGF2 concentration. The concentration of FGF2 was then interpolated within a given sample based upon standard controls. Utilizing the FGF2 BD FlexSet, we observed thermal instability of FGF2 as similarly shown by (Levenstein, 2006) within iPSC culture at 37°C **(Figure 3.4)**. The FGF2 concentration was quantified at 0 hour when fresh media was replaced, 4 hours and 24 hours after 37°C incubation. Then replaced media was quantified at 24 hours as well as overnight and fresh media at 48 hours and 72 hours. While these time points did not allow us to determine distinct kinetics of FGF2 degradation, it allowed us to observe the drastic fluctuations of FGF2 concentration under current protocols (Thomson, 1998). Statistical analysis was performed by applying the student's t-test correlating significant differences in FGF2 concentrations over time relative to

0 hour concentration. With replenishment of fresh mTesR1 every 24 hours, greater than 50% of the soluble FGF2 had degenerated within 4 hours and was nearing 80% by 24 hours. Unlike soluble FGF2 within mTeSR1, FGF2 loaded microspheres were able to withstand thermal instability while steadily releasing FGF2 into solution between 9.5 and 10 ng/ml after 72 hours **(Figure 3.5)**. After calculating a linear regression curve with an R^2 value greater than 95%, it was seen that our FGF2 loaded microspheres followed zero-order release kinetics as the rate was independent of FGF2 concentration within mTesR1 **(Figure 3.6)**. Zero-order kinetic release indicates that FGF2 is released from the microspheres at a rate independent of media concentrations.

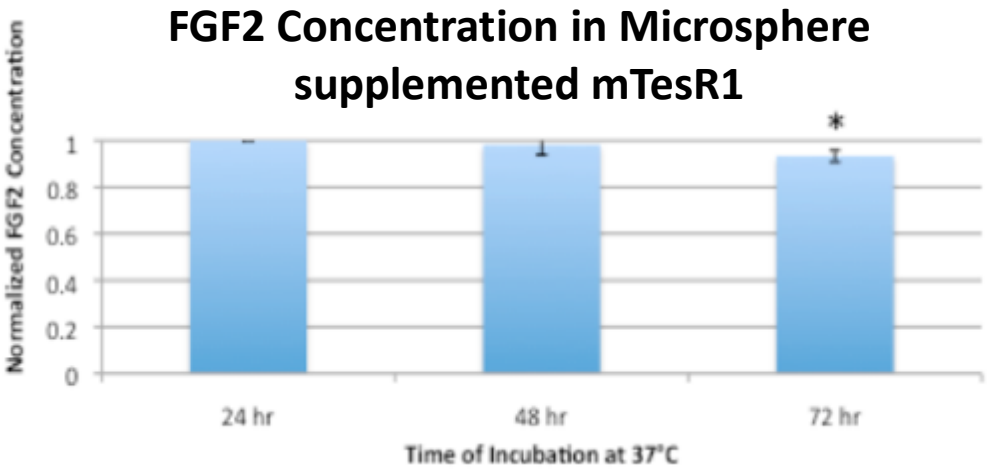

Figure 3.5 FGF2 Concentration in Microsphere supplemented mTesR1.

$$[A]_t = -kt + [A]_0$$

$$[FGF2]_t = -kt + [FGF2]_0$$

$$[FGF2]_t = -0.0335t + [1.0387]_0$$

Figure 3.6 Zero Order kinetics. FGF2 release from microspheres follows zero-order kinetics proving FGF2 concentration is independent of its own amount in solution.

FGF2 Loaded PLGA Microspheres Support Pluripotency

FGF2 loaded microspheres were then investigated for their ability to support pluripotency within iPSCs through an extended duration of culture upon MEF feeder cells **(Figure 3.7)**. The six conditions investigated are described in **TABLE 2.** As the microspheres could sustain FGF2 concentration through 72 hours, replacing media supplemented with FGF2 loaded microspheres every third day became a feeding condition to quantify iPSC pluripotency relative to control daily feeds. The 15 ul/ml microspheres added to the media attained 10 ng/ml FGF2 as determined by BD FlexSet titer. Our hESCs were all passaged from the same initial population to create the six sample conditions. The feeding paradigms were then carried out through 5 passages: on days 0, 7, 14, 21, 28, 35 and by feeding and/or adding FGF2 microspheres on the allotted days. When the iPSC conditions were passaged, 85% were harvested for flow cytometry analysis and the remainder for propagation of the experiment. The markers for analysis are described in **TABLE 3.**

Table 2: Feeding Conditions for Microsphere Experiment			
Feeding Schedule:			
No Microspheres:	Feed Once/Week	Feed Every 3rd Day	Feed Every Day
Microspheres:	15 λ/µl Every 3rd Day		5 λ/µl Once/Week

Table 3: hESC Antibodies			
hESC Markers:	**Protein:**	**Observed:**	**References:**
SSEA 1	3-FAL	Differentiated hESCs	Yuan, 2011
SSEA 3	Oct-4.	Undifferentiated hESCs	Evans, 2011
SSEA 4	Oct-4.	Undifferentiated hESCs	Pruszak, 2009
TRA-1-60	Sox2	Undifferentiated hESCs	

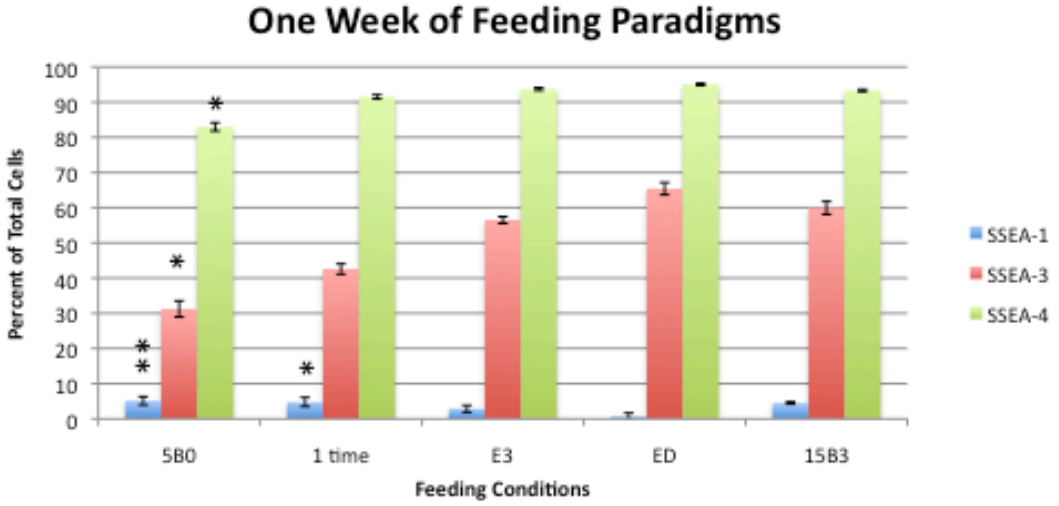

Figure 3.7 One Week of Feeding Paradigm. Pluripotency analysis with FACS Aria II of stem cells after one week. 5BO: 5ul microspheres/ml media change once a week. 15B3: 15ul microspheres/ml media change every 3 days. E3: Media change once every 3 days. ED: Media change every day (control). 1time: Media change once a week. SSEA-1 indications differentiated cells as SSEA-3 and 4 indicates pluripotent stem cells. (n=5) and Student t-test provided statistical significance as * ($p<0.05$) ** ($p<0.005$) ***($p<0.0001$). Error bars are defined by standard error.

An optimal indicator for pluripotency is the quantification of stage-specific embryonic antigen (SSEA) antibodies. hESCs were incubated with SSEAs and Tra-1-60 antibodies and then analyzed with flow cytometry of FACS Aria II (References included in Table 3). Cells expressing SSEA 3, SSEA 4 and TRA-1-60 on the surface indicated pluripotency, whereas cell surface SSEA 1 indicated differentiated iPSCs. **Figure 3.7** displays the data obtained from FACS Aria II analysis. It was observed within the first week that all conditions provided cell populations to be near 100% SSEA4 positive, 80% SSEA3 positive and 5% SSEA1 positive

(Figure 3.7). The conclusion from this experiment was that feeding once every three days with our microspheres was as sufficient as feeding daily to maintain iPSC pluripotency **(Figure 3.8)**. **Figure 3.8** specifically shows that the cell pluripotency profiles with microsphere supplemented media replaced every third day (B3) and control mTesR1 feeds (ED) had statistically identical SSEA 3 and 4 percentages. In conclusion, the microspheres maintain a sustained concentration of FGF2 within mTesR1 that provided expression of pluripotency markers after five weeks similar to our control daily feed condition.

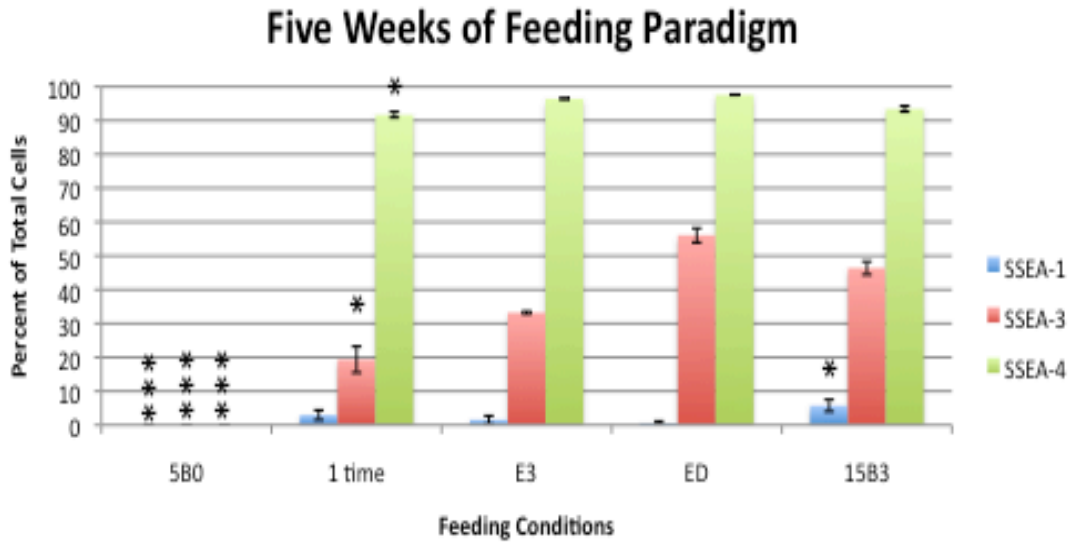

Figure 3.8 five week of feeding paradigm. Pluripotency analysis with FACS Aria II of stem cells after five weeks. 5BO: 5ul microspheres/ml media change once a week. 15B3: 15ul microspheres/ml media change every 3 days. E3: Media change once every 3 days. ED: Media change every day (control). 1time: Media change once a week. SSEA-1 indications differentiated cells as SSEA-3 and 4 indicates pluripotent stem cells. Student t-test provided statistical significance as * ($p<0.05$) ** ($p<0.005$) ***($p<0.0001$). Error bars are defined by standard error. (n=5)

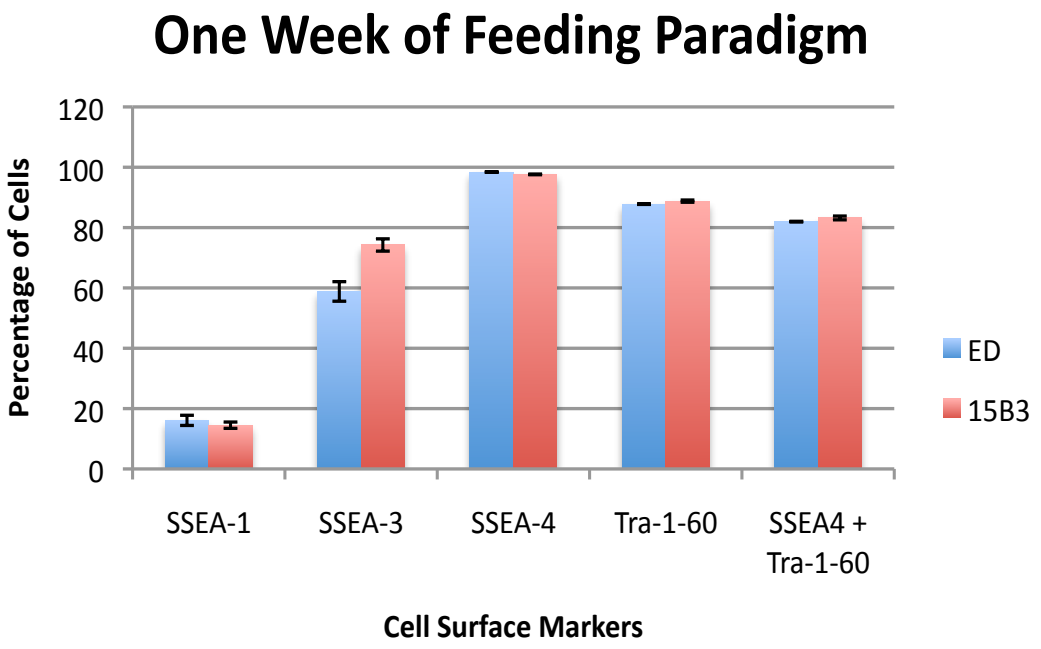

Figure 3.9 pluripotency markers after 1 week. FACS analysis was performed once a week though a month of culturing stem cells with both conditions B3 and ED. The SSEA and TRA antibodies allowed quantification of pluripotency. (n=5)

We then duplicated our long-term stem cell culture with microsphere-supplemented feeds every third day compared to a control daily feed. The results from the first and last week of FACS Aria II cellular analysis of our triplicate samples were graphed in **Figure 3.9**. After one week of the feeding conditions, the microspheres provided ample support to provide pluripotency similar to that of daily control feeds **(Figure 3.9).** After a month of these conditions, we revisited our cell pluripotency with flow cytometry **(Figure 3.10)**. At the conclusion of the experiment, mTesR1 feeding every third day with microspheres was statistically sufficient to keep our iPSCs as pluripotent as the control daily mTesR1 feeds. The sustained FGF2 concentration relative to varying amounts confirmed the hypothesis that microsphere-supplemented feeds would reduce spontaneous differentiation.

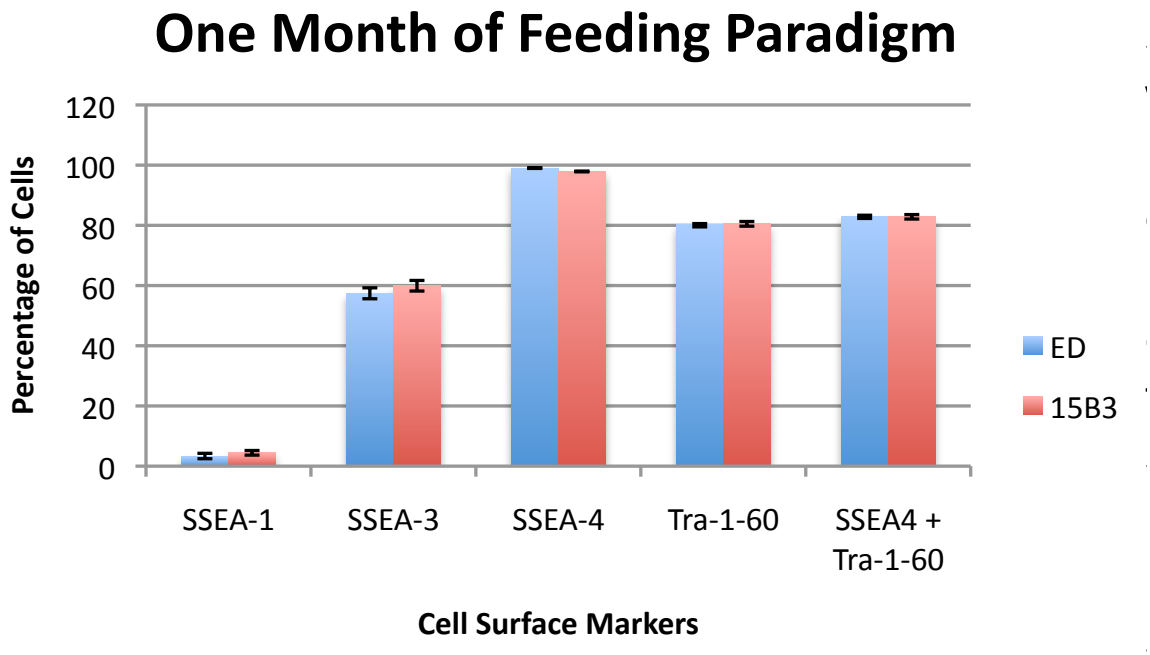

Figure 3.10. Pluripotency cell surface markers after 1 month. FACS analysis was performed once a week though a month of culturing stem cells upon both conditions B3 and ED. The SSEA and TRA antibodies allowed quantification of pluripotency. (n=6)

FGF2 Loaded Microspheres Increase Differentiation Potential in iPSCs

We have shown that we can maintain an equivalent level of pluripotency within iPSCs by stabilizing trophic FGF2 within FGF2 loaded microspheres. To determine if mTesR1 with microsphere feeding had an effect upon differentiation potential, hESCs were guided through neural induction to determine efficiency. hESCs were enzymatically detached from cell culture dishes with accutase (Invitrogen) after 4 weeks of microsphere and control feeds and plated at a density of 250,000 cells upon matrigel coated dishes with Rho Associated Protein Kinase (ROCK) inhibitor (Watanabe, 2007). ROCK inhibition diminishes hESC apoptosis due to reduced cell-to-cell contact (Watanabe, 2007). Four days post plating**,** it was observed that single cells from a previous microsphere conditioning proliferated and divided much faster than those cells under control conditions. We then directed neural induction through ten-day dual SMAD inhibition blocking TGFβ and Bone Morphogenetic Protein (BMP) pathways directing mesoderm and endoderm lineage through differentiation (Chambers, 2009) **(Figure 3.11).**

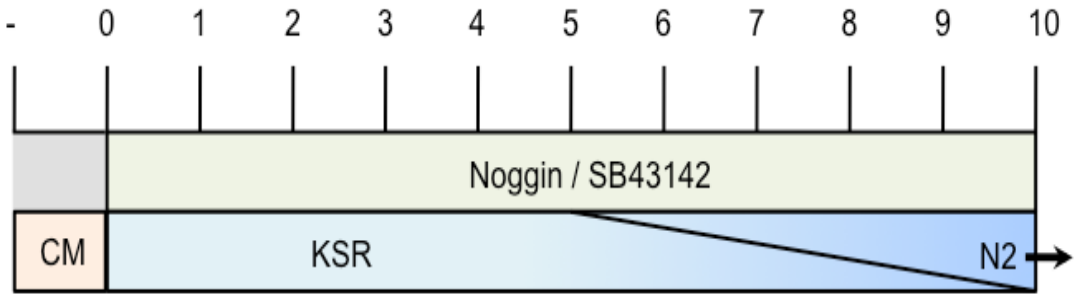

Figure 3.11 Schematic of iPSC neural induction and blockage of endoderm and mesoderm. Timeline of culture conditions to obtain stem cells derived neural precursor cells. Once cells reach confluency within the culture dish, they are switched from stem cell media with FGF2 to neural differentiation media. This dual SMAD inhibition media allows for an efficient and directed neural induction.

Table 4: NPC Flow Cytometry Analysis		
Cell Sample	**Population:**	**Percentage of Total**
ED Control	CD44- / CD271-	48.8
ED Control	CD189+ / CD24+	25.4
ED Control	CD44- / CD271- / CD189+ / CD24+	12.4
15 λ/µl Every 3rd Day	CD44- / CD271-	37.8
15 λ/µl Every 3rd Day	CD189+ / CD24+	77.0
15 λ/µl Every 3rd Day	CD44- / CD271- / CD189+ / CD24+	29.1

At day 10, a previously described flow cytometry analysis (Yuan, 2011) was followed to observe NPC induction efficiency. This study investigated a protocol for the quantification of the population percentage of NPCs with cell surface markers. It was shown that NPCs could express CD184 and CD24 while not expressing CD44 and CD271. CD184 is a cell surface marker for neural cells capable of differentiation to neurons while CD24 is a marker for a neural cell adhesion molecule, both providing a signature true to NPCs. CD271 is a marker for hESCs and neural crest while CD44 is a marker for glial progenitors and astrocytes, neither being indicative of NPCs (Yuan, 2011). At Day 10 of neural induction, our cell populations were then analyzed for efficiency in generating $CD184^{+}/CD24^{+}/CD44^{-}/CD271^{-}$ cells. The first step of flow cytometry analysis was gating out cellular debri and clusters of cells (**Figure 3.12A,D**). The population of $CD44^{-}/CD271^{-}$ cells was then analyzed and gated (**Figure 3.12B,E**). Of those cells not expressing non-NPC cell surface markers, the percentage of cells

$CD184^{+}/CD24^{+}$ (**Figure 3.12C,F**) provided a relative percentage of the total cell population witha NPC identity (Yuan, 2011). Such NPCs should have the ability to derive glia, neurons and continue proliferation (Yuan, 2011). **Table 4** displays the percentages of such cellular populations within both culture conditions. It was found that hESCs exposed to FGF2 loaded microspheres have a higher differentiation potential presumably from lesser spontaneous differentiation relative to that with daily control media.

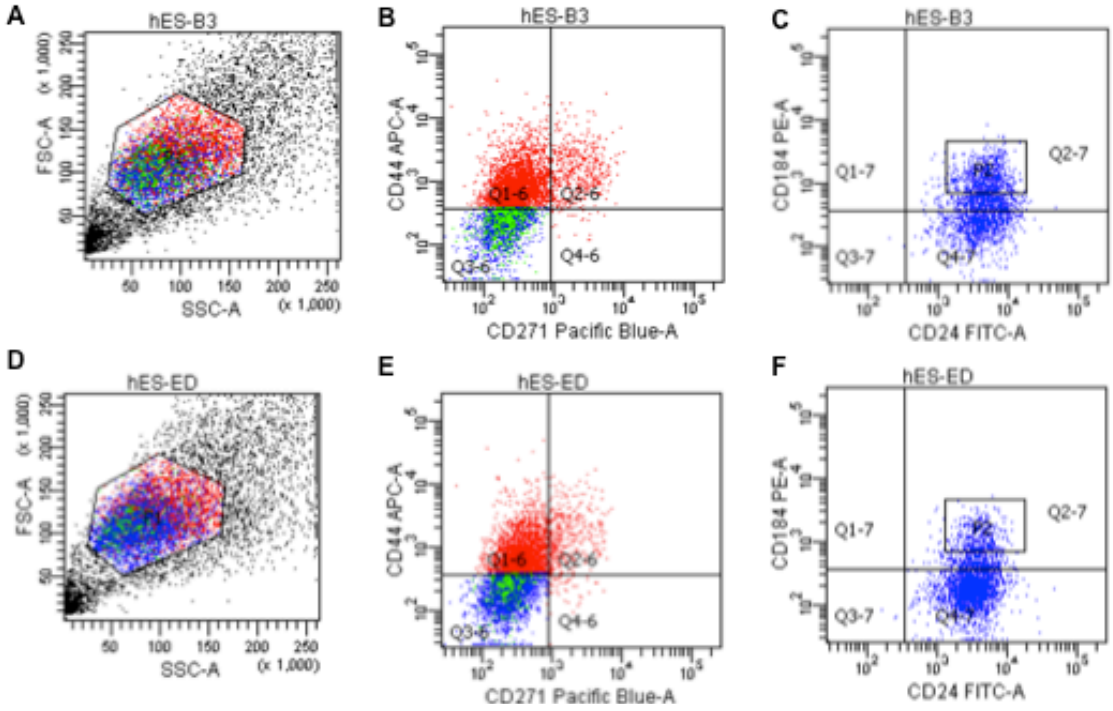

Figure 3.12 Neural Induction to test whether we can improve differentiation kinetics. As another strategy to determine pluripotency of stem cells within our two feeding paradigms, cells were plated as single cells post-accutase treatment. Once cells were to grown to confluency, they were exposed to dual SMAD inhibition to efficiently drive neural induction. After the 11 day protocol, the cells were treated with accutase and analyzed via FACS Aria II. (A-F) with CD44, CD271, CD184, and CD24 to determine what percentage of the population attained neural precursor state. (n=5)

To corroborate our flow cytometry analysis, we analyzed immunohistochemical protein markers of fixed cells at the same induction point **(Figure 3.13)**. We first observed staining of Dapi, TUJ1 and PAX6. Cell nuclei are marked by Dapi. The two conditions display comparable cellular densities indicating growth and proliferation **(Figure 3.13 A,D).** TUJ1 was then used to mark neuron specific beta-tubulin. It appeared that there were TUJ1 positive

cells with longer cellular extensions in our control condition compared to that with cells previously cultured with microspheres. This suggested that such cells previously exposed to a constant FGF2 level do not commit and differentiate to a neural lineage as readily as our control population **(Figure 3.13 B,E)**. Staining for PAX6 then signified successful neurectodermal induction. There appeared to be equal or greater amounts of PAX6 positive cells in microsphere treated cells than with our controls. This suggested that a constant FGF2 concentration within hESCs prior to neural induction allowed for a more efficient induction to cells containing the neurectoderm fate determinant PAX6 and ability to then differentiate towards neurons.

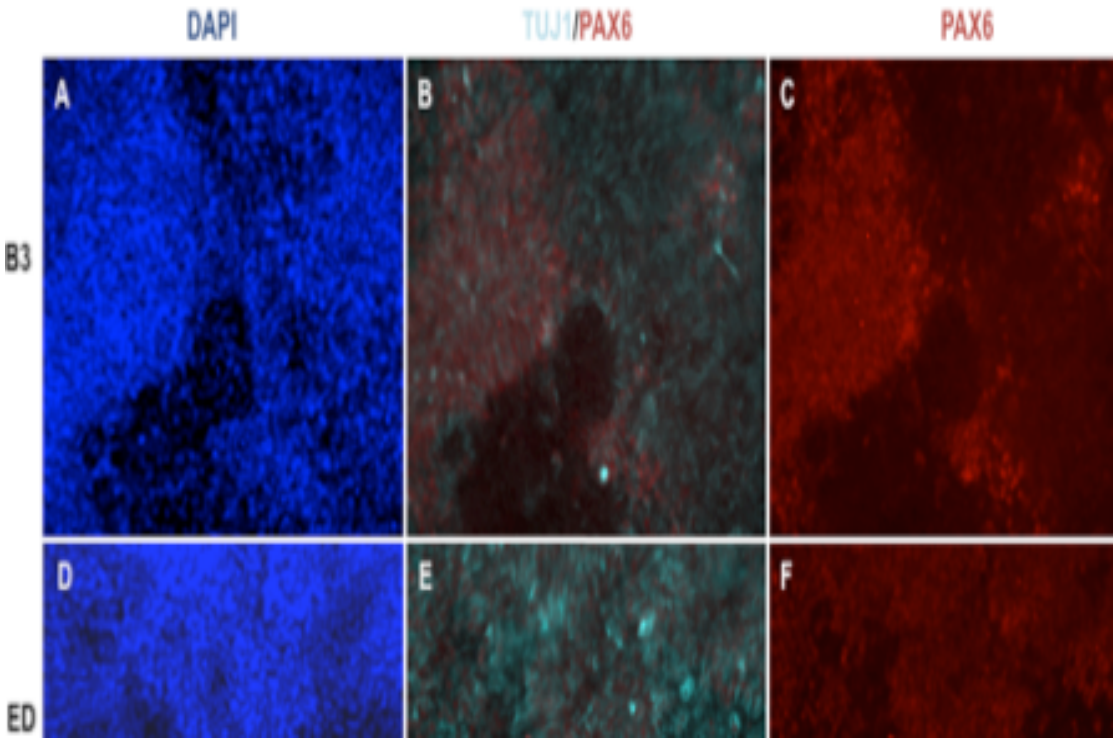

Figure 3.13 Neural induction ICC to better understand effects of microspheres. Cells were treated with control stem cell media daily feeds or supplemented with FGF2 loaded microspheres every three days for the duration of one month. To supplement the data observed by flow cytometry, protein expression was also observed upon fixed neural precursors (A-F). These panels of neural precursors showed TUJ1, PAX6, and DAPI: indicative of neurons, neuroectoderm fate determinant and cell nuclei respectively. Magnification at 4x

We next carried out staining of Dapi, Nestin and SOX2. We saw similar Dapi staining signifying cell nuclei and general cell density **(Figure 3.14 A,D)** to that in **Figure 3.13**. SOX2 is a protein that is preeminent in self-renewal of hESCs and NPCs that are undifferentiated, that has been shown to interact with PAX6 (Aota, 2003). There was comparable SOX2 staining in both conditions indicating similar levels of self-renewal between cells previously exposed to microspheres or not **(Figure 3.14 B,E)**. Nestin is an intermediate filament protein involved in neuron axonal growth (Guerette, 2007) **(Figure 3.14 C,F)**. There was similar if not more nestin within cells exposed to microspheres relative to the control cells implying comparable axonal growth in the two conditions. Taking **Figure 3.11** through **Figure 3.14** together, it was observed that a higher percentage of cells specifically at the NPC state can be generated by the end of a previously described 10-day neural induction (Chambers, 2009) upon cells exposed to microspheres during hESC culture. Cells were not counted and fluorescent intensities were not quantified in this study, but both approaches could be valuable future methods for distinct analysis of NPC generation efficiency.

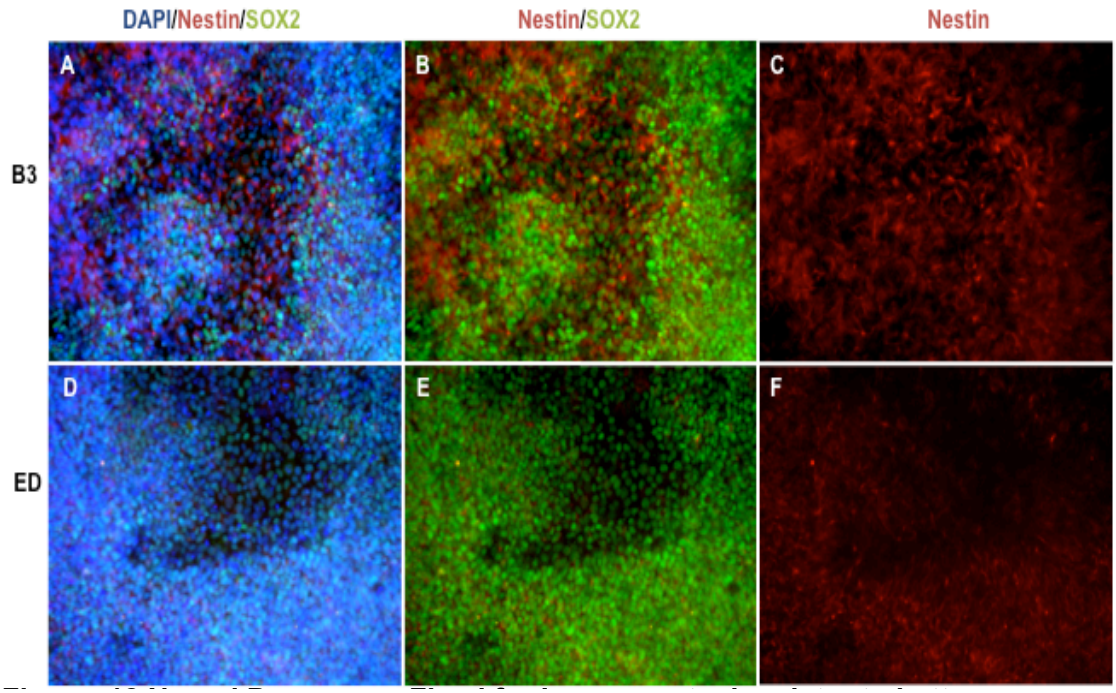

Figure 3.14: Neural Precursors fixed for immunocytochemistry to better understand neural induction after microsphere supplemented media. Cells were treated with control stem cell media or stem cell media supplemented with FGF2 loaded microspheres every three days for the duration of one month. To further supplement the data observed by flow cytometry, protein expression was also showed upon fixed neural precursors (A-F). these panels of neural precursors observed SOX2, Nestin, and Dapi staining: indicative of stem cell pluripotency, developing neural axons and cell nuclei respectively. Magnification at 4x

Novel iPSC Feeding Paradigm with FGF2 Loaded Microspheres

FGF2 loaded microspheres when supplemented into HuESM and only fed every third day of culture can yield hESCs or iPSCs equally if not more pluripotency than that observed with traditional daily feeds (Thompson, 1998). These findings yielded three very substantial benefits: microsphere-supplemented cells have maintained pluripotency, increased differentiation potential, and greatly reduced contact, which has the potential cell interaction to cause contamination. We have shown that cells fed with FGF2 loaded microspheres maintain pluripotency such to lead to increased differentiation potential. Every time researchers open incubators and handle cell culture dishes there is increased possibility of hESCs and iPSCs being exposed to contaminants. Reducing feeding events reduces

contamination potential. The cells can remain unhandled within the incubators at 37°C except for one feed every 72 hours.

iPSC Derivation techniques: FACS derivation of iPSCs

Previous studies have demonstrated that downregulation of the human fibroblast marker CD13[8], and upregulation of the pluripotency markers SSEA4 and TRA-1-60 occurs during reprogramming (Thorstan *et al.,* 2011). These studies suggest that isolation of fully reprogrammed iPSCs during the early stages of reprogramming may be accomplished by FACS using a combination of positive and negative surface markers. While current sorting strategies for purification of pluripotent cells rely on positive selection (Manos *et al.*, 2011), it is possible that a significant proportion of clones isolated using this method may not be fully reprogrammed. To test this hypothesis, I first optimized the conditions for survival of live-cell sorted, fully reprogrammed cells by examining the expression levels of three surface markers in a manually derived, early passage clone (p4) of an iPSC line (1018) cultured on MEFs. Populations of cells expressing all three markers were found in the culture suggesting a heterogeneous mixture of cells containing parental and partially reprogrammed fibroblasts **Figure 3.15**. I then sorted the $CD13^{-}SSEA4^{+}Tra\text{-}1\text{-}60^{+}$ (Tra- $1\text{-}60^{+}$) population and, as a control, the $CD13^{-}SSEA4^{+}Tra\text{-}1\text{-}60^{-}$ (Tra-$1\text{-}60^{-}$) population to approximately 70% purity directly into one well of a 6 well plate containing MEFs in the presence of ROCK inhibitor Y-27632. The sorted populations were maintained for 20 days on MEFs without ROCK inhibitor or removal of differentiated cells or splitting prior to reanalysis by flow cytometry. At 20 days post-sorting (dps), the cultures originating from the enriched Tra $1\text{-}60^{+}$ population contained fewer Tra-$1\text{-}60^{-}$differentiated cells and no detectable $CD13^{+}$ parental fibroblasts. The Tra-$1\text{-}60^{+}$ population was present in these cultures at approximately double the proportion found in the Tra-$1\text{-}60^{-}$ enriched culture (30% vs. 14%). Conversely, at 20 dps the culture originating from the Tra-1-

60- enriched population contained a Tra-1-60+ population at a similar proportion to the originally sorted culture (18%T vs. 14%T). However, these cultures also contained a higher proportion of differentiated or transformed cells (CD13- SSEA4-Tra-1-60-) as well as adult fibroblasts (CD13+) suggesting that our FACS conditions allow for purification of fully reprogrammed cells from contaminating cell types.

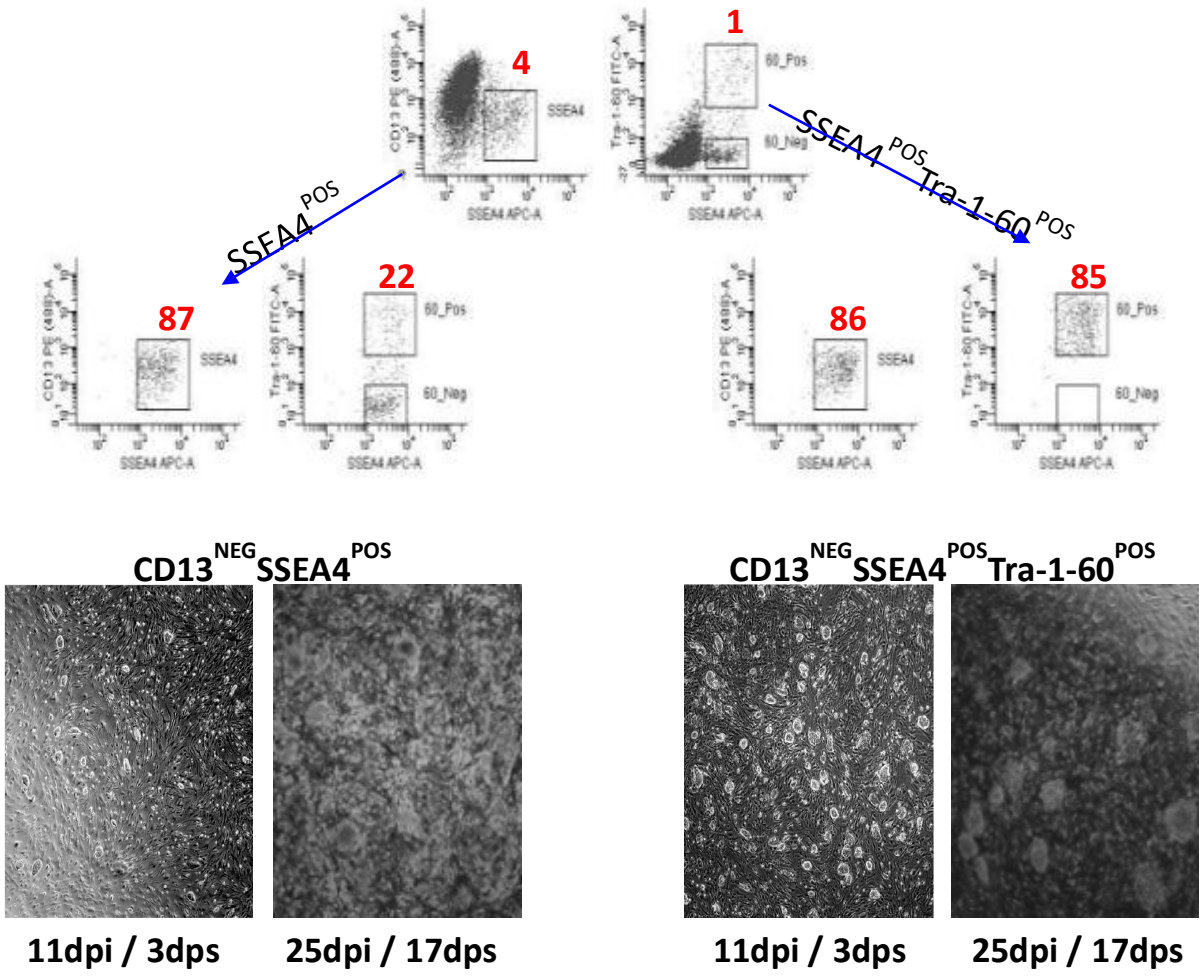

Figure 3.15 Sorting of iPSCs. CD13^{NEG}SSEA4^{PO}STra-1-60^{NEG} and CD13^{NEG}SSEA4^{POS}Tra-1-60^{POS} populations from the manually derived 1018 clone were sorted onto MEF feeder layers and expanded for 20 days prior to reanalysis by flow cytometry to assess retention of sorted surface markers. dpi = days post infection. dps = days post sort.

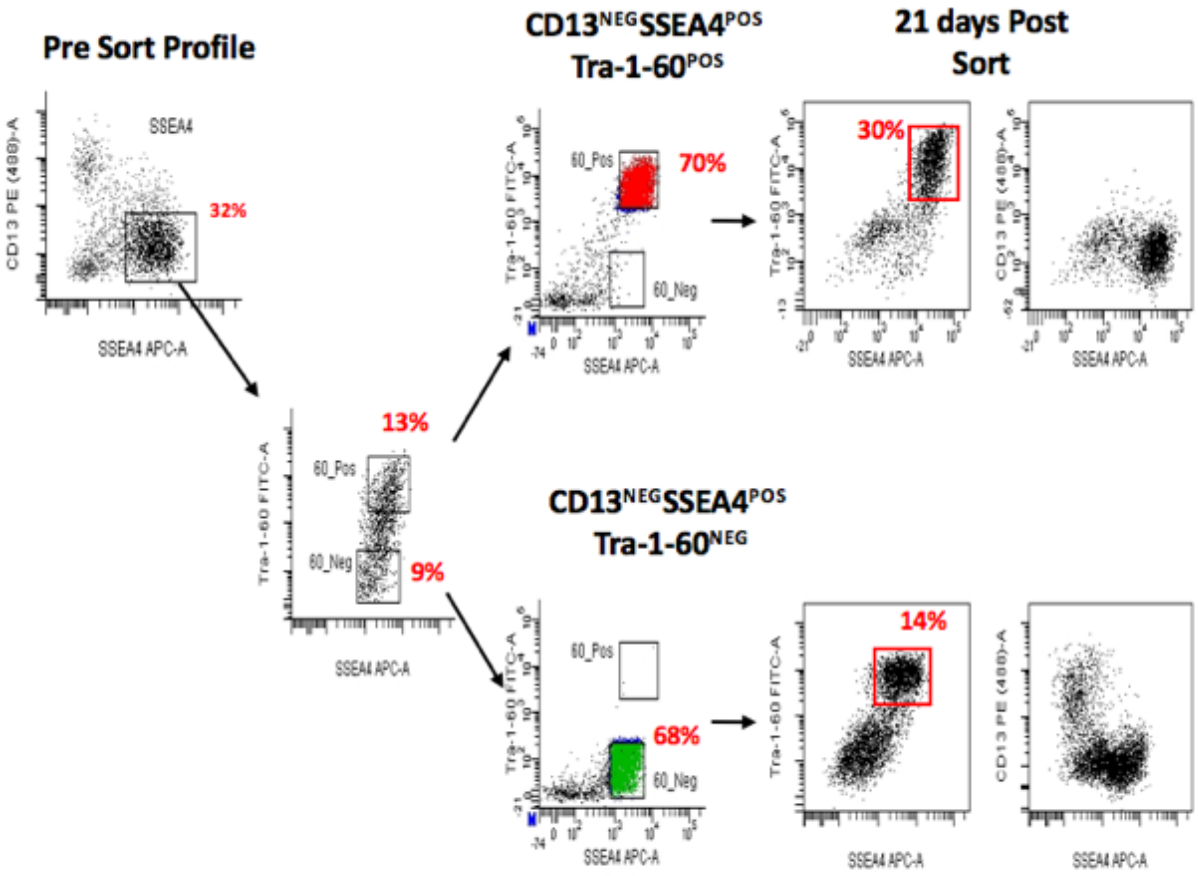

Figure 3.16 Pre-Sort Profile. Gating structure used to sort the CD13^{NEG}SSEA4^{POS}Tra-1-60^{PO}S populations for all cell lines derived in this study. Live cell are first defined using forward (FSC) and side (SSC) light scattering properties. The CD13^{NEG}SSEA4^{POS} population is then selected from the live cell gate. The highest Tra-1-60^{POS} expressing cells are then selected from the CD13^{NEG}SSEA4P^{OS} population and sorted for expansion and characterization.

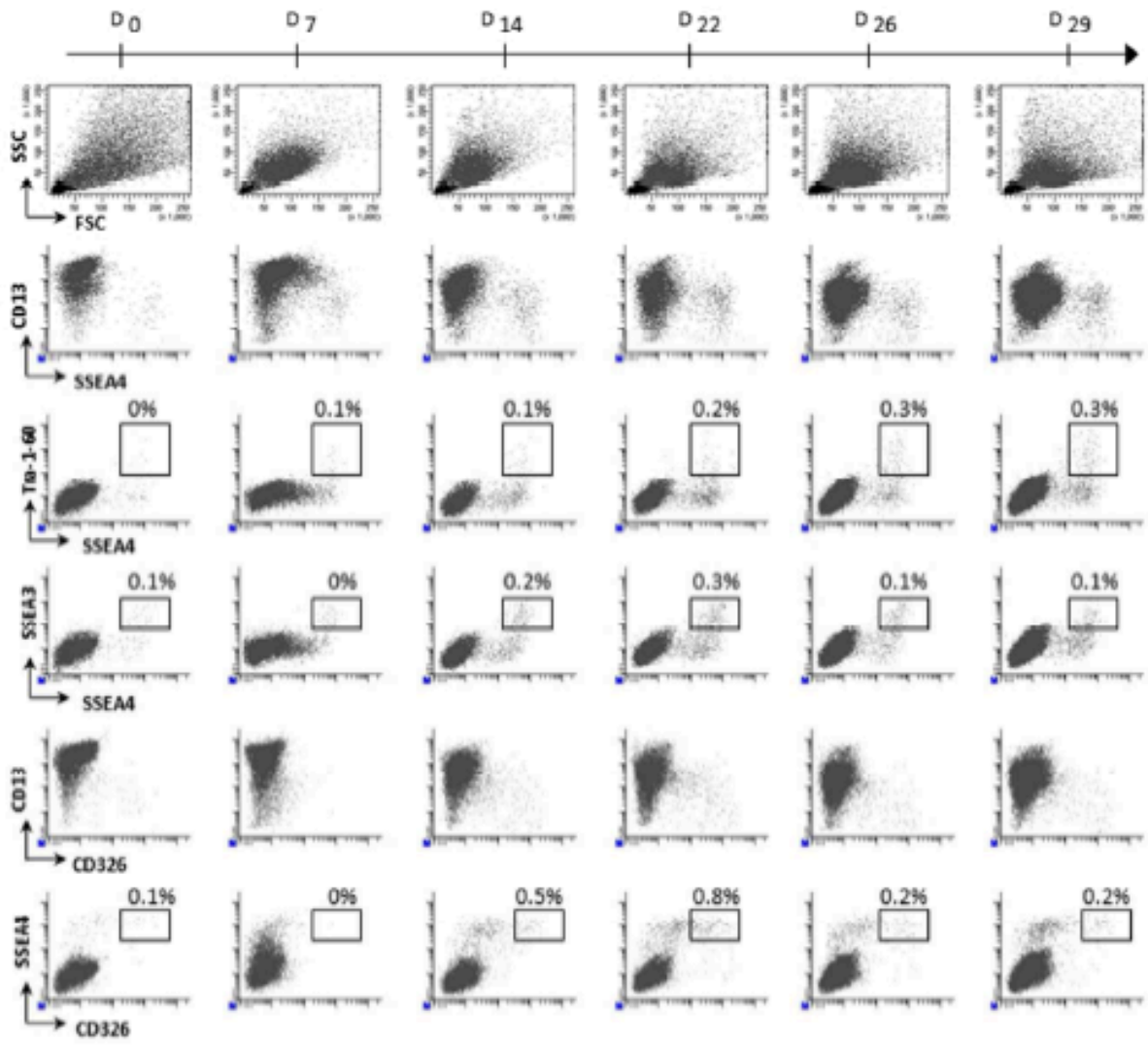

Figure 3.17 Time Course analysis of retroviral reprogrammed fibroblasts. A fibroblast line was analyzed for changes in pluripotent surface marker expression by flow cytometry at ~7 dpi intervals following retroviral reprogramming to determine the earliest time point at which the $CD13^{-}SSEA4^{+}Tra\text{-}1\text{-}60^{+}$ population appears. Values indicate percent of total cells in the culture expressing the indicated markers

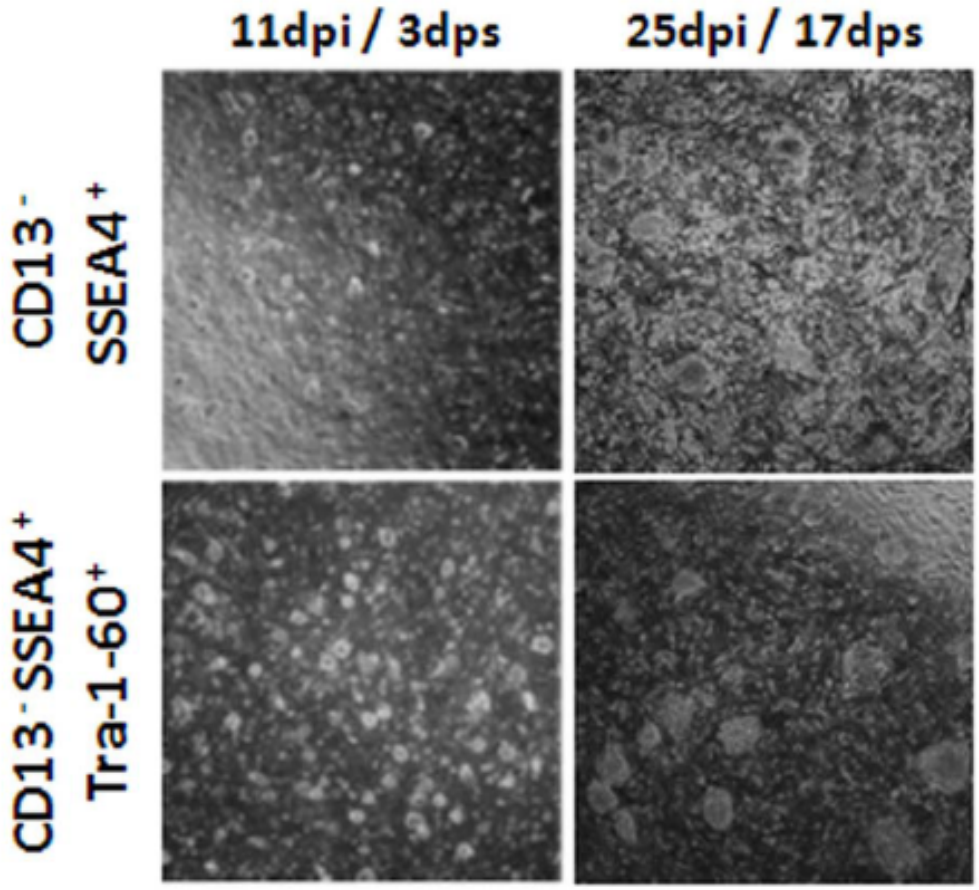

Figure 3.18 Sorting 11 dpi early derivation iPSCs. $CD13^{NEG}SSEA4^{POS}$ and $CD13^{NEG}SSEA4^{POS}$Tra-1- 60^{POS} populations were sorted onto MEF layers at seven days post infection and imaged at 3 and 17 dps to assess colony formation.

To confirm this strategy, adult skin fibroblasts at 8 days post infection (dpi) were sorted based on the CD13-SSEA4+TRA-1-60+ surface marker profile. As a control, the CD13 SSEA4+ population that contained two subpopulations of cells expressing either Tra-1-60+ or Tra-1-60- was isolated in parallel. 5,000 or 10,000 cells from each population were sorted directly into MEF-containing plates, and monitored for the formation of colonies. Small but distinct colonies were evident in both sorted populations as early as 3 days post sort (dps), with the CD13 SSEA4+Tra-1-60+ population producing larger and more abundant colonies than the CD13 SSEA4+ population (3 dps, 11 dpi; **Figure 3.18).** Following an additional 2 weeks of expansion without manual removal of differentiated cells, wells containing the CD13–SSEA4+ population had become overgrown with transformed and

differentiated cells, whereas wells containing the sorted CD13–SSEA4+Tra-1-60+ cells contained large, well-separated colonies with few differentiated cells between the colonies and lacked cells with a transformed morphology (17 dps, 25 dpi; **Figure 3.18**). We observed a 3-4 fold increase in the number of colonies present in wells containing the sorted CD13–SSEA4+Tra-1-60+ cells compared to the sorted CD13–SSEA4+ cells **Figure 3.19.**

Sorted Population	Sorted Cell #	Colonies
SSEA4$^+$	5000	35
SSEA4$^+$	10000	129
SSEA4$^+$Tra-1-60$^+$	5000	132
SSEA4$^+$Tra-1-60$^+$	10000	363

Figure 3.19 Colony counts arising from the sorted cell populations shown in Panel B at 17 dps (25 dpi).

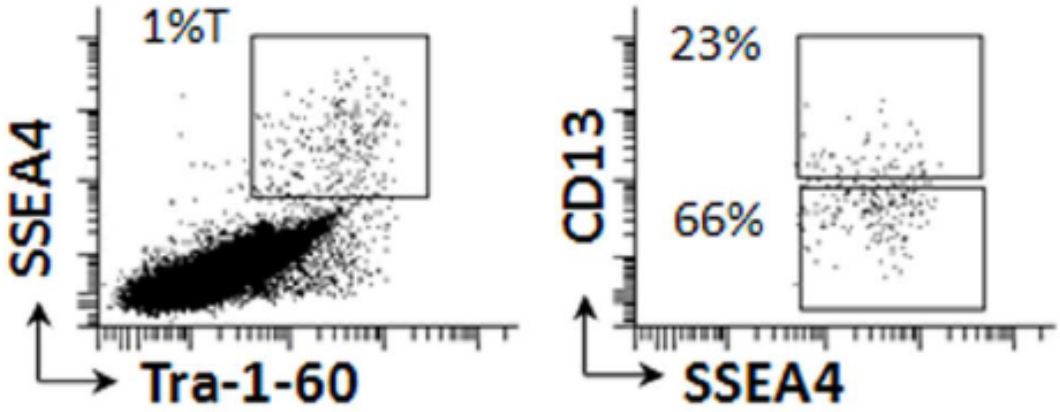

Figure 3.20 Pluripotency sorting parameters. Gating structure used in the analysis of CD13+ cells present within the SSEA4^{POS}Tra-1-60^{POS} population at 7 dpi

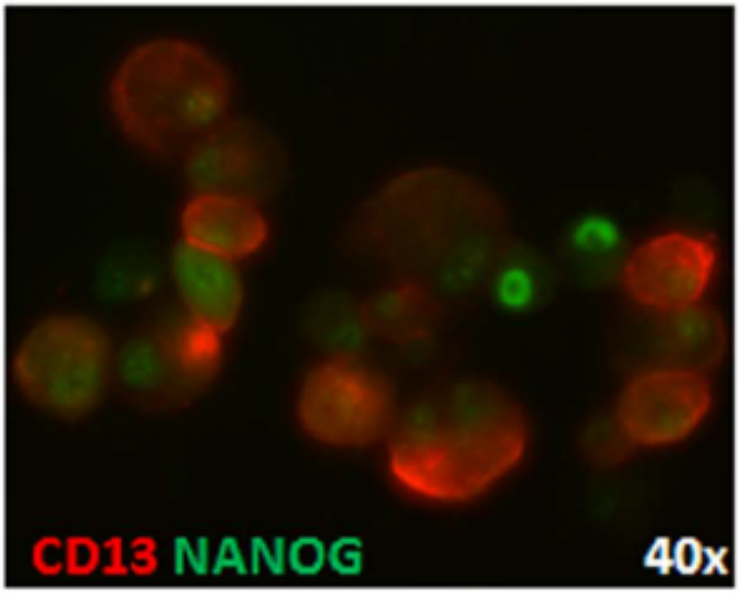

Figure 3.21 Nanog expression and CD13. Fluorescence microscopy demonstrating NANOG expression in CD13+ cell at 7 dpi. 40x magnification. CD13 shown in red. Nanog in shown in green.

I then analyzed CD13 expression within the SSEA4+Tra-1-60+ population of reprogrammed fibroblasts at 7 dpi. Roughly one quarter of the SSEA4+Tra-1-60+ population expressed CD13 indicating the presence of a heterogeneous population of fully reprogrammed, transformed, or transitioning cells (23% CD13+, 66% CD13-; **Figure 3.20**), some of which expressed both Nanog and CD13 **Figure 3.21**. Because surface marker expression during reprogramming is dynamic, I wanted to first identify the earliest time point at which to enrich fully reprogrammed iPSCs. Time course analysis conducted by flow cytometry following retroviral reprograming suggested that SSEA4+Tra-1-60+ cells were detectable as early as 7 dpi, and their proportion increased up to 21 dpi, then remained constant as marker negative cells outgrew the reprogrammed cells **Figure 3.17**. The SSEA4+Tra-1-60+ population also expressed the SSEA3 and CD326 pluripotency markers (Kahler *et al.*, 2013). SSEA4+CD13+ cells appeared by 7 dpi and while most of this

population disappeared by 14 dpi, a proportion remained in the culture. To test whether this timing was consistent among different skin samples, I analyzed cultures derived from a foreskin fibroblast line (0825), a healthy adult control fibroblast line (1023), and a fibroblast line from a subject with HCM (1018) for up to 21 dpi. The three fibroblast cell lines showed a consistent emergence of pluripotent surface markers with SSEA4+Tra-1-60+ cells present at low numbers at 7 dpi (D7, 0.3%-0.4% **Figure 3.22**), increasing in proportion at 14 dpi (D14, 1.4%-2.2%), and decreasing by day 21 as other cells overtook the culture (D21, 0.7%), suggesting a consistent appearance of potentially early reprogrammed cells between 7 and 14 dpi. However, at early time points, the majority of SSEA4+Tra-1-60+ cells also expressed CD13 (D7, 98%-100%). The proportion of CD13+SSEA4+Tra-1-60+ decreased approximately half by day 14 post infection (D14, 37%-54%), suggesting loss of this fibroblast marker on cells undergoing reprogramming. Interestingly, the CD13+SSEA4+Tra-1-60+ population increased again by day 21, suggesting that this population was expanding or that CD13- cells were lost from the culture.

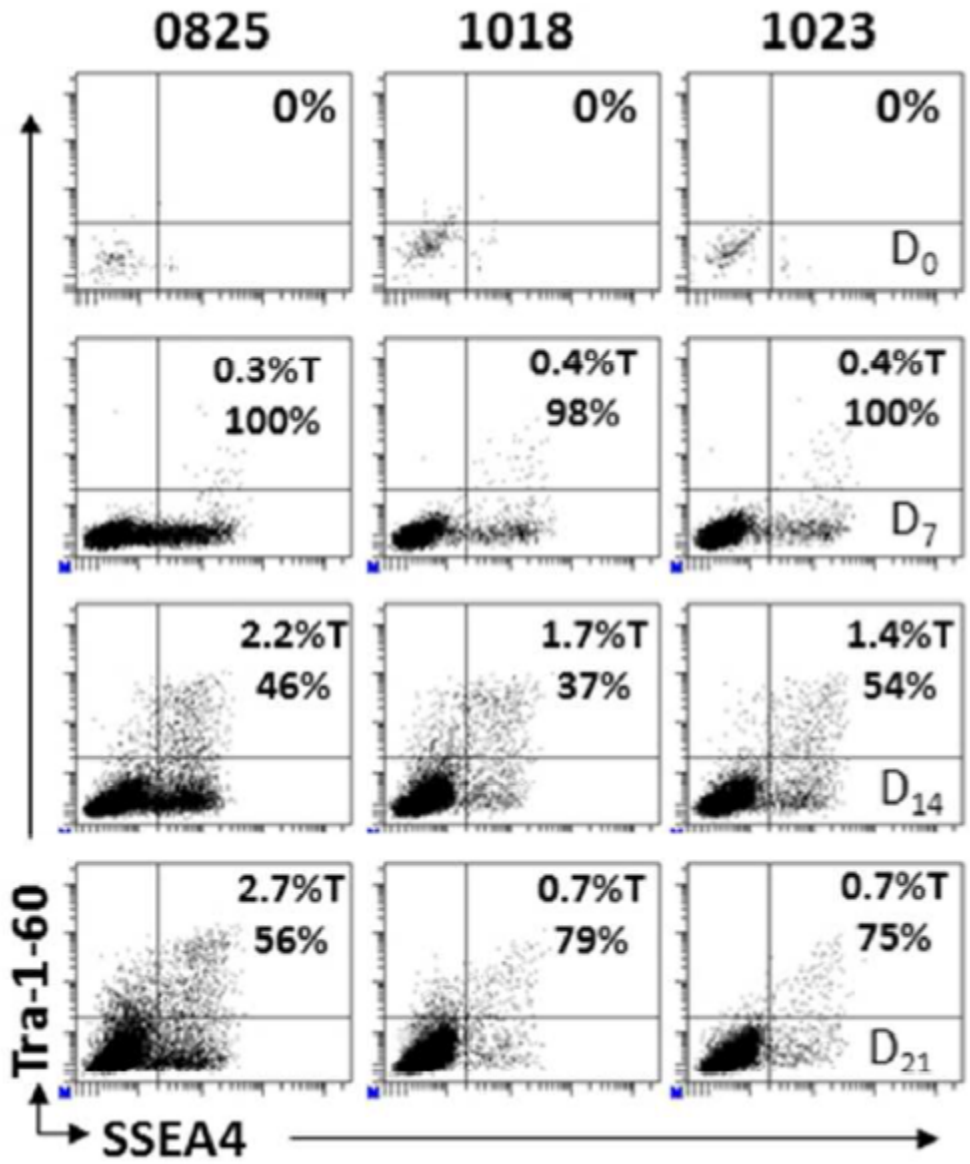

Figure 3.22 Foreskin (0825) and adult dermal fibroblast (1018 and 1023) lines underwent four factor retroviral reprogramming and were analyzed by flow cytometry for the emergence of the CD13NEGSSEA4POSTra-1-60POS population at seven day intervals post infection. Values designated %T indicates proportion of total cells within the culture positive for the indicated combinations of surface markers. Values without T designation indicate the proportion of cells positive within the parent gate.

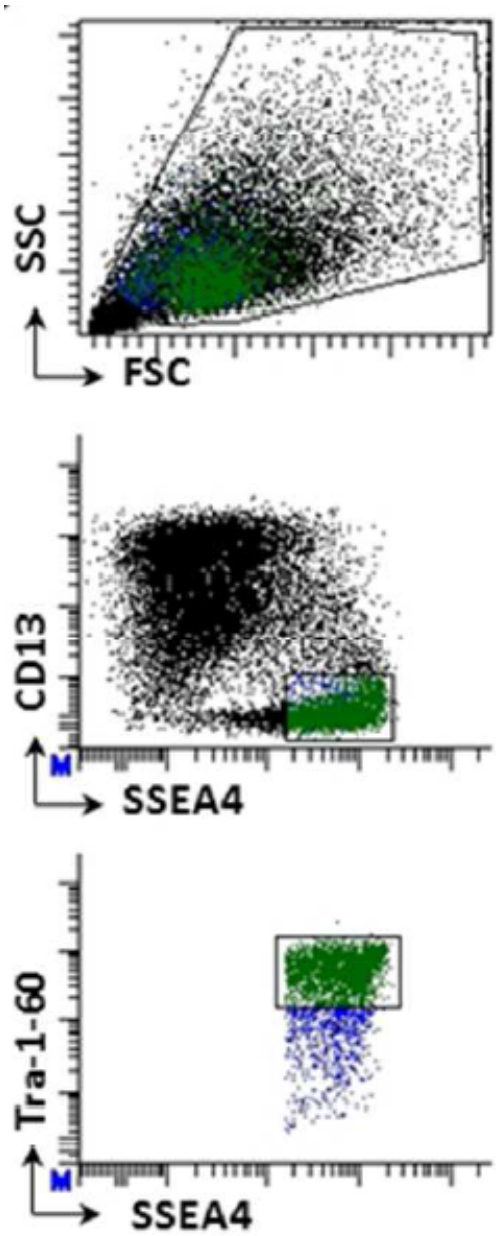

Figure 3.23 Gating structure used to sort the CD13NEGSSEA4POSTra-1-60POS populations for all cell lines derived in this study. Live cell are first defined using forward (FSC) and Side (SSC) light scattering properties. The CD13NEGSSEA4POS population is then selected from the live cell gate (blue cells). The highest Tra-1-60POS expressing cells are then selected from the CD13NEGSSEA4POS population (Green cells) and sorted for expansion and characterization.

Based on these results we developed the sorting strategy shown in **Figure 3.23** which omits the contaminating partially reprogrammed CD13+SSEA4+ population by selecting the highest Tra-1-60+ expressing cells within the CD13-SSEA4+ population. Using this strategy, I FACS derived 228 individual iPSC lines from over 75 fresh or frozen fibroblast lines

generated from biopsies harvested from healthy or disease patients using either integrating (retroviral) or non-integrating (Sendai virus) reprogramming vectors and performed extensive characterization on a subset of those lines which is described in the data that follows. I further characterized the first 2 weeks of the reprogramming process on 128 FACS derived iPSC line.. As shown in **Figure 3.24**, a higher percentage of SSEA4+TRA-1-60+ cells were generated with Sendai infections compared to retroviral infections over the entire time course. However, Sendai infections demonstrated a delayed reduction in the proportion of SSEA4+TRA1-60+CD13+ cells (**Figure 3.25**). By the second week of induction, the proportion of the CD13+ population between the cultures was similar.

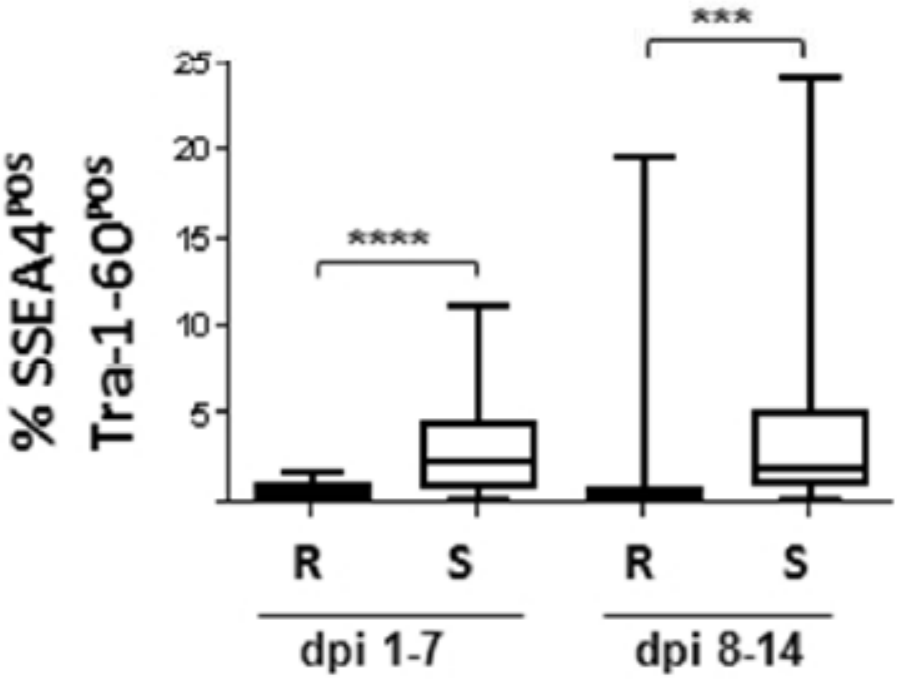

Figure 3.24 Comparison of $SSEA4^{POS}Tra\text{-}1\text{-}60^{POS}$ populations present in Retro (R) or Sendai (S) viral infected fibroblast cultures during first two weeks of programming. Dpi 1–7:(R) n=29, (S) n=21. Dpi 8–14: (R) n=32, (S) n=46. Total n=228. Statistical significance was assessed via Student's t-Test. * p<=0.05, ** p<=0.001, *** p<=0.001, ****p<=0.0001.
.

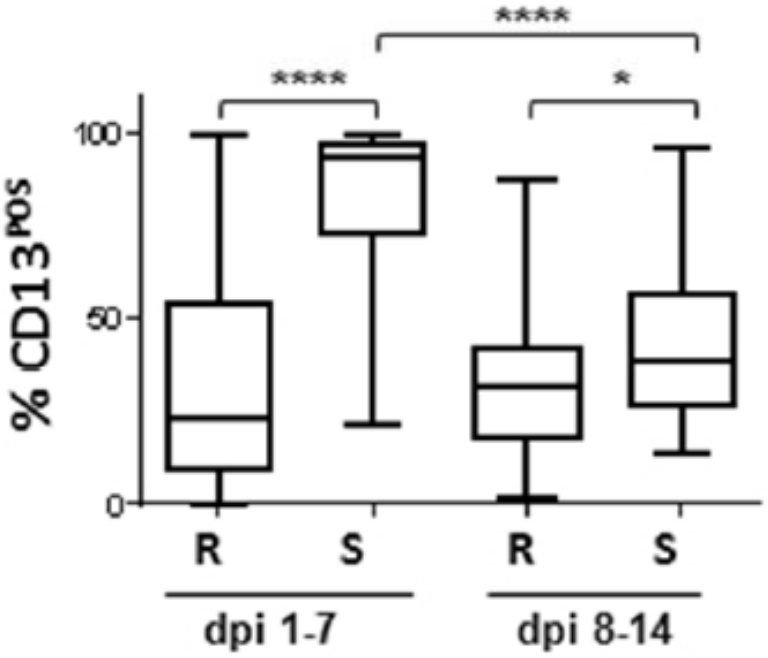

Figure 3.25 Comparison of $CD13^{POS}$ cells present within the $SSEA4^{POS}Tra\text{-}1\text{-}60^{POS}$ populations during first two weeks of programming following Retro (R) or Sendai (S) infection. Dpi 1-7:(R) n=29, (S) n= 21. Dpi 8-14: (R) n=32, (S) n= 46. Total n=228. Statistical significance was assessed via Student's t-Test. * p <= 0.05, ** p <= 0.001, *** p <= 0.001, ****p <= 0.0001.

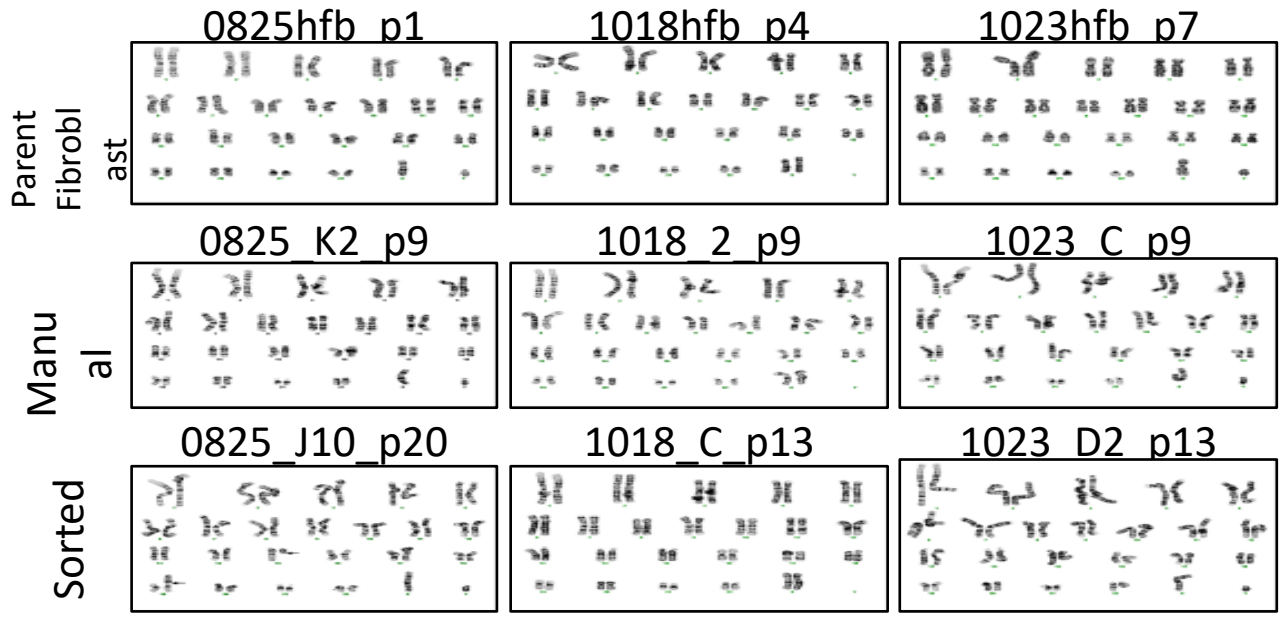

Figure 3.26 Karyotype of FACS and Manually Derived retroviral iPS lines possess a normal karyotype and match the parent fibroblast. Karyotype was assessed using 20 G-banded metaphase cells from each fibroblast and reprogrammed cell lines at passages indicated. All lines possess a normal karyotype and match the parent fibroblast. Karyotype was assessed using 20 G-banded metaphase cells from each fibroblast and reprogrammed lines at passages indicated. Fibroblasts and FACS derived lines possess a normal karyotype and match the parent fibroblast. Three out of 20 cells from the manually derived line displayed an unbalanced translocation between the short arm of chromosomes 11 and 22 resulting in trisomy of the short arm of chromosome 11.

FACS derived lines are pluripotent

To further characterize this defined selection strategy, I compared the phenotype and function of the FACS-derived iPSC clones to manually picked clones. First, the 0825, 1018, and 1023 fibroblast lines shown in Figure 2A reprogrammed using the 4-factor retroviral protocol were subjected to either FACS derivation at 7 dpi or standard picking techniques. For each method, one clone from each line was randomly selected for expansion and further characterization by a standard battery of assays, including karyotypic analysis, DNA fingerprint, pluripotent surface marker expression, qRT-PCR, and teratoma formation. All fibroblasts and reprogrammed iPSC lines displayed normal karyotypes, and had DNA fingerprints matching the parental fibroblast line **Figure 3.26**. Clones from the 0825 foreskin fibroblast line had a DNA fingerprint that matched a major subpopulation in the parental

fibroblasts that contained a contaminating subpopulation with a different genotype, suggesting isolation of clonal cultures from a mixed population.

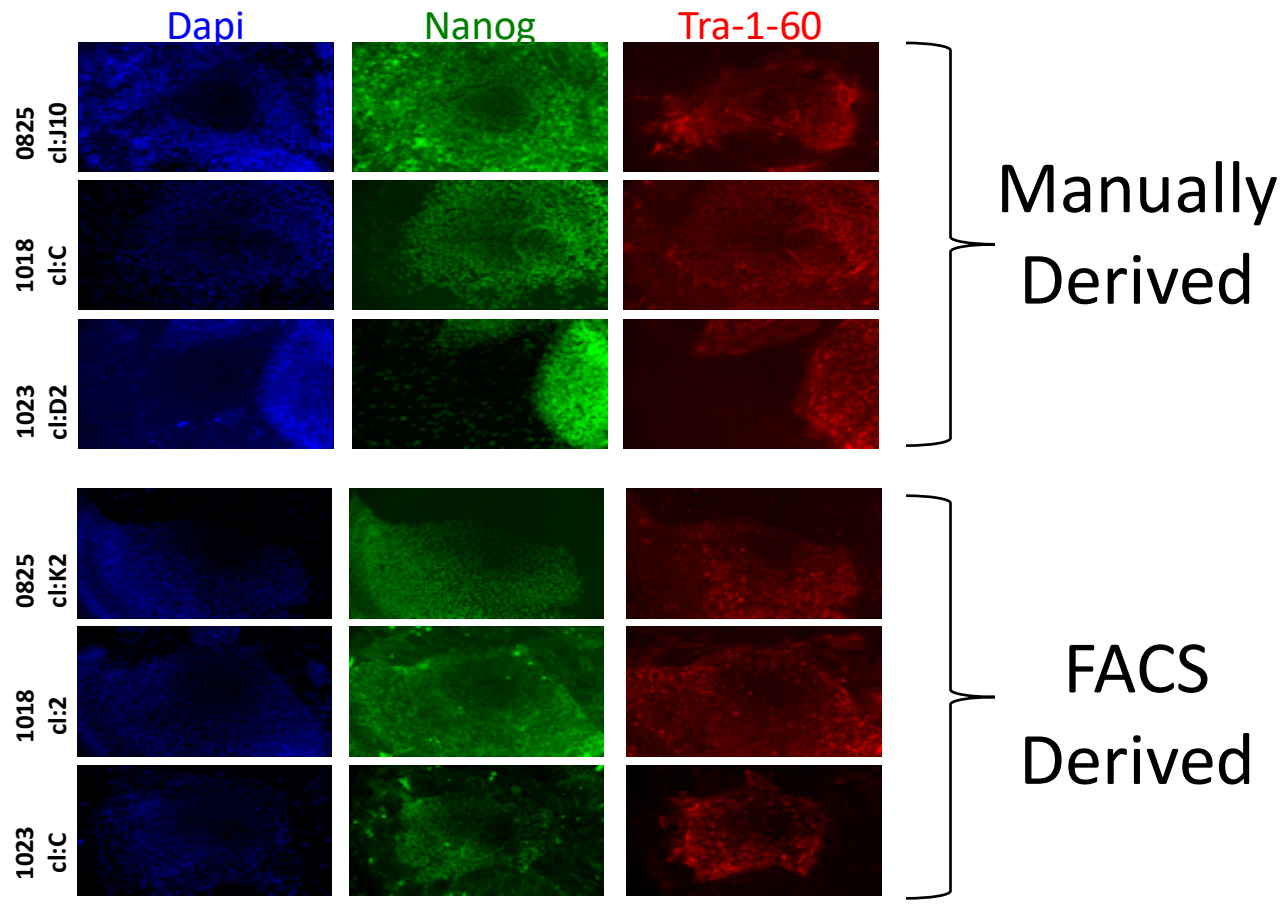

Figure 3.27 Characterization of Fluorescence Activated Cell Sorted and Manually Derived IPSC Lines. Immunofluorescence microscopy of the three cell lines demonstrating expression of common markers of pluripotency Nanog and Tra-1-60 by FACS or Manually Derived IPSC lines.

Both the manually and FACS-derived iPSC lines expressed common markers of pluripotency, including the surface marker Tra-1-60 and the transcription factor Nanog, and generated compact colonies morphologically consistent with normal hESCs, **Figure 3.27**. Next, the cell lines were expanded for ten passages and the expression of endogenous Nanog, Oct4, Sox2, cMyc, and Klf4, and silencing of the viral transgenes Oct4, Sox2, Klf4, and cMyc were assayed. I used a probebased Nanostring nCounter transcript quantification assay, to assess pluripotency by detecting both activation of endogenous gene expression **Figure**

3.28 and silencing of retroviral transgenes **Figure 3.29**. However, two of the three manually derived clones (1018_2 and 1023_C) maintained much higher expression of the viral transgenes than the sorted clones **Figure 3.29**. Additionally, the 1018_2 cultures expressed CD13, indicating the presence of non-reprogrammed or partially transformed human fibroblasts in the manually picked lines **Figure 3.29**. These analyses suggest that selection of single cells based on CD13–SSEA4+Tra-1-60+ expression can be used to select against partially reprogrammed or contaminating cell types in reprogrammed cultures.

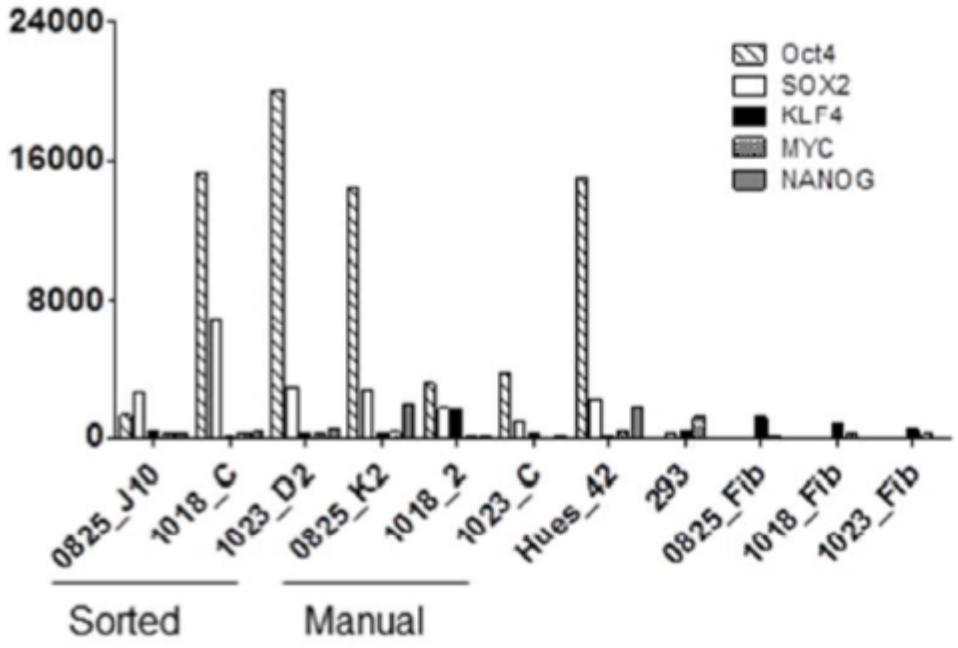

Figure 3.28 RNA expression. Activation of endogenous gene expression

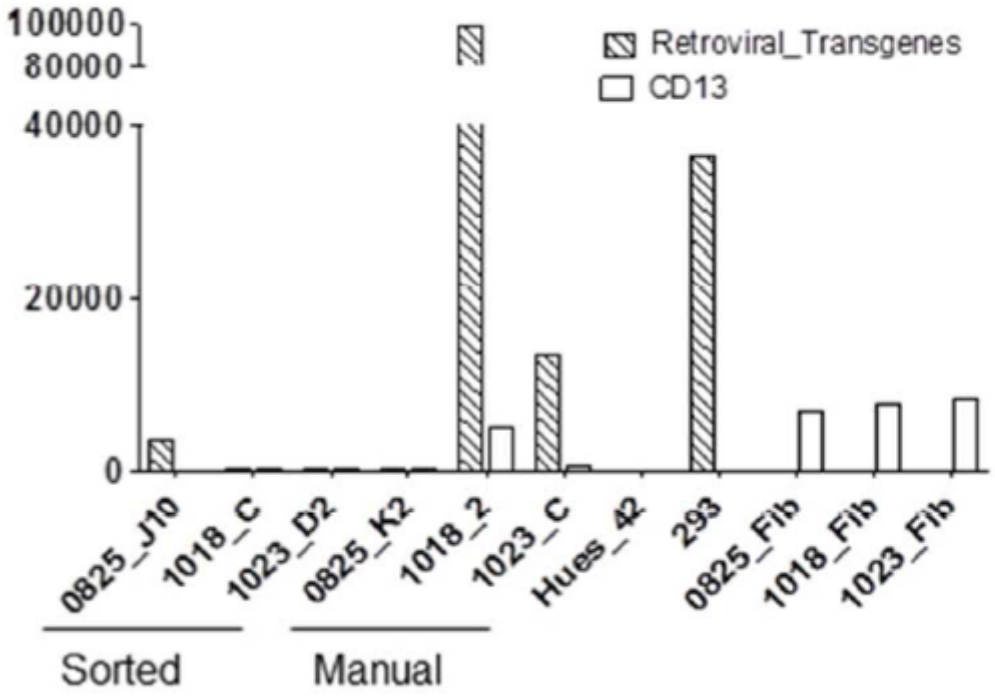

Figure 3.29 Silence of viral genes. silencing of gene expression and presence of unreprogrammed and transformed fibroblasts CD13+ in manually derived clones

Determination of differentiation potential

I next examined undirected EB formation to measure the *in vitro* differentiation potential of FACS and manually-derived iPSCs clones. Following differentiation for 5 weeks, EBs were collected and assayed for markers of three embryonic germ layers endoderm, mesoderm, and ectoderm by immunohistochemistry for α1-fetoprotein (AFP), smooth muscle actin (αSMA), and beta III tubulin (Tuj1), respectively. EBs derived from FACS or manually picked clones expressed markers associated with formation of the three germ layers **Figure 3.30**. To further define the differentiation potential of the derived lines, RNA from the EBs were collected after two weeks of differentiation and tested against a panel of lineage-specific nCounter probes previously validated to detect expression of genes commonly found in the three germ layers (Manos *et al.*, 2011) **Figure 3.31**. With the exception of the FACS-derived 0825 line, all lines expressed comparable levels of the germ layer-associated genes,

indicating they have similar potential to spontaneously differentiate *in vitro* into any germ layer.

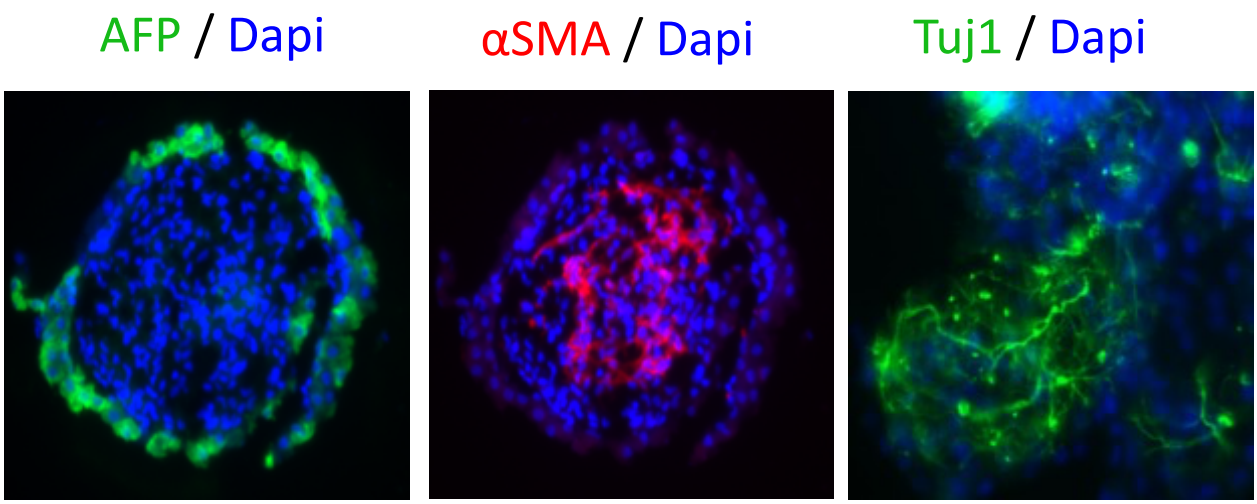

Figure 3.30 ICC differentiation of iPSCs. Embryoid bodies were derived from FACS and stained for expression of alpha fetoprotein, smooth muscle actin and beta III tubulin (Tuj1) to demonstrate differentiation potential *in vitro* potential. 10x Magnification

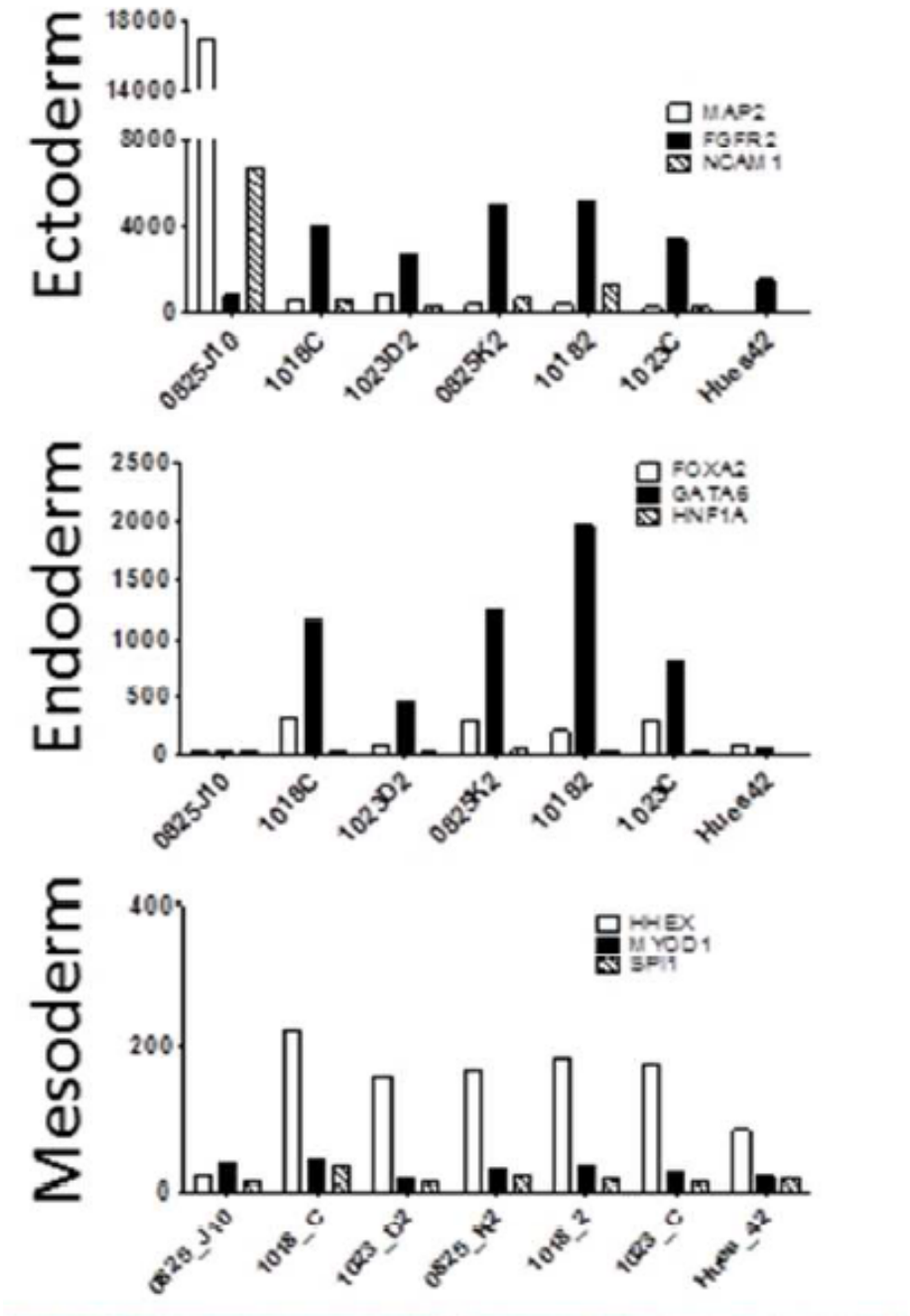

Figure 3.31 nCounter Pluripotency Panel. Differentiation potential of the derived lines for expression of germ layer genes present in the Lineage scorecard assay.

In vivo differentiation potential

To measure the *in vivo* differentiation potential of the iPSCs, immunocompromized mice were injected with FACS or manually derived clones from the 1023 fibroblast line. The resulting teratomas were sectioned and examined by H&E staining. This analysis showed that teratomas generated from sorted Figure 4 or manually derived Figure 4E clones formed all three germ layer tissues, including gutlike epithelial tissues (endoderm), cartilage (mesoderm), and retinal pigment epithelium (ectoderm). Together, these analyses validate the use of CD13–SSEA4+Tra 1-60+ expression as a surface marker signature compatible with FACS that can be used to isolate a population of fully reprogrammed iPSCs.

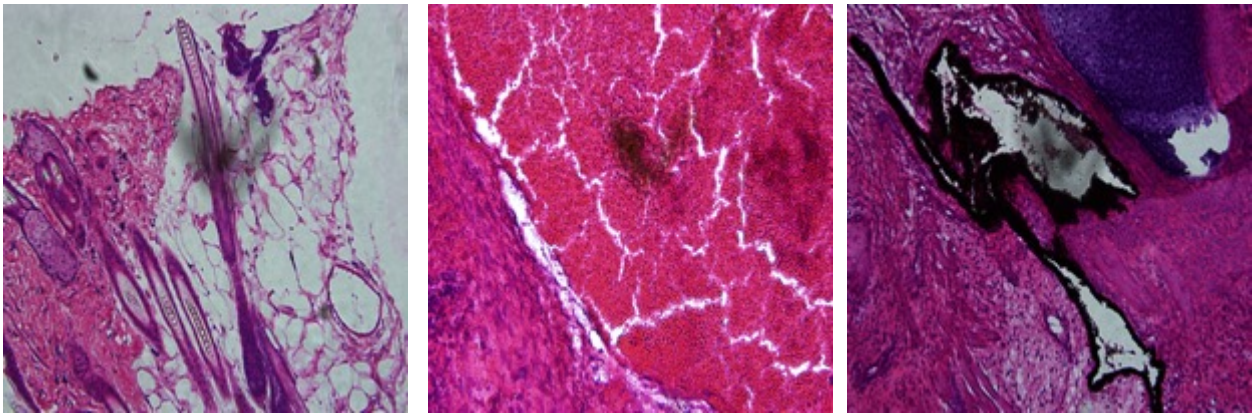

Figure 3.32 Teratomas generated from iPSCs. *In vivo* differentiation potential of the iPSCs, immunocompromised mice were injected with FACS derived clones. Resulting teratomas were sectioned and examed with H&E staining.

FACS derivation produces independent clones

Because iPSC lines can arise from rare apparently stochastic events at early time points during reprogramming, it was important to establish that FACS sorting could isolate multiple independent reprogramming events. To determine whether FACS derivation can produce unique cell lines in a similar manner to manual picking, we performed Southern blotting on several clones derived by both methods. Klf4 and Oct4 probes were used to identify the endogenous and virally integrated forms of the genes. Different banding patterns indicate differences in the chromosomal integration sites and, in some cases, varying

numbers of detectable integration events. As shown in **Figure 3.33,** all three sorted clones from line 1023 have different integration sites for both Klf4 and Oct4, demonstrating they are independent clones. In contrast, two of the three picked clones from line 1023 have identical banding patterns for Klf4 and Oct4, suggesting they are the same clone. Of the iPSC lines generated from three different fibroblast lines, 8/9 FACS-derived lines were independent clones, while 7/9 manually picked lines were independent (data not shown), suggesting equivalent ability to generate clonal cultures. Therefore, FACS sorting between 7-14 dpi using CD13– SSEA4+Tra-1-60+ can generate independent clonal cultures following retroviral reprogramming.

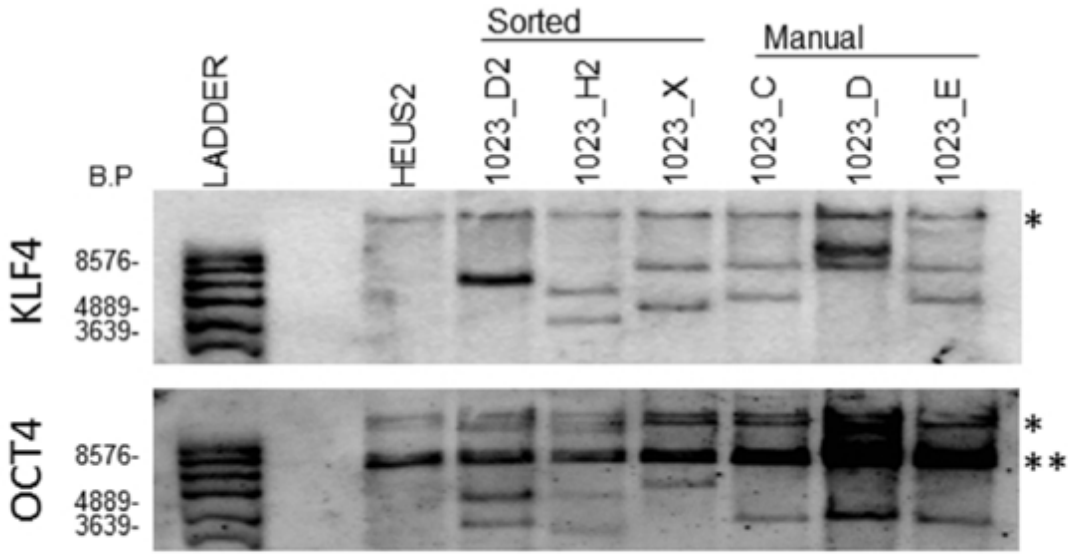

Figure 3.33 Southern Blot analysis on iPSC clonality. Three sorted and three picked lines from patient 1023 were used to compare the ability of both methods to generate independent clones. 10 µg of genomic DNA were cut overnight with BglII and submitted to Southern blotting. The HuES line HES2 was used as a positive control for endogenous KLF4/OCT4, and as a negative control for transgene insertions. Samples were first blotted for KLF4, then stripped and reblotted for OCT4. Picked clones 1023 C and E are consistent with being the same clone by both KLF4 and OCT4 blotting. * indicated the predicted endogenous KLF4/OCT4 bands, and ** indicated a consistent band found in all samples blotted with OCT4.

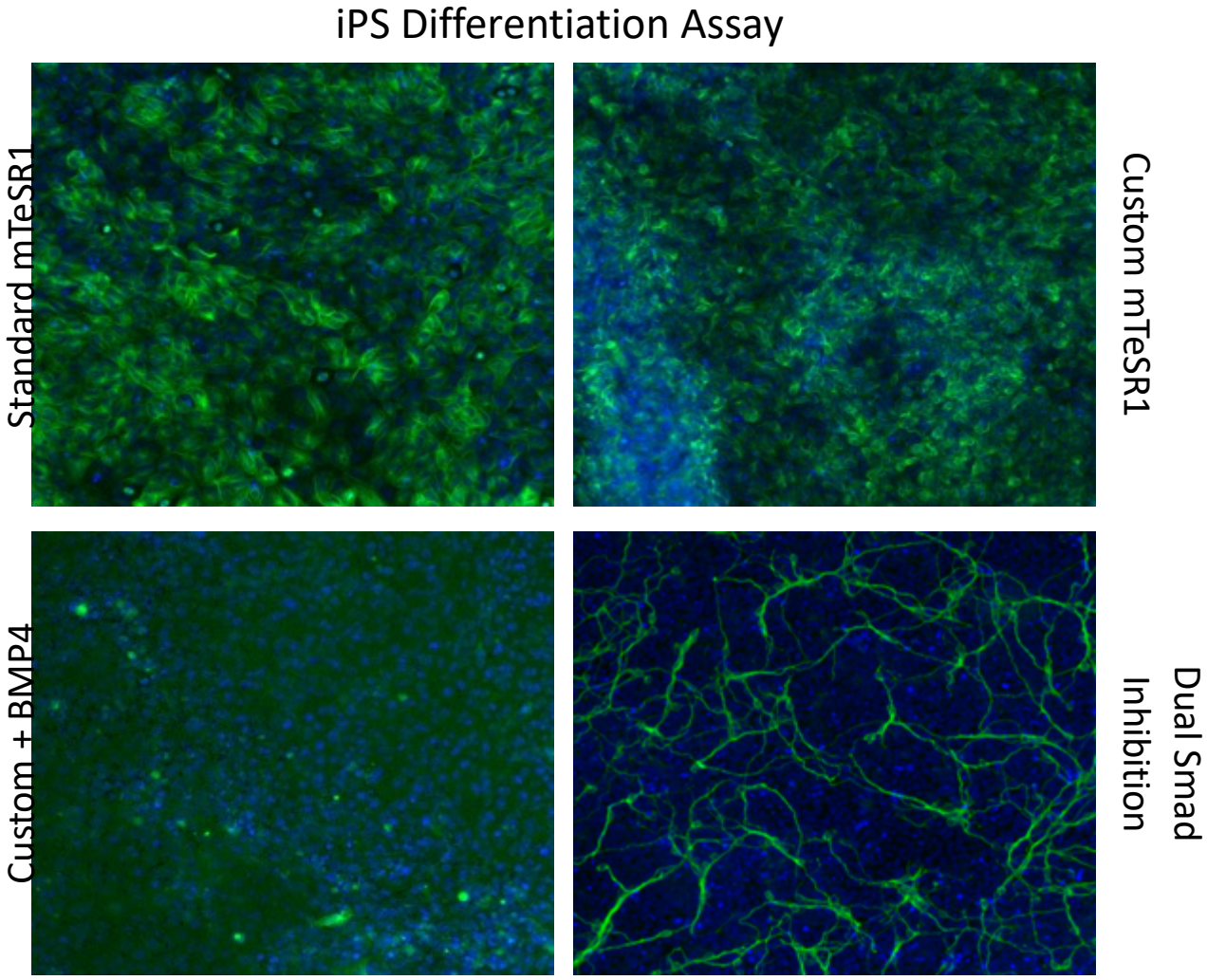

Figure 3.34 IPS differentiation in different culture mediums. Distribution of TUJ1 staining in various differentiation based media's. Dual SMAD inhibition yields morphologically distinct neural cells. Magnification 4x

3.3 Discussion

PLGA microspheres are biocompatible and can be very functional and stable in supplying factors to hESCs consistently over extended amounts of time. There are many other possible applications for biocompatible microspheres, through the loading of proteins and pharmaceuticals other than FGF2. Another group has described dually loaded microspheres with both dexamethasone (DEX) and FGF2 for rMSCs (Liang, 2012). The next initiative to utilize microspheres would be to encapsulate other proteins or compounds for a steady release. One specific example is that hESC derived neural induction is greatly dependant upon dual

SMAD inhibition. If microspheres were then to be loaded with Noggin and SB431542, replenishment of media and feeding occurrences could be reduced during the 10-day induction. Microspheres also have potential *in vivo* with use for drug delivery. With endless possibilities, there is a great need for imagination and optimization when regarding PLGA microspheres.

Clinical application of iPSC technology will require standardized and reproducible methods for each step of derivation and differentiation into relevant cell types. I have found that the majority of manually derived iPSC lines contain CD13+ cells even after prolonged culture suggesting that these lines were either not fully reprogrammed or that CD13+ cells were carried over during passage. While both manual picking and FACS sorting methods (Kahler *et al.*, 2013) have been used to isolate reprogrammed pluripotent cells, I demonstrated that inclusion of a negative selection marker such as CD13 has significant advantages in improving the purity of reprogrammed cultures. Here, I have validated a surface marker profile that enables selection of early reprogrammed iPSCs following reprogramming with either DNA-integrating or non-integrating viruses by FACS. Employing this strategy as early as 7 dpi isolates a highly purified starting population of fully functional CD13–SSEA4+Tra-1-60+ cells that are depleted of contaminating non-transduced and transformed fibroblasts. To make this clinically applicable I have successfully generated and characterized 228 individual iPSC lines in the past 4 years from 76 fibroblast lines obtained from fresh biopsies, frozen stocks, and cell line repositories harvested from healthy and individuals possessing various forms of diabetes, neurodegenerative, cardiac and autoimmune diseases. Moreover, I've routinely used FACS for maintenance of established cell lines to remove differentiated cells and to dispense graded numbers of highly purified CD13- SSEA4+Tra-1-60+ populations cells for use in high-throughput derivation and screening assays which include directed differentiation and automated drug screening and phenotyping experiments. This is an important property because the results of these assays could be unequivocally attributed to a defined population of

reprogrammed cells rather than to a heterogeneous mixture of cells. Taken together, these results suggest that isolation of the CD13–SSEA4+Tra-1-60+ population following reprogramming, including integrating or non-integrating viral technologies, allows for the rapid isolation of high quality iPSC lines. Negative selection against CD13+ cells significantly reduces the appearance of transformed cells in iPSC cultures and suggests that negative selection for a marker present on the starting somatic cells can be used to exclude nonreprogrammed or transformed cells from the cultures. Future studies will be needed to determine if this strategy applies to derivation from other somatic cell types or reprogramming methods.

Rationale to develop optimized techniques in pluripotent stem cell biology

Human pluripotent stem cells (hPSCs) provide powerful resources for application in regenerative medicine and pharmaceutical development. In the past decade, various methods have been developed for large-scale hPSC culture that rely on combined use of multiple growth components, including media containing various growth factors, extracellular matrices, three-dimensional environmental (3D) cues and modes of multicellular association. It has been critical to dissect these growth components by comparing cell culture methods and identifying the benefits and pitfalls associated with each one before delving in to establishing differentiation paradigms. This chapter has helped inform and further provide criteria, considerations, and suggestions to achieve optimal cell growth for hPSC expansion, which in turn improves capabilities in differentiation, and use in future therapeutic applications.

CHAPTER 4: DIRECTED DIFFERENTIATION OF PLURIPOTENT STEM CELL LINES TOWARDS MATURE ATRIAL CARDIOMYOCYTES.

Chapter 4: Directed Differentiation of pluripotent stem cell lines towards mature atrial cardiomyocytes.

4.1 Introduction

Adult somatic cells are stringently programmed to execute very precise functions that involve both structural and intracellular components in order to accomplish specific tasks. Throughout post-implantation embryo development, there is a certain degree of plasticity with cells being specified as development continues. However, after a certain point natural plasticity is halted and the cells have already become determined as to which cell fate is acquired after birth. Strategies to induce reprogramming of somatic cells after birth started as early as 1958, when Sir John Gurdon and colleagues in Cambridge, UK, pioneered nuclear transfer in frogs (Evans, 2011). Decades later Sir Ian Wilmut cloned Dolly the sheep (Wilmut *et al.*, 2001) . Since Sir John Gurdon and colleagues, progress slowed in the field, until 20 years ago it was realized that the technique could be used to regenerate tissue and develop *in vitro* models of disease for drug testing and genetic manipulations. As a result, this ushered in a massive expansion within the field for developing reprogramming techniques which include somatic cell nuclear transfer, forced gene expression, microRNA strategies, chemical inducers to derive pluripotent stem cells as well as directly converting somatic cells towards desired cell fates. All of which have shed light on the mechanisms of directed differentiation towards cardiomyocytes.

Lessons from developmental biology: generation of cardiomyocytes from PSCs

The power of developmental biology has given us fundamental insights, into the intricacies and mechanisms by which commitment towards cardiac cell fates occur. Gastrulation begins with mesoderm induction through nodal signaling in the primitive ectoderm. Nodal, a cytokine belonging to the TGF-b superfamily, plays a critical role during the formation of the primitive streak and germ layers. During gastrulation, cardiac cells are

amongst the first cell lineages to be established from cells fated to become the mesoderm which emerges from the primitive streak. The cells arising from this anatomical space, contain mesoderm transcription factors such as: mesp1, bmp4, wnt3, and brachyury (Evans, 2011). These genes act to induce and regulate cardiovascular lineage specification and commitment and in turn activate factors involved in cardiac differentiation and maturation, as well as drive gene expression of nkx2.5, gata4, mef2c, and tbx5 (Sanders *et al*., 2016). Interestingly, in human iPSCs MESP-1 also represses early mesoderm induction through direct inhibition of WNT and nodal signaling pathways by DKK1 and CER (Sanders *et al*., 2016). Accordingly, induction of cardiac differentiation of human PSCs can be initiated by sequential stimulation with specific recombinant growth factors such as basic fibroblast growth factor (bFGF), BMP4, WNT3, and activinA, followed by addition of DKK1 or other WNT inhibitors (Bylund and Hatzopoulos, 2016). Newer protocols have relied on modulation of WNT signaling in order to achieve ventricular cardiomyocyte specification (Bylund and Hatzopoulos, 2016). Further cytokines have been reported to increase the differentiation efficiency such as the vascular endothelial growth factor (VEGF) (Bylund and Hatzopoulos, 2016), Noggin (Liu *et al*., 2004) (BMP antagonist), and IWR-1/IWP-276 (inhibitors of WNT) (Hao *et al*., 2008) among others. Taken together, insights from lineage tracing studies have better informed us in generating novel protocols allowing the production of ventricular CMs from PSCs (Hao *et al*., 2008). Coincidently, these efforts have not addressed purity, maturation, as well as subtype specific lineage generation (Evans, 2011).

Improvement of CMs differentiation

Many strategies have been proposed to improve the differentiation and maturation of iPSC derived CMs. In particular, hypoxic culture conditions (Sheng *et al.*, 2014) knockdown

of selected genes, (Sheng *et a*l., 2014) and forced aggregation of iPSCs-derived EBs in a chemically defined medium (Sheng *et al.*, 2014) have shown promising results.

Further, a high-throughput screening system has been established to identify small molecules that promote the differentiation of CMs from iPSCs. Among these, vitamin C (Xie *et al.*, 2014) cyclosporine A (Takahashi and Yamanaka, 2006) (immunosuppressant), and triiodothyronine (Takahashi and Yamanaka, 2006) (T3, thyroid hormone) showed a marked induction of cardiac differentiation. Of note, the exogenous expression of human Apolipoprotein-A1(Takahashi and Yamanaka, 2006) or induction of the Wnt/b-catenin signaling pathway(Takahashi and Yamanaka, 2006) have been shown to enhance cardiac differentiation and maturation of hESCs and hiPSCs. These cardiogenic effects are thought to be mediated by the BMP4/SMAD signaling pathway. A recent publication of highly reproducible and efficient differentiation protocols, via temporal modulation of canonical Wnt signaling (90% of differentiation), (Kim *et al.*, 2001) sets the path for clinically scalable applications. Aside from all the different iPSC to CM differentiation protocols that are being considered, a crucial parameter influencing the differentiation potential is the cellular origin of the iPSCs (Kim *et al.*, 2001). This is likely to be due to the "epigenetic memory" of iPSCs, which manifests as differential gene expression.

Lesson from embryology and factors involved in hPSC cardiac differentiation.

During mouse embryonic development at E5.5 gastrulation occurs by the formation of the primitive streak. An epithelial to mesenchymal transition (EMT) of anterior primitive ectoderm allows cells to move laterally between primitive ectoderm and visceral endoderm. At E6.5 cells located proximally to the primitive ectoderm go on to form the extraembryonic mesoderm. Cells adjacent to this zone form heart, blood and mesoderm derivatives. The most distal portion of the primitive streak gives rise to endoderm cells. At E7.0 the lateral plate

mesoderm is formed which delaminates to form two layers. Cardiac mesoderm goes on to form the first heart field (FHF) laterally and more ventrally the second heart field (SHF) is formed both by coordinated expression of Dkk1, MESP1, Nodal and WNT signaling. Other cardiogenic signals, such as BMP and FGF, activate cardiac-specific transcription factors such as Nkx2.5, GATA4, HAND2, which coordinate to move both heart fields to the midline. Whereby at E7.5, the FHF progenitors form the heart tube which later contributes to the left ventricle. SHF progenitors join with the CMs of the FHF which leads to the rightward looping of the cardiac tube which eventually progresses towards formation of cardiac chambers. In brief, the two major factors determining iPSC differentiation to CMs are the starting cell population and the cardio-inductive growth factors used.

Clinical applicability limitations

Following differentiation, even if great yields are obtained, only pure CMs could potentially be used clinically. The iPSCs derived CMs therefore need to be purified and enriched before potential implantation to avoid risks of teratoma formation or inappropriate tissue engraftment. Frequently used methods include manual dissection of spontaneously beating CMs using a pulled-glass micropipette (Raynaud *et al.*, 2015) cell separation based on density gradient, (Kim *et al.*, 2001) and fluorescence-activated cell sorting (FACS). Physical enrichment by manual dissection or density gradient separation has limited success due to their low yield. The FACS technique relies on a positive selection of CMs cells that are phenotypically different from other cells. This can be realized by tagging cardiac-specific proteins with fluorescent antibodies followed by a subsequent step of detection and sorting using a FACS machine. Hence, a panel of surface markers is being used for the enrichment of CMs. This panel includes the following surface markers: CD166, vascular endothelial growth factor 2 (VEGFR2) and platelet-derived growth factor-a (PDGFR-a), elastin microfibril

interface 2 (EMILIN2), (signal regulatory protein-a (SIRPA-a), and vascular cell adhesion protein1 (VCAM1). (Sheng *et al.*, 2014) (Ehrlich *et al.*, 2005) (Cardin *et al.*, 2003) (Hayashi *et al.*, 2017)

A major limitation for this approach is the lack of specific CM surface markers that could specifically identify and select only cardiac cells from a pool of differentiating/undifferentiating cells (Melkoumian *et al.*, 2010a) Therefore, genetically modified hESCs lines have been developed to select the terminally differentiated CMs based on the expression of a luminescent reporter gene (e.g the green fluorescent protein, GFP) coupled to the regulatory sequence of a cardiac-specific gene like MYH6(Willems *et al.*, 2011) Nkx2.5 (Willems *et al.*, 2011), myosin light chain 2V (MLC2V) (Willems *et al.*, 2011), and insulin gene enhancer protein 1 (ISL1) (Willems *et al.*, 2011), The expression level of the reporter fluorescent proteins reflects the transcriptional activity of the attached cardiac gene. Although the latter method showed a marked CMs purification and enrichment, they obviously cannot be used on a larger scale or for clinical applications. Interestingly, Hattori et al. reported that a fluorescent dye that labels mitochondria may serve as a selective marker of hESCs/hiPSCs derived CMs. The authors claimed that a significant enrichment of CMs with a high degree of purity (99%) could be obtained by FACS with this dye (Hattori *et al.*, 2010) . Purification and enrichment of PSC derived CMs is an important limiting step for cell-based therapy for cardiac regeneration. Though different protocols for purification and enrichment of CMs have been proposed, their efficiency is controversial. An efficient method of purification should be fast, specific, and scalable with no genetic modifications. Such a method would greatly enhance the potential of iPSC derived CMs in the cardiology clinic.

Cell-type specificity and maturation

Maturation of iPSC-derived CMs Beyond the differentiation protocol improvements, much work focused on the maturation of PSC derived CMs. Indeed, the maturity of generated CMs remains a critical bottleneck. For instance, despite the fact that iPSC derived CMs present most of the characteristics of adult CMs (self-induced action potential, proteins/genes expression), the generated cells lack maturity for the most part (no expression of mlc2v contractile protein, lack of organization, absence of M-band etc) and more closely resemble embryonic CMs than adult CMs (Verma and Mcneill, 1976) . A remarkable publication by Murry and colleagues (Chong *et al.*, 2014) showed that implantation of a large number of human embryonic stem cell-derived CMs in non-human primates following heart failure could lead to re-muscularization of infarcted heart and even electromechanical junctions with surrounding muscle, but even over a three month period, cells failed to completely mature, and the non-human primate ultimately experienced arrhythmic complications. Long term culture of PSC derived CMs has been shown to improve the maturity of differentiating cells, but remains of restricted interest for potential clinical applications (Chong *et al.*, 2014). Our group and others have previously demonstrated that a forced alignment of the cells improves the maturity of the CMs generated (Melkoumian *et al.*, 2010b). The mechanical and electrical stimulation of derived CMs has also been proven to favor maturation of cells toward an adult phenotype (Rangarajan *et al.*, 2014). Besides, the use of scaffolds for maturation of CMs may lead to their potential interest for clinical use.

IPSCs and targeted gene therapy

While use of iPSCs proposes to circumvent the autologous hurdle of cell therapy, this technique cannot be used straight away for patients presenting disorders linked to genetic abnormalities. The ability to generate gene targeted mutations or manipulations in iPSCs has opened new areas of research in dissecting multifaceted genetic interactions. It has become

increasingly easy to utilize genome engineering techniques which involve site-specific nucleases acting as DNA scissors that introduce double strand breaks, allowing expression of nucleotide alterations, knockin reporters, and small insertions or deletions to study loss of function mutations. The possibility of using iPSCs for targeted gene therapy reflects further their promising therapeutic potential. Hockemeyer et al. demonstrated in 2011 the possibility of genetic engineering hESCs and hiPSCs using TALE nuclease (Hockemeyer *et al*., 2011). Reversion of disease mutation was further demonstrated in hPSCs by various groups utilizing CRISPR-Cas and TALENs (Jessup *et al*., 2015). For example, Jessup *et al*. showed that overexpression of SERCA2a via gene therapy can improve the contractility of iPSCs derived CMs of dilated cardiomyopathy patients. (Jiang *et al.,* 2014) Jiang *et al*. demonstrated that the allele specific silencing of a dominant mutation could suppress hypertrophic cardiomyopathy condition in mice. Subsequently, other groups have introduced conversion of normal genes to disease models by genome editing, targeting specific mutations to mimic known diseases and syndromes in hPSCs. (Gonzalez *et. al.,* 2016) Gonzalez and colleagues., have even combined two gene editing tools, TALEN and CRISPR/Cas systems, developing a more efficient platform which can rapidly and simultaneously introduce multiple gene alterations along with stage specific inducible genetic alterations which they named the iCRISPR platform (González *et al.*, 2014). Thus, the possibility to use the high proliferative capacity of iPSCs would enable the expansion of clonal populations of genetically modified iPSCs *ex vivo* followed by their subsequent differentiation and subtype-specific maturation.

4.3 Results

Isolation and expansion of cardiac cells from stem cells

It should be emphasized that the human atrial cardiomyocyte derivation from iPSCs was established for the first time in the lab. Prior to starting my DPhil studies, I had been involved in developing various iPSC derivation and differentiation techniques for derivation of neural cells and ventricular cardiomyocytes. It was my belief that within the cardiovascular field, we would need to understand the development of all three types of cardiovascular cell types (ventricular, atrial, and nodal) in order to address the regenerative potential of cardiomyocytes in cellular therapeutic applications.

iPSC characteristics

In order to investigate, as proof of principle, the feasibility of deriving patient-specific human iPSCs from patient samples as described in Chapter 3 of this thesis, were kindly provided by Prof. Magdi Yacoub from the Magdi Yacoub Institute, Imperial College London, UK. The fibroblasts were transduced with Sendai virus vectors encoding OCT4, KLF4, SOX2 and c-MYC as previously reported in Chapter 3. These cells were expanded from frozen vials. After plating, human iPSCs adhered on to a matrigel-coated surface. A monolayer of compact cell colonies with high nuclear to cytoplasmic ratio started to appear 3 days post plating. After approximately 7 days, small round phase bright cells could be seen all over the matrigel coated dish. As shown in **Figure 4.1**, the photomicrographs show the small, tightly packed cells with large nuclei that make up the colonies. These iPSCs continued to proliferate and expand prior to harvesting for differentiation experiments.

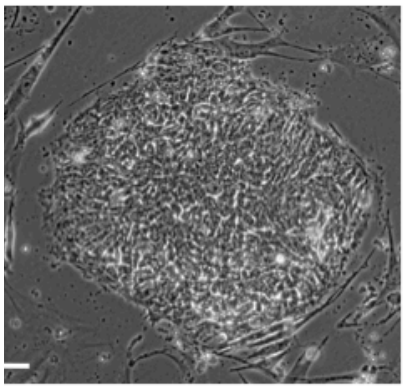

Figure 4.1 Characterization of iPSC. Representative normal morphologies of iPSCs used here and in all subsequent experiments.

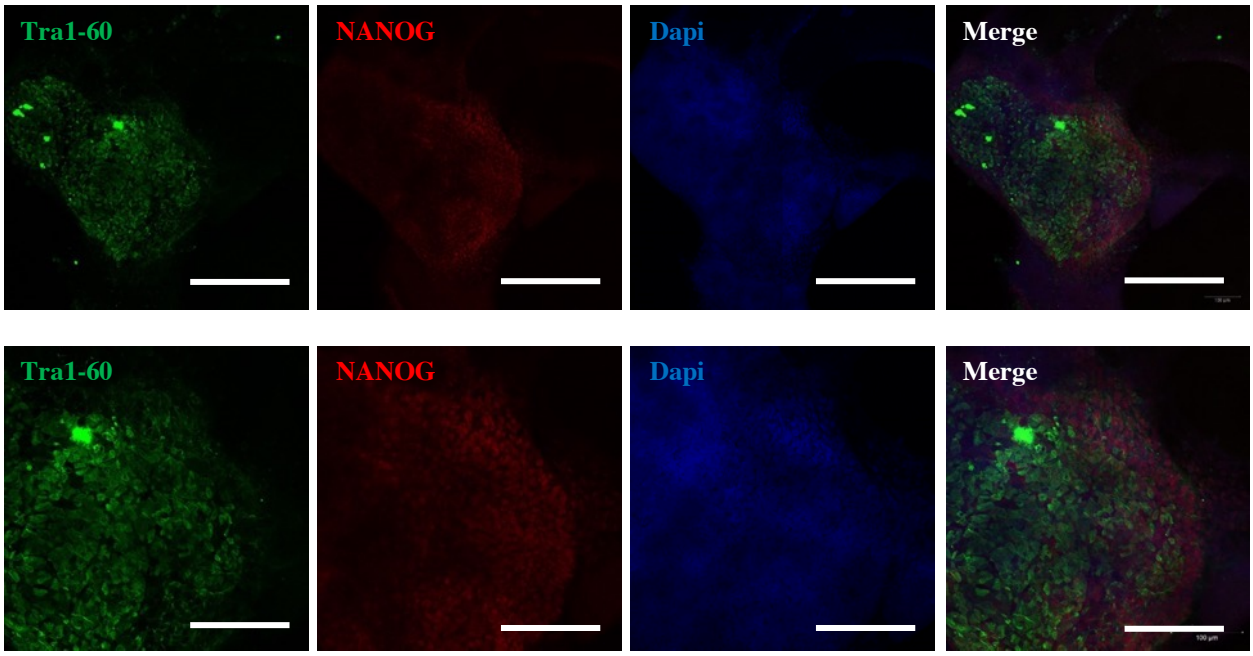

Figure 4.2 Immunocytochemical analysis of iPSCs. Immunocytochemical analysis of pluripotent marker expression (TRA-1-60, NANOG) in iPSCs. Scale bars represent 50μm,

Pluripotency is known to be maintained by the expression of a range of markers including transcription factors Oct3/4 and Nanog and further characterized by the expression of cell surface markers Tra-1-60 and SSEA-4 (Kahler *et al.*, 2013). In order to investigate the expression of these pluripotency markers by the iPSC lines used in this study, cells were stained and analyzed by immunocytochemistry. All the iPSC lines generated in this study, were assayed for phenotypic analysis by formation of ES-like colonies (Figure 4.1, 4.2, and 4.3). This includes, nuclear and surface markers characteristic of human stem cells. Of the cells used for subsequent studies I checked for adequate morphology, low persistence of

transgene expression, ability to form embryoid bodies and in some instances I performed teratoma assays. Figure 4.2 shows images from iPSC01 and iPSC02 positive for both cell surface marker Tra-1-60 and transcription factor NANOG. Subsequently Figure 4.3 shows all of the iPSCs used for directed differentiation exhibited SOX2 staining which is also a pluripotent stem cell marker. Taken together, the results indicate that the iPSCs represent a homogenous cell population of pluripotent stem cells which has the potential to form any somatic cell type.

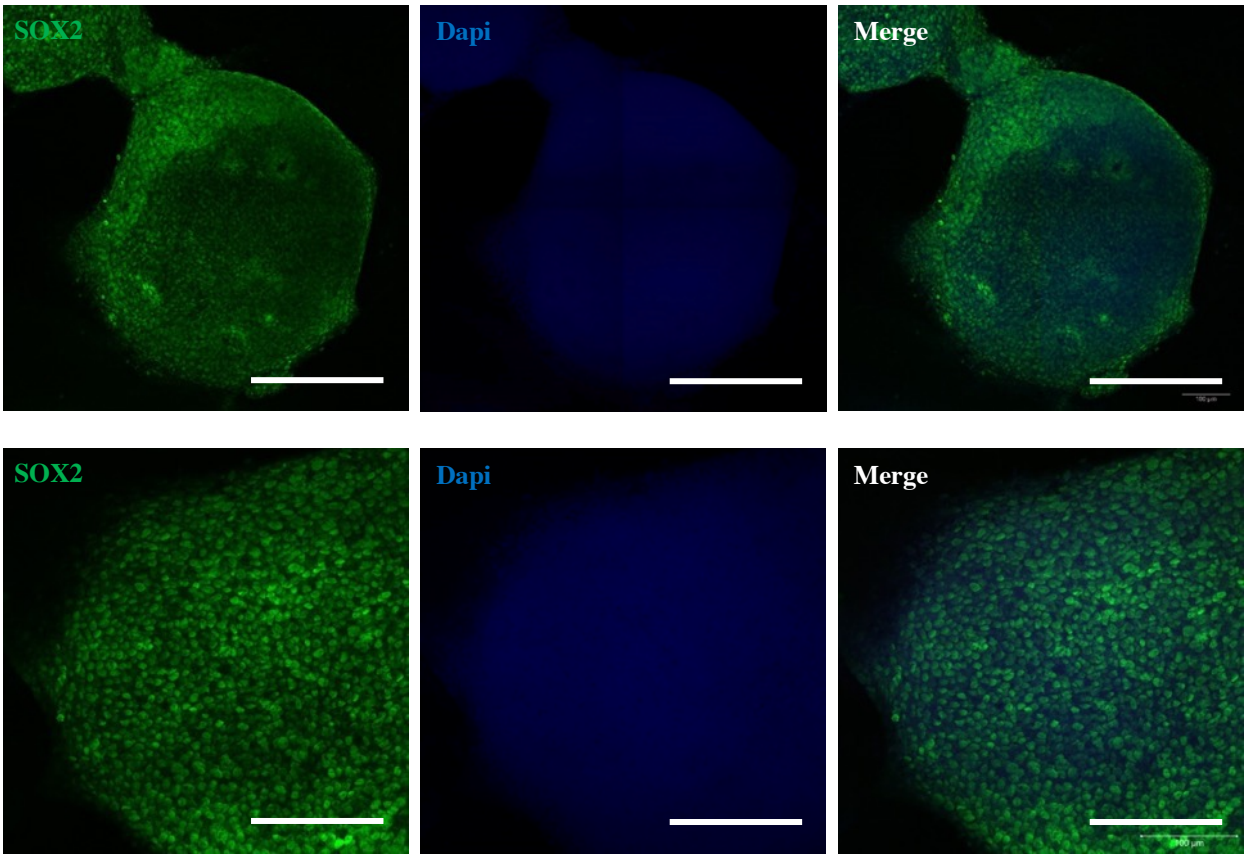

Figure 4.3 Immunocytochemical analysis of iPSCs. Immunocytochemical analysis of pluripotent marker expression (Sox2) in iPSCs. Scale bars represent 50μm,

Pluripotency Gene Expression of iPSCs.

Once the cells were confirmed by bright field and fluorescent microscopy, I next inspected the iPSCs during the expansion phase, towards transcriptome analysis of pluripotency genes using qRT-PCR. It appears that the cell lines generated and expanded

using the techniques developed in chapter 3 of this thesis suggest adequate levels of pluripotency genes. As shown in Figure 4.4, 4.5, and 4.6, all three cell lines show increase levels of SOX2, NANOG, and OCT4. Having shown the phenotypic characteristics of the iPSCs both here and in Chapter 3 that are consistent with their pluripotency, it was investigated whether these iPSCs could be expanded and successfully differentiated in to pan-cardiac cells.

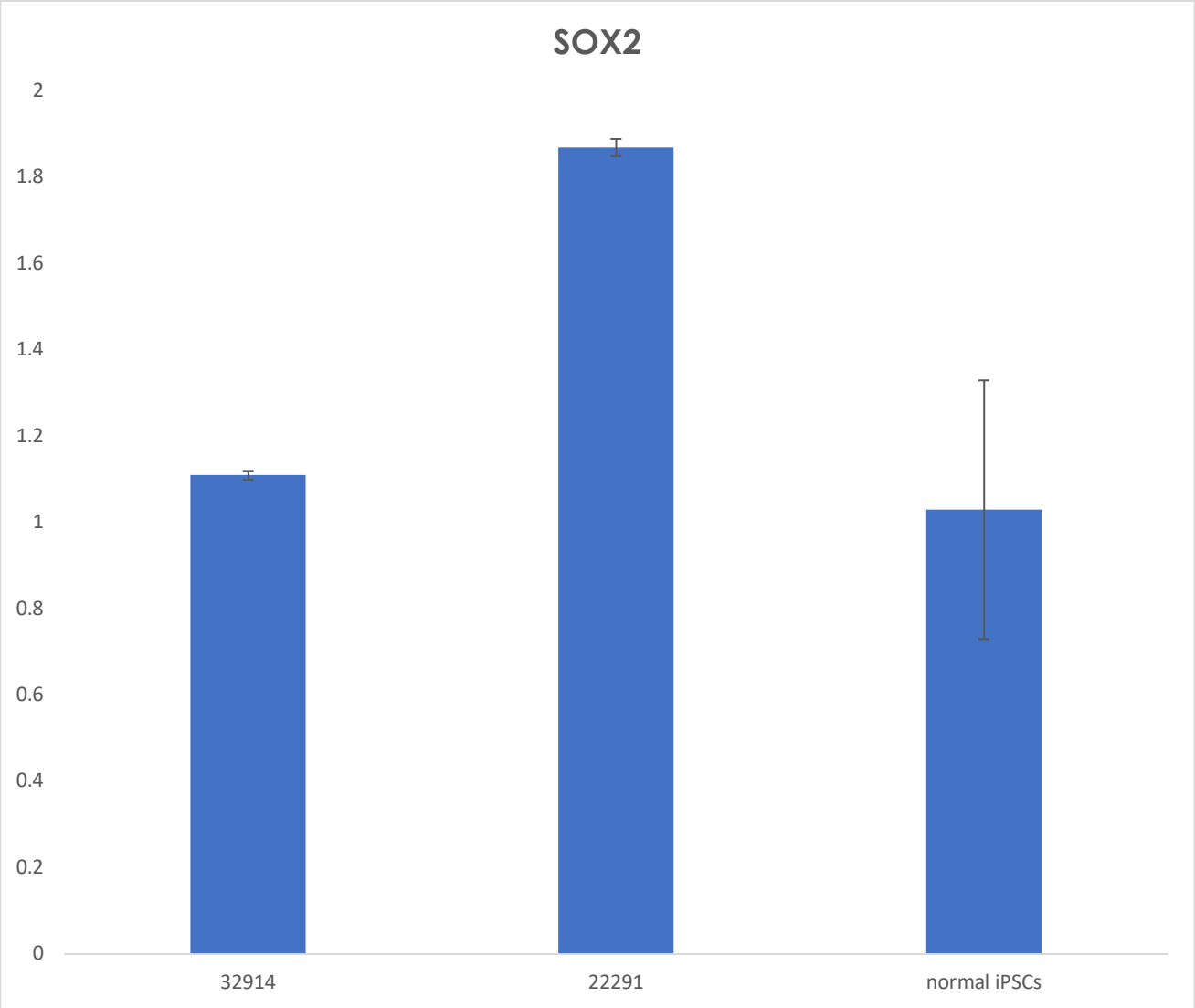

Figure 4.4 Levels of pluripotentcy gene expression in 2 disease patients and 1 normal iPSC line measured by qRT-PCR. Samples were normalized to the gene HPRT. The experiment was repeated twice with similar results.

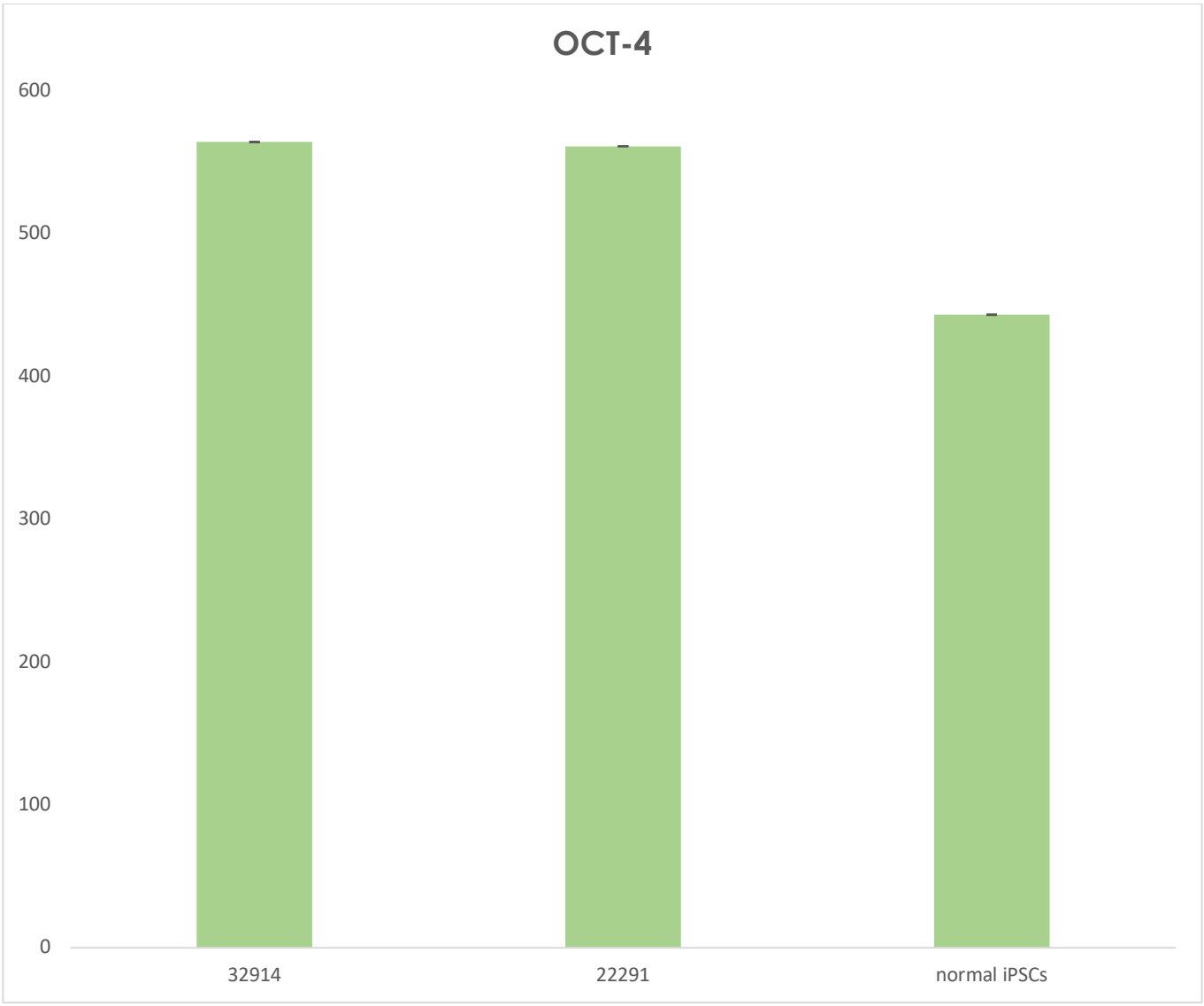

Figure 4.5 Levels of pluripotentcy gene expression in 2 disease patients and 1 normal iPSC line measured by qRT-PCR. Samples were normalized to the gene HPRT. The experiment was repeated twice with similar results.

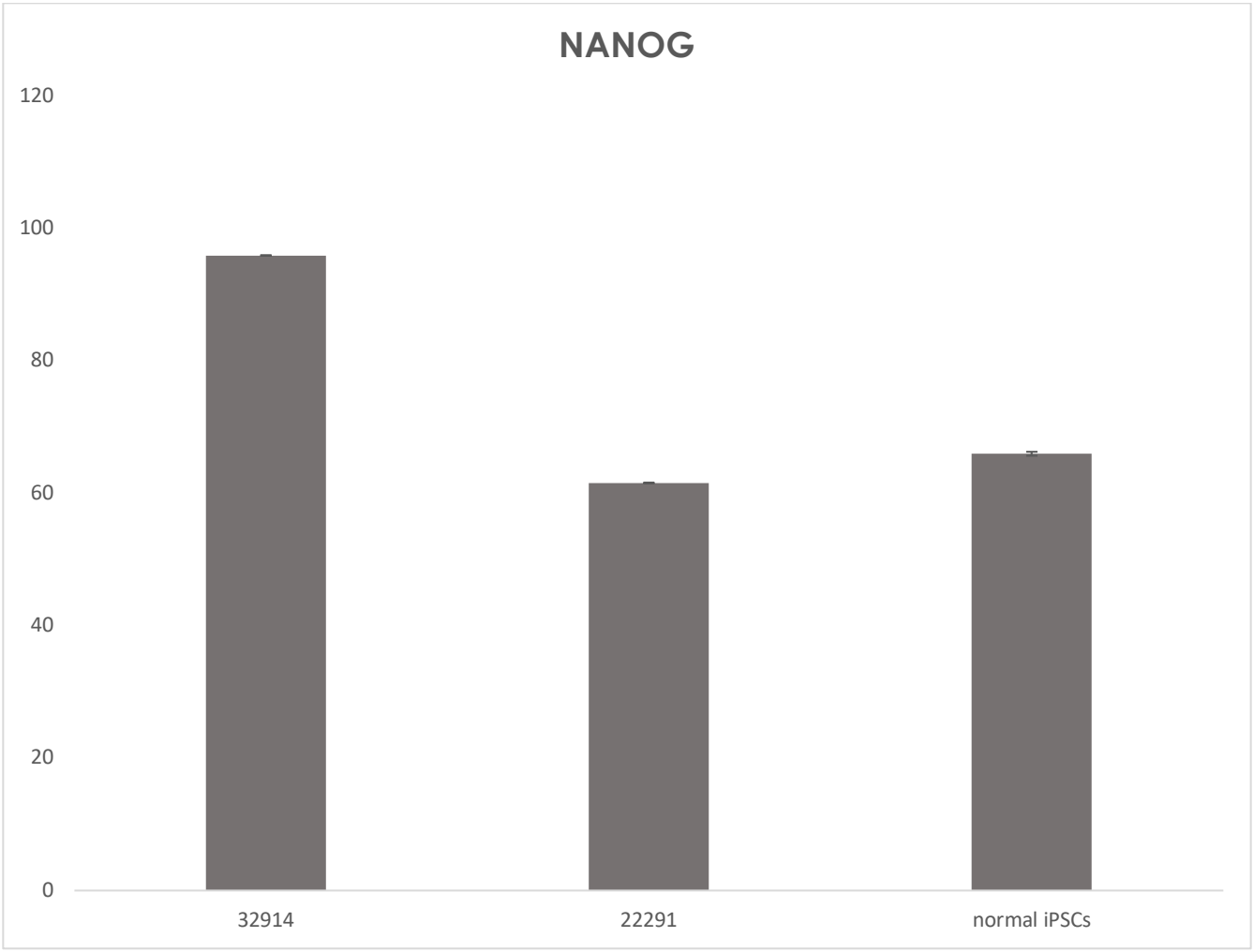

Figure 4.6 Levels of pluripotentcy gene expression in 2 disease patients and 1 normal iPSC line measured by qRT-PCR. Samples were normalized to the gene HPRT. The experiment was repeated twice with similar results.

Differentiation of ventricular cardiomyocytes from iPSCs.

Once the iPSCs were cultured to 80% confluency, cells were harvested and plated on matrigel coated dishes for differentiation. Modulating levels of cytokines during the differentiation within the media allows cells to be directed in their differentiation towards the mesoderm lineage for generation of cardiomyocyte-like cells.

As a first step toward analyzing the effects of modulating the differentiation paradigm in order to increase subtype specific atrial cardiomyocyte generation, I differentiated one iPSC line per patient into ventricular cardiomyocytes using a 14 day monolayer based protocol (Lian *et al.*, 2012) that generated majority cultures of ventricular myocytes, and fewer atrial and sinoatrial node cells. All 4 patient specific iPSCs were used to generate the cardiomyocytes with comparable efficiency to the control iPSC01 cell line used as measured by the cardiomyocyte marker TNNT2 as shown in **Figure 4.8**. I further adapted this monolayer differentiation protocol with addition of RA at 500nM concentration from Days 4-12 and Grem2 at 5ug/ml concentration on day 4 **(Figure4.7)**. The protocol used for ventricular differentiation was the same with the exception of adding RA and Grem2 as shown in the schematic in **Figure 4.7**.

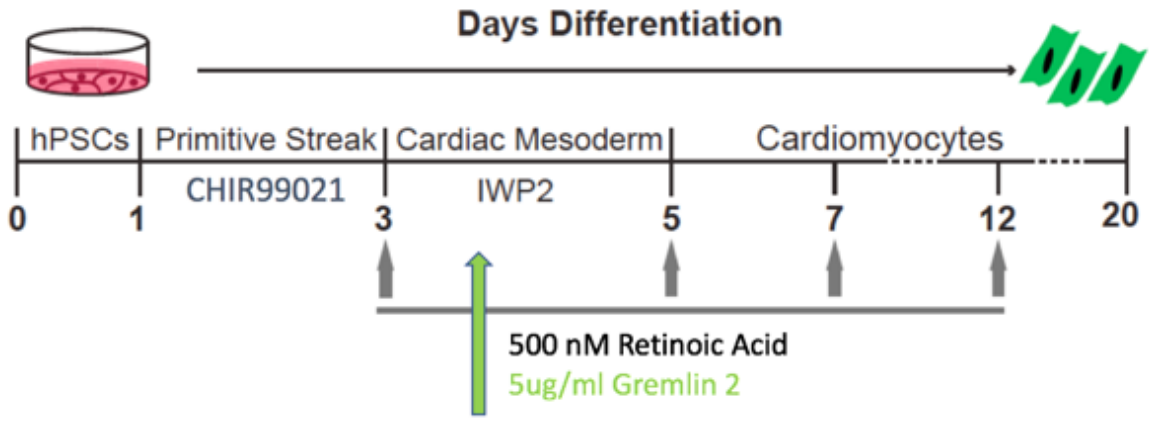

Figure 4.7 Directed differentiation towards atrial cardiomyocytes from human iPSCs. Schematic of the hiPSC cardiomyocyte differentiation protocol indicating developmental stages and timing of RA addition and Grem2.

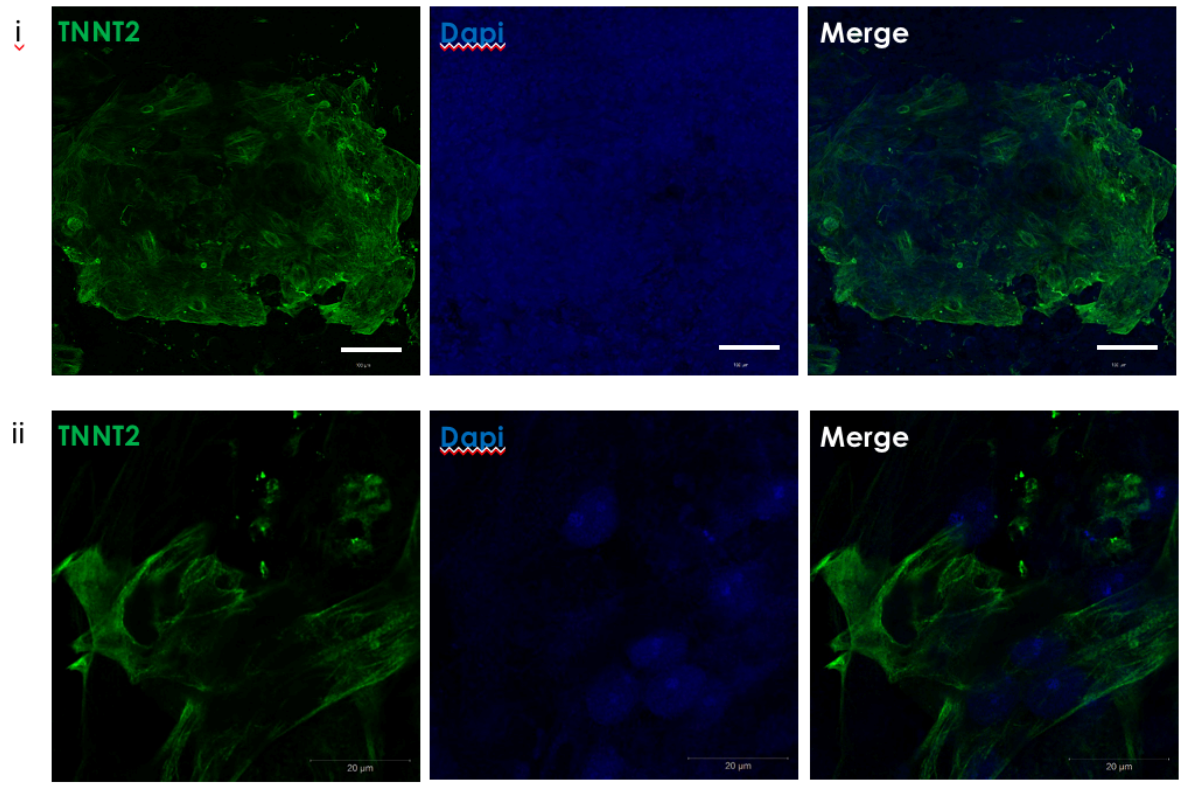

Figure 4.8 TNNT2 expression for cardiomyocytes. Photomicrograph showing immunostaining of TNNT2 to identify all cardiomyocytes and DAPI to visualize all cells. (i) Scale bars represent 100μm, (ii) Scale bars represent 20μm

Differentiation of atrial cardiomyocytes from iPSCs.

Following optimizing conditions for generating ventricular cardiomyocytes from human iPSCs, I hypothesized that spatial and temporal changes during the early stages of mesoderm commitment could be accessed via addition of pro-atrial factors in order to devise a differentiation paradigm to skew cells towards an atrial phenotype. Building on observations to investigate the developmental origin of ventricular and atrial lineages, I next sought to investigate further the functionality of RA signaling and the Grem2 pathway in cardiac development which is conserved across species (Devalla *et al*, 2015, Zhang *et al,* 2011).

As a first step, it was critical to ascertain the expression pattern of Grem2 relative to other BMP antagonism during the differentiation of atrial and ventricular cell lineages. I analyzed expression profiles of Grem2 and Cer1 over a 20 day time course experiment collecting RNA on alternate days and running quantitative PCR. BMP antagonists are expressed at varying quantities during differentiation days 0-10 in the presence of RA and Grem2 as shown in **Figure 4.9** and **4.10.** The expression of Cer1 seems to be expressed transiently between days 1-3 which may indicate when germ layer formation occurs. This is then followed by sustained Grem2 expression following day 10. Tanwar et al, have tabulated expression studies of BMP ligands (Tanwar *et al*, 2016) and show that between days 3-4 remaining BMP ligands begin to be expressed, suggesting a role for activity of Grem2 which becomes more noticeable throughout establishment of successive differentiation of lineage-specific progenitor cells.

Insofar, my data remains consistent with embryonic development as the pattern of gene expression holds true for Grem2 which is upregulated during the time when lineage specification occurs for the endoderm, endothelium, blood and heart. Conversely, the

expression of both BMP antagonists and agonists suggest very strict control of BMP signaling during the lineage specification process.

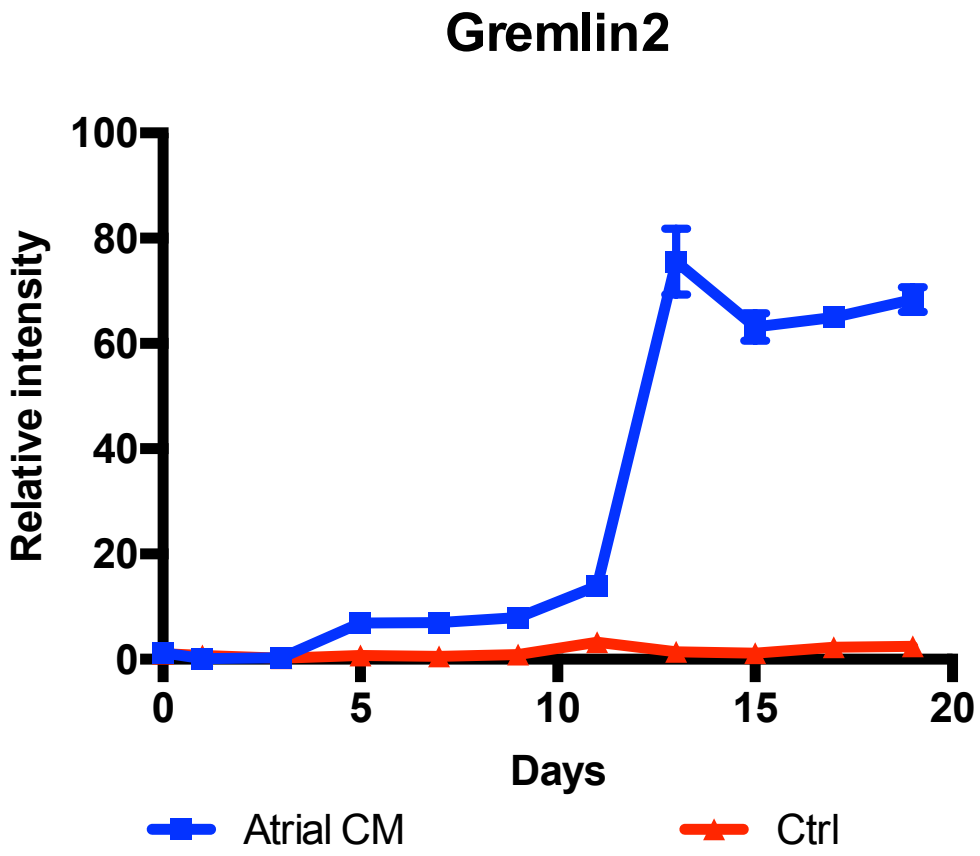

Figure 4.9 Grem2 expression during differentiation of iPSCs using Gremlin2. iPSC01 were allowed to differentiate, RNA samples were collected at successive differentiation days, and expression of BMP antagonist Gremlin2 was analyzed by quantitative PCR. (n=7)

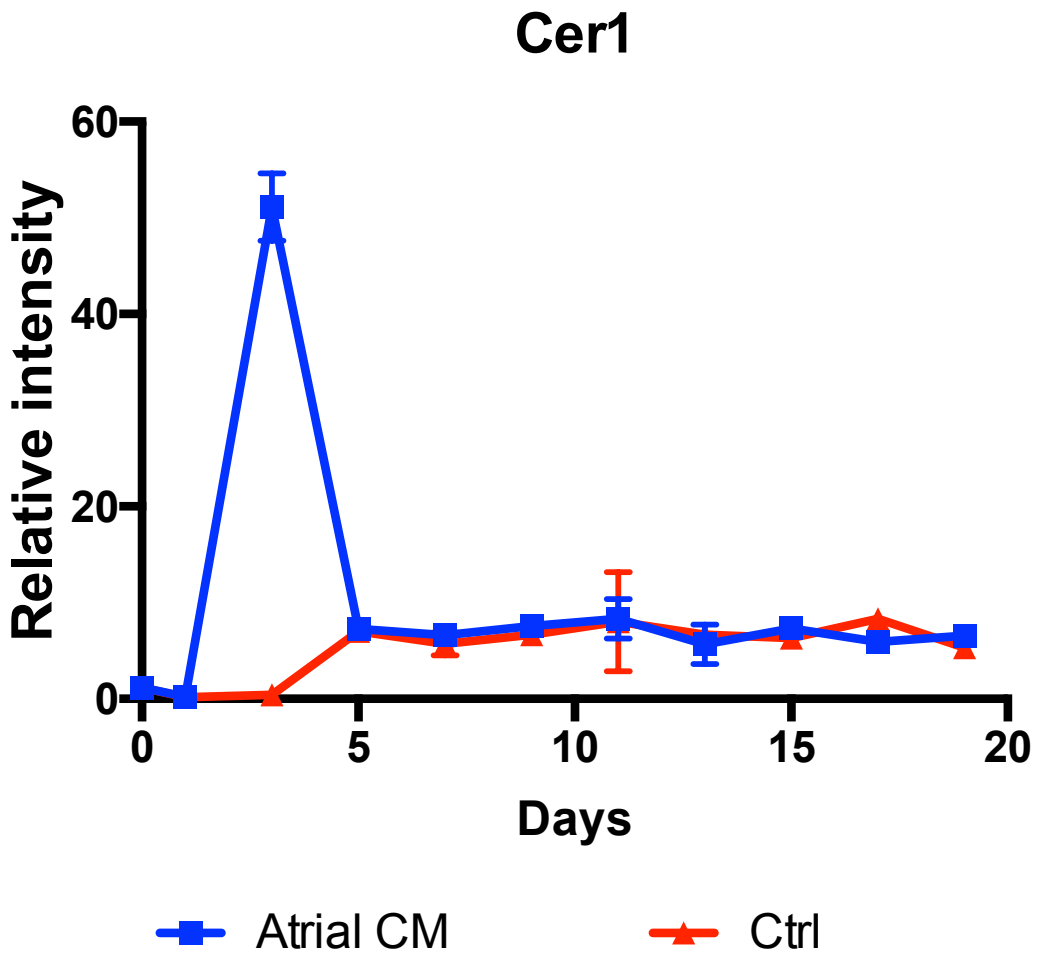

Figure 4.10 Cer1 expression during differentiation of iPSCs using Gremlin2. iPSC01 were allowed to differentiate, RNA samples were collected at successive differentiation days, and expression of BMP antagonist Gremlin2 was analyzed by quantitative PCR. **, p <.01 (n=7)

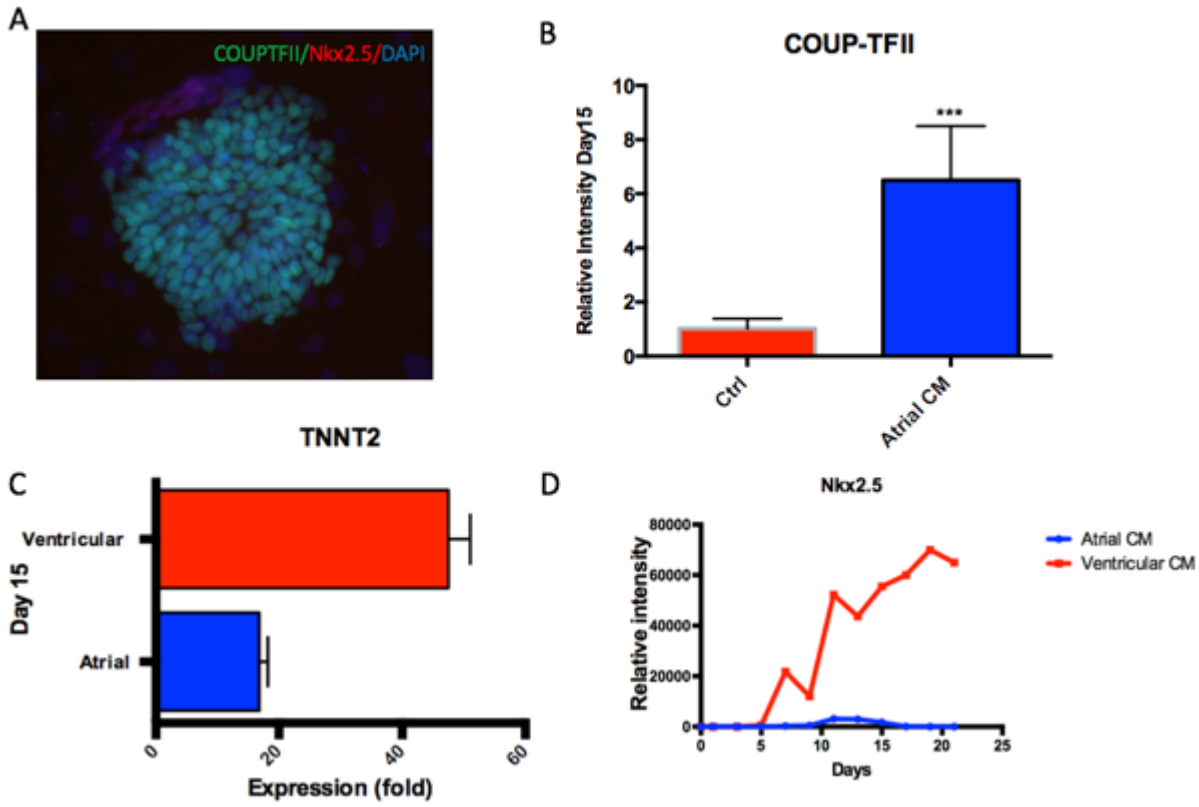

Figure 4.11 Early and late mesoderm lineage markers profiled. (A) Photomicrograph of COUPTFII and Nkx2.5 immunocytochemistry expression (B) qPCR gene analysis of COUP-TFII transcription factor. (C) qPCR gene analysis of pan-cardiomyocyte gene TNNT2. (D) qPCR gene expression of early cardiomyocyte transcription factor Nkx2.5. Statistical significance was assessed via Student's t-Test. * p<=0.05, ** p<=0.001, *** p<=0.001, ****p<=0.0001. (n=5)

Normal iPSCs were treated with Grem2 at day 4 of differentiation and subsequently treated with RA between days 4-12. Treatment with Grem2 and RA was chosen at day 4 because Grem2 transcripts emerge in differentiating human iPSCs, to enrich and consequently uncover the effects of Grem2 on atrial specification. Differentiating monolayer cultures showed similar expression levels of human Troponin T2 (TNNT2), a marker of pan-cardiac cells (**Figure 4.11C**). **Figure 4.11A** is an immunocytochemistry photomicrograph of atrial differentiating cells stained for expression of human COUPTFII and human NKX2.5. human COUPTFII is a chick ovalbumin upstream promoter of transcription factors I and II (COUP-TFI and II or NR2F1 and NR2F2) and these have been shown to be highly expressed in atrial cardiomyocytes, but not in ventricular cardiomyocytes (Devalla *et al.,* 2015, Tanwar

et al., 2016). **Figure 4.11B** thus shows high expression of COUPTFII in atrial differentiating cells. Throughout murine cardiovascular development, COUP-TFII expression is initially detected within the sinus venosus and visceral mesoderm, next proceeds to the atrium, and subsequently turns out to be restricted to cardiomyocytes of the atrial-specific chambers upon late stages of development (Pereira *et al.,* 1999; Wu *et al.,* 2013). Transcription profiling experiments revealed that COUP-TFII is highly upregulated in human iPSC atrial CMs. Based on previous reports by others indicating a role for COUP transcription factors (Tanwar *et al.,* 2016), I postulated that these genes may be critical downstream of Grem2/RA treatment during atrial differentiation. This hypothesis is further supported by data which indicates here, that COUP-TFII is an important atrial-enriched transcription factor.

Our data also demonstrate that atrial cardiomyocytes are born within different subpopulations of mesoderm progenitors. qPCR analysis shown in **Figure 4.11D** that cells only transiently turn on Nkx2.5 transcription factor expression in atrial fated populations whereas, in contrast the expression of this factor is maintained in ventricular fated populations. This finding coupled with the human COUPTFII data demonstrate that we have shown enhanced generation of subpopulations of cardiomyocytes within the differentiation paradigm using Grem2 and RA. To further assess the differentiation of these subpopulations towards atrial versus ventricular cells, qPCR analysis shown in **Figure 4.12C** demonstrates robust expression of human NPPA within the atrial differentiated subpopulations while this is virtually nonexistent within the ventricular differentiation protocol. NPPA is the gene encoding atrial natriuretic peptide (ANP). NPPA expression pattern has mainly been observed in governing cardiac chamber development and the expression of NPPA is initiated within the developing atrial myocardium (Christoffels *et al.*, 2006).

As a follow up towards analyzing the effects of GREM2 and RA treatment on human iPSCs, I used a 12 day differentiation treatment protocol which was optimized in the lab in

order to generate cells with atrial identity. **Figure 4.12A** and **4.12B** show generation of either ventricular or atrial cells, assessed by immunostaining for a pan-cardiac marker troponin (TNNT2) and the gene encoding ANP (NPPA). Atrial cells that were generated by this protocol showed positive expression of NPPA while ventricular cells showed little to zero expression of NPPA. Thus, hiPSCs that differentiated towards atrial cardiomyocytes showed preferential upregulation of NPPA protein, whilst their ventricular cardiomyocyte counterparts did not upregulate the atrial cardiomyocyte marker NPPA. To confirm if the resulting atrial cardiomyocytes were indeed atrial-like cells, the maintained expression of various atrial specific markers was investigated. One of which was Myl7, also known as myosin regulatory light chain 2, atrial isoform (MLC2a) in humans is a gene encoded by the Myl7 gene. Its expression has been found to be restricted to cardiac muscle of the atria in healthy individuals, whereas, Myl7 expression is altered in patients with hypertrophic cardiomyopathy and other cardiac related disorders (Lim *et al.*, 2001). To determine if the resulting cardiomyocytes maintained atrial gene signatures I monitored expression of Myl7 using qPCR as shown in **Figure 4.12D**, these observations show a 20 fold increase in expression within the atrial myocyte differentiation protocol. Levels of Myl7 protein were not measured due to lack of a reliable signal on western blot. These findings are also in agreement with reports of an increased abundance of Myl7 in adult atrial cardiomyocytes (Lim *et al.*, 2001).

I next asked whether atrial-like cardiomyocytes from iPSCs displayed the kcnj2 gene which encodes Kir2.1. The cardiac inward rectifier potassium current (I_{k1}) is known for stabilizing the resting membrane potential (RMP) and contributes to repolarization of action potential in both atrial and ventricular populations (Ehrlich *et al.*, 2003). The K^+ channels which mediate I_{k1} expression is composed of Kir2.x family of subunits. In order to assess the functionality of our atrial and ventricular cells I examined gene expression signatures of

many of the genes within the Kir subfamily. Real-time PCR data of KCNJ2 shown in **Figure 4.12E** confirm abundance of KCNJ2 within the atrial cardiomyocytes and to a significantly lesser extent in the ventricular cardiomyocytes. These observations are perhaps indicative of the role of I_{k1} expression in delineating a more mature cardiac phenotype within the Grem2 and RA protocol, characteristics that I will delve more deeply in to chapter 5 of this thesis.

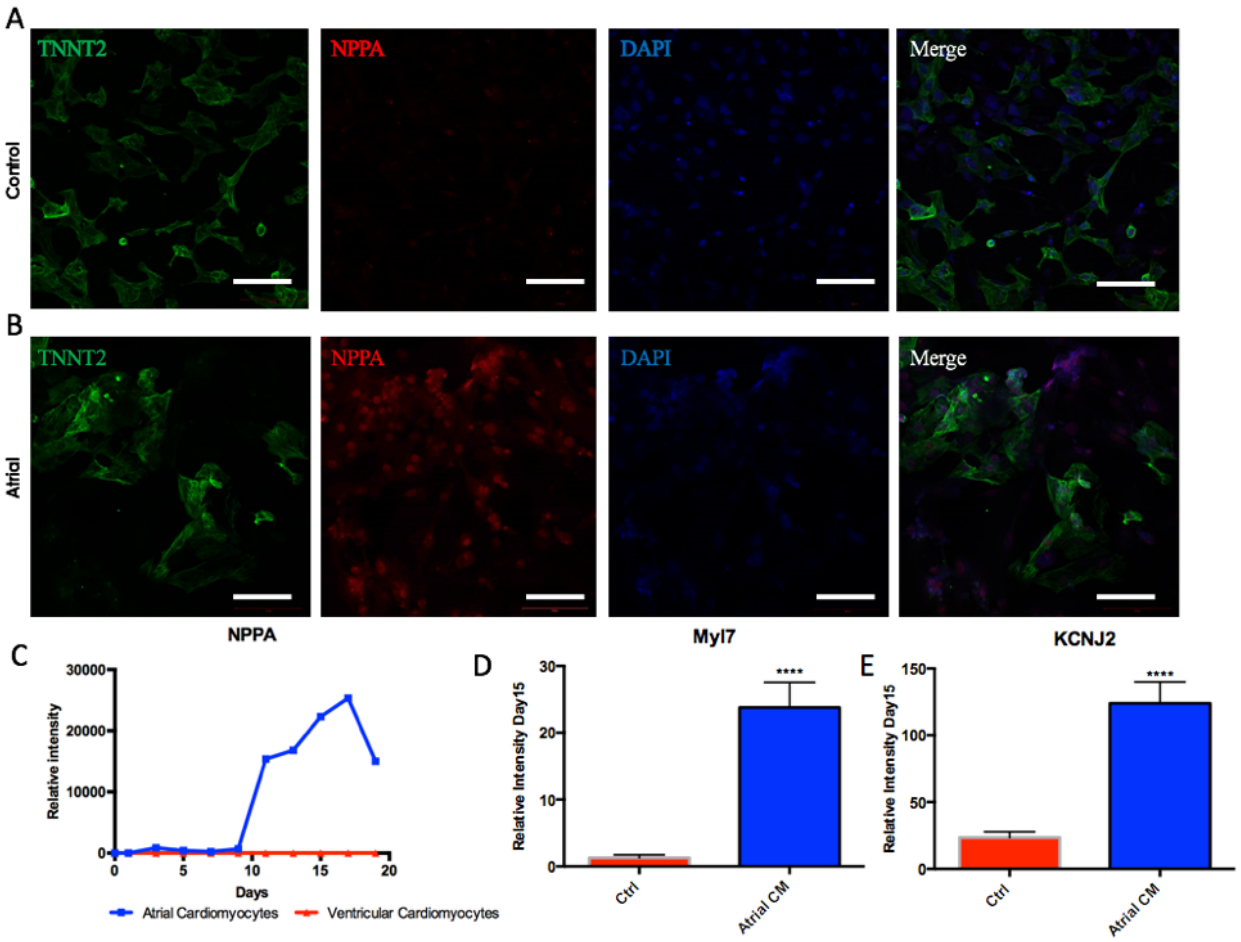

Figure 4.12 Atrial lineage markers profiled. (A) Photomicrograph of TNNT2 and NPPA immunocytochemistry expression in ventricular cells (B) Photomicrograph of TNNT2 and NPPA immunocytochemistry expression in atrial cells (C) qRT-PCR gene analysis of NPPA over a 20-day time course (D) qRT-PCR gene analysis of atrial gene marker Myl7. (E) qRT-PCR gene expression of KCNJ2 gene. Statistical significance was assessed via Student's t-Test. * p<=0.05, ** p<=0.001, *** p<=0.001, ****p<=0.0001. (n=5) Scale bars represent 50μm.

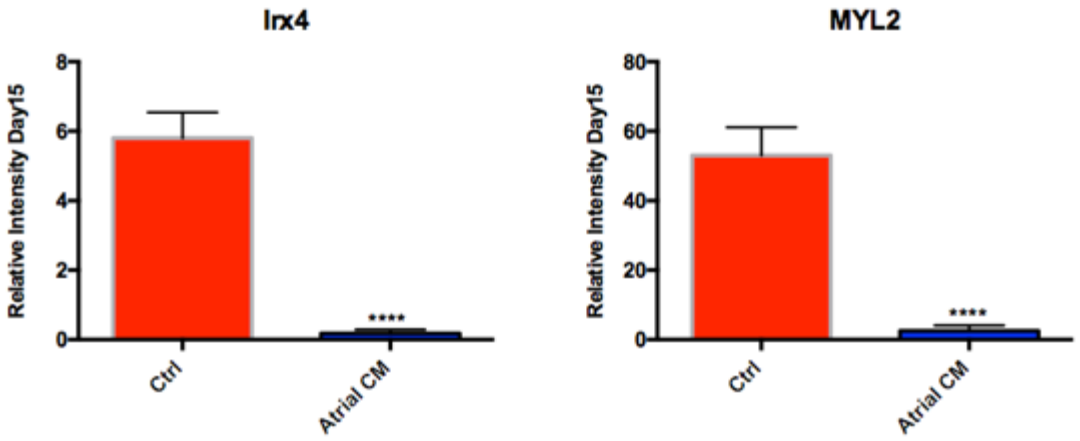

Figure 4.13 Ventricular lineage markers profiled. qRT-PCR based analyses directly compaing the atrial differentiation protocol that employed Grem2 and RA and ventricular differentiation protocol. Cell populations were analyzed at differentiation day 15. The Grem2/RA protocol was able to generate cells that lacked ventricular markers (MYL2 and IRX4). Values are shown relative to housekeeping gene HPRT. Error bars represent standard deviation of the mean from the values of independent experiments. Statistical significance was assessed via Student's t-Test. * p<=0.05, ** p<=0.001, *** p<=0.001, ****p<=0.0001. (n=5)

Shown earlier, molecular characterization of the two differentiation protocols revealed that the Grem2/RA based atrial differentiation protocol, in comparison to the control (ventricular) protocol, generated cells that expressed higher levels of atrial specific markers NPPA (natriuretic peptide type A) and Myl7 genes. As shown in **Figure 4.13**, the control differentiation protocol similarly showed higher levels of expression of ventricular specific markers such as the ventricular paralog of the regulatory light chain of myosin (Myl2), and the Iroquois-class homeodomain protein IRX-4 (IRX4). Hence Grem2/RA induced genes that encode atrial proteins Myl7, NPPA, COUP-TFII. In contrast, Grem2/RA treatment did not have a significant effect on ventricular markers for contractile proteins Myl2 (Mlc2v) or IRX4 genes.

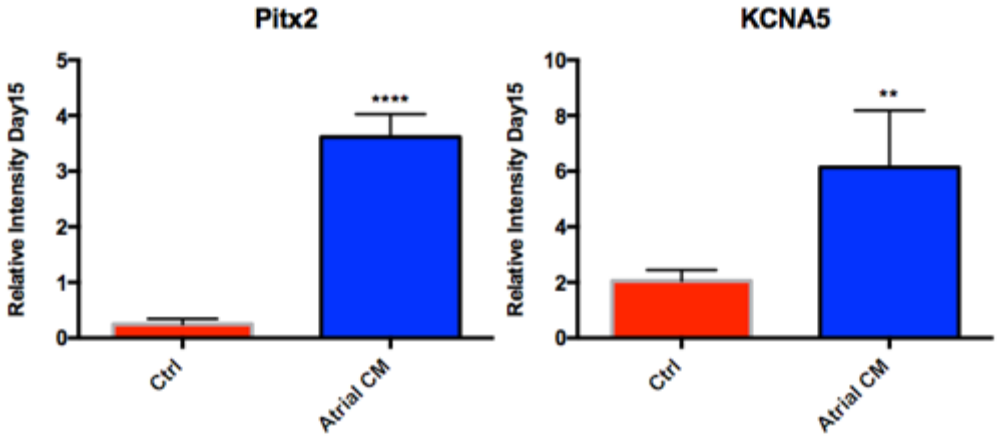

Figure 4.14 Atrial lineage markers profiled. qRT-PCR based analyses directly comparing the atrial differentiation protocol that employed Grem2/RA and ventricular differentiation protocol. Cell populations were analyzed at differentiation day 15. The Grem2/RA protocol was able to generate cells that highly expressed atrial transcription factor markers (Pitx2) and atrial-specific ion channel gene (KCNA5) encoding Kv1.5. Values are shown relative to housekeeping gene HPRT. Error bars represent standard deviation of the mean from the values of independent experiments. Statistical significance was assessed via Student's t-Test. * p<=0.05, ** p<=0.001, *** p<=0.001, ****p<=0.0001. (n=5)

Further analysis was performed to demonstrate atrial specificity which included observations of atrial-specific ultra-rapid delayed rectifier K+ current gene KCNA5 (IKur). There is a general consensus that the Kv1.5 subunit is responsible for a large part of the IKur in human atrial myocytes (Dobrev and Ravens, 2003) . It has been shown that this subunit is much less abundant in ventricular than in atrial myocardium. Therefore, it appears to be quite specific to atrial cardiomyocytes. The pharmacology of KV1.5 channels has been studied extensively studied. In a goat model of atrial fibrillation (AF), inhibition of KV1.5 channels have been shown to normalize action potential (AP) duration and refractory period which in turn quenches AF (Honore et al., 1994). Within human atrial fibers some chronic AF patients receive pharmacological inhibition of I_{Kur} which reestablishes AP duration (Al Ghamdi and Hassan, 2009). **Figure 4.14** provides strong evidence that the KCNA5 gene which encodes the atrial specific ion channel KV1.5 is abundantly expressed at a 3-fold higher concentration within the atrial cardiomyocyte differentiation program in respect to the ventricular protocol.

Moreover, the transcriptional archetype that deliberates robustness of cardiac rhythm is tightly controlled by cardiac channel gene expression, since imbalances of channel expression can cause arrhythmias (Roden *et al.*, 1996). Human AF studies have indicated various transcription factor networks important in regulating perturbations in atrial rhythm, which includes TBX5 and PITX2. PITX2, is a paired-like homeodomain transcription factor that plays a crucial role in heart development and adult rhythm control (Harvey, 2002) . PITX2 is also frequently reported as an AF-susceptibility locus (Harvey, 2002) . PITX2 is regulated by TBX5 and it was found that TBX5 haploinsufficiency can be rescued with PITX2, therefore, uncovering a multilevel gene regulatory network for atrial rhythm and atrial homeostasis (Nadadur *et al.*, 2016). The PITX2 gene is highly (**Figure 4.14**) upregulated during the differentiation of atrial cardiomyocytes as compared to ventricular cardiomyocytes which may account for appropriate atrial rhythm and allow for further genetic manipulation studies in order to delineate diverse mechanisms in atrial homeostasis that will clue us in on AF phenotypes.

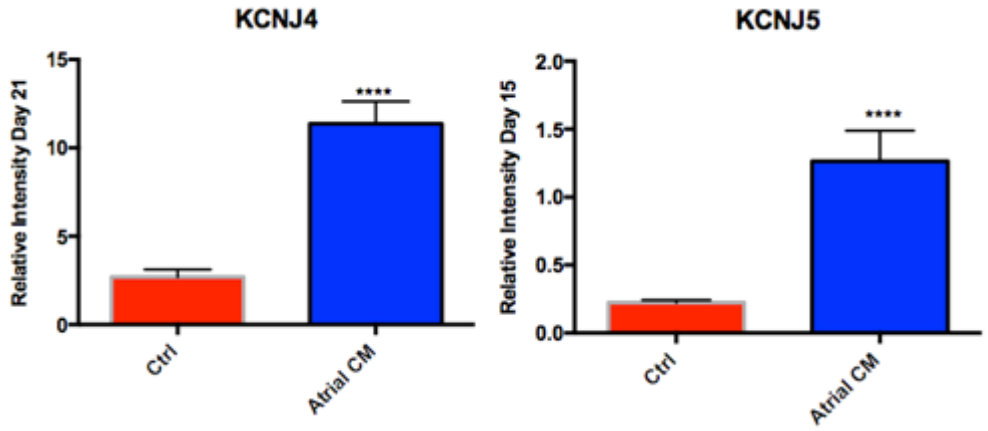

Figure 4.15 Inward rectifier ion channel genes profiled. qRT-PCR based analyses directly comparing the atrial differentiation protocol that employed Grem2/RA and ventricular differentiation protocol. Cell populations were analyzed at differentiation day 15. The Grem2/RA protocol was able to generate cells that highly expressed ion channel genes (KCNJ4 and KCNJ5) encoding Kv2.3 and Kv3.4 respectively. Values are shown relative to housekeeping gene HPRT. Error bars represent standard deviation of the mean from the values of independent experiments. Statistical significance was assessed via Student's t-Test. * p<=0.05, ** p<=0.001, *** p<=0.001, ****p<=0.0001. (n=5)

As mentioned above, an important requirement for cardiomyocytes to maintain appropriate resting membrane potentials is the presence of IK1 ion channels also known as the inward rectifier currents that control resting potential. Human atrial cardiomyocytes are typically polarized at a resting membrane potential of near -80mV. This negative resting potential is crucial for the normal propagation of the depolarizing wave. Within dilated atria or during AF in humans, some areas lose their negative resting potential which contributes to the formation of arrhythmogenic substrate for AF. Kir2.3 subunit has been found to be more abundant in the atrium than in the ventricle (Schram *et al.*, 2002). Typically Kir2.1, Kir2.2, and Kir2.3 contribute to IK1, and Kir2.1 is the isoform that is known to be the underlying factor regulating IK1 activity within the ventricle. Conversely Kir2.3 expression is higher within the atria, which is more abundant in the atria as opposed to the ventricle. **Figure 4.15** also enhances the notion that expression of human KCNJ4 within the atrial cardiomyocyte population higher as compared to that in ventricular myocytes.

Interestingly, Kir3.4 subunits are functionally enhanced by β-adrenergic stimulation (Schram *et al.*, 2002). Kir3.4 (KCNJ5) is an important mediator of vagally induced bradycardia and contributes to the shortening of action potential duration. Kir3.4 is expressed mainly in the sinoatrial node (SAN) and atrial cardiomyocytes (Schram *et al.*, 2002) and these proteins are found to be the main underlying mechanism for regulating heart rate. I have shown that within the atrial differentiation protocol, expression of Kir3.4 (KCNJ5) gene expression is higher in atrial cardiomyocytes, perhaps owing to more functionally responsive cardiomyocytes which will be assessed more clearly in Chapter 5 of this thesis.

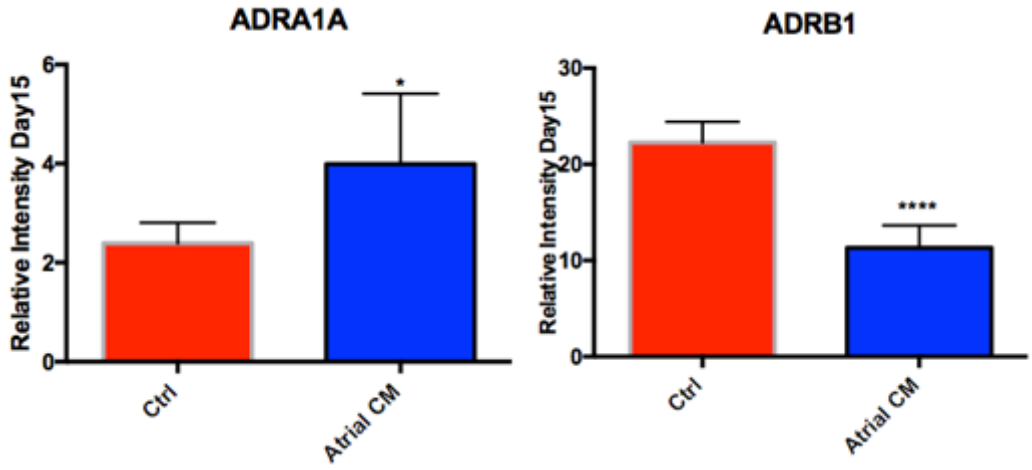

Figure 4.16 expression qRT-PCR based analyses directly comparing the atrial differentiation protocol that employed Grem2/RA and ventricular differentiation protocol. Cell populations were analyzed at differentiation day 15. The Grem2/RA protocol was able to generate atrial cells. qRT-PCR analysis for ADRA1A and ADRB1 were performed. Values are shown relative to housekeeping gene HPRT. Error bars represent standard deviation of the mean from the values of independent experiments. Statistical significance was assessed via Student's t-Test. * p<=0.05, ** p<=0.001, *** p<=0.001, ****p<=0.0001. (n=5)

Phenylephrine (PE) is an α_1 adrenoceptor agonist coupled to G_q that would be expected to have high expression within both atrial and ventricular cardiomyocytes. Therefore, **Figure 14.16** investigates expression of α_1 adrenoceptor (ADRA1A). Others have shown that ADRA1A during human cardiogenesis is not detectable in differentiated human iPSCs or human ESCs and nor is there a physiological response to PE (Földes *et al.*, 2014).

However, in our case I observed expression of ADRA1A in both atrial and ventricular derived cardiomyocytes. Further I will demonstrate responsiveness of our atrial cardiomyocytes to PE in Chapter 5 of this thesis.

Similarly, I was interested in following the expression pattern of the β1 adrenoceptor gene (ADRB1). β1 receptors are present in the adult heart. Stimulation of β1 receptors in the cardiomyocytes activates adenylyl cyclase through a Gs-coupled system (Földes *et al.*, 2014). Increased adenylyl cyclase activity increases cytoplasmic cAMP, which in turn activates PKA, which then goes on to phosphorylate various target genes. The summation of phosphorylation events increases Ca^{2+} activity. There are also various chronotropic and ionotropic effects of β1 adrenergic agonists that exert various affects. For instance, these increase the strength of myocardial contraction, which is in part determined by the amount of Ca^{2+} present. Therefore, studying expression and control of β1 receptors within a human cellular model would be critical to establish appropriate preclinical treatment modalities. As shown in **Figure 14.16** there is expression of β1 adrenergic (ADRB1) receptors within both atrial and ventricular derived cardiomyocytes. α_1 adrenoceptor and β1 adrenoceptor regulation in isolation as well as in tandem within the human cellular context would be able to give key insights hitherto, in Ca^{2+} signaling regulation in health and disease. It would be prudent to investigate whether expression of α_1 adrenoceptor and β1 adrenoceptor might influence atrial cardiomyocyte Ca^{2+} transients before and after the application of phenylephrine or isoprenaline.

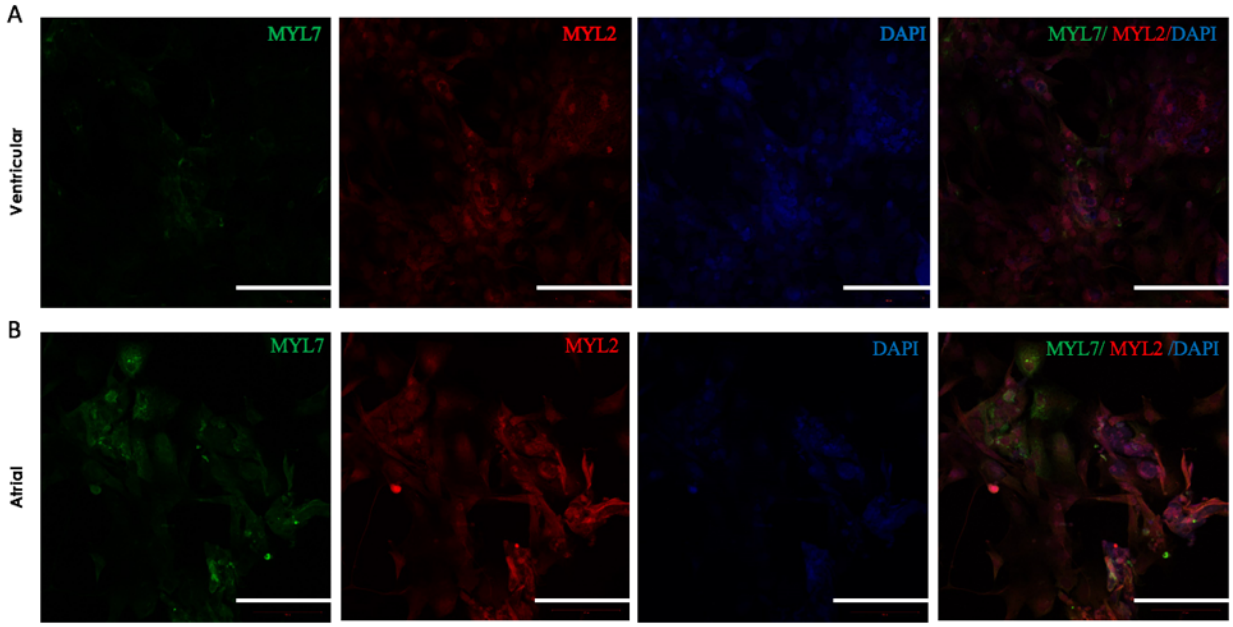

Figure 4.17 Atrial and Ventricular specific light chains. (A) Photomicrograph of MYL7 and MYL2 immunocytochemistry expression in ventricular cells (B) Photomicrograph of MYL7 and MYL2 immunocytochemistry expression in atrial cells. Scale bars represent 50μm.

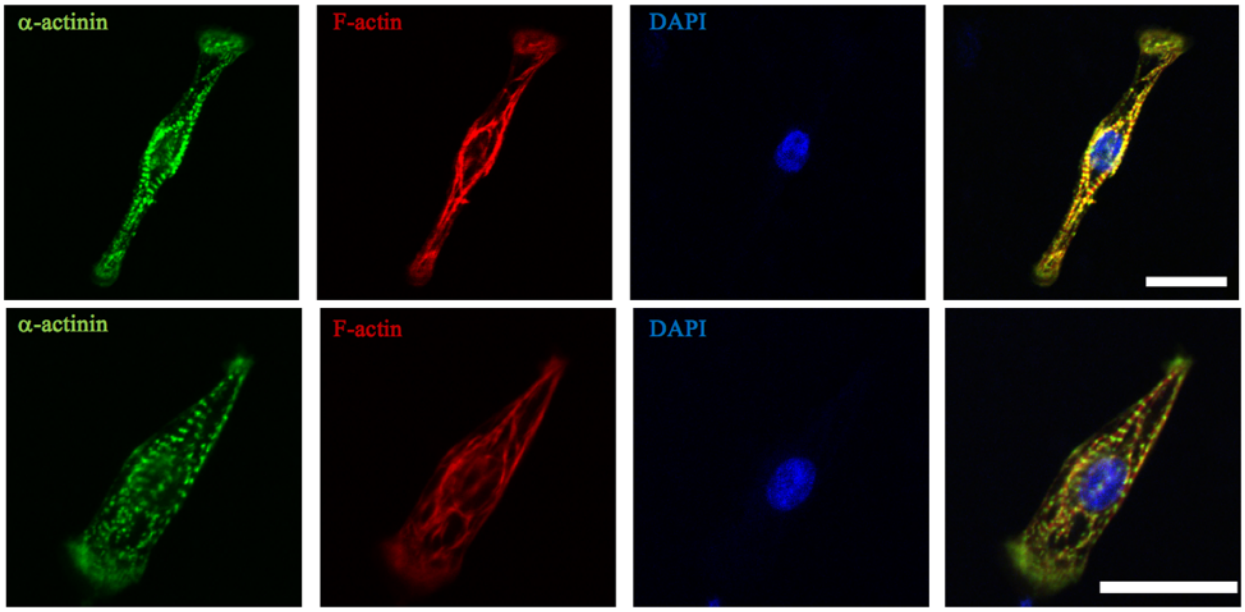

Figure 4.18 Immunophenotype characterization of isolated human iPSC derived single cells. Immunolabelling of α-actinin and F-actin on human iPSC derived atrial myocytes showed a striated pattern that maintain morphological characteristics of adult atrial myocytes. Note: Images shown are the representative immunolabelling of the majority of cells. Secondary antibodies consisted of the following AF488 (green) and AF568 (red) Scale bar represents 25μm.

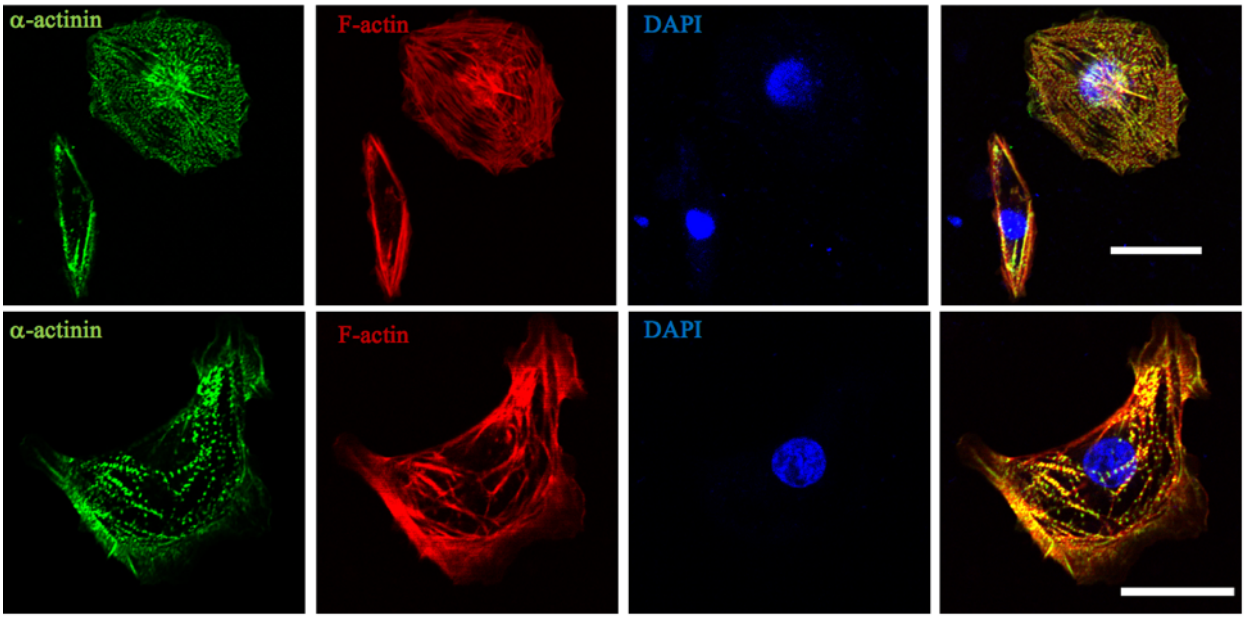

Figure 4.19 Immunophenotype characterization of isolated human iPSC derived single cells. Immunolabelling of α-actinin and F-actin on human iPSC derived atrial myocytes showed a striated pattern that maintain morphological characteristics of adult atrial myocytes. Note: Images shown are the representative immunolabelling of the majority of cells. Secondary antibodies consisted of the following AF488 (green) and AF568 (red) Scale bar represents 25 μm .

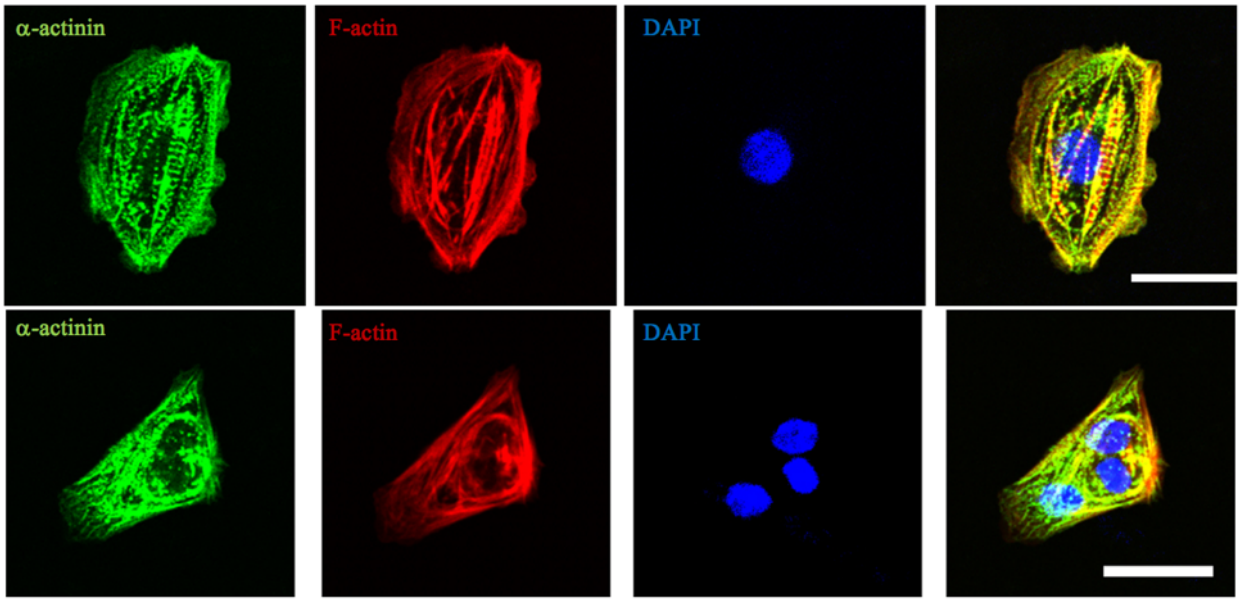

Figure 4.20 Immunophenotype characterization of isolated human iPSC derived single cells. Immunolabelling of α-actinin and F-actin on human iPSC derived atrial myocytes showed a striated pattern that maintain morphological characteristics of adult atrial myocytes. Note: Images shown are the representative immunolabelling of the majority of cells. Secondary antibodies consisted of the following AF488 (green) and AF568 (red) Scale bar represents 25 μm .

Myosin is an essential component of cardiac muscle, from the onset of cardiogenesis through to the adult heart (Brand, 2003). Myosin heavy-chain and myosin light-chain proteins are required for a correctly formed heart (Brand, 2003). MLC2v (MYL2) is restricted to the ventricles, both throughout the developing and adult human heart (Schram *et al.*, 2002). Mutations of the human *MYL2* gene have been associated with hypertrophic cardiomyopathy (Lim *et al.*, 2001). MLC2a (MYL7) is expressed in humans at high levels in the atrium postnatally, throughout the linear heart during development (Honore *et al.*, 1994). I sought to observe the expression of MYL7 and MYL2 in iPSC derived atrial and ventricular cells. Cells were fixed and stained once contracting myocytes were detected at day 30 of differentiation. **Figure 4.17** shows MYL7 staining was restricted to cells differentiated using the Grem2/RA protocol to derive atrial cells. In contrast, MYL2 had overlapping expression within both atrial and ventricular fated cells. I hypothesized that atrial-like cells could be identified and isolated from these cultures using MYL7. Future molecular genetic strategies may be employed in order to purify atrial like cellular populations. Previously, I showed robust expression by qRT-PCR for MYL7 but not MYL2 in atrial cardiomyocytes. Further investigations need to be performed to delineate the role of MYL2 which is a ventricular myosin light chain marker. It seems that the MYL7 gene which encodes myosin light chain 2a is more specific to atrial cardiomyocytes, whereas, MYL2 may maintain expression within atrial cells albeit to a lesser extent. Myosin structural proteins are expressed in a restricted manner in the developing heart and play vital roles in early cardiogenesis. However, there remain many gaps in knowledge with as yet a comprehensive understanding of the role that myosin heavy and light chains play in cardiogenesis still lacking. In the future, further genetic and molecular studies will elucidate precise roles for the myosins in human heart development and how the myosins are regulated at different developmental stages.

Quantitative data from electron microscopy (EM) studies of atrial tissue sections from the adult heart, show typical morphological features different from ventricular myocytes (Peters *et al.*, 1993). Within the literature there are differences in transverse tubules (TT), prominent perinuclear Golgi complexes associated with atria specific granules, numerous peripheral sarcoplasmic reticulum (SR) cisterns which form discontinuous membrane contacts, and high density of mitochondria (Peters *et al.*, 1993) However, the fundamental feature that is different between ventricular cardiomyocytes, atrial cardiomyocytes typically have only one nucleus and are roughly 100um long rod-shaped polar cells while ventricular cells derived from iPSCs typically do not follow conventional adult phenotype (Blundo, 2010). Novel observations represented in Figures 4.18, 4.19, and 4.20 are photomicrographs of human iPSC derived atrial cardiomyocytes differentiated using Grem2/RA. Amongst the images shown five of the six cells show this very unique archetypical structure of adult atrial like cells. A large majority of our cells show the above morphological features which are consistent with data from adult non-human atrial cardiomyocytes. Previous reports, from various groups who specialize in differentiating human iPSCs towards various cardiomyocytes have not shown morphological features reminiscent of an adult cardiac cell. This is in part explained by the theory that iPSC derived cells almost never achieve complete maturation, and the majority of the cells shown are mainly spherical in orientation.

4.3 Discussion

For myocardial injury and chronic HF, the clinical application of stem cell therapeutics using cellular transplantation is limited by heterogeneous populations of cells and lack of maturity. This chapter has confirmed the feasibility of deriving cells from iPSCs that resemble atrial cardiomyocytes in their morphology, surface phenotype and extensive gene expression analysis. Therefore, given that iPSCs may be derived in an autologous manner, the possibility of generating large populations of patient specific atrial cardiomyocytes appears entirely feasible.

Isolation, expansion and characterization of human iPSCs

A variety of iPSCs were generated for the purpose of developing a cellular model of atrial cardiomyocytes for use in drug screening and cellular therapeutics studies. In the present study, iPSCs were isolated from reprogramming human fibroblasts using the sendai virus particles developed by engineering the Yamanaka factors which include Oct3/4, Sox2, Klf4, and c-Myc. These cells were characterized using immunocytochemistry, flow cytometry targeting specific proteins associated with the identification of iPSCs. In agreement with previous reports from my work (Ahmad *et al*, 2013) and in Chapter 3, the immunocytochemical analysis showed that *in vitro* cultured iPSCs were a homogenous population of cells expressing, Oct4, Nanog, Tra-1-60. Flow cytometric analysis further confirmed and quantified the cells expressing pluripotent cell surface markers for SSEA4 and Tra-1-60 while downregulating expression of CD13 which I presume to mainly be indicative of human fibroblasts.

GREM2 mediated cardiac differentiation

Bone morphogenetic proteins (BMPs) employ pleiotropic properties on morphogenesis and cardiomyocyte maturation (Tanwar *et al.*, 2014) . The morphogenetic processes include cardiac looping (Tanwar *et al.*, 2014), valve formation, and ventricular development (Willems *et al.*, 2011). In addition to forward BMP signaling, BMP antagonists such as Noggin are also necessary for cardiac development. Taken together, these observations indicate that fine-tuning BMP activity may be required for developing atrial cardiomyocytes. Traditionally, previous data have shown that BMP agonists upregulate gene expression of cardiac contractile proteins whereas early inhibition of BMP signaling enhances cardiogenic potential (Tanwar *et al.*, 2014).

I hypothesized based on developmental data, that Gremlin2 (Grem2) also known as Protein Related to Dan and Cereberus (PRDC) could potentially influence atrial specification. Grem2 is a secreted BMP antagonist that belongs to the CAN family (Brand, 2003). The mechanism by which BMP antagonism occurs with Grem2 is by inhibiting Bmp2 and Bmp4 signaling (Tanwar *et al.*, 2014). Work from Antonis Hatzopoulos's lab indicated in mouse studies that Grem2 was necessary for cardiac laterality and atrial differentiation during development (Tanwar *et al.*, 2014). In line with this evidence they determined that Human Grem2 variants resulted in familial atrial fibrillation. Here I have demonstrated that Grem2 treatment shifts human pluripotent stem cell differentiation to cardiomyocytes with atrial biomolecular and electrophysiological properties (Chapter 5). These findings provide a novel tool to probe mechanistic insights into cell type specific cardiomyocyte differentiation and stem cell platform to study atrial abnormalities.

Our data demonstrate that the Grem2 morphogen and RA, which regulates atrial formation and establishment of cardiac rhythm during embryonic development, can be used to promote differentiation of pluripotent stem cells to cardiomyocytes with

electrophysiological and molecular properties characteristic of atrial cells. Grem2/RA treatment leads to 20–120-fold expansion of myocytes and comparable induction levels in the expression of genes encoding atrial-specific contractile, gap junction and ion channel proteins such as Myl7, KCNA5, NPPA, and Kcnj5. Interestingly, Grem2/RA decreases ventricular myocyte differentiation and the expression levels of corresponding ventricular-specific genes such as Myl2, and Irx4. Consistent with these findings, electrophysiology data show that Grem2.RA-induced (Chapter 5), iPSC-derived cardiomyocytes have action potentials typical of atrial myocytes.

In contrast, cardiomyocytes in control which are ventricular cardiomyocyte, samples display a wide heterogeneity of electrical properties. Activation or suppression of downstream signaling gene networks conferring chamber identity mechanisms could explain the Grem2/RA effects. A recent elegant analysis of cardiac-specific CoupTFII knockout mice demonstrated that inactivation of CoupTFII leads to ventricularized atria with loss of atrial-specific genes Hey1, Myl7, Gja5, Kcnj3, and Kcnj5 and gain of ventricular-specific genes Hey2, Irx4, and Myl2 (Tanwar *et al.*, 2014). In complementary fashion, overexpression of CoupTFII in ventricles leads to increased Myl7 and decreased Myl2 expression, further suggesting a critical role of CoupTFII in regulating atrial identity. Our data show that Grem2/RA treatment of differentiating iPSCs leads to induction of CoupTFII and has similar effects as gain of CoupTFII function in mouse hearts, suggesting that Grem2/RA acts upstream of CoupTFII to confer atrial identity. The Notch signaling pathway promotes cardiac cell proliferation and differentiation and thus is required for multiple aspects of cardiovascular development. Hairy related transcription factors Hey1 and Hey2 are downstream targets of Notch signaling. Hey2 is specifically expressed in ventricular cardiomyocytes and is known to suppress atrial-specific gene expression, including

CoupTFII. Therefore, it is also possible that Grem2/RA induces atrial phenotype through direct Hey2 downregulation, thus, removing the suppression of CoupTFII.

Our data further show that stimulation of atrial cardiomyocyte differentiation is confined to the gremlin subfamily of BMP antagonists and does not depend singularly on BMP inhibition. In data not shown, other tested BMP antagonists such as Noggin, DAN, Chordin, and Dante do not induce atrial or cardiac differentiation at this stage of iPSC differentiation. Interestingly, JNK signaling activation by noncanonical Wnt ligands such as Wnt (Lian *et al.*, 2012) is required for cardiac induction during development (Lian *et al.*, 2012) and differentiation of iPSC-derived cardiac progenitor cells to cardiomyocytes (Lian *et al.*, 2012). However, unlike noncanonical Wnt signaling, Grem2-mediated JNK activation specifically induces atrial cardiomyocytes, acting upstream of CoupTFII and Hey1.

The molecular mechanisms of Grem2 function at the protein structure level are currently being discovered. Unlike BMP ligands that have similar structures, BMP antagonists are structurally diverse, suggesting that their mode of inhibition of BMP signaling varies. Consistent with this possibility, the Grem2 3D protein structure has been recently resolved and shows that Grem2 forms head-to-tail dimers unlike the head-to-head pairing in Noggin complexes (Yeung *et al.*, 2014). Although the Grem2/BMP complex structure has not yet been resolved, this arrangement predicts that Grem2 does not completely surround BMP complexes as Noggin does. As a result, it is likely that Grem2 selectively hinders the interaction of BMP ligands with their receptors, allowing stimulation of downstream signaling through counter activation of compensatory feedback loop mechanisms. Additionally, Grem2, unlike Noggin, shows structural characteristics of growth factors. Therefore, it is possible that Grem2 binds and activates yet to be determined receptors that lead to JNK phosphorylation, independently of BMP signaling. Resolution of the

BMP/Grem2 structural complexes and their interaction with BMP receptors may shed light on these different scenarios.

Nkx2.5 has been a widely used transcription factor gene to mark for the cardiomyocyte lineage (Lian *et al.*, 2012). The gene has also been shown to regulate a critical set of genes to maintain proper cardiac formation and function, including NPPA which is the gene that encodes atrial natriuretic peptide A (ANF) (Tanwar *et al.*, 2014). To our knowledge, this study is the first to systematically show restriction of Nkx2.5 gene expression as NPPA gene expression expands within the context of atrial differentiation. Other studies have shown that Nkx2.5 binds at specific genomic sites in the ANF gene locus. These binding elements were found to be sufficient for transactivating a reporter gene in hearts mirroring endogenous ANF gene expression (Lian *et al.*, 2012). The authors further showed that the repressor Hey2 contributes to spatial expression pattern of the reporter gene in the developing heart. This suggests that Nkx2.5 mediates activation of NPPA and in turn activates repressors of Nkx2.5 to turn off Nkx2.5 gene in order to direct differentiation towards an atrial phenotype.

Similarly, Pitx2 gene is a transcription factor that I see is upregulated in our atrial differentiation platform. Studies have shown that Pitx2 mRNA levels contribute to atrial resting membrane potential (RMP). Overexpression and underexpression studies with Pitx2 gene has been found to be associated with AF in humans (Nadadur *et al.*, 2016). This signifies the need to have appropriate models to study AF within normal Pitx2 conditions, and I believe that our platform will allow future studies to probe for therapeutics involving Pitx2 regulation. In general, the entire scope of the activities and interactions of PITX2 are yet to be elucidated, it is clear that *PITX2* has important functions in the adult left atrium, and there is evidence in animal models that reduced *Pitx2* mRNA levels predispose atria to AF by changing its electrical function, whether by abnormal pacemaker activity or adverse electrical

remodeling. While complete deletion of *Pitx2* results in structural abnormalities, moderate reduction in atrial *Pitx2* levels primarily alters electrical function of the atria, for example the resting membrane potential and ion channel function. Emerging evidence that *PITX2* not only contributes to AF but could be used to predict effectiveness of rhythm control therapy, coupled with further investigations into the key co-factors, regulators and targets of *PITX2* could change the current strategies used to determine the choice of anti-arrhythmic drugs. Therefore, I will need reliable methods to identify alterations in *PITX2* expression in humans which may help to make an informed choice about anti-arrhythmic drug therapy.

Moving on to the importance of IK1 channels in promoting atrial specificity, considerable progress has been made to dissect the functions of distinct atrial potassium (K^+) channels. Interestingly, some K^+ channels are expressed at high levels only in atria, providing potential targets for tissue-specific treatment of atrial arrhythmias as well as guided differentiation platforms to make more atrial cardiomyocytes ideally without effects in ventricles. For example, in human atria, Kv1.5 provides the transmembrane channel pore that underlies the ultra-rapid delayed rectifier current (I_{Kur}) responsible for fast phase-2 repolarization. Because of exclusive atrial Kv1.5 expression as observed in our iPS derived atrial cardiomyocytes, I_{Kur} may function as a major repolarizing current that shortens phase-2 only in atrial but not ventricular myocytes as shown in Chapter 5 of this thesis. Kv1.5 is also considered a promising target for the development of new antiarrhythmic drugs and an important strategy to avoid potentially life-threatening adverse drug effects in the ventricle, a common problem in patients with atrial rhythm disorders. Conversely, in isolated canine atrial compared to ventricular myocytes, inwardly rectifying K^+ channels, in particular Kir2.1, were shown to be expressed at significantly lower levels consistent with only one third of I_{K1} current density relevant for atrial AP phases-3/4. Constitutively lower I_{K1} currents may contribute to the slow depolarization observed in phase-4, which determines the

threshold of cell excitability and hence atrial automaticity as well as maintaining a more negative resting membrane potential in our hands.

In summary, I have directed the differentiation of iPSCs towards atrial like cardiomyocytes, which warrants further investigation in to the role of these transcription factors in cardiac development and disease. Moreover, generation and characterization of cardiomyocyte subtypes such as atrial, ventricular and pacemaker cells *in vitro* is essential for their applicability in pre-clinical and clinical testing. In this chapter, I addressed the impending need for a pre-clinical screening model resembling the biomolecular and physiological characteristics of a human atrial cardiomyocyte. The finding that iPSC-atrial CMs are a robust model for atrial-selective pharmacology has major implications for drug discovery and development to combat AF.

CHAPTER 5: PROBING ADRENOCEPTOR SIGNALING IN IPSC DERIVED CARDIOMYOCYTES INCLUDING THOSE WITH AN ADULT ATRIAL PHENOTYPE.

Chapter 5: Probing Adrenoceptor Signaling in iPSC Derived Cardiomyocytes Including Those With An Adult Atrial Phenotype

5.1 Introduction

Understanding human adrenoceptor signaling

Receptors are defined by their ability to recognize hormones, neurotransmitters or drugs of a specific class through direct binding interactions and, of equal importance, to translate the binding event into a biological response (Stadel, 1991). There are two adrenergic receptors associated with the heart. In animal models studied, α and β adrenoceptors have been found to be different in terms of the effects of the drug each receptor binds: β adrenoceptors effects exhibit a larger increase of relaxation than of contraction (Skomedal *et al,* 1986). This is referred to as a selective relaxant effect, e.g. shortened time to reach peak tension, while α adrenergic receptors do not have a selective relaxant effect (Skomedal *et al*, 1986). α adrenergic effects also develop more slowly than β adrenergic effects (Osnes, 1978). The inotropic effects of β-receptor stimulation and α-receptor stimulation (phenylephrine combined with propranolol) were studied in isolated perfused rat hearts, atria and papillary muscles. The β-effect reached maximum before the α-effect (Osnes, 1978). The α-effect followed a three-phase course in reference to time indicating both stimulatory and inhibitory components (Osnes, 1978).

Two common drugs that are shown to exhibit α adrenoceptor effects are epinephrine and phenylephrine. While epinephrine is largely used for cardiopulmonary resuscitation and increases cerebral blood flow to a much bigger extent, phenylephrine exhibits this effect to a smaller extent (Brown, 1986). Phenylephrine is an α1 adrenergic agonist and is used primarily as a decongestant. It works by constricting arteries to decrease blood supply to nasal mucosa and decrease mucosal edema (Verma, 1976). It is also used to increase blood pressure, e.g resulting from septic shock. An IV bolus of phenylephrine is short lived and needs to be reassessed every so often. According to a study in the 70s, injections of

phenylephrine into isolated perfused guinea pig hearts increased cyclic AMP and phosphorylase (Verma, 1976). However, this was refuted later since phenylephrine does not activate cardiac adenylate cyclase (Benfey, 1971). The increase in cyclic AMP was then understood to be due to β-receptor stimulation making it a weak β agonist.

Phenylephrine stimulates myocardial beta receptors indirectly at low concentrations through the release of noradrenaline (Schumann, 1974) and directly through high concentrations (10uM). Phenylephrine is also known to cause hypertrophy and recent studies have attempted to find ways to treat hypertrophy induced by phenylephrine. A study done in 2017 found that phenylephrine-induced cardiac hypertrophy is attenuated by a histone acetylase inhibitor and a Chinese herbal extract, anacardic acid in mice (Peng, 2017). Overall, phenylephrine is relatively safe with no dependence and can be used long term by patients carrying a low incidence of side effects.

As stated earlier, the ionotropic effects of an alpha adrenergic are independent of cyclic AMP but are dependent on cyclic AMP for a beta adrenergic agonist. An example of a beta agonist would be isoprenaline, a drug used to treat bradycardia. Isoprenaline was tested on cardiac Purkinje fibers in comparison to noradrenaline and showed that isoprenaline increases the slope of phase 2 of repolarization and decreases the plateau length; the resulting decrease in action potential duration is concentration dependent, but not rate dependent (Giotti, 1973). Recent work shows an increase in duration followed by a decrease, which perhaps effects via L-type Ca^{2+} channels with a slower but dominant effect via potassium channels (perhaps IKs). The effect of isoprenaline on the action potential duration was entirely blocked by propranolol, a beta blocker but unaffected by phentolamine, an alpha blocker (Giotti, 1973). It has been shown to induce coronary spasm. Isoprenaline has also been tested as an inhalation agent for asthmatic patients without a statistically significant risk to the heart.

Prazosin was approved by the Food and Drug Administration for the treatment of hypertension in 1976. Structurally, it combines the 4- amino pyrimidine moiety found in cyclic AMP and the dimethoxy benzo moiety of papaverine, a recognized inhibitor of phosphodiesterase (Graham et al, 1977). Prazosin is a peripherally acting selective a1 blocker used for the treatment of hypertension, anxiety and posttraumatic stress disorder. It has also been used to decrease urinary obstruction and relieve symptoms associated with symptomatic benign prostatic hyperplasia. α1-receptors mediate contraction and hypertrophic growth of smooth muscle cells. Antagonism of these receptors leads to smooth muscle relaxation in the peripheral vasculature and prostate gland (Graham et al, 1977). After blocking the postsynaptic receptors, both arteries and veins exhibit indirect vasodilation. Prazosin causes less reflex tachycardia than do other vasodilator agents. In a study, the vasodilatory and alpha adrenergic blocking properties of prazosin were studied in rats and compared with the direct-acting vasodilator, diazoside (Graham et al, 1977). The hypotensive action of prazosin was completely abolished, over a 10-fold dose range, after ganglion or alpha adrenoreceptor blockade and it failed in all hypotensive doses, to attenuate its angiotensin II pressor responses (Graham et al, 1977). At this time, Prazosin was shown to possess potent alpha adrenoceptor blocking properties, attenuating norepinephrine pressor responses and causing reversal of epinephrine pressor responses. Furthermore, evidence shows that unlike direct-acting vasodilators, prazosin causes little reflex stimulation of renin release (Graham et al., 1977).

Development of Small Molecule PAK1 Activators

Heart Failure (HF) is a growing subclass of cardiovascular disease with the highest morbidity and mortality and it currently lacks innovative, effective therapies. Maladaptive hypertrophy is the key step leading to HF regardless of initial pathological stimulus. Increasing evidence indicates modulating specific intracellular signaling pathways that regulate

myocardial remodeling offers potential new therapeutic strategies for the management of HF. One such strategy is the activation of P21-activated kinase (PAK1), which has shown to be anti-hypertrophic in various mouse models of pathological hypertrophy.

My colleague James Bae developed a small molecule PAK1 activator as a novel drug for the treatment for HF, through attenuating pathological maladaptive hypertrophic remodeling. We have already successfully translated from the PAK1-activating peptide to a small molecule PAK1 activator (current lead compound JB79) and designed a number of lead analogues. We have shown that the analogues can directly activate PAK1, and PAK1 activators are currently in the process of studying the structure-activity relationship (SAR). Functional studies of JB79 treated cardiomyocytes have shown significant improvement in Ca^{2+} handling through PAK1 activation. Finally, the immunohistochemistry of JB79 treated cells exhibited significantly higher fluorescence of PAK1, further validating evidence for drug induced PAK1 activation. From these developed small molecule PAK1 activator compounds, I would like to further optimize the current lead compound JB79 as a candidate drug for future clinical studies as an application to attenuate adrenoceptor signaling within human iPSC derived atrial cardiomyocytes.

Mechanisms of PAK1 activators

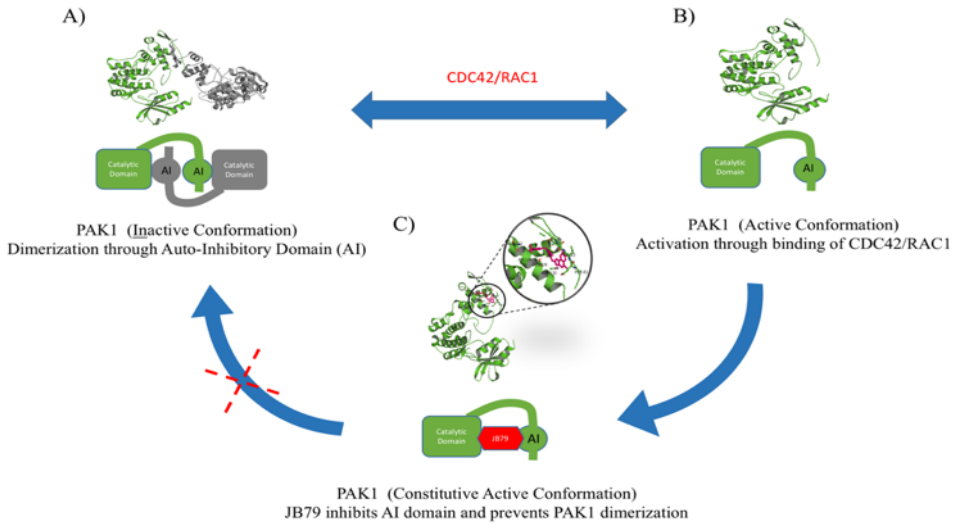

Figure 5.1 Mechanisms of the PAK1 small molecule activator.

As demonstrated in figure 5.1, PAK1 dimerization through the auto-inhibitory domain (AI) conceals the catalytic domain of PAK1 and subsequently, keeps PAK1 in an inactive conformation. Upon binding of regulator modulators such as CDC42 and RAC1 enzymes, PAK1 dissociates into monomers. This allows the catalytic domain to be exposed and to activate downstream enzymes that are responsible for providing cardio protective mechanisms. JB79 is a compound that binds to the AI domains and prevents PAK1 monomers from dimerizing again. This keeps PAK1 at a monomeric active form and continuous to activate the downstream beneficial proteins and provide protection against cardiac stress inducers.

The aim of the experiments presented in this chapter is to investigate any possible effects of adrenergic receptors on Ca^{2+} signaling in human iPSC derived atrial myocytes. Next, the development of therapeutically relevant compounds that may augment adrenergic signaling in human cellular models like in the case of PAK1 activators (JB79). In addition, human iPSC derived atrial myocytes maintain a more mature atrial-like electrophysiological

characteristics than previously reported. Finally, I address the void for a humanized preclinical screening platform for atrial-selective pharmacology.

5.2 Results

Effects of the α_1-adrenoceptor agonist phenylephrine

To functionally evaluate whether the presence of α_1-adrenoceptor receptor signaling is intact in human iPSC derived atrial cardiomyocytes, I tested the effects of phenylephrine's ability to enhance atrial Ca^{2+} transients. Phenylephrine is an α_1-adrenoceptor agonist paired to G_q that would be expected to increase cellular IP_3 levels. Therefore, to investigate whether this mechanism might influence human atrial myocyte EC coupling, human atrial myocyte Ca^{2+} transients were recorded before and after the application of phenylephrine. Atrial cardiomyocytes from Days 25-30 post initiation of differentiating human iPSC derived atrial cardiomyocytes were used to assess the effect of phenylephrine on Ca^{2+} transient amplitude. Figure 5.2 shows that 10μM phenylephrine increased the Ca^{2+} transient amplitude by 28 ± 10 % as measured from the fluo-4 fluorescence ($P < 0.05$, n = 5) but had no effect on the Ca^{2+} transient rise time or decay time. Figure 5.3 shows that 1 μM prazosin, a selective α_1 adrenoceptor antagonist, had no effect on control Ca^{2+} transients ($P < 0.05$, n = 5) and that in the presence of prazosin, phenylephrine had no effect on Ca^{2+} transients, consistent with blockade of alpha adrenoceptors by prazosin and the consequent suppression of the action of the agonist phenylephrine under these conditions ($P < 0.05$, n = 5).

Within our group there is significant interest in exploring the possible mechanism by which phenylephrine may enhance human atrial Ca^{2+} transients through the stimulation of Ca^{2+} sensitive adenylyl cyclase's (AC) by Ca^{2+} released by IP_3. It seems possible that Ca^{2+} released from IP_3Rs might regulate the activity of Ca^{2+} stimulated ACs. If this were the case, then inhibitors of ACs or of PKA would be expected to reduce the effects of phenylephrine, as this has been shown by Dr. Tom Collins, a former DPhil student in the lab. In similar experiments using optical mapping techniques, application of 10 μM phenylephrine in human atrial

cardiomyocytes pre-treated with 2-APB did not have inhibitory effects on Ca^{2+} transient amplitude (data not shown).

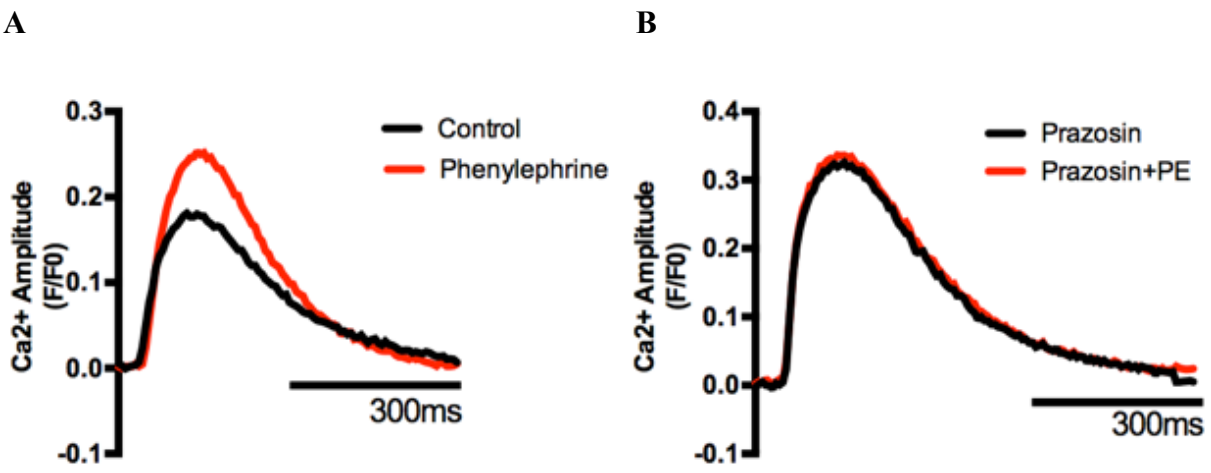

Figure 5.2 Representative Ca^{2+} transients recorded from Atrial CM derived from human iPSCs showing effects of 10μM phenylephrine and 1μM prazosin. Cells were loaded with fluo-4 at 37°C. (A)Phenylephrine evoked an increased Ca^{2+} transient amplitude within control experiments. (B) Pre-treatment with 1μM prazosin with and without 10μM phenylephrine evoked significantly smaller increases with pre-treatment with prazosin. (n=5)

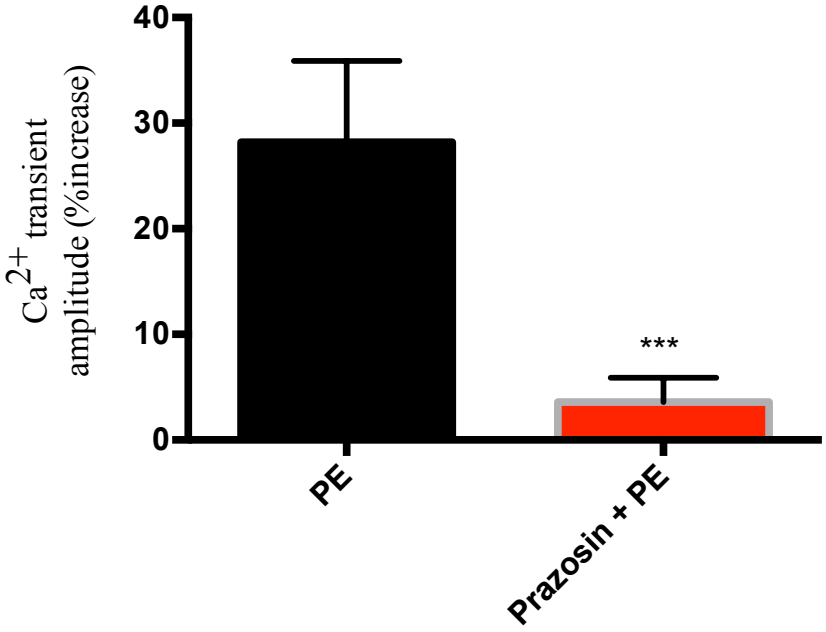

Figure 5.3 Effect of 10μM Phenylephrine on the mean Ca^{2+} transient amplitudes of Atrial CM derived from human iPSCs showing effects of 1μM prazosin. Cells were loaded with fluo-4 at 37°C. Phenylephrine evoked an increase in Ca^{2+} transient amplitude within control experiments. Pre-treatment with 1μM prazosin followed by application of 10μM phenylephrine with pre-treatment of prazosin. Data are expressed as the percentage change in Fluo4 fluorescence transient amplitude compared control values. Statistical significance was assessed via Student's t-Test. * p<=0.05, ** p<=0.001, *** p<=0.001, ****p<=0.0001. (n=5)

Effects of the β-adrenoceptor agonist isoprenaline

To functionally evaluate whether β-adrenoceptor signaling is intact in human iPSC derived atrial cardiomyocytes, I tested the effects of isoprenaline's ability to enhance atrial Ca^{2+} transients. Overall, β-adrenoceptors are G-protein Coupled Receptors (GPCRs) that contain 7 transmembrane spanning domains and couple to heterotrimeric GTP-binding proteins. Isoprenaline is a β-adrenoceptor agonist with a mode of action through G_s and G_i. Within atrial and ventricular cells β_1-adrenoceptors are activated by agonists, bound GDP is exchanged for GTP and the $G\alpha_s$ subunit is activated and remains so until it hydrolyses the GTP. $G\alpha_s$ dissociates from βγ and activates ACs to produce cAMP. The cAMP then binds to and activates PKA, which then phosphorylates LTCCs, PLB, TnI and possibly RyRs to produce an increase in the force of contraction and in the rate of relaxation. Therefore, to investigate whether this mechanism might influence human atrial myocyte EC coupling, human atrial myocyte Ca^{2+} transients were recorded before and after the application of isoprenaline. Atrial cardiomyocytes from Days 25-30 post initiation of differentiating human iPSC derived atrial cardiomyocytes were used to assess the effect of isoprenaline on Ca^{2+} transient amplitude. Figure 5.4 shows that 100nM isoprenaline increased Ca^{2+} transient amplitude by 36 ± 10 % as measured from the fluo-4 fluorescence ($P < 0.05$, n = 5) but had no effect on the Ca^{2+} transient rise time or decay time. Figure 5.5 shows that 600 nM CGP20712A, a selective β_1 adrenoceptor antagonist, had no effect on control Ca^{2+} transients ($P < 0.05$, n = 5) but that in the presence of CGP20712A, isoprenaline had no effect on Ca^{2+} transients ($P < 0.05$, n = 5). The results revealed that the major contributor in evoking the Ca^{2+} transient amplitude effects of isoprenaline was occurring through the activation of the β_1 pathway.

A **B**

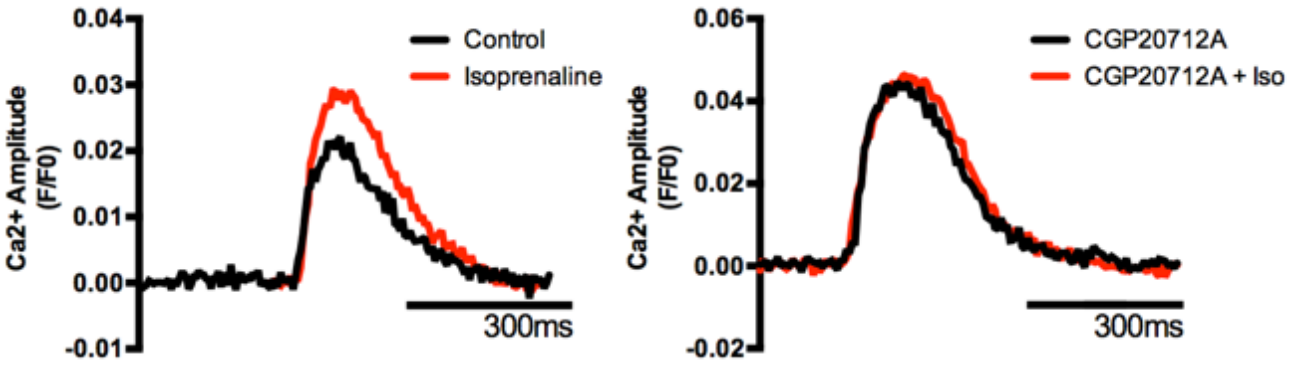

Figure 5.4 Representative Ca^{2+} transients recorded from Atrial CM derived from human iPSCs showing effects of 100nM isoprenaline and 600nM CGP20712A. Cells were loaded with fluo-4 at 37°C. (A) Isoprenaline evoked an increase Ca^{2+} transient amplitude within control experiments. (B) Pre-treatment with 600nM CGP20712A with 100nM isoprenaline evoked significantly smaller increases when pre-treated with CGP20712A alone. (n=5)

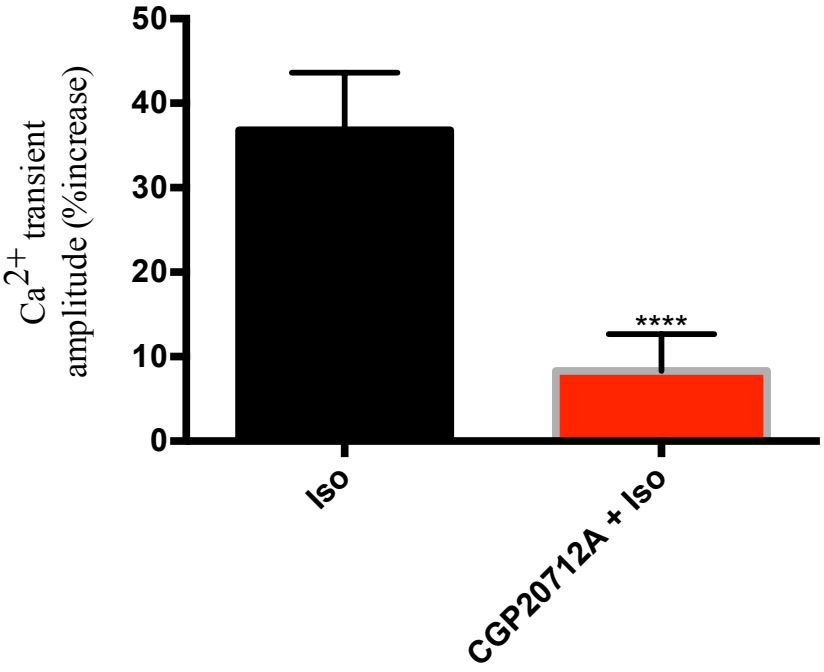

Figure 5.5 Effect of 100nM Isoprenaline on the mean Ca^{2+} transient amplitudes of Atrial CM derived from human iPSCs showing effects of 600nM CGP20712A. Cells were loaded with fluo-4 at 37°C. Isoprenaline evoked an increased Ca^{2+} transient amplitude within control experiments. Pre-treatment with 600nM CGP20712A followed by application of 100nM isoprenaline with pre-treatment of CGP20712A. Data are expressed as percentage change in Fluo4 fluorescence transient amplitude from control values. Statistical significance was assessed via Student's t-Test. * p<=0.05, ** p<=0.001, *** p<=0.001, ****p<=0.0001. (n=5).

Pak1 agonist JB79

To study PAK1 function in the heart, our group has created a PAK1 knock-out mice (Lei *et al.*, 2000). The study revealed that PAK1 deficiency in cardiomyocytes showed an exacerbated pressure overload-induced hypertrophy, as well as the sensitization of PAK1 KO to heart failure due to prolonged load stress (Lei *et al.*, 2000). Work from Prof. Ming's group demonstrated that PAK1 was able to repress ISO-induced arrhythmias by restoring both the L-type Ca^{2+} current and the delayed rectifier K+ current. The current hypothesis about these anti-adrenergic effects are that they occur through PAK1 activation of protein phosphatase 2A (PP2A), one of the main serine-threonine phosphatases active in maintaining cell homeostasis by inhibiting most kinase-driven intracellular signaling pathways. Lei et al, identified numerous examples that suppressing the effect of active PAK1 on the response to beta-adrenergic stimulations could partially be reversed (Lei *et al.*, 2000). These observations thus identified a key signaling mechanism for anti-adrenergic function and thereby, I could use our iPSC platform for both cardiotoxicity testing and probing adrenergic signaling mechanisms.

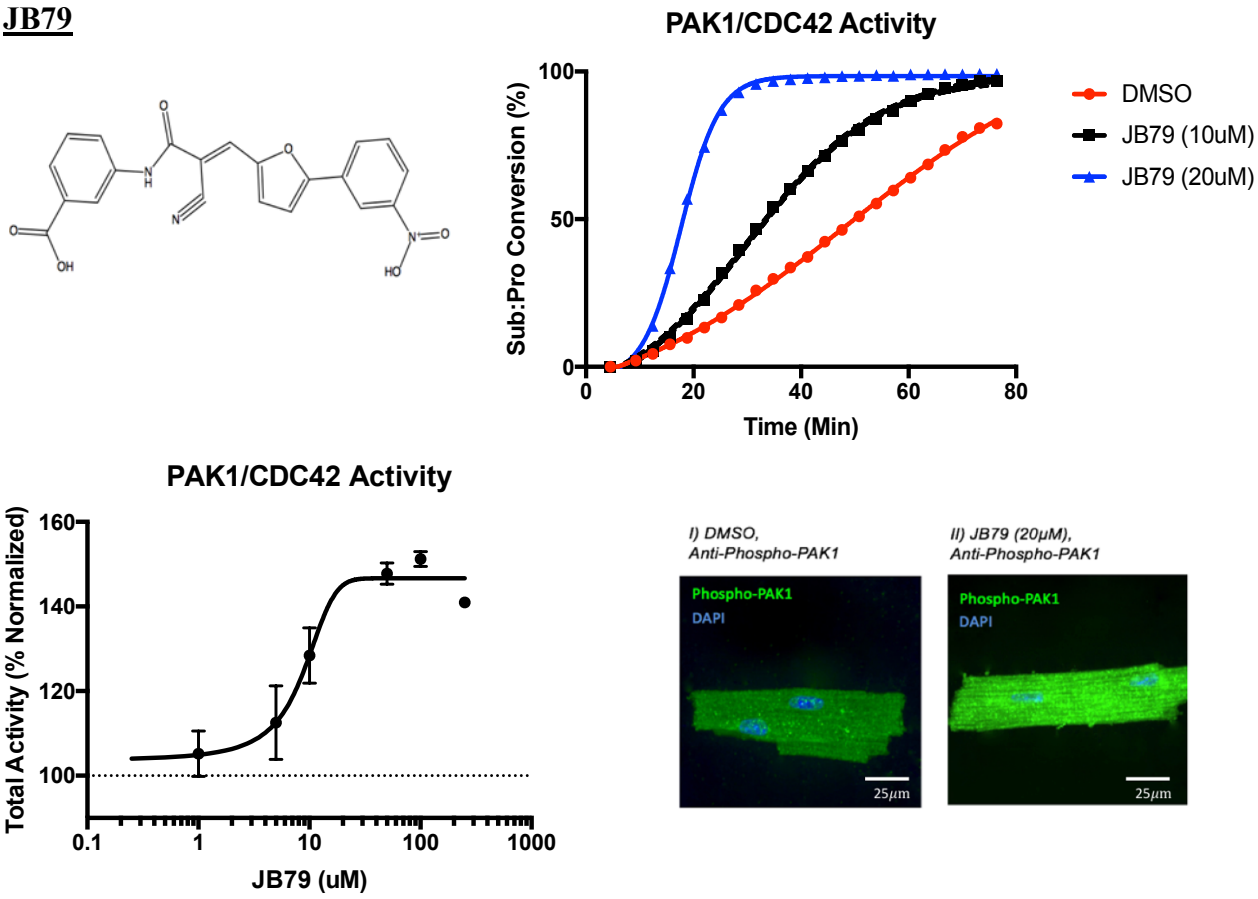

Figure 5.6 A) Structures JB79 B) RF-mass spectrometry results in PAK1/CDC42 activity. The rates of substrate to product (substrate phosphorylation) conversion were compared to PAK1/CDC42 kinase reaction in the presence of JB79 (20um), JB79 (10uM), and DMSO. C) Dose response test measuring the effects of JB79 on PAK1/CDC42 kinases using ADP-GLO assay. D) Immunofluorescent staining of mouse cardiomyocytes with phospho-PAK1 (Thr423) antibody (■) after 30 minutes of i) DMSO ii) JB79 (20μM). JB79 is permeable and able to activate intrinsic PAK1 in cardiomyocytes. Scale bars represent 25μm.

Effects of the α_1-adrenoceptor agonist phenylephrine in response to JB79

To functionally evaluate whether presence of α_1-adrenoceptor receptor signaling is intact in human iPSC derived atrial cardiomyocytes, I tested the effects of phenylephrine's ability to enhance atrial Ca^{2+} transients. Phenylephrine is an α_1-adrenoceptor agonist paired to G_q that would be expected to increase cellular IP_3 levels. Therefore, to investigate whether this mechanism might influence human atrial myocyte EC coupling, human atrial myocyte Ca^{2+} transients were recorded before and after the application of phenylephrine. Atrial

cardiomyocytes from days 25-30 post initiation of differentiating human iPSC derived atrial cardiomyocytes were used to assess the effect of phenylephrine on Ca^{2+} transient amplitude. Figure 5.7 shows that 10μM phenylephrine increased Ca^{2+} transient amplitude by 30 ± 10 % as measured from the fluo-4 fluorescence ($P < 0.05$, n = 5) but had no effect on the Ca^{2+} transient rise time or decay time. Figure 5.8 shows that 20μM JB79, a selective PAK1 small molecule activator, had no effect on control Ca^{2+} transients ($P < 0.05$, n = 5) and that in the presence of JB79, phenylephrine had no effect on Ca^{2+} transients ($P < 0.05$, n = 5).

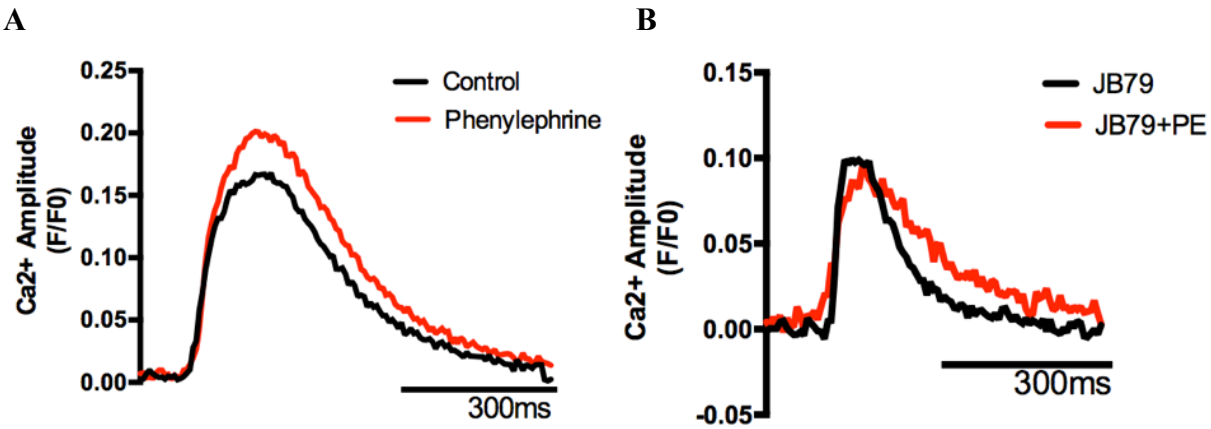

Figure 5.7 Representative Ca^{2+} transients recorded from Atrial CM derived from human iPSCs showing effects of 10µM phenylephrine and 20µM JB79. Cells were loaded with fluo-4 at 37°C. (A)Phenylephrine evoked an increase Ca^{2+} transient amplitude within control experiments. (B) 20µM JB79 pre-treatment with and without addition of 10µM phenylephrine induced significantly smaller increases than pre-treatment with JB79.

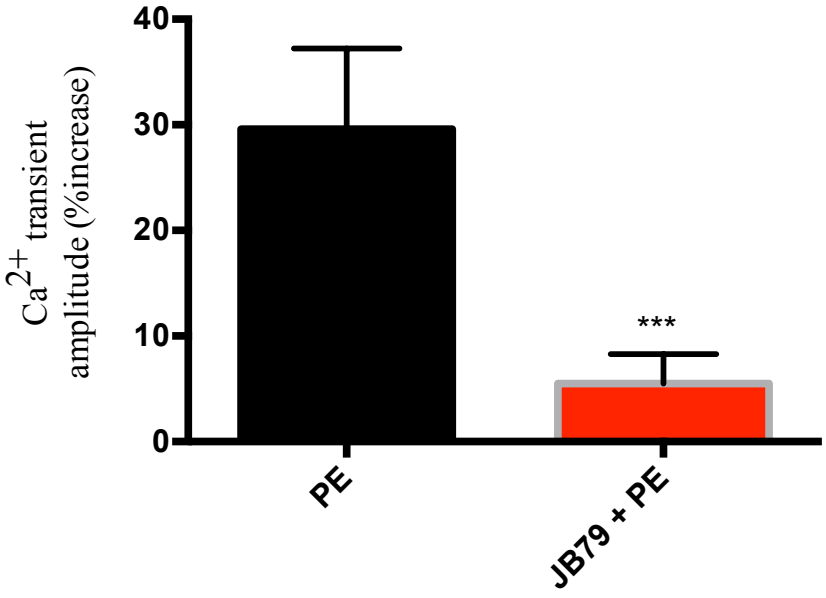

Figure 5.8 Representative Ca^{2+} transients recorded from Atrial CM derived from human iPSCs showing effects of 10µM phenylephrine and 20µM JB79. Cells were loaded with fluo-4 at 37°C. (A)Phenylephrine induced an increase in Ca^{2+} transient amplitude within control experiments. (B) Cells pre-treated with 20µM JB79 with and without application of 10µM phenylephrine evoked significantly smaller increases per pre-treatment with JB79. Statistical significance was assessed via Student's t-Test. * p<=0.05, ** p<=0.001, *** p<=0.001, ****p<=0.0001. (n=5)

Effects of the β-adrenoceptor agonist isoprenaline in response to JB79

To functionally evaluate whether presence of β-adrenoceptor signaling is intact in human iPSC derived atrial cardiomyocytes, I tested the effects of isoprenaline's ability to enhance atrial Ca^{2+} transients. Overall, β-adrenoceptors are G-protein Coupled Receptors (GPCRs) that contain 7 transmembrane spanning domains and couple to heterotrimeric GTP-binding proteins. Isoprenaline is an β-adrenoceptor agonist whose mode of action is through G_s and G_i. Within atrial and ventricular cells β_1-adrenoceptors are activated by agonists, bound GDP is exchanged for GTP and the $G\alpha_s$ subunit is activated and remains so until it hydrolyses the GTP. $G\alpha_s$ dissociates from $\beta\gamma$ and activates ACs to produce cAMP. The cAMP then binds to and activates PKA, which then phosphorylates LTCCs, PLB, TnI and possibly RyRs to produce an increase in the force of contraction and rate of relaxation. Therefore, to investigate whether this mechanism might influence human atrial myocyte EC coupling, human atrial myocyte Ca^{2+} transients were recorded before and after the application of isoprenaline. Atrial cardiomyocytes from days 25-30 post initiation of differentiating human iPSC derived atrial cardiomyocytes were used to assess the effect of isoprenaline on Ca^{2+} transient amplitude. Figure 5.9 shows that 100nM isoprenaline increased Ca^{2+} transient amplitude by 39 ± 10 % as measured from the fluo-4 fluorescence ($P < 0.05$, n = 5) but had no effect on the Ca^{2+} transient rise time or decay time. Figure 5.10 shows that 20uM JB79, a selective PAK1 activator, had no effect on control Ca^{2+} transients ($P < 0.05$, n = 5) and that in the presence of JB79, isoprenaline had no effect on Ca^{2+} transients ($P < 0.05$, n = 5). The results revealed that the major contributor in evoking the Ca^{2+} transient amplitude effects of isoprenaline was abolished by the PAK1 small molecule compound (JB79).

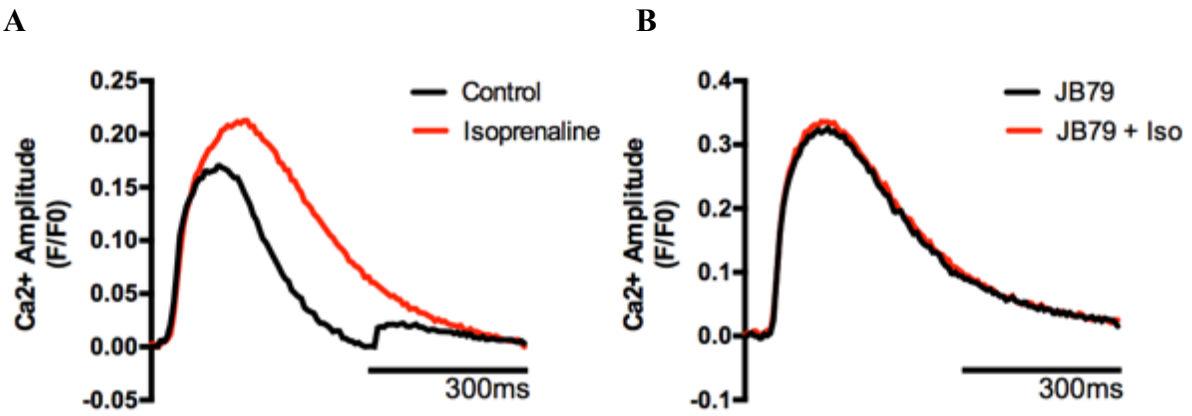

Figure 5.9 Representative Ca^{2+} transients recorded from Atrial CM derived from human iPSCs showing effects of 100nM isoprenaline and 20µM JB79. Cells were loaded with fluo-4 at 37°C. (A) Addition of isoprenaline evoked an increased Ca^{2+} transient amplitude within control experiments. (B) Cells were subjected to Pre-treatment with 20µM JB79 with and without application of 100nM isoprenaline induced significantly smaller increases than pre-treatment with JB79.

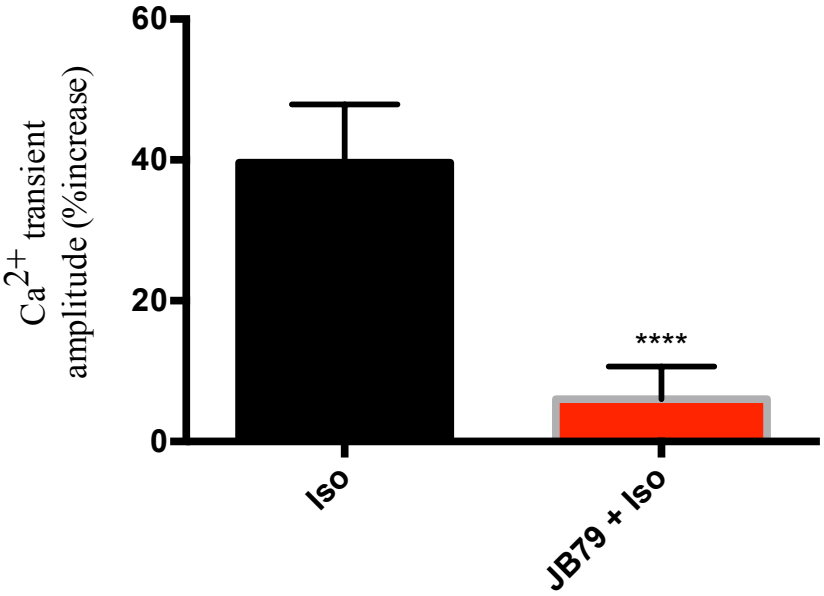

Figure 5.10 Representative Ca^{2+} transients recorded from Atrial CM derived from human iPSCs showing effects of 100nM isoprenaline and 20µM JB79. Cells were loaded with fluo-4 at 37°C. (A)Isoprenaline evoked an increase Ca^{2+} transient amplitude within control experiments. (B) Pre-treatment with 20µM JB79 with and without application of 100nM isoprenaline evoked significantly smaller increases with pre-treatment with JB79. Statistical significance was assessed via Student's t-Test. * p<=0.05, ** p<=0.001, *** p<=0.001, ****p<=0.0001. (n=5)

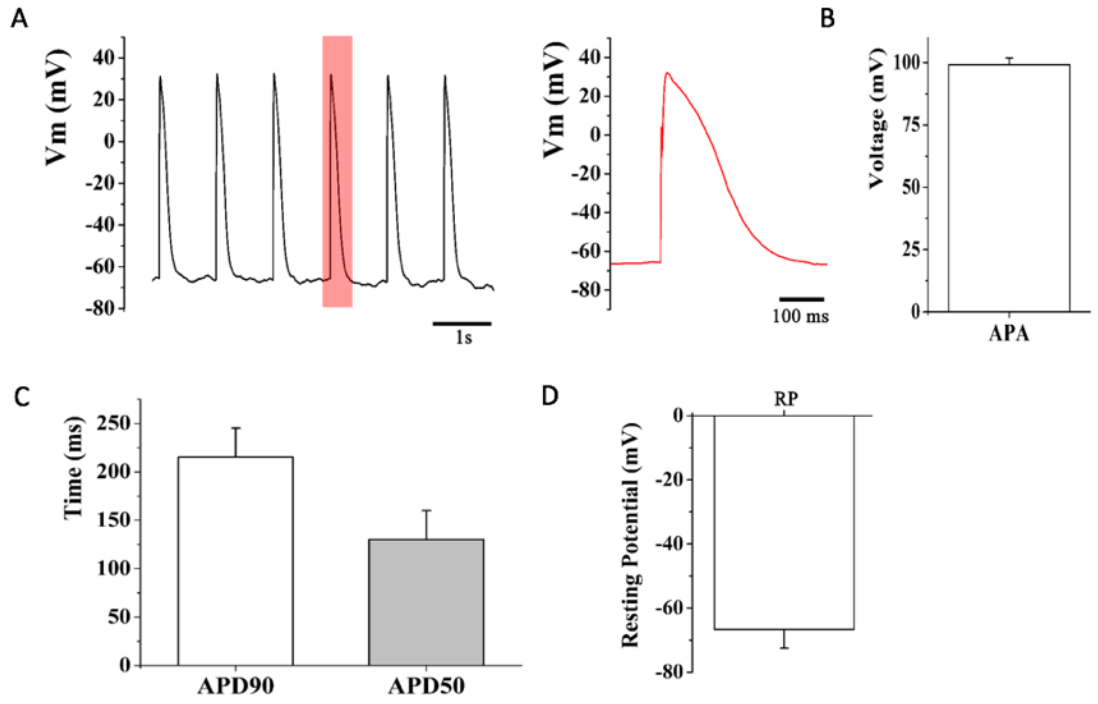

Figure 5.11 Representative action potentials recorded from human iPSC derived atrial cardiomyocytes patched in the whole cell configuration and stimulated once every second. (A) Showing representative AP recordings with magnifying a single AP at 0.5-4 Hz (B) Average action potential amplitude (APA) of the seven examined cells was 99.15 ± 2.74 mV (n=7). (C) Average action potential duration (APD) at 90% and 50% repolarization (APD90 and APD50) of the seven examined cells are 215.36 ± 29.88 ms and 130.12 ± 29.73 ms. (D) Average resting potential (RP) of the seven examined cells was -66.67 ± 5.85 mV (n=7). Data are presented as Mean ± SEM.

To further test my *in vitro* findings, which identified high levels of COUP-TF, NPPA and various other transcriptional requirements of adult atrial myocytes presented in Chapter 4, I along with collaborators in China sought to study the electrical phenotype of human iPSC derived atrial myocytes. We measured action potential (AP) of dissociated single cells using the patch-clamp method (Figure 5.11) Representative APs stimulated at 1Hz are shown in Figure 5.11A. The AP of an atrial myocyte depicts an AP with a fast phase-1 repolarization and a plateau phase with a repolarization to a more negative potential compared to previous published reports Figure 5.11B & Figure 5.11D. Average resting membrane potential's (RMP) (Figure 5.11D) were between ranges of -70 to -80mV. In particular, APs of atrial myocytes had a 100mV amplitude (APA), which is consistent with studies in atrial cardiomyocytes from

animal models. Figure 5.11C also demonstrates a shorter APD90 and APD50 as compared to previous published reports compared to ventricular myocytes. Of the 10 cells measured from the atrial myocyte group, 90% of the cells showed atrial-like action potential properties. Figure 5.12 demonstrates the architecture of AP recordings from a spontaneously beating cell. And broadly, the AP characteristics are similar to observed AP morphology for an atrial cell. It is important to note that the cultures showed spontaneous beating, but that after dissociation of these cultures into individual myocytes, it appeared that a small fraction of the individual cells showed spontaneous electrical activity (as in this figure) while many cells were electrically quiescent until stimulated as in Figure 5.11.

The differences observed in AP duration and APA between atrial myocytes and published reports of ventricular myocytes closely matched the AP differences observed between atrial and ventricular myocytes *in vivo* (Nerbonne & Kass, 2005). Taken together, gene expression signature, adrenergic signaling properties, and electrophysiological properties demonstrate that the atrial myocytes derived from human iPSC differentiation displayed atrial-like phenotype (hereby referred to as hiPSC-atrial CM)

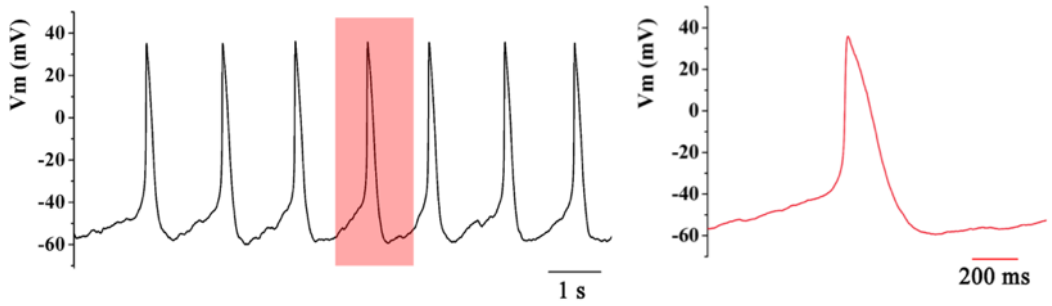

Figure 5.12 Representative action potentials recorded from human iPSC derived atrial cardiomyocytes that are spontaneously beating Showing representative architecture of AP recordings by magnifying a single AP without electrical stimulation. Action potential recordings of one representative quiescent cardiomyocyte.

5.3 Discussion

Cardiovascular disease is the leading cause of death in the United Kingdom. As such a constant and reliable source of CMs from both atrial and ventricular CM is necessary for disease modeling, drug screening or tissue engineering studies.

Here I compare the production of atrial cardiomyocytes. An advantage of directing differentiation towards atrial versus ventricular myocytes is the ability to perform side by side comparisons of atrial versus ventricular myocytes. Ultimately the true usefulness of iPSCs is being able to analyze genotypes associated with rich clinical information; the inclusion of atrial cells to probe cardiotoxic and physiological effects *in vitro* will only add further power to the study being performed. Thus the need to have either robust protocols for directed differentiation towards more mature cells for their performance in a particular drug testing protocol is in requirement of critical attention.

Studies of α_1-adrenoceptor and β-adrenoceptor signaling during the differentiation and maturation of human stem cell derived atrial cardiomyocytes have not been reported to date. Others have demonstrated β-adrenergic signaling during the differentiation and maturation of ventricular fated iPSC-CMs where they have found that despite some immature features, β-adrenergic signaling can induce inotropic and chronotropic regulation of contractile function in iPSC-CMs (Hwang *et al.*, 2015). Prof. Joseph Wu's lab have found that despite some immature features, β-adrenergic signaling can induce inotropic and chronotropic regulation of contractile function in iPSC-CMs, however they have not observed Ca^{2+} transient amplitude via optical mapping techniques.

The majority of previous studies have focused on ventricular iPSC models, which have their own limitations as indicated by often not being able to reach a fully mature state. However, ventricular models still offer an attractive human tissue based experimental platform to model cardiovascular diseases for mechanistic research and drug discovery. The

ability to direct human iPSCs towards an atrial cardiomyocyte phenotype had not been discovered. In fact, when I first enrolled as a DPhil candidate there existed no known protocols for the successful derivation of purified populations of atrial cardiomyocytes. Differentiation paradigms continue to use cell-based systems where the conditions are undefined. In this thesis, I believe I have made significant advances in curtailing a novel protocol to generate more functionally responsive atrial cardiomyocytes human iPSCs via temporal regulation of WNT and BMP signaling to drive this specification and subsequently the maturation of these cells. I have combined advances in differentiation techniques in the context of a human cellular model whereby discerning the functionality of atrial cardiomyocytes and their role in arrhythmogenic perturbations have been largely unmet. I hope to bring together expertise's in pluripotent stem cell biology, cellular modeling, and functionally relevant pharmacological testing in order to create a more accurate representation of health and disease mechanisms that will have profound implications in developing therapeutics within the broader cardiovascular field.

An important cause of drug withdrawals from the market in the past several decades has been cardiotoxicity (Christoffels *et al.*, 2006). Often, these drugs were associated with a potentially fatal form of ventricular arrhythmia, referred to as Torsades de Pointes (TdP) (Christoffels *et al.*, 2006). A significant number of these drugs were terminated in the late preclinical studies where it is very costly. This leads to the need for predictive assays that allow for assessment of potential cardiotoxic side effects of lead compounds early in the drug discovery process. The application of Ca^{2+} flux measurements to spontaneously contracting cardiomyocytes addresses several critical needs for development of *in vitro* assays suitable for safety and efficacy testing. Kinetic fluorescence recording is used to monitor cell beating rates and other temporal parameters to assess compound-induced changes in the phenotypic behavior of the cardiomyocytes. The automated data acquisition and analysis methods are

well suited for high-throughput environments. The assay precision is also sufficient for screening of compounds and can potentially allow early determination of their suitability for drug development. The ability to measure phenotypic response of human-derived cell models provides a system that shows good initial concordance with clinical data. A number of limitations of currently employed methods are overcome with this technique. Electrophysiology methods use mammalian cell lines over expressing ion channels, which might not be representative of native human cardiomyocytes.

Observation of Ca^{2+} flux in smooth muscle cell contraction was reported in 1986 (Hwang *et al.*, 2015) . Intracellular Ca^{2+} oscillations associated with spontaneous cardiomyocyte contractions (Hwang *et al.*, 2015) are monitored with Ca2+-sensitive fluorescent dyes (Christoffels *et al.*, 2006). This phenomenon was originally termed Ca^{2+} sparks because of the fast, transient nature of the response (Hwang *et al.*, 2015). The Ca^{2+} fluxes associated with contractions of cardiac cells have been established as physiologically relevant and a predictive indicator of myocardial performance (Christoffels *et al.*, 2006). iPSC-derived atrial cardiomyocytes recapitulate the expected genomic, biochemical, mechanical, and electrophysiological behaviors of native human cardiomyocytes and are available in large quantities required for high-throughput environments. The assays described herein, can be used to assess pharmacologic modulators of ion channels and adrenergic receptors and other targets that effect cardiac contraction.

Phenylephrine increased Ca^{2+} transient amplitude through a mechanism that could be inhibited by prazosin. This is consistent with phenylephrine activating α_1 adrenoceptors resulting in the production of IP_3, which is required for the increase in Ca^{2+} transient amplitude. This is consistent with previous studies that have used agonists coupled to PLC, which produce a sustained increase in the amplitude of electrically stimulated Ca^{2+} transients (Christoffels *et al.*, 2006).

CHAPTER 6: GENERAL DISCUSSION

6.1. General Discussion

A large motivation for the research within our lab is the understanding of intrinsic biological mechanisms within human induced pluripotent stem cells and their ability to differentiate to the cardiovascular lineage. This developmental knowledge can translate into potential therapeutics in hopes of improving the quality of life for those suffering from cardiac injury or disabilities such as AF. Regenerative medicine therapeutics are predicated upon optimal pluripotent stem cell culture and the ability to efficiently direct subtype specific cardiac differentiation.

Before iPSCs can be utilized as *in vitro* models for development or disease, they must be optimally maintained in a state of pluripotency. FGF2 is particularly unstable at 37°C and daily replenishment of stem cell media fails to provide consistent FGF2 concentration through incubation. FGF2 was encapsulated with the stabilizing cofactor heparin (Furue, 2007) within PLGA microspheres. It was revealed that FGF2 shielding from the harsh incubation conditions of 37°C for iPSCs provided a sustained release at an optimal concentration of 10 ng/ml over 72 hours. Supplementing HuESM with FGF2 loaded microspheres provided a novel feeding paradigm for iPSCs that not only provides trophic nourishment but a stable concentration of FGF2 through the noted 72 hours. The reduction of media replenishment by 67% minimizes risk of contaminants as cell culture dishes are previously exposed to open air in tissue culture hoods at daily frequencies. Most notable: maintaining a dependable concentration of FGF2 provides a iPSC population with greater differentiation potential as they can maintain high levels of pluripotency.

My results (Chapter 3) demonstrated that culture conditions with sustained FGF2 exposure not only aided in maintaining iPSC pluripotency, but also augmented directed induction towards naïve NPCs. Following the 10-day dual SMAD neural induction (Chambers, 2009), hESCs that were previously exposed to microspheres were capable of

generating 29.1% true NPCs (Yuan, 2011) relative to control conditions (Thomson, 1998) generating 12.4%. These data leads us to speculate that iPSCs exposed to microspheres on a consistent basis would have greater differentiation potential to derive any of the three germ layers and specific terminal cell types therein. Our studies have been furthered, by observing the generation of mesoderm lineage cells that consists of atrial and ventricular cardiomyocytes. It is my belief, that maintaining appropriate trophic conditions of support for iPSCs, that cellular differentiation could be performed more efficiently, and advances in regenerative medicine could progress more rapidly.

For myocardial injury and chronic HF, the clinical application of stem cell therapeutics using cellular transplantation is limited by heterogeneous populations of cells and lack of maturity. Chapter 4 confirmed the feasibility of deriving cells from iPSCs that resemble atrial cardiomyocytes in their morphology, surface phenotype and extensive gene expression analysis. Therefore, given that iPSCs may be derived in an autologous manner, the possibility of generating large populations of patient specific atrial cardiomyocytes appears entirely feasible.

Bone morphogenetic proteins (BMPs) employ pleiotropic properties on morphogenesis and cardiomyocyte maturation. The morphogenetic processes include cardiac looping, valve formation, and ventricular development. In addition to forward BMP signaling, BMP antagonists such as Noggin are also necessary for cardiac development. I hypothesized based on developmental data, that Gremlin2 (Grem2) also known as Protein Related to Dan and Cereberus (PRDC) could potentially influence atrial specification. Grem2 is a secreted BMP antagonist that belongs to the CAN family. The mechanism by which BMP antagonism occurs with Grem2 is by inhibiting Bmp2 and Bmp4 signaling . Work from Antonis Hatzopoulos's lab indicated in mouse studies that Grem2 was necessary for cardiac laterality and atrial differentiation during development (Christoffels *et al.*, 2006).

Here in Chapter 4, I have demonstrated that Grem2 treatment shifts human pluripotent stem cell differentiation to cardiomyocytes with atrial biomolecular and electrophysiological properties (Chapter 4). These findings provide a novel tool to probe mechanistic insights into cell type specific cardiomyocyte differentiation and stem cell platform to study atrial abnormalities.

Grem2/RA treatment leads to 20–120-fold expansion of myocytes and comparable induction levels in the expression of genes encoding atrial-specific contractile, gap junction and ion channel proteins such as Myl7, KCNA5, NPPA, and Kcnj5. Interestingly, Grem2/RA decreases ventricular myocyte differentiation and the expression levels of corresponding ventricular-specific genes such as Myl2, and Irx4. Consistent with these findings, electrophysiology data show that Grem2.RA-induced (Chapter 5), iPSC-derived cardiomyocytes have action potentials typical of atrial myocytes.

I have also re-established the importance of IK1 channels in promoting atrial specificity within the context of iPSC derived atrial cardiomyocytes. In summary, I have directed the differentiation of iPSCs towards atrial like cardiomyocytes, which warrants further investigation in to the role of these transcription factors in cardiac development and disease. Moreover, generation and characterization of cardiomyocyte subtypes such as atrial, ventricular and pacemaker cells *in vitro* is essential for their applicability in pre-clinical and clinical testing. The finding that iPSC-atrial CMs are a robust model for atrial-selective pharmacology has major implications for drug discovery and development to combat AF.

Studies of α_1-adrenoceptor and β-adrenoceptor signaling during the differentiation and maturation of human stem cell derived atrial cardiomyocytes have not been reported to date. While others have demonstrated β-adrenergic signaling during the differentiation and maturation of ventricular fated iPSC-CMs where they have found that despite some immature features, β-adrenergic signaling can induce inotropic and chronotropic regulation of

contractile function in iPSC-CMs (Hwang *et al.*, 2015). Ca^{2+} transient amplitude via optical mapping techniques have not been reported for iPSC derived atrial cardiomyocytes. In our literature survey, I believe I am the first to demonstrate adrenoceptor signaling in human atrial myocytes using optical techniques. The data garnered in this thesis is also strengthened by observations previously made within animal models studying atrial cell biology.

Study limitations

Clinical applications using cardiac stem cell engineering with autologous pluripotent stem cells face the limitation of scaling up sufficient cells *in vitro*. Although atrial and ventricular cells could be derived and grown from normal or disease patients as shown here, characterization of long-term cultured atrial or ventricular cells derived from iPSCs following multiple passages was not conducted regarding karyotype (chromosomal stability), phenotype (stemness) and function (contractility after differentiation, calcium transients, regenerative potential).

Future work

Following observations reported in this thesis that support the expression of mature atrial markers, the topological orientation of cardiac contractile proteins are yet to be determined. Various labeling and gene editing tools need to be used in order to follow more appropriately the developmental mechanisms whereby, Grem2 and RA elicit effects in the directed differentiation of iPSCs towards atrial cardiomyocytes (González *et al.*, 2014). These tools, or similar specific labeling agents, for targeting iPSCs will be useful in the study of various genes implicated in atrial pathophysiology. Our lab has had a longstanding interest in studying the expression of CD38 within the context of human atrial biology. The regulation of the expression of type-II or type-III CD38 is also worth studying as this will

provide further insight in to their expression levels in human cardiac tissue is altered in the disease state or upon hormonal stimulation. The relative contribution of type-III CD38 versus the type-II CD38 in terms of generating Ca2+-mobilizing molecules can also be investigated using pharmacological agents that inhibit the substrate/product transport mechanisms, which are pivotal for the type-II CD38 to act as an efficient enzyme.

It is necessary to optimize methods to efficiently guide differentiation of iPSCs into three major cardiac lineages (i.e., cardiac myocytes, endothelial and smooth muscle cells) *in vitro* using well-defined culture media supplemented with inducing chemical reagents or recombinant growth factors. Alternatively, another approach would be to differentiate iPSCs cultured within alginate- or collagen-based scaffold with assistance from signals arising from cell-to-ECM interactions. It would be important to conduct cardiomyogenic differentiation on substrates that provide maturation cues to determine if there is a biological mechanism to acutely alter levels of maturation within the differentiation paradigm.

In addition, to recellularize the decellularized ECM scaffold into a functional bioartificial organ for regenerative medicine, it is imperative to establish a suitable culture system resembling the *in vivo* physiological environment in terms of hemodynamic load and electro-mechanical coupling. During maturation, there are many fundamental and functional characterizations required. Undoubtedly, this is an ambitious and exciting goal, and requires a multidisciplinary team to work towards these achievements.

In short, a number of follow-up experiments should include: further optimization of *in vitro* cardiac lineage differentiation of iPSCs to generate homogenous atrial versus ventricular beating cardiomyocytes that could be subjected to the measurement of calcium transients, optimisation of scalable differentiation paradigms, cardiomyocyte maturation techniques, characterization of long-term cultured iPSC derived cardiomyocytes, and *in vivo* functional study of regenerative potential.

REFERENCES

References

Akopian, V, Andrews, PW, Beil, S, Benvenisty, N, Brehm, J, Christie, M*, et al.* (2010). Comparison of defined culture systems for feeder cell free propagation of human embryonic stem cells. *In Vitro Cellular & Developmental Biology-Animal* **46**: 247-58.

Al Ghamdi, B, Hassan, W (2009). Atrial Remodeling And Atrial Fibrillation: Mechanistic Interactions And Clinical Implications. *Journal of atrial fibrillation* **2**.

Banerji, CR, Miranda-Saavedra, D, Severini, S, Widschwendter, M, Enver, T, Zhou, JX*, et al.* (2013). Cellular network entropy as the energy potential in Waddington's differentiation landscape. *Scientific reports* **3**: 3039.

Beenken, A, Mohammadi, M (2009). The FGF family: biology, pathophysiology and therapy. *Nature reviews Drug discovery* **8**: 235-53.

Belus, A, Piroddi, N, Scellini, B, Tesi, C, Amati, GD, Girolami, F*, et al.* (2008). The familial hypertrophic cardiomyopathy-associated myosin mutation R403Q accelerates tension generation and relaxation of human cardiac myofibrils. *J Physiol (Lond)* **586**: 3639-44.

Bizy, A, Guerrero-Serna, G, Hu, B, Ponce-Balbuena, D, Willis, BC, Zarzoso, M*, et al.* (2013). Myosin light chain 2-based selection of human iPSC-derived early ventricular cardiac myocytes. *Stem cell research* **11**: 1335-47.

Blundo, JT (2010). *Biomechanics in the Heart and Bone: The Role of Electromechanical Forces in Deriving Cardiac Myocytes from Human Embryonic Stem Cells and the Role of Focal Adhesion Kinase in Osteoblast Mechanotransduction.* Stanford University.

Bolton, E, Bayliss, R, Kalungia, CA, Bloor-Young, D, da Silva, MR, Parrington, J*, et al.* (2013). The involvement of NAADP and two-pore Ca2 channels in the cardiac beta-adrenergic response. *Biophys J* **104**: 614a.

Bradley, A, Evans, M, Kaufman, MH & Robertson, E (1984). Formation of germ-line chimaeras from embryo-derived teratocarcinoma cell lines. *Nature* **309**: 255-6.

Brand, T (2003). Heart development: molecular insights into cardiac specification and early morphogenesis. *Dev Biol* **258**: 1-19.

Breckenridge, RA, Mohun, TJ & Amaya, E (2001). A role for BMP signalling in heart looping morphogenesis in Xenopus. *Dev Biol* **232**: 191-203.

Burridge, PW, Li, YF, Matsa, E, Wu, H, Ong, S, Sharma, A*, et al.* (2016). Human induced pluripotent stem cell-derived cardiomyocytes recapitulate the predilection of breast cancer patients to doxorubicin-induced cardiotoxicity. *Nat Med* **22**: 547-56.

Burridge, PW, Matsa, E, Shukla, P, Lin, ZC, Churko, JM, Ebert, AD*, et al.* (2014). Chemically defined generation of human cardiomyocytes. *Nature methods* **11**: 855-60.

Burridge, PW, Thompson, S, Millrod, MA, Weinberg, S, Yuan, X, Peters, A*, et al.* (2011). A universal system for highly efficient cardiac differentiation of human induced pluripotent stem cells that eliminates interline variability. *PloS one* **6**: e18293.

Bylund, JB, Hatzopoulos, AK (2016). Differentiation of atrial cardiomyocytes from pluripotent stem cells using the BMP antagonist Grem2. *JoVE (Journal of Visualized Experiments)*: e53919-.

Calcraft, PJ, Ruas, M, Pan, Z, Cheng, X, Arredouani, A, Hao, X*, et al.* (2009). NAADP mobilizes calcium from acidic organelles through two-pore channels. *Nature* **459**: 596-600.

Cambridge, D, Davey, MJ & Massingham, R (1977). Prazosin, a selective antagonist of post-synaptic alpha-adrenoceptors [proceedings. *Br J Pharmacol* **59**: 514P-5P.

Capecchi, MR (1989). Altering the genome by homologous recombination. *Science* **244**: 1288-92.

Cardin, S, Li, D, Thorin-Trescases, N, Leung, T, Thorin, E & Nattel, S (2003). Evolution of the atrial fibrillation substrate in experimental congestive heart failure: angiotensin-dependent and-independent pathways. *Cardiovasc Res* **60**: 315-25.

Carlsson, L (2006). In vitro and in vivo models for testing arrhythmogenesis in drugs. *J Intern Med* **259**: 70-80.

Caspi, O, Itzhaki, I, Kehat, I, Gepstein, A, Arbel, G, Huber, I*, et al.* (2009). In vitro electrophysiological drug testing using human embryonic stem cell derived cardiomyocytes. *Stem cells and development* **18**: 161-72.

Chambers, SM, Fasano, CA, Papapetrou, EP, Tomishima, M, Sadelain, M & Studer, L (2009). Highly efficient neural conversion of human ES and iPS cells by dual inhibition of SMAD signaling. *Nat Biotechnol* **27**: 275-80.

Chang Liao, ML, de Boer, TP, Mutoh, H, Raad, N, Richter, C, Wagner, E*, et al.* (2015). Sensing Cardiac Electrical Activity With a Cardiac Myocyte--Targeted Optogenetic Voltage Indicator. *Circ Res* **117**: 401-12.

Chen, G, Gulbranson, D, Yu, P, Hou, Z & Thomson, J (2011). Thermal stability of FGF protein is a determinant factor in regulating self-renewal, differentiation and reprogramming in human pluripotent stem cells. *Stem Cells* **30**: 623-30.

Chocron, S, Verhoeven, MC, Rentzsch, F, Hammerschmidt, M & Bakkers, J (2007). Zebrafish Bmp4 regulates left–right asymmetry at two distinct developmental time points. *Dev Biol* **305**: 577-88.

Chong, JJ, Yang, X, Don, CW, Minami, E, Liu, Y, Weyers, JJ*, et al.* (2014). Human embryonic-stem-cell-derived cardiomyocytes regenerate non-human primate hearts. *Nature* **510**: 273-7.

Christoffels, VM, Mommersteeg, MT, Trowe, MO, Prall, OW, de Gier-de Vries, C, Soufan, AT*, et al.* (2006). Formation of the venous pole of the heart from an Nkx2-5-negative precursor population requires Tbx18. *Circ Res* **98**: 1555-63.

Coppini, R, Ferrantini, C, Yao, L, Fan, P, Del Lungo, M, Stillitano, F*, et al.* (2013). Late sodium current inhibition reverses electromechanical dysfunction in human hypertrophic cardiomyopathy. *Circulation* **127**: 575-84.

Cowan, CA, Klimanskaya, I, McMahon, J, Atienza, J, Witmyer, J, Zucker, JP*, et al.* (2004). Derivation of embryonic stem-cell lines from human blastocysts. *N Engl J Med* **350**: 1353-6.

Dailey, L, Ambrosetti, D, Mansukhani, A & Basilico, C (2005). Mechanisms underlying differential responses to FGF signaling. *Cytokine Growth Factor Rev* **16**: 233-47.

Daily, NJ, Santos, R, Vecchi, J, Kemanli, P & Wakatsuki, T (2017). Calcium transient assays for compound screening with human iPSC-derived cardiomyocytes: Evaluating new tools. *Journal of evolving stem cell research* **1**: 1.

Darbar, D, Roden, DM (2013). Genetic mechanisms of atrial fibrillation: impact on response to treatment. *Nature Reviews Cardiology* **10**: 317-29.

de Pater, E, Ciampricotti, M, Priller, F, Veerkamp, J, Strate, I, Smith, K*, et al.* (2012). Bmp signaling exerts opposite effects on cardiac differentiation. *Circ Res* **110**: 578-87.

Denning, C, Anderson, D (2009). Cardiomyocytes from human embryonic stem cells as predictors of cardiotoxicity. *Drug Discovery Today: Therapeutic Strategies* **5**: 223-32.

Devalla, HD, Schwach, V, Ford, JW, Milnes, JT, El-Haou, S, Jackson, C*, et al.* (2015). Atrial-like cardiomyocytes from human pluripotent stem cells are a robust preclinical model for assessing atrial-selective pharmacology. *EMBO Mol Med* **7**: 394-410.

Di Pasquale, E, Lodola, F, Miragoli, M, Denegri, M, Avelino-Cruz, J, Buonocore, M*, et al.* (2013). CaMKII inhibition rectifies arrhythmic phenotype in a patient-specific model of catecholaminergic polymorphic ventricular tachycardia. *Cell death & disease* **4**: e843.

Dobrev, D, Ravens, U (2003). Remodeling of cardiomyocyte ion channels in human atrial fibrillation. *Basic Res Cardiol* **98**: 137-48.

Doetschman, TC, Eistetter, H, Katz, M, Schmidt, W & Kemler, R (1985). The in vitro development of blastocyst-derived embryonic stem cell lines: formation of visceral yolk sac, blood islands and myocardium. *J Embryol Exp Morphol* **87**: 27-45.

Doherty, KR, Talbert, DR, Trusk, PB, Moran, DM, Shell, SA & Bacus, S (2015). Structural and functional screening in human induced-pluripotent stem cell-derived cardiomyocytes accurately identifies cardiotoxicity of multiple drug types. *Toxicol Appl Pharmacol* **285**: 51-60.

Doherty, KR, Wappel, RL, Talbert, DR, Trusk, PB, Moran, DM, Kramer, JW*, et al.* (2013). Multi-parameter in vitro toxicity testing of crizotinib, sunitinib, erlotinib, and nilotinib in human cardiomyocytes. *Toxicol Appl Pharmacol* **272**: 245-55.

Dooley, DJ, Bittiger, H (1987). Quantitative assessment of central β1 and β2-adrenoceptor regulation using CGP 20712 A. *J Pharmacol Methods* **18**: 131-6.

Du, DT, Hellen, N, Kane, C & Terracciano, CM (2015). Action potential morphology of human induced pluripotent stem cell-derived cardiomyocytes does not predict cardiac chamber specificity and is dependent on cell density. *Biophys J* **108**: 1-4.

Dubois, NC, Craft, AM, Sharma, P, Elliott, DA, Stanley, EG, Elefanty, AG*, et al.* (2011). SIRPA is a specific cell-surface marker for isolating cardiomyocytes derived from human pluripotent stem cells. *Nat Biotechnol* **29**: 1011-8.

Dvorak, P, Hampl, A (2005). Basic fibroblast growth factor and its receptors in human embryonic stem cells. *Folia histochemica et Cytobiologica* **43**: 203-8.

Ehrlich, JR, Cha, T, Zhang, L, Chartier, D, Melnyk, P, Hohnloser, SH*, et al.* (2003). Cellular electrophysiology of canine pulmonary vein cardiomyocytes: action potential and ionic current properties. *J Physiol (Lond)* **551**: 801-13.

Ehrlich, JR, Zicha, S, Coutu, P, Hébert, TE & Nattel, S (2005). Atrial fibrillation-associated minK38G/S polymorphism modulates delayed rectifier current and membrane localization. *Cardiovasc Res* **67**: 520-8.

Ekerot, M, Stavridis, MP, Delavaine, L, Mitchell, MP, Staples, C, Owens, DM*, et al.* (2008). Negative-feedback regulation of FGF signalling by DUSP6/MKP-3 is driven by ERK1/2 and mediated by Ets factor binding to a conserved site within the DUSP6/MKP-3 gene promoter. *Biochem J* **412**: 287-98.

Eschenhagen, T, Mummery, C & Knollmann, BC (2015). Modelling sarcomeric cardiomyopathies in the dish: from human heart samples to iPSC cardiomyocytes. *Cardiovasc Res* **105**: 424-38.

Evans, M (2011). Discovering pluripotency: 30 years of mouse embryonic stem cells. *Nature Reviews Molecular Cell Biology* **12**: 680-6.

Evans, MJ, Kaufman, MH (1981). Establishment in culture of pluripotential cells from mouse embryos. *Nature* **292**: 154-6.

Farkasfalvi, K, Stagg, MA, Coppen, SR, Siedlecka, U, Lee, J, Soppa, GK*, et al.* (2007). Direct effects of apelin on cardiomyocyte contractility and electrophysiology. *Biochem Biophys Res Commun* **357**: 889-95.

Fermini, B, Hancox, JC, Abi-Gerges, N, Bridgland-Taylor, M, Chaudhary, KW, Colatsky, T*, et al.* (2016). A new perspective in the field of cardiac safety testing through the comprehensive in vitro proarrhythmia assay paradigm. *Journal of biomolecular screening* **21**: 1-11.

Földes, G, Matsa, E, Kriston-Vizi, J, Leja, T, Amisten, S, Kolker, L*, et al.* (2014). Aberrant α-adrenergic hypertrophic response in cardiomyocytes from human induced pluripotent cells. *Stem cell reports* **3**: 905-14.

Fonoudi, H, Ansari, H, Abbasalizadeh, S, Blue, GM, Aghdami, N, Winlaw, DS*, et al.* (2016). Large-scale production of cardiomyocytes from human pluripotent stem cells using a highly reproducible small molecule-based differentiation protocol. *JoVE (Journal of Visualized Experiments)*: e54276-.

Furue, MK, Na, J, Jackson, JP, Okamoto, T, Jones, M, Baker, D*, et al.* (2008). Heparin promotes the growth of human embryonic stem cells in a defined serum-free medium. *Proc Natl Acad Sci U S A* **105**: 13409-14.

González, F, Zhu, Z, Shi, Z, Lelli, K, Verma, N, Li, QV*, et al.* (2014). An iCRISPR platform for rapid, multiplexable, and inducible genome editing in human pluripotent stem cells. *Cell stem cell* **15**: 215-26.

Graham, RM, Pettinger, WA (1979). Prazosin. *N Engl J Med* **300**: 232-6.

Graham, RM, Oates, HF, Stoker, LM & Stokes, GS (1977). Alpha blocking action of the antihypertensive agent, prazosin. *J Pharmacol Exp Ther* **201**: 747-52.

Greber, B, Wu, G, Bernemann, C, Joo, JY, Han, DW, Ko, K*, et al.* (2010). Conserved and divergent roles of FGF signaling in mouse epiblast stem cells and human embryonic stem cells. *Cell stem cell* **6**: 215-26.

Guan, X, Wang, Z, Czerniecki, S, Mack, D, Francois, V, Blouin, V*, et al.* (2015). Use of adeno-associated virus to enrich cardiomyocytes derived from human stem cells. *Human Gene Therapy Clinical Development* **26**: 194-201.

Guinamard, R, Chatelier, A, Demion, M, Potreau, D, Patri, S, Rahmati, M*, et al.* (2004). Functional characterization of a Ca2 -activated non-selective cation channel in human atrial cardiomyocytes. *J Physiol (Lond)* **558**: 75-83.

Hao, J, Daleo, MA, Murphy, CK, Paul, BY, Ho, JN, Hu, J*, et al.* (2008). Dorsomorphin, a selective small molecule inhibitor of BMP signaling, promotes cardiomyogenesis in embryonic stem cells. *PloS one* **3**: e2904.

Harvey, RP (2002). Organogenesis: Patterning the vertebrate heart. *Nature Reviews Genetics* **3**: 544.

Hattori, F, Chen, H, Yamashita, H, Tohyama, S, Satoh, Y, Yuasa, S*, et al.* (2010). Nongenetic method for purifying stem cell–derived cardiomyocytes. *Nature methods* **7**: 61.

Hay, M, Thomas, DW, Craighead, JL, Economides, C & Rosenthal, J (2014). Clinical development success rates for investigational drugs. *Nat Biotechnol* **32**: 40-51.

Hayashi, K, Tada, H & Yamagishi, M (2017). The genetics of atrial fibrillation. *Curr Opin Cardiol* **32**: 10-6.

Heng, BC, Vinoth, KJ, Liu, H, Hande, MP & Cao, T (2006). Low temperature tolerance of human embryonic stem cells. *Int J Med Sci* **3**: 124-9.

Hinson, JT, Chopra, A, Nafissi, N, Polacheck, WJ, Benson, CC, Swist, S*, et al.* (2015). HEART DISEASE. Titin mutations in iPS cells define sarcomere insufficiency as a cause of dilated cardiomyopathy. *Science* **349**: 982-6.

Honore, E, Barhanin, J, Attali, B, Lesage, F & Lazdunski, M (1994). External blockade of the major cardiac delayed-rectifier K+ channel (Kv1.5) by polyunsaturated fatty acids. *Proc Natl Acad Sci U S A* **91**: 1937-41.

Hwang, HS, Kryshtal, DO, Feaster, TK, Sanchez-Freire, V, Zhang, J, Kamp, TJ*, et al.* (2015). Comparable calcium handling of human iPSC-derived cardiomyocytes generated by multiple laboratories. *J Mol Cell Cardiol* **85**: 79-88.

Itzhaki, I, Maizels, L, Huber, I, Zwi-Dantsis, L, Caspi, O, Winterstern, A*, et al.* (2011). Modelling the long QT syndrome with induced pluripotent stem cells. *Nature* **471**: 225-9.

Jaenisch, R (1988). Transgenic animals. *Science* **240**: 1468-74.

Jessup, M, Brozena, S (2003). Heart Failure. *N Engl J Med* **348**: 2007-18.

Jiang, J, Han, P, Zhang, Q, Zhao, J & Ma, Y (2012). Cardiac differentiation of human pluripotent stem cells. *J Cell Mol Med* **16**: 1663-8.

Johnson-Kerner, BL, Ahmad, FS, Diaz, AG, Greene, JP, Gray, SJ, Samulski, RJ*, et al.* (2014). Intermediate filament protein accumulation in motor neurons derived from giant axonal neuropathy iPSCs rescued by restoration of gigaxonin. *Hum Mol Genet* **24**: 1420-31.

Kahler, DJ, Ahmad, FS, Ritz, A, Hua, H, Moroziewicz, DN, Sproul, AA*, et al.* (2013). Improved methods for reprogramming human dermal fibroblasts using fluorescence activated cell sorting. *PloS one* **8**: e59867.

Kamao, H, Mandai, M, Okamoto, S, Sakai, N, Suga, A, Sugita, S*, et al.* (2014). Characterization of human induced pluripotent stem cell-derived retinal pigment epithelium cell sheets aiming for clinical application. *Stem cell reports* **2**: 205-18.

Kami, D, Watakabe, K, Yamazaki-Inoue, M, Minami, K, Kitani, T, Itakura, Y*, et al.* (2013). Large-scale cell production of stem cells for clinical application using the automated cell processing machine. *BMC biotechnology* **13**: 102.

Kattman, SJ, Huber, TL & Keller, GM (2006). Multipotent flk-1 cardiovascular progenitor cells give rise to the cardiomyocyte, endothelial, and vascular smooth muscle lineages. *Developmental cell* **11**: 723-32.

Kaufman, MH, Robertson, EJ, Handyside, AH & Evans, MJ (1983). Establishment of pluripotential cell lines from haploid mouse embryos. *J Embryol Exp Morphol* **73**: 249-61.

Ke, Y, Lei, M & Solaro, RJ (2008). Regulation of cardiac excitation and contraction by p21 activated kinase-1. *Prog Biophys Mol Biol* **98**: 238-50.

Keller, G (2005). Embryonic stem cell differentiation: emergence of a new era in biology and medicine. *Genes Dev* **19**: 1129-55.

Kim, RY, Robertson, EJ & Solloway, MJ (2001). Bmp6 and Bmp7 are required for cushion formation and septation in the developing mouse heart. *Dev Biol* **235**: 449-66.

Klug, MG, Soonpaa, MH, Koh, GY & Field, LJ (1996). Genetically selected cardiomyocytes from differentiating embronic stem cells form stable intracardiac grafts. *J Clin Invest* **98**: 216-24.

Kolossov, E, Lu, Z, Drobinskaya, I, Gassanov, N, Duan, Y, Sauer, H*, et al.* (2005). Identification and characterization of embryonic stem cell-derived pacemaker and atrial cardiomyocytes. *FASEB J* **19**: 577-9.

Lanner, F, Rossant, J (2010). The role of FGF/Erk signaling in pluripotent cells. *Development* **137**: 3351-60.

Lee, P, Klos, M, Bollensdorff, C, Hou, L, Ewart, P, Kamp, TJ*, et al.* (2012). Simultaneous voltage and calcium mapping of genetically purified human induced pluripotent stem cell-derived cardiac myocyte monolayers. *Circ Res* **110**: 1556-63.

Lehmann, M (2014). *A Novel Model System to Study the Role of Catecholamines in Cardiac Lineage Commitment of Embryonic Stem Cells and Functional Response to Proarrhythmic Drugs*.

Lei, M, Brown, HF & Terrar, DA (2000). Modulation of delayed rectifier potassium current, iK, by isoprenaline in rabbit isolated pacemaker cells. *Exp Physiol* **85**: 27-35.

Lei, M, Lu, W, Meng, W, Parrini, M, Eck, MJ, Mayer, BJ*, et al.* (2000). Structure of PAK1 in an autoinhibited conformation reveals a multistage activation switch. *Cell* **102**: 387-97.

Levenstein, ME, Ludwig, TE, Xu, R, Llanas, RA, VanDenHeuvel-Kramer, K, Manning, D*, et al.* (2006). Basic fibroblast growth factor support of human embryonic stem cell self-renewal. *Stem Cells* **24**: 568-74.

Lewis, AM, Aley, PK, Roomi, A, Thomas, JM, Masgrau, R, Garnham, C*, et al.* (2012). ß-Adrenergic receptor signaling increases NAADP and cADPR levels in the heart. *Biochem Biophys Res Commun* **427**: 326-9.

Leyton-Mange, JS, Mills, RW, Macri, VS, Jang, MY, Butte, FN, Ellinor, PT*, et al.* (2014). Rapid cellular phenotyping of human pluripotent stem cell-derived cardiomyocytes using a genetically encoded fluorescent voltage sensor. *Stem Cell Reports* **2**: 163-70.

Lian, X, Zhang, J, Azarin, SM, Zhu, K, Hazeltine, LB, Bao, X*, et al.* (2013). Directed cardiomyocyte differentiation from human pluripotent stem cells by modulating Wnt/β-catenin signaling under fully defined conditions. *Nature protocols* **8**: 162-75.

Lian, X, Hsiao, C, Wilson, G, Zhu, K, Hazeltine, LB, Azarin, SM*, et al.* (2012). Robust cardiomyocyte differentiation from human pluripotent stem cells via temporal modulation of canonical Wnt signaling. *Proc Natl Acad Sci U S A* **109**: E1848-57.

Liang, C, Li, H, Tao, Y, Zhou, X, Yang, Z, Xiao, Y*, et al.* (2012). Dual delivery for stem cell differentiation using dexamethasone and bFGF in/on polymeric microspheres as a cell carrier for nucleus pulposus regeneration. *J Mater Sci Mater Med* **23**: 1097-107.

Liang, P, Lan, F, Lee, AS, Gong, T, Sanchez-Freire, V, Wang, Y*, et al.* (2013). Drug screening using a library of human induced pluripotent stem cell-derived cardiomyocytes reveals disease-specific patterns of cardiotoxicity. *Circulation* **127**: 1677-91.

Liberski, AR, Al-Noubi, MN, Rahman, ZH, Halabi, NM, Dib, SS, Al-Mismar, R*, et al.* (2013). Adaptation of a commonly used, chemically defined medium for human embryonic stem cells to stable isotope labeling with amino acids in cell culture. *Journal of proteome research* **12**: 3233-45.

Lim, D, Roberts, R & Marian, AJ (2001). Expression profiling of cardiac genes in human hypertrophic cardiomyopathy: insight into the pathogenesis of phenotypes. *J Am Coll Cardiol* **38**: 1175-80.

Lin, WK, Bolton, E, Maciejewska, M, Wang, Y, Cortopassi, W, O'Brien, F*, et al.* (2016). Intracellular CD38 Mediates Cardiac Synthesis of NAADP and CADPR. *Biophys J* **110**: 262a.

Liu, W, Selever, J, Wang, D, Lu, MF, Moses, KA, Schwartz, RJ*, et al.* (2004). Bmp4 signaling is required for outflow-tract septation and branchial-arch artery remodeling. *Proc Natl Acad Sci U S A* **101**: 4489-94.

Liu, W, Zi, M, Naumann, R, Ulm, S, Jin, J, Taglieri, DM*, et al.* (2011). Pak1 as a novel therapeutic target for antihypertrophic treatment in the heart. *Circulation* **124**: 2702-15.

Liu, W, Zi, M, Tsui, H, Chowdhury, SK, Zeef, L, Meng, QJ*, et al.* (2013). A novel immunomodulator, FTY-720 reverses existing cardiac hypertrophy and fibrosis from pressure overload by targeting NFAT (nuclear factor of activated T-cells) signaling and periostin. *Circ Heart Fail* **6**: 833-44.

Lohse, MJ, Engelhardt, S & Eschenhagen, T (2003). What is the role of beta-adrenergic signaling in heart failure? *Circ Res* **93**: 896-906.

Lombardi, R, Marian, AJ (2010). Arrhythmogenic right ventricular cardiomyopathy is a disease of cardiac stem cells. *Curr Opin Cardiol* **25**: 222-8.

Lotz, S, Goderie, S, Tokas, N, Hirsch, SE, Ahmad, F, Corneo, B*, et al.* (2013). Sustained levels of FGF2 maintain undifferentiated stem cell cultures with biweekly feeding. *PloS one* **8**: e56289.

Lowry, WE, Richter, L, Yachechko, R, Pyle, AD, Tchieu, J, Sridharan, R*, et al.* (2008). Generation of human induced pluripotent stem cells from dermal fibroblasts. *Proc Natl Acad Sci U S A* **105**: 2883-8.

Lubitz, SA, Benjamin, EJ & Ellinor, PT (2010). Atrial fibrillation in congestive heart failure. *Heart failure clinics* **6**: 187-200.

Lundy, SD, Gantz, JA, Pagan, CM, Filice, D & Laflamme, MA (2014). Pluripotent stem cell derived cardiomyocytes for cardiac repair. *Current treatment options in cardiovascular medicine* **16**: 319.

Ma, J, Guo, L, Fiene, SJ, Anson, BD, Thomson, JA, Kamp, TJ*, et al.* (2011). High purity human-induced pluripotent stem cell-derived cardiomyocytes: electrophysiological properties of action potentials and ionic currents. *American Journal of Physiology-Heart and Circulatory Physiology* **301**: H2006-17.

Ma, L, Lu, MF, Schwartz, RJ & Martin, JF (2005). Bmp2 is essential for cardiac cushion epithelial-mesenchymal transition and myocardial patterning. *Development* **132**: 5601-11.

Macgregor, A, Yamasaki, M, Rakovic, S, Sanders, L, Parkesh, R, Churchill, GC*, et al.* (2007). NAADP controls cross-talk between distinct Ca2+ stores in the heart. *J Biol Chem* **282**: 15302-11.

Manos, PD, Ratanasirintrawoot, S, Loewer, S, Daley, GQ & Schlaeger, TM (2011). Live-Cell Immunofluorescence Staining of Human Pluripotent Stem Cells. *Current protocols in stem cell biology*: 1C. 12.1,1C. 12.14.

Marcus, FI, McKenna, WJ, Sherrill, D, Basso, C, Bauce, B, Bluemke, DA*, et al.* (2010). Diagnosis of arrhythmogenic right ventricular cardiomyopathy/dysplasia: proposed modification of the Task Force Criteria. *Eur Heart J* **31**: 806-14.

Marinho, PA, Chailangkarn, T & Muotri, AR (2015). Systematic optimization of human pluripotent stem cells media using Design of Experiments. *Scientific reports* **5**: srep09834.

Martin, GR (1981). Isolation of a pluripotent cell line from early mouse embryos cultured in medium conditioned by teratocarcinoma stem cells. *Proc Natl Acad Sci U S A* **78**: 7634-8.

Matsa, E, Rajamohan, D, Dick, E, Young, L, Mellor, I, Staniforth, A*, et al.* (2011). Drug evaluation in cardiomyocytes derived from human induced pluripotent stem cells carrying a long QT syndrome type 2 mutation. *Eur Heart J* **32**: 952-62.

Mauritz, C, Martens, A, Rojas, SV, Schnick, T, Rathert, C, Schecker, N*, et al.* (2011). Induced pluripotent stem cell (iPSC)-derived Flk-1 progenitor cells engraft, differentiate, and improve heart function in a mouse model of acute myocardial infarction. *Eur Heart J* **32**: 2634-41.

McCulley, DJ, Kang, J, Martin, JF & Black, BL (2008). BMP4 is required in the anterior heart field and its derivatives for endocardial cushion remodeling, outflow tract septation, and semilunar valve development. *Developmental Dynamics* **237**: 3200-9.

Melkoumian, Z, Weber, JL, Weber, DM, Fadeev, AG, Zhou, Y, Dolley-Sonneville, P*, et al.* (2010). Synthetic peptide-acrylate surfaces for long-term self-renewal and cardiomyocyte differentiation of human embryonic stem cells. *Nat Biotechnol* **28**: 606.

Miragoli, M, Gaudesius, G & Rohr, S (2006). Electrotonic modulation of cardiac impulse conduction by myofibroblasts. *Circ Res* **98**: 801-10.

Mitcheson, JS, Hancox, JC & Levi, AJ (1998). Cultured adult cardiac myocytes: future applications, culture methods, morphological and electrophysiological properties. *Cardiovasc Res* **39**: 280-300.

Mohamed, F, van der Walle, Christopher F (2008). Engineering biodegradable polyester particles with specific drug targeting and drug release properties. *J Pharm Sci* **97**: 71-87.

Moorman, JE, Rudd, RA, Johnson, CA, King, M, Minor, P, Bailey, C*, et al.* (2007). National surveillance for asthma—United States, 1980–2004. *MMWR Surveill Summ* **56**: 1-54.

Moretti, A, Bellin, M, Welling, A, Jung, CB, Lam, JT, Bott-Flügel, L*, et al.* (2010). Patient-specific induced pluripotent stem-cell models for long-QT syndrome. *N Engl J Med* **363**: 1397-409.

Moretti, A, Caron, L, Nakano, A, Lam, JT, Bernshausen, A, Chen, Y*, et al.* (2006). Multipotent embryonic isl1 progenitor cells lead to cardiac, smooth muscle, and endothelial cell diversification. *Cell* **127**: 1151-65.

Mudd, JO, Kass, DA (2008). Tackling heart failure in the twenty-first century. *Nature* **451**: 919-28.

Muller, II, Melville, DB, Tanwar, V, Rybski, WM, Mukherjee, A, Shoemaker, MB*, et al.* (2013). Functional modeling in zebrafish demonstrates that the atrial-fibrillation-associated gene GREM2 regulates cardiac laterality, cardiomyocyte differentiation and atrial rhythm. *Dis Model Mech* **6**: 332-41.

Mummery, C, Ward-van Oostwaard, D, Doevendans, P, Spijker, R, van den Brink, S, Hassink, R*, et al.* (2003). Differentiation of human embryonic stem cells to cardiomyocytes: role of coculture with visceral endoderm-like cells. *Circulation* **107**: 2733-40.

Mummery, CL, Zhang, J, Ng, ES, Elliott, DA, Elefanty, AG & Kamp, TJ (2012). Differentiation of human embryonic stem cells and induced pluripotent stem cells to cardiomyocytes: a methods overview. *Circ Res* **111**: 344-58.

Murry, CE, Reinecke, H & Pabon, LM (2006). Regeneration gaps. *J Am Coll Cardiol* **47**: 1777-85.

Nadadur, RD, Broman, MT, Boukens, B, Mazurek, SR, Yang, X, van den Boogaard, M*, et al.* (2016). Pitx2 modulates a Tbx5-dependent gene regulatory network to maintain atrial rhythm. *Sci Transl Med* **8**: 354ra115.

Ni, TT, Rellinger, EJ, Mukherjee, A, Xie, S, Stephens, L, Thorne, CA*, et al.* (2011). Discovering small molecules that promote cardiomyocyte generation by modulating Wnt signaling. *Chem Biol* **18**: 1658-68.

Novak, A, Barad, L, Lorber, A, Gherghiceanu, M, Reiter, I, Eisen, B*, et al.* (2015). Functional abnormalities in iPSC-derived cardiomyocytes generated from CPVT1 and CPVT2 patients carrying ryanodine or calsequestrin mutations. *J Cell Mol Med* **19**: 2006-18.

Olesen, MS, Nielsen, MW, Haunsø, S & Svendsen, JH (2014). Atrial fibrillation: the role of common and rare genetic variants. *European Journal of Human Genetics* **22**: 297-306.

Olson, H, Betton, G, Robinson, D, Thomas, K, Monro, A, Kolaja, G*, et al.* (2000). Concordance of the toxicity of pharmaceuticals in humans and in animals. *Regulatory Toxicology and Pharmacology* **32**: 56-67.

Onizuka, T, Yuasa, S, Kusumoto, D, Shimoji, K, Egashira, T, Ohno, Y*, et al.* (2012). Wnt2 accelerates cardiac myocyte differentiation from ES-cell derived mesodermal cells via non-canonical pathway. *J Mol Cell Cardiol* **52**: 650-9.

Papapetrou, EP, Tomishima, MJ, Chambers, SM, Mica, Y, Reed, E, Menon, J*, et al.* (2009). Stoichiometric and temporal requirements of Oct4, Sox2, Klf4, and c-Myc expression for efficient human iPSC induction and differentiation. *Proc Natl Acad Sci U S A* **106**: 12759-64.

Paull, D, Sevilla, A, Zhou, H, Hahn, AK, Kim, H, Napolitano, C*, et al.* (2015). Automated, high-throughput derivation, characterization and differentiation of induced pluripotent stem cells. *Nature methods* **12**: 885-92.

Peters, MF, Lamore, SD, Guo, L, Scott, CW & Kolaja, KL (2015). Human stem cell-derived cardiomyocytes in cellular impedance assays: bringing cardiotoxicity screening to the front line. *Cardiovascular toxicology* **15**: 127-39.

Peters, NS, Green, CR, Poole-Wilson, PA & Severs, NJ (1993). Reduced content of connexin43 gap junctions in ventricular myocardium from hypertrophied and ischemic human hearts. *Circulation* **88**: 864-75.

Pittenger, MF, Mackay, AM, Beck, SC, Jaiswal, RK, Douglas, R, Mosca, JD*, et al.* (1999). Multilineage potential of adult human mesenchymal stem cells. *Science* **284**: 143-7.

Polak, S, Pugsley, MK, Stockbridge, N, Garnett, C & Wiśniowska, B (2015). *Early drug discovery prediction of proarrhythmia potential and its covariates*.

Prystowsky, E (1996). Prystowsky EN, Benson DW Jr, Fuster V, Hart RG, Kay GN, Myerburg RJ, NaccarelliGV, Wyse DG. Management of patients with atrial fibrillation. A Statement for HealthcareProfessionals. From the Subcommittee on Electrocardiography and Electrophysiology, American Heart Association. *Circulation* **93**: 1262-77.

Rai, M, Walthall, JM, Hu, J & Hatzopoulos, AK (2011). Continuous antagonism by Dkk1 counter activates canonical Wnt signaling and promotes cardiomyocyte differentiation of embryonic stem cells. *Stem cells and development* **21**: 54-66.

Rakovic, S, Galione, A, Ashamu, GA, Potter, BV & Terrar, DA (1996). A specific cyclic ADP-ribose antagonist inhibits cardiac excitation–contraction coupling. *Current Biology* **6**: 989-96.

Rakovic, S., Terrar, D.A. (2002). Calcium signaling by cADPR in cardiac myocytes. In: Anonymous *Cyclic ADP-Ribose and NAADP*Springer, pp 319-341.

Ramachandra, CJ, Mehta, A, Wong, P & Shim, W (2016). ErbB4 activated p38γ MAPK isoform mediates early cardiogenesis through NKx2. 5 in human pluripotent stem cells. *Stem Cells* **34**: 288-98.

Rangarajan, S, Madden, L & Bursac, N (2014). Use of flow, electrical, and mechanical stimulation to promote engineering of striated muscles. *Ann Biomed Eng* **42**: 1391-405.

Raynaud, CM, Ahmad, FS, Allouba, M, Abou-Saleh, H, Lui, KO & Yacoub, M (2015). Reprogramming for cardiac regeneration. *Global Cardiology Science and Practice*: 44.

Reiffel, JA (2014). Atrial fibrillation and stroke: epidemiology. *Am J Med* **127**: e15-6.

Roden, DM, Lazzara, R, Rosen, M, Schwartz, PJ, Towbin, J & Vincent, GM (1996). Multiple mechanisms in the long-QT syndrome. Current knowledge, gaps, and future directions. The SADS Foundation Task Force on LQTS. *Circulation* **94**: 1996-2012.

Rohr, S (2009). Myofibroblasts in diseased hearts: new players in cardiac arrhythmias? *Heart Rhythm* **6**: 848-56.

Rosamond, W, Flegal, K, Furie, K, Go, A, Greenlund, K, Haase, N*, et al.* (2008). Heart disease and stroke statistics--2008 update: a report from the American Heart Association Statistics Committee and Stroke Statistics Subcommittee. *Circulation* **117**: e25-146.

Rouleau, J, Chatterjee, K, Benge, W, Parmley, WW & Hiramatsu, B (1982). Alterations in left ventricular function and coronary hemodynamics with captopril, hydralazine and prazosin in chronic ischemic heart failure. *Circulation* **65**: 671-8.

Sanders, LN, Schoenhard, JA, Saleh, MA, Mukherjee, A, Ryzhov, S, McMaster, WG,Jr*, et al.* (2016). BMP Antagonist Gremlin 2 Limits Inflammation After Myocardial Infarction. *Circ Res* **119**: 434-49.

Saunders, CM, Larman, MG, Parrington, J, Cox, LJ, Royse, J, Blayney, LM*, et al.* (2002). PLC zeta: a sperm-specific trigger of Ca(2+) oscillations in eggs and embryo development. *Development* **129**: 3533-44.

Savio-Galimberti, E, Darbar, D (2014). Atrial fibrillation and SCN5A variants. *Cardiac electrophysiology clinics* **6**: 741-8.

Schram, G, Pourrier, M, Melnyk, P & Nattel, S (2002). Differential distribution of cardiac ion channel expression as a basis for regional specialization in electrical function. *Circ Res* **90**: 939-50.

Schulz, H, Kolde, R, Adler, P, Aksoy, I, Anastassiadis, K, Bader, M*, et al.* (2009). The FunGenES database: a genomics resource for mouse embryonic stem cell differentiation. *PLoS One* **4**: e6804.

Schurmann, A, Mooney, AF, Sanders, LC, Sells, MA, Wang, HG, Reed, JC*, et al.* (2000). P21-Activated Kinase 1 Phosphorylates the Death Agonist Bad and Protects Cells from Apoptosis. *Mol Cell Biol* **20**: 453-61.

Scott, CW, Peters, MF & Dragan, YP (2013). Human induced pluripotent stem cells and their use in drug discovery for toxicity testing. *Toxicol Lett* **219**: 49-58.

Sheng, J, Shim, W, Lu, J, Lim, SY, Ong, BH, Lim, TS*, et al.* (2014). Electrophysiology of human cardiac atrial and ventricular telocytes. *J Cell Mol Med* **18**: 355-62.

Shiba, Y, Fernandes, S, Zhu, W, Filice, D, Muskheli, V, Kim, J*, et al.* (2012). Human ES-cell-derived cardiomyocytes electrically couple and suppress arrhythmias in injured hearts. *Nature* **489**: 322-5.

Sirenko, O, Crittenden, C, Callamaras, N, Hesley, J, Chen, Y, Funes, C*, et al.* (2013). Multiparameter in vitro assessment of compound effects on cardiomyocyte physiology using iPSC cells. *Journal of biomolecular screening* **18**: 39-53.

Solloway, MJ, Robertson, EJ (1999). Early embryonic lethality in Bmp5;Bmp7 double mutant mice suggests functional redundancy within the 60A subgroup. *Development* **126**: 1753-68.

Spencer, CI, Baba, S, Nakamura, K, Hua, EA, Sears, MA, Fu, C*, et al.* (2014). Calcium transients closely reflect prolonged action potentials in iPSC models of inherited cardiac arrhythmia. *Stem cell reports* **3**: 269-81.

Stubbs, SL, Crook, JM, Morrison, WA & Newcomb, AE (2011). Toward clinical application of stem cells for cardiac regeneration. *Heart, Lung and Circulation* **20**: 173-9.

Takahashi, K, Yamanaka, S (2006). Induction of pluripotent stem cells from mouse embryonic and adult fibroblast cultures by defined factors. *Cell* **126**: 663-76.

Tamaddon, HS, Vaidya, D, Simon, AM, Paul, DL, Jalife, J & Morley, GE (2000). High-resolution optical mapping of the right bundle branch in connexin40 knockout mice reveals slow conduction in the specialized conduction system. *Circ Res* **87**: 929-36.

Tanaka, T, Tohyama, S, Murata, M, Nomura, F, Kaneko, T, Chen, H*, et al.* (2009). In vitro pharmacologic testing using human induced pluripotent stem cell-derived cardiomyocytes. *Biochem Biophys Res Commun* **385**: 497-502.

Tanaka, A, Yuasa, S, Mearini, G, Egashira, T, Seki, T, Kodaira, M*, et al.* (2014). Endothelin-1 induces myofibrillar disarray and contractile vector variability in hypertrophic cardiomyopathy-induced pluripotent stem cell-derived cardiomyocytes. *J Am Heart Assoc* **3**: e001263.

Tanwar, V, Bylund, JB, Hu, J, Yan, J, Walthall, JM, Mukherjee, A*, et al.* (2014). Gremlin 2 promotes differentiation of embryonic stem cells to atrial fate by activation of the JNK signaling pathway. *Stem Cells* **32**: 1774-88.

Terami, H, Hidaka, K, Katsumata, T, Iio, A & Morisaki, T (2004). Wnt11 facilitates embryonic stem cell differentiation to Nkx2. 5-positive cardiomyocytes. *Biochem Biophys Res Commun* **325**: 968-75.

Terrenoire, C, Wang, K, Tung, KW, Chung, WK, Pass, RH, Lu, JT*, et al.* (2013). Induced pluripotent stem cells used to reveal drug actions in a long QT syndrome family with complex genetics. *J Gen Physiol* **141**: 61-72.

Tesar, PJ, Chenoweth, JG, Brook, FA, Davies, TJ, Evans, EP, Mack, DL*, et al.* (2007). New cell lines from mouse epiblast share defining features with human embryonic stem cells. *Nature* **448**: 196-9.

Thomson, JA, Itskovitz-Eldor, J, Shapiro, SS, Waknitz, MA, Swiergiel, JJ, Marshall, VS*, et al.* (1998). Embryonic stem cell lines derived from human blastocysts. *Science* **282**: 1145-7.

Thomson, JR, Machado, RD, Pauciulo, MW, Morgan, NV, Humbert, M, Elliott, GC*, et al.* (2000). Sporadic primary pulmonary hypertension is associated with germline mutations of the gene encoding BMPR-II, a receptor member of the TGF-beta family. *J Med Genet* **37**: 741-5.

Thul, R, Coombes, S, Roderick, HL & Bootman, MD (2012). Subcellular calcium dynamics in a whole-cell model of an atrial myocyte. *Proc Natl Acad Sci U S A* **109**: 2150-5.

Tohyama, S, Hattori, F, Sano, M, Hishiki, T, Nagahata, Y, Matsuura, T*, et al.* (2013). Distinct metabolic flow enables large-scale purification of mouse and human pluripotent stem cell-derived cardiomyocytes. *Cell stem cell* **12**: 127-37.

Turbendian, HK, Gordillo, M, Tsai, SY, Lu, J, Kang, G, Liu, TC*, et al.* (2013). GATA factors efficiently direct cardiac fate from embryonic stem cells. *Development* **140**: 1639-44.

Vallier, L, Alexander, M & Pedersen, RA (2005). Activin/Nodal and FGF pathways cooperate to maintain pluripotency of human embryonic stem cells. *J Cell Sci* **118**: 4495-509.

Verma, SC, Mcneill, JH (1976). Biochemical and mechanical effects of phenylephrine on the heart. *Eur J Pharmacol* **36**: 447-50.

Voigt, N, Maguy, A, Yeh, Y, Qi, X, Ravens, U, Dobrev, D*, et al.* (2007). Changes in IK, ACh single-channel activity with atrial tachycardia remodelling in canine atrial cardiomyocytes. *Cardiovasc Res* **77**: 35-43.

Wang, R, Wang, Y, Lin, WK, Zhang, Y, Liu, W, Huang, K*, et al.* (2014). Inhibition of angiotensin II-induced cardiac hypertrophy and associated ventricular arrhythmias by a p21 activated kinase 1 bioactive peptide. *PloS one* **9**: e101974.

Wang, Y, Tsui, H, Ke, Y, Shi, Y, Li, Y, Davies, L*, et al.* (2014). Pak1 is required to maintain ventricular Ca(2)(+) homeostasis and electrophysiological stability through SERCA2a regulation in mice. *Circ Arrhythm Electrophysiol* **7**: 938-48.

Wang, Z, Fermini, B & Nattel, S (1993). Sustained depolarization-induced outward current in human atrial myocytes. Evidence for a novel delayed rectifier K+ current similar to Kv1.5 cloned channel currents. *Circ Res* **73**: 1061-76.

Watanabe, K, Ueno, M, Kamiya, D, Nishiyama, A, Matsumura, M, Wataya, T*, et al.* (2007). A ROCK inhibitor permits survival of dissociated human embryonic stem cells. *Nat Biotechnol* **25**: 681-6.

Wei, WJ, Sun, HY, Ting, KY, Zhang, LH, Lee, HC, Li, GR*, et al.* (2012). Inhibition of cardiomyocytes differentiation of mouse embryonic stem cells by CD38/cADPR/Ca2+ signaling pathway. *J Biol Chem* **287**: 35599-611.

Willems, E, Spiering, S, Davidovics, H, Lanier, M, Xia, Z, Dawson, M*, et al.* (2011). Small-molecule inhibitors of the Wnt pathway potently promote cardiomyocytes from human embryonic stem cell-derived mesoderm. *Circ Res* **109**: 360-4.

Wilmut, I, Campbell, K & Tudge, C (2001). *The second creation: Dolly and the age of biological control.* Harvard University Press.

Witchel, HJ, Hancox, JC (2000). Familial and acquired long QT syndrome and the cardiac rapid delayed rectifier potassium current. *Clinical and Experimental Pharmacology and Physiology* **27**: 753-66.

Wobus, AM, Kaomei, G, Shan, J, Wellner, MC, Rohwedel, J, Ji, G*, et al.* (1997). Retinoic acid accelerates embryonic stem cell-derived cardiac differentiation and enhances development of ventricular cardiomyocytes. *J Mol Cell Cardiol* **29**: 1525-39

World Health Organization (2012). World health statistics: a snapshot of global health.

Wu, Q, Tang, S & Yuan, Z (2015). Gremlin 2 inhibits adipocyte differentiation through activation of Wnt/β-catenin signaling. *Molecular medicine reports* **12**: 5891-6.

Wu, SM, Fujiwara, Y, Cibulsky, SM, Clapham, DE, Lien, C, Schultheiss, TM*, et al.* (2006). Developmental origin of a bipotential myocardial and smooth muscle cell precursor in the mammalian heart. *Cell* **127**: 1137-50.

Xie, M, Cao, N & Ding, S (2014). Small molecules for cell reprogramming and heart repair: progress and perspective. *ACS chemical biology* **9**: 34-44.

Yamamizu, K, Iwasaki, M, Takakubo, H, Sakamoto, T, Ikuno, T, Miyoshi, M*, et al.* (2017). In vitro modeling of blood-brain barrier with human iPSC-derived endothelial cells, pericytes, neurons, and astrocytes via notch signaling. *Stem cell reports* **8**: 634-47.

Yang, L, Soonpaa, MH, Adler, ED, Roepke, TK, Kattman, SJ, Kennedy, M*, et al.* (2008). Human cardiovascular progenitor cells develop from a KDR embryonic-stem-cell-derived population. *Nature* **453**: 524-8.

Yang, T, Rubart, M, Soonpaa, MH, Didié, M, Christalla, P, Zimmermann, W*, et al.* (2015). Cardiac engraftment of genetically-selected parthenogenetic stem cell-derived cardiomyocytes. *PloS one* **10**: e0131511.

Yap, J, Liew, R (2014). Understanding arrhythmogenic right ventricular cardiomyopathy: Use of patient-specific induced pluripotent stem cell models. *Journal of Arrhythmia* **30**: 350-2.

Ye, L, Chang, Y, Xiong, Q, Zhang, P, Zhang, L, Somasundaram, P*, et al.* (2014). Cardiac repair in a porcine model of acute myocardial infarction with human induced pluripotent stem cell-derived cardiovascular cells. *Cell stem cell* **15**: 750-61.

Yeung, CC, Gossan, N, Lu, Y, Hughes, A, Hensman, JJ, Bayer, ML*, et al.* (2014). Gremlin-2 is a BMP antagonist that is regulated by the circadian clock. *Scientific reports* **4**: 5183.

Yu, J, Vodyanik, MA, Smuga-Otto, K, Antosiewicz-Bourget, J, Frane, JL, Tian, S*, et al.* (2007). Induced pluripotent stem cell lines derived from human somatic cells. *Science* **318**: 1917-20.

Yuasa, S, Itabashi, Y, Koshimizu, U, Tanaka, T, Sugimura, K, Kinoshita, M*, et al.* (2005). Transient inhibition of BMP signaling by Noggin induces cardiomyocyte differentiation of mouse embryonic stem cells. *Nat Biotechnol* **23**: 607-11.

Zeevi-Levin, N, Itskovitz-Eldor, J & Binah, O (2012). Cardiomyocytes derived from human pluripotent stem cells for drug screening. *Pharmacol Ther* **134**: 180-8.

Zhang, H, Bradley, A (1996). Mice deficient for BMP2 are nonviable and have defects in amnion/chorion and cardiac development. *Development* **122**: 2977-86.

Zhang, J, Klos, M, Wilson, GF, Herman, AM, Lian, X, Raval, KK*, et al.* (2012). Extracellular matrix promotes highly efficient cardiac differentiation of human pluripotent stem cells: the matrix sandwich method. *Circ Res* **111**: 1125-36.

Zhang, J, Wilson, GF, Soerens, AG, Koonce, CH, Yu, J, Palecek, SP*, et al.* (2009). Functional cardiomyocytes derived from human induced pluripotent stem cells. *Circ Res* **104**: e30-41.

Zhang, X, Ibrahimi, OA, Olsen, SK, Umemori, H, Mohammadi, M & Ornitz, DM (2006). Receptor specificity of the fibroblast growth factor family. The complete mammalian FGF family. *J Biol Chem* **281**: 15694-700.

Zhu, MX, Ma, J, Parrington, J, Calcraft, PJ, Galione, A & Evans, AM (2010). Calcium signaling via two-pore channels: local or global, that is the question. *Am J Physiol Cell Physiol* **298**: C430-41.

Zhu, WZ, Xie, Y, Moyes, KW, Gold, JD, Askari, B & Laflamme, MA (2010). Neuregulin/ErbB signaling regulates cardiac subtype specification in differentiating human embryonic stem cells. *Circ Res* **107**: 776-86.

Zimmermann, W, Melnychenko, I & Eschenhagen, T (2004). Engineered heart tissue for regeneration of diseased hearts. *Biomaterials* **25**: 1639-47.

Zimmermann, W, Melnychenko, I, Wasmeier, G, Didié, M, Naito, H, Nixdorff, U*, et al.* (2006). Engineered heart tissue grafts improve systolic and diastolic function in infarcted rat hearts. *Nat Med* **12**: 452

Al Ghamdi, B, Hassan, W (2009). Atrial Remodeling And Atrial Fibrillation: Mechanistic Interactions And Clinical Implications. *Journal of atrial fibrillation* **2**.

Blundo, JT (2010). *Biomechanics in the Heart and Bone: The Role of Electromechanical Forces in Deriving Cardiac Myocytes from Human Embryonic Stem Cells and the Role of Focal Adhesion Kinase in Osteoblast Mechanotransduction.* Stanford University.

Brade, T, Pane, LS, Moretti, A, Chien, KR & Laugwitz, KL (2013). Embryonic heart progenitors and cardiogenesis. *Cold Spring Harb Perspect Med* **3**: a013847.

Brand, T (2003). Heart development: molecular insights into cardiac specification and early morphogenesis. *Dev Biol* **258**: 1-19.

Capecchi, MR (1989). Altering the genome by homologous recombination. *Science* **244**: 1288-92.

Chong, JJ, Yang, X, Don, CW, Minami, E, Liu, Y, Weyers, JJ*, et al.* (2014). Human embryonic-stem-cell-derived cardiomyocytes regenerate non-human primate hearts. *Nature* **510**: 273.

Christoffels, VM, Mommersteeg, MT, Trowe, MO, Prall, OW, de Gier-de Vries, C, Soufan, AT*, et al.* (2006). Formation of the venous pole of the heart from an Nkx2-5-negative precursor population requires Tbx18. *Circ Res* **98**: 1555-63.

Dobrev, D, Ravens, U (2003). Remodeling of cardiomyocyte ion channels in human atrial fibrillation. *Basic Res Cardiol* **98**: 137-48.

Ehrlich, JR, Cha, T, Zhang, L, Chartier, D, Melnyk, P, Hohnloser, SH*, et al.* (2003). Cellular electrophysiology of canine pulmonary vein cardiomyocytes: action potential and ionic current properties. *J Physiol (Lond)* **551**: 801-13.

Földes, G, Matsa, E, Kriston-Vizi, J, Leja, T, Amisten, S, Kolker, L*, et al.* (2014). Aberrant α-adrenergic hypertrophic response in cardiomyocytes from human induced pluripotent cells. *Stem cell reports* **3**: 905-14.

Furue, MK, Na, J, Jackson, JP, Okamoto, T, Jones, M, Baker, D*, et al.* (2008). Heparin promotes the growth of human embryonic stem cells in a defined serum-free medium. *Proc Natl Acad Sci U S A* **105**: 13409-14.

Glukhov, AV, Balycheva, M, Sanchez-Alonso, JL, Ilkan, Z, Alvarez-Laviada, A, Bhogal, N*, et al.* (2015). Direct Evidence for Microdomain-Specific Localization and Remodeling of Functional L-Type Calcium Channels in Rat and Human Atrial Myocytes. *Circulation* **132**: 2372-84.

González, F, Zhu, Z, Shi, Z, Lelli, K, Verma, N, Li, QV*, et al.* (2014). An iCRISPR platform for rapid, multiplexable, and inducible genome editing in human pluripotent stem cells. *Cell stem cell* **15**: 215-26.

Harvey, RP (2002). Organogenesis: Patterning the vertebrate heart. *Nature Reviews Genetics* **3**: 544.

Hattori, F, Chen, H, Yamashita, H, Tohyama, S, Satoh, Y, Yuasa, S*, et al.* (2010). Nongenetic method for purifying stem cell–derived cardiomyocytes. *Nature methods* **7**: 61.

Honore, E, Barhanin, J, Attali, B, Lesage, F & Lazdunski, M (1994). External blockade of the major cardiac delayed-rectifier K+ channel (Kv1.5) by polyunsaturated fatty acids. *Proc Natl Acad Sci U S A* **91**: 1937-41.

Hwang, HS, Kryshtal, DO, Feaster, TK, Sanchez-Freire, V, Zhang, J, Kamp, TJ*, et al.* (2015). Comparable calcium handling of human iPSC-derived cardiomyocytes generated by multiple laboratories. *J Mol Cell Cardiol* **85**: 79-88.

Kahler, DJ, Ahmad, FS, Ritz, A, Hua, H, Moroziewicz, DN, Sproul, AA*, et al.* (2013). Improved methods for reprogramming human dermal fibroblasts using fluorescence activated cell sorting. *PloS one* **8**: e59867.

Kamao, H, Mandai, M, Okamoto, S, Sakai, N, Suga, A, Sugita, S*, et al.* (2014). Characterization of human induced pluripotent stem cell-derived retinal pigment epithelium cell sheets aiming for clinical application. *Stem cell reports* **2**: 205-18.

Lei, M, Lu, W, Meng, W, Parrini, M, Eck, MJ, Mayer, BJ*, et al.* (2000). Structure of PAK1 in an autoinhibited conformation reveals a multistage activation switch. *Cell* **102**: 387-97.

Lian, X, Hsiao, C, Wilson, G, Zhu, K, Hazeltine, LB, Azarin, SM*, et al.* (2012). Robust cardiomyocyte differentiation from human pluripotent stem cells via temporal modulation of canonical Wnt signaling. *Proc Natl Acad Sci U S A* **109**: E1848-57.

Liang, C, Li, H, Tao, Y, Zhou, X, Yang, Z, Xiao, Y*, et al.* (2012). Dual delivery for stem cell differentiation using dexamethasone and bFGF in/on polymeric microspheres as a cell carrier for nucleus pulposus regeneration. *J Mater Sci Mater Med* **23**: 1097-107.

Lim, D, Roberts, R & Marian, AJ (2001). Expression profiling of cardiac genes in human hypertrophic cardiomyopathy: insight into the pathogenesis of phenotypes. *J Am Coll Cardiol* **38**: 1175-80.

Manos, PD, Ratanasirintrawoot, S, Loewer, S, Daley, GQ & Schlaeger, TM (2011). Live-Cell Immunofluorescence Staining of Human Pluripotent Stem Cells. *Current protocols in stem cell biology*: 1C. 12.1,1C. 12.14.

Melkoumian, Z, Weber, JL, Weber, DM, Fadeev, AG, Zhou, Y, Dolley-Sonneville, P*, et al.* (2010a). Synthetic peptide-acrylate surfaces for long-term self-renewal and cardiomyocyte differentiation of human embryonic stem cells. *Nat Biotechnol* **28**: 606.

Melkoumian, Z, Weber, JL, Weber, DM, Fadeev, AG, Zhou, Y, Dolley-Sonneville, P*, et al.* (2010b). Synthetic peptide-acrylate surfaces for long-term self-renewal and cardiomyocyte differentiation of human embryonic stem cells. *Nat Biotechnol* **28**: 606.

Mohamed, F, van der Walle, Christopher F (2008). Engineering biodegradable polyester particles with specific drug targeting and drug release properties. *J Pharm Sci* **97**: 71-87.

Nadadur, RD, Broman, MT, Boukens, B, Mazurek, SR, Yang, X, van den Boogaard, M*, et al.* (2016). Pitx2 modulates a Tbx5-dependent gene regulatory network to maintain atrial rhythm. *Sci Transl Med* **8**: 354ra115.

Peters, NS, Green, CR, Poole-Wilson, PA & Severs, NJ (1993). Reduced content of connexin43 gap junctions in ventricular myocardium from hypertrophied and ischemic human hearts. *Circulation* **88**: 864-75.

Pittenger, MF, Mackay, AM, Beck, SC, Jaiswal, RK, Douglas, R, Mosca, JD*, et al.* (1999). Multilineage potential of adult human mesenchymal stem cells. *Science* **284**: 143-7.

Rangarajan, S, Madden, L & Bursac, N (2014). Use of flow, electrical, and mechanical stimulation to promote engineering of striated muscles. *Ann Biomed Eng* **42**: 1391-405.

Raynaud, CM, Ahmad, FS, Allouba, M, Abou-Saleh, H, Lui, KO & Yacoub, M (2015). Reprogramming for cardiac regeneration. *Global Cardiology Science and Practice*: 44.

Roden, DM, Lazzara, R, Rosen, M, Schwartz, PJ, Towbin, J & Vincent, GM (1996). Multiple mechanisms in the long-QT syndrome. Current knowledge, gaps, and future directions. The SADS Foundation Task Force on LQTS. *Circulation* **94**: 1996-2012.

Schram, G, Pourrier, M, Melnyk, P & Nattel, S (2002). Differential distribution of cardiac ion channel expression as a basis for regional specialization in electrical function. *Circ Res* **90**: 939-50.

Tanwar, V, Bylund, JB, Hu, J, Yan, J, Walthall, JM, Mukherjee, A*, et al.* (2014). Gremlin 2 promotes differentiation of embryonic stem cells to atrial fate by activation of the JNK signaling pathway. *Stem Cells* **32**: 1774-88.

Verma, SC, Mcneill, JH (1976). Biochemical and mechanical effects of phenylephrine on the heart. *Eur J Pharmacol* **36**: 447-50.

Willems, E, Spiering, S, Davidovics, H, Lanier, M, Xia, Z, Dawson, M*, et al.* (2011). Small-molecule inhibitors of the Wnt pathway potently promote cardiomyocytes from human embryonic stem cell-derived mesoderm. *Circ Res* **109**: 360-4.

Wilmut, I, Campbell, K & Tudge, C (2001). *The second creation: Dolly and the age of biological control.* Harvard University Press.

Xie, M, Cao, N & Ding, S (2014). Small molecules for cell reprogramming and heart repair: progress and perspective. *ACS chemical biology* **9**: 34-44.

Yeung, CC, Gossan, N, Lu, Y, Hughes, A, Hensman, JJ, Bayer, ML*, et al.* (2014). Gremlin-2 is a BMP antagonist that is regulated by the circadian clock. *Scientific reports* **4**: 5183.